DEVELOPMENT OF HOLLOW FIBER MEMBRANE BIOREACTORS FOR TWO-PHASE BIODEGRADATION OF PHENOL

PRASHANT PRAVEEN

(***B. Tech. (Hons.), SASTRA University, India***)

A THESIS SUBMITTED FOR THE DEGREE OF DOCTOR OF PHILOSOPHY

DEPARTMENT OF CHEMICAL AND BIOMOLECULAR ENGINEERING

NATIONAL UNIVERSITY OF SINGAPORE

2012

DECLARATION

I hereby declare that the thesis is my original work and it has been written by me in its entirety. I have duly acknowledged all the sources of information which have been used in the thesis.

This thesis has also not been submitted for any degree in any university previously.

Prashant Praveen

Prashant Praveen

April 02, 2013

ACKNOWLEDGEMENTS

The past four years of PhD has been a roller coaster ride, filled with a myriad of emotions, some pleasure, some adventure and some frustration. As I prepare to conclude my dissertation, it is now time to thank all the people who helped me complete this arduous journey.

First of all, I would like the express my gratitude to my thesis supervisor, Associate Professor Loh Kai-Chee. I would like to thank him for all the independence, the trust, the encouragement, the motivation, the finances, the discussions, the criticism, the corrections, for instilling in me tremendous confidence and data interpretations skills, for my first job as a scientist, and for being the inspiration I am so keen to emulate.

I would like to thank all my current and former lab mates, Dr. Satyen Gautam, Dr. Karthiga Nagarajan, Dr. Vivek Vasudevan, Dr. Cheng Xiyu and Ms. Phay Jia-Jia. My special thanks to my fellow riders Ms. Nguyen Thi Thuy Duong and Ms. Vu-Tran Khanh Linh for being wonderful friends, and for all the stolen moments from their busy schedule which were translated into laughter and jollification.

I thank our lab officers Ms. Tay Alyssa, Mr. Ang Wee Siong and Ms. Xu Yanfang for all the help rendered in this research, and Ms. Ng Sook Poh for designing the glass modules for membrane contactor fabrication.

Finally, I would like to thank my parents, my wife and my brother. It is their love, prayers and blessings which have been my strength to carry on. I would not have achieved whatever I have, if not for them. Not to forget are my dear friends, especially Mr. Rahul Modi who is keenly awaiting my graduation date. I thank them all.

TABLE OF CONTENTS

ACKNOWLEDGEMENTS i
TABLE OF CONTENTS ii
SUMMARY v
LIST OF TABLES ix
LIST OF FIGURES xi
LIST OF ABBREVIATIONS xv
LIST OF SYMBOLS xvii
1 Introduction 1
1.1 Background and Motivations 1
1.2 Research Objectives and Scope 8
1.3 Thesis Organization 11
2 Literature Review 12
2.1 Two-Phase Partitioning Bioreactors 12
2.1.1 Design Considerations 12
2.1.2 Liquid/Liquid TPPB 17
2.1.3 Solid/liquid TPPB 21
2.2 Membrane Enhanced Solvent Extraction 25
2.2.1 Non-Dispersive Solvent Extraction 26
2.2.2 Hollow Fiber Supported Liquid Membranes 29
2.3 Hollow Fiber Membrane Bioreactors in Biodegradation 36
2.4 Conclusions 40
3 Materials & Methods 41
3.1 Microorganisms, Culture Conditions, and Chemicals 41
3.2 Solvent Selection 42
3.2.1 Determination of Distribution Coefficients 42
3.2.2 Biodegradation of Organic Solvents 43
3.2.3 Biocompatibility of Organic Solvents 43
3.3 Membrane Contactor Fabrication 44
3.4 Preparation of the EIHFMs 47
3.5 EIHFM Contactor Fabrication 47
3.6 Membrane Contactor Sterilization 48

3.7 Experimental Setup 48
3.7.1 TPPB Operation 48
3.7.2 HFMB Operation 49
3.7.3 HFSLMB Operation 52
3.7.4 Adsorption/Desorption of Phenol on EIHFMs 53
3.7.5 EIHFMB Operation 54
3.8 Analytical Methods 55
4 Two-phase Biodegradation of Phenol in a Hollow Fiber Membrane Bioreactor 57
4.1 Introduction 57
4.2 Results and Discussions 59
4.2.1 Single-phase Biodegradation of Phenol 59
4.2.2 Solvent Selection 61
4.2.3 TPPB Operation 62
4.2.4 HFMB Operation 64
4.2.5 Comparison between HFMB and TPPB 73
4.2.6 Simultaneous Extraction and Biodegradation 76
4.3 Conclusions 80
5 Kinetic Modeling of Two-Phase Biodegradation in a Hollow Fiber Membrane Bioreactor 82
5.1 Introduction 82
5.2 Theory 85
5.2.1 Cell Growth Kinetics 85
5.2.2 Overall Mass Transfer Coefficients 86
5.2.3 Resistance in Series Model 88
5.2.4 Estimation of Mass Transfer Coefficients 90
5.3 Model Equations 92
5.4 Results & Discussion 93
5.4.1 Parameter Estimation 93
5.4.2 Model Validation and Analysis 95
5.4.3 Parameter Sensitivity Analysis 100
5.4.4 Model Simulations 101
5.5 Conclusions 110
6 Simultaneous Extraction and Biodegradation of Phenol in a Hollow Fiber Supported Liquid Membrane Bioreactor 112
6.1 Introduction 112
6.2 Results & Discussion 116
6.2.1 Two-phase biodegradation of phenol 116

6.2.2 Effects of substrate concentration 121
6.2.3 Effects of Phase Ratio 125
6.2.4 Effect of flow rates 126
6.2.5 Effects of interfacial area 130
6.2.6 Bioreactor Sustainability 134
6.3 Conclusions 139
7 Development of Extractant Impregnated Hollow Fiber Membranes for Adsorption of Phenol from Wastewater 140
7.1 Introduction 140
7.2 Theoretical 143
7.2.1 Adsorption kinetics modeling 143
7.2.2 Adsorption isotherm 145
7.3 Results and Discussion 146
7.3.1 Characterization of EIHFM 146
7.3.2 Adsorption/Desorption on EIHFM 148
7.3.3 Adsorption kinetics 151
7.3.4 Regeneration and Stability 155
7.3.5 Application to TPPB 158
7.4 Conclusions 161
8 Two-Phase Biodegradation of Phenol in an Extractant Impregnated Hollow Fiber Membrane Bioreactor 162
8.1 Introduction 162
8.2 Results and Discussion 165
8.2.1 Cell Growth and Biodegradation 165
8.2.2 Biodegradation Stages 169
8.2.3 Effects of Substrate Concentration 172
8.2.4 Effects of Interfacial Area 175
8.2.5 Effects of Flow Rate 176
8.2.6 Bioreactor Stability 178
8.3 Conclusions 181
9 Conclusions and Recommendations for Future Work 182
9.1 Conclusions 182
9.2 Recommendations for Future Work 186
REFERENCES 190
LIST OF PUBLICATIONS AND PRESENTATIONS 209

SUMMARY

The advent of two-phase partitioning bioreactors (TPPB) can be hailed as one of the most significant developments in the fields of biodegradation in the past decade. These bioreactors utilize a non-aqueous sequestering phase to reduce the effective concentration of toxic substrates in the cell culture medium, thereby enabling suspended bacteria to withstand and metabolize high substrate concentrations. In this research, we aimed to develop hollow fiber membrane-based bioreactors to mitigate the challenges encountered in conventional TPPBs during two-phase biodegradation. The model pollutant selected was phenol and *Pseudomonas putida* was the biodegrading bacterium. Introducing hollow fiber membranes between the aqueous and the organic phases prevented phase dispersion, which eliminated various operating problems in TPPBs and provided a solvent-free growth environment to the microorganisms. In a further study, hollow fiber membranes impregnated with solid extractant TOPO using carrier solvent dichloromethane transformed the membrane itself into the partitioning phase.

A hollow fiber membrane bioreactor (HFMB) resembling a shell and tube dialysis module was first developed for aqueous/organic two-phase biodegradation of phenol and the results were compared with that in a conventional TPPB. The suspended cells in the HFMB could biodegrade inhibitory phenol concentrations at 600-2000 mg/L without experiencing severe substrate inhibition. For example, 1000 mg/L phenol was completely biodegraded in 46 hours at a maximum specific growth rate of 0.49 hr^{-1}. Phenol removal started at an exponential rate subsequently taking on a linear profile under nutrient limitation. The HFMB offered a better growth environment for the cells as evident from the absence of the lag phase and could mitigate the dispersion-

associated problems of foaming and emulsification. It was also observed that for comparable mass transfer flux across the aqueous/organic interface, biodegradation was faster in the HFMB as compared to that in the TPPB.

During simultaneous extraction and biodegradation of phenol from wastewater, phenol concentrations of 1000, 1500 and 2000 mg/L were biodegraded within 28, 36 and 45 hours, respectively. The cell growth rates and biomass yields were comparable to those observed in single-phase biodegradation systems. A kinetics model was developed to elucidate the mass transfer mechanism and phenol metabolism in the HFMB. The overall mass transfer coefficients in the shell and the lumen sides were determined to be 4.58×10^{-8} and 1.51×10^{-6} m/s, respectively, using relevant empirical correlations. The model corroborated the experimental data very well and it was applied to simulate cell growth and biodegradation profiles for various case studies involving variations in the operating conditions.

In the second part of this research, an improvement in the biodegradation performance was brought about by limiting the presence of the organic solvent to a liquid membrane supported on the hollow fiber membranes. The resulting hollow fiber supported liquid membrane bioreactor (HFSLMB) offered improved biodegradation performance during concomitant extraction and biodegradation of phenol. In the HFSLMB, phenol was extracted from the wastewater by dispersing a small amount of organic phase into the wastewater, whereas mass transfer between the solvent and the culture medium was non-dispersive. This semi-dispersive configuration stabilized the liquid membrane and facilitated solvent-free cell growth environment analogous to that in the HFMB. *P. putida* could biodegrade phenol at 1000-4000 mg/L without experiencing severe substrate inhibition. For example, 4000 mg/L phenol was biodegraded within 76 hours while the specific growth rate and biomass yield were

0.31 hr^{-1} and 0.26 g/g, respectively. Substrate removal occurred in two sequential steps: removal during log growth phase and removal under diffusion limitation. The biodegradation rates were enhanced by changing the phase ratio, hydrodynamic conditions and the interfacial area. Repeated batch runs were conducted for more than 400 hours to evaluate long term stability of the HFSLMB.

The focus of the third part of the thesis was the incorporation of the organic phase into the hollow fiber membranes for solid/liquid two-phase biodegradation of phenol. A technique was developed to impregnate polypropylene hollow fiber membranes with an organic extractant – trioctylphosphine oxide (TOPO). Scanning electron microscopy showed white deposits of TOPO dispersed non-uniformly within the cross sections and external surface of the extractant-impregnated hollow fiber membranes (EIHFM). The EIHFMs manifested high sorption capacity and mass transfer rates, with adsorption equilibrium attained within 10-30 minutes of operation. Adsorption kinetics was examined using pseudo-first-order, pseudo-second-order and intraparticle diffusion models, while the sorption capacities were modeled after the Langmuir and Freundlich isotherms. Desorption of phenol from the EIHFMs was comparatively slower but the regeneration of the adsorbents was quite effective. During repeated operation with 1000 mg/L phenol, the adsorption capacities of the EIHFMs remained constant at 32.2 ± 1.3 and 52.3 ± 0.9 mg/g, with indicates high stability of TOPO immobilization in the polypropylene membranes.

The EIHFMs, when used as the non-aqueous phase in a TPPB, alleviated substrate inhibition on *P. putida* by rapidly reducing aqueous phenol concentrations to sub-inhibitory levels. Although a short lag phase was observed during each experiment, subsequent high specific growth rates exhibited by the cells resulted in rapid removal

of 800-2500 mg/L phenol in the extractant impregnated hollow fiber membrane bioreactor (EIHFMB). It was also demonstrated that a higher concentration of phenol could be biodegraded by increasing the length of the EIHFMs. Since the changes in the flow rate did not affect biodegradation rate, it was inferred that biodegradation in the EIHFMB was not limited by mass transfer. The EIHFMB also exhibited high performance stability over a period of 400 hours.

The results from this research demonstrate the strengths and potential of the combination of the hollow fiber membrane technology with TPPBs. In the aqueous/organic configuration, the hollow fiber membranes acted as the semi-permeable barrier to alleviate phase dispersion and its associated problems without compromising the biodegradation performance. The resulting HFMB and HFSLMB extricated mass transfer rates from high energy agitation and facilitated simultaneous extraction and biodegradation. On the other hand, the EIHFM combined the advantages of both solvent extraction and adsorption, resulting in a solventless TPPB with high flexibility in the bioreactor's configuration and operation. It can thus be concluded that the hollow fiber membrane based TPPBs are promising alternatives to conventional two-phase biodegradation systems for the biodegradation of phenolic compounds in wastewater treatment.

LIST OF TABLES

Table 2.1 NAP selection criteria in TPPBs.....14

Table 2.2 Summary of research on liquid/liquid TPPB.....18

Table 2.3 Summary of research on solid/liquid TPPB.....22

Table 3.1 Composition of mineral medium.....42

Table 3.2 Specifications for the hollow fiber membranes.....44

Table 3.3 Specifications for the two membrane contactors.....45

Table 4.1 Solvent screening for the selection of organic phase in two-phase biodegradation of phenol.....61

Table 4.2 Effects of phenol concentration on biodegradation parameters in TPPB.....64

Table 4.3 Effects of phenol concentration on biodegradation parameters in HFMB.....67

Table 4.4 Effects of membrane length on two-phase biodegradation of phenol in the HFMB.....72

Table 4.5 Performance comparison of TPPBs in biodegradation of phenol.....73

Table 4.6 Comparison of TPPB and HFMB based on the operating problems typically observed during two-phase biodegradation of phenol.....76

Table 4.7 Effects of phenol concentration on biodegradation parameters in simultaneous extraction and biodegradation of phenol in the HFMB.....78

Table 5.1 Physical properties, equilibrium parameters and membrane characteristics used for simultaneous extraction and biodegradation in HFMB.....97

Table 5.2 Mass transfer coefficients at the operating conditions in the HFMB.....98

Table 6.1 Summary of the experimental runs in the HFSLMB.....115

Table 6.2 Effects of initial phenol concentration on two-phase biodegradation in the HFSLMB.....122

Table 6.3 Effects of organic to aqueous phase ratio on two-phase biodegradation in the HFSLMB.....127
Table 6.4 Effects of interfacial surface area on two-phase biodegradation in the HFSLMB 132
Table 7.1 Experimental sorption capacities using four sets of EIHFMs for different phenol concentrations 151
Table 7.2 Kinetic rate constants (k), equilibrium adsorption capacities (Q_e) and regression coefficients (R^2) obtained using different models for removal of phenol using TOPO-containing EIHFM 152
Table 7.3 Langmuir and Freundlich isotherm parameters for the four different sets of EIHFM 154
Table 7.4 Adsorption capacities (Q_e) of EIHFMs after washing with DCM.....158
Table 8.1 Performance of conventional TPPBs in two-phase biodegradation of phenol 170
Table 8.2 Effects of substrate inhibition on two-phase biodegradation of phenol in EIHFMB 173
Table 8.3 Effect of aqueous flow rate on bioreactor parameters during biodegradation of 1000 mg/L phenol 178

LIST OF FIGURES

Figure 1.1 Schematic layout of the research program and the specific objectives 10

Figure 2.1 Schematic diagram of an aqueous/organic TPPB 13

Figure 3.1 Schematic diagram of the HFMB 50

Figure 3.2 Schematic diagram of the HFMB in simultaneous extraction and biodegradation 51

Figure 3.3 Schematic diagram of the HFSLMB 53

Figure 3.4 Schematic diagram of the EIHFMB 55

Figure 4.1 Effects of substrate inhibition on: (a) cell growth; (b) specific growth rate and biomass yield, during biodegradation of phenol in single-phase 60

Figure 4.2 Temporal concentration profiles of biomass and phenol during biodegradation of 1000 mg/L phenol in TPPB 63

Figure 4.3 Temporal concentration profiles of biomass, aqueous phenol, organic phenol and total phenol in biodegradation of 1000 mg/L phenol in HFMB 66

Figure 4.4 Effects of substrate concentration on: (a) phenol distribution between two-phases and (b) effect of mass transfer limitation on biodegradation, for initial phenol concentrations of 600, 1000, and 2000 mg/L 69

Figure 4.5 Temporal concentration profiles of biomass and phenol in HFMB with twin modules at initial substrate concentration of 2000 mg/L 70

Figure 4.6 Effects of the membrane length on (a) aqueous phenol concentration; and (b) phenol removal rate 71

Figure 4.7 Comparison of the TPPB and HFMB of 60 cm effective length: (a) substrate distribution between the aqueous and organic phases, and the distribution in TPPB after offsetting the lag phase; (b) total phenol removal profiles 75

Figure 4.8 Temporal concentration profiles of biomass, aqueous phenol, organic phenol, feed phenol and total phenol in the HFMB during simultaneous extraction and biodegradation of 1000 mg/L phenol 78
Figure 5.1 Schematic diagram of mass transfer process in extraction of phenol from feed solution to the organic solvent 88
Figure 5.2 Specific growth rate of *P. putida* (ATCC 11172) on phenol 94
Figure 5.3 Two-phase biodegradation of 1000 mg/L of phenol in the HFMB: (a) feed and organic phenol concentration profile; and, (b) biomass and aqueous phenol concentration profile 96
Figure 5.4 Experimental and modeled total phenol concentration profiles in the biodegradation of 1000 mg/L phenol in the HFMB 100
Figure 5.5 Parameter sensitivity: (a) effects of b on the cell growth; and, (b) effects of ψ_B on the organic phase phenol concentration 102
Figure 5.6 Comparison of the experimental data and model simulations at feed phenol concentration of 1500 mg/L: (a) feed and organic phenol concentration; and, (b) aqueous phenol and biomass concentrations 104
Figure 5.7 Comparison of the experimental data and model simulations at feed phenol concentration of 1500 mg/L: (a) feed and organic phenol concentration; and, (b) aqueous phenol and biomass concentrations 105
Figure 5.8 Effects of flow rate on HFMB performance: (a) lumen side flow rate of 12 mL/min; and (b) shell side flow rate of 8 mL/min 107
Figure 5.9 Model simulations to study: (a) effects of effect membrane length; and, (2) effects of fiber packing density 109
Figure 6.1 Temporal concentration profiles of biomass and phenol concentrations during two-phase biodegradation of 1000 mg/L phenol in the HFSLMB 118

Figure 6.2 Two-phase biodegradation of 1500 mg/L phenol in the HFLMB: (a) three different stages of phenol removal; (b) changes in the distribution of phenol between the organic and the two aqueous phases during biodegradation 120
Figure 6.3 Effects of initial phenol concentration on two-phase biodegradation in the HFLMB: (a) aqueous phase phenol concentration in the cell culture; (b) removal rates under diffusion limitation.....123
Figure 6.4 Temporal concentration profiles of biomass and phenol concentrations during two-phase biodegradation of 4000 mg/L phenol in the HFSLMB at organic to aqueous phase ratio of 1:6.67 126
Figure 6.5 Effects of lumen side flow rate on two-phase biodegradation of phenol in the HFSLMB: (a) total phenol concentration profiles; (b) removal rates under mass transfer limitation 128
Figure 6.6 Effects of shell side flow rate on two-phase biodegradation of phenol in the HFSLMB.....129
Figure 6.7 Effects of interfacial area on two-phase biodegradation of phenol in the HFSLMB: (a) phenol concentration in the organic phase; (b) phenol concentration in the cell culture; (c) removal rates under diffusion limitation.....131
Figure 6.8 Bioreactor sustainability studies for the HFSLMB: (a) feed phenol concentration profiles; (b) Total phenol concentration profiles, for the 20 consecutive runs 136
Figure 6.9. Bioreactor sustainability studies for the HFSLMB: (a) biodegradation time and; (b) biomass yields, for the 20 consecutive runs 137
Figure 7.1 Cross-sections (a and b) and external surface (c) of untreated polypropylene membrane and; cross-sections (d and e) and external surface (f) of the EIHFMs.....147
Figure 7.2 Effects of contact time on adsorption of 1000 mg/L phenol for the four sets of EIHFMs with varying TOPO concentration 149

Figure 7.3 Effects of contact time on adsorption using EIHFM containing 100 g/L TOPO at varying initial phenol concentrations.....150
Figure 7.4 Pseudo-second-order sorption kinetics of 1000 mg/L phenol using different sets of EIHFM with varying TOPO concentration.....153
Figure 7.5 Langmuir isotherms for EIHFMs containing varying TOPO concentration (markers represent experimental values and the dotted lines represent modeled values) 155
Figure 7.6 Effects of contact time on desorption of phenol using all four sets of EIHFMs with varying TOPO concentration after adsorption of phenol at 1000 mg/L 156
Figure 7.7 Sorption capacities of 50 and 200 g/L TOPO containing EIHFMs during consequent runs at initial phenol concentration of 1000 mg/L.....157
Figure 7.8 Cell growth and substrate removal profiles in the TPPB at initial phenol concentrations of: (a) 1000 mg/L and, (b) 2000 mg/L.....159
Figure 8.1 Temporal cell growth and phenol concentration profiles during biodegradation of 1000 mg/L in EIHFMB.....167
Figure 8.2 Temporal cell growth and phenol concentration profiles during biodegradation of 2000 mg/L in EIHFMB.....169
Figure 8.3 Two-phase biodegradation of 1500 mg/L phenol in the EIHFMB: (a) different stages of phenol removal; (b) different stages of cell growth.....171
Figure 8.4 Cell growth and phenol removal profiles during biodegradation of 3000 mg/L phenol at effective EIHFM length of 90 cm in the EIHFMB 176
Figure 8.5 Effects of aqueous flow rate on the removal of 1000 mg/L phenol in the EIHFMB 177
Figure 8.6 Comparison of cell growth and biodegradation profiles at initial phenol concentration of 1000 mg/L, carried out after an interval of 400 hours of operation in the

EIHFMB. Solid shapes represent original profiles whereas open shapes represent the profiles after 400 hours of repeated operation 180

LIST OF ABBREVIATIONS

Aq	Aqueous
BTX	Benzene, Toluene, Xylene
Conc	Concentration
DCM	Dichloromethane
EIHFM	Extractant impregnated hollow fiber membranes
EIHFMB	Extractant impregnated hollow fiber membrane bioreactor
EPS	Extra polymeric substances
EVA	Poly(ethylene-co-vinylacetate)
GAC	Granular activated carbon
GC	Gas chromatography
HFCLM	Hollow fiber contained liquid membrane
HFMB	Hollow fiber membrane bioreactor
HFRLM	Hollow fiber renewal liquid membrane
HFSLM	Hollow fiber supported liquid membrane
HFSLMB	Hollow fiber supported liquid membrane bioreactor
MSDS	Material safety data sheet
NAP	Non-aqueous phase
OD	Optical density
OMMT	Organic modified montmorillonite
Org	Organic
PAH	Poly aromatic hydrocarbons
PCP	Pentachlorophenol

PEHFSD	Pseudo-emulsion-based hollow fiber strip dispersion
PSF	Polysulfone
PTFE	Polytetrafluoroethylene
PVA	Polyvinyl alcohol
PVDF	Polyvinylidene fluoride
RPM	Revolutions per second
SEM	Scanning electron microscopy
SLM	Supported liquid membrane
TBP	Tributyl phosphate
TCE	Trichloroethylene
TOA	Trioctylamine
TOPO	Trioctyl phosphine oxide
TPPB	Two phase partitioning bioreactor
TSP	Tetrasodium pyrophosphate
VOC	Volatile organic contaminant
VVM	Volume of gas per reactor volume per minute

LIST OF SYMBOLS

A_{in}	Interfacial area on the lumen side
A_{lm}	Log mean area of the membrane
A_{out}	Interfacial area on the shell side
Au	Gold
b	Fraction of total biomass present as biofilms
C^{*}_{feed}	Hypothetical phenol concentration in aqueous phase that is in equilibrium with that in the organic phase in the HFMB
C^{*}_{org}	Hypothetical phenol concentration in organic phase that is in equilibrium with that in the aqueous phase in the HFMB
C_e	Equilibrium concentration of the solute in the solution
C_{feed}	Phenol concentration in feed wastewater
C^{i}_{feed}	Aqueous phenol concentration at the aqueous/organic interface
C^{i}_{org}	Organic phenol concentration at the aqueous/organic interface
C^{m}_{org}	Phenol concentration in solvent wetted membranes
C_{org}	Phenol concentration in organic solvent
D_{aq}	Diffusivity of phenol in water
d_h	Hydraulic diameter
d_{in}	Inside diameter of the membranes
d_{lm}	Log mean diameter of the membranes
d_{out}	Outside diameter of the membranes
D_{org}	Diffusivity of phenol in 2-undecanone
J	Flux of phenol from one phase to another
J_{feed}	Flux of phenol from aqueous feed to solvent phase

J_{org}	Flux of phenol from solvent to aqueous phase
k_1	Pseudo-first-order rate constant
k_2	Pseudo-second-order rate constant
K_{aq}	Overall mass transfer coefficient on the aqueous side
n,k_F	Freundlich isotherm constants
k_i	Intraparticle diffusion rate constant
K_I	Substrate inhibition constant
k_L	Langmuir adsorption constant
k_m	Mass transfer coefficient in the membranes
K_{org}	Overall mass transfer coefficient on the organic side
K_s	Substrate affinity constant
k_s	Mass transfer coefficient in the shell side boundary layer
k_t	Mass transfer coefficient in the lumen side boundary layer
L	Effective length of the membranes
M_B	Molecular weight of 2-undecanone
P	Partition coefficient
Q_{aq}	Aqueous flow rate
Q_e	Amount of phenol adsorbed at equilibrium
Q_{max}	Maximum adsorption capacity
Q_{org}	Organic flow rate
Q_t	Amount of phenol adsorbed at any time
R^2	Coefficient of regression
Re	Reynolds number
Sc	Schmidt number

Sh	Sherwood number
T	Temperature
t	Time
V_A	Molar volume of phenol as liquid at its boiling point
V_{aq}	Volume of the aqueous phase
v_{aq}	Aqueous flow rate
V_{org}	Volume of the organic phase
X	Biomass concentration
Y_{xs}	Yield coefficient
δ	Membrane thickness
ε	Porosity
η	Viscosity of 2-undecanone
η_{aq}	Viscosity of water
μ	Specific growth rate
μ_m	Maximum specific growth rate
ρ_{aq}	Density of water
τ	Tortuosity
φ	Packing density
ψ_B	Association parameter for 2-undecanone

1 Introduction

1.1 Background and Motivations

Research in biodegradation of toxic aromatic compounds has made significant strides in the past two decades. These developments have been propelled by the isolation of microbial strains capable of metabolizing, hitherto, non-biodegradable xenobiotics (Jain *et al.* 2005; Paul *et al.* 2005; Rieger *et al.* 2000); evolution of novel metabolic pathways by genetic and metabolic engineering of existing biodegrading microorganisms (Lovley 2003; Perez-Pantoja *et al.* 2008; Timmis and Pieper 1999); and proteomics analysis of cellular responses to biodegradation (Cao and Loh 2008; Loh and Cao 2008; Zhang *et al.* 2009). On the engineering front, several innovative bioreactor designs (Daugulis *et al.* 2011; Juang *et al.* 2008; Loh *et al.* 2000; Loh and Liu 2001; Saravanan *et al.* 2008; Singh *et al.* 2006; Tepe and Dursun 2008) with the potential to metabolize high inhibitory concentrations of toxic aromatics have been proposed. Most of these bioreactors, however, are based on cell immobilization and do not exhibit high biodegradation rates.

Recently, two-phase partitioning bioreactors (TPPB) have been investigated as an alternative to immobilized cell bioreactors in mitigating substrate inhibition. TPPBs are based on the equilibrium distribution of a toxic substrate between the cell culture medium and an immiscible non-aqueous phase (NAP), which can either be an organic solvent (Juang *et al.* 2010; Munoz *et al.* 2008) or a polymeric adsorbent (Khan and Daugulis 2011; Tomei *et al.* 2010). Due to the high affinity for the NAP, most of the substrate partitions into the NAP during equilibration, resulting in a sub-inhibitory substrate concentration in the aqueous phase, which is suitable for cell growth. Microbial metabolism of the substrate disrupts the equilibrium resulting in a

unidirectional transport of the substrate from the NAP to the cell culture, which eventually leads to the complete removal of the substrate from both the phases (Daugulis *et al.* 2011).

This unique bioreactor configuration with biocompatible NAPs enables suspended cells to withstand and metabolize high inhibitory concentrations of toxic aromatic compounds at unprecedented high biodegradation rates. In one of the earliest reported studies on TPPB, phenol concentrations up to 28 g/L were biodegraded by *Pseudomonas putida* without experiencing severe substrate inhibition, using 2-undecanone as the organic phase. The volumetric biodegradation rates reported were 135 mg/L-hr during batch operation and 175 mg/L-hr during fed-batch operation (Collins and Daugulis 1997).

Most of the studies on two-phase biodegradation systems have been carried out using organic solvents as the partitioning phase. These aqueous/organic TPPBs have been very effective against the aromatic compounds and would have constituted an ideal system; but a plethora of operating problems resulting from phase dispersion limits their applicability. The primary challenge in these bioreactors is the presence of emulsions which inflicts high downstream separation cost (Amsden *et al.* 2003). Stable emulsions may also result in incomplete phase separation and consequent release of the organic solvent into the environment as a secondary waste. The emulsified cell growth medium is also prone to foaming when aerated, resulting in the loss of the solvent into the environment (Quijano *et al.* 2009). Furthermore, the presence of organic solvent laden with the toxic substrate in the cell culture medium is harmful for the microorganisms and this often gives rise to long lag phases. It has also been observed that some of the biosurfactants produced by the cells actually enhanced emulsion stability (Cruickshank *et al.* 2000), further aggravating the massive task of

phase separation. The reliance of the TPPBs on high agitation rates for improved performance is another limitation of these bioreactors which can be quite energy intensive, especially when the solvent has a high viscosity. Agitation rates as high as 600 RPM have been reported during pyrene biodegradation using silicone oil as the organic phase (Mahanty *et al.* 2008), which may be difficult to realize in a large-scale bioreactor.

Some of the problems encountered using organic solvents in TPPBs have been overcome by substituting the NAPs with polymeric adsorbents. These polymers provide a cheaper, bio-friendlier and eco-friendlier alternative to conventional solvents and are finding increasing application in two-phase biodegradation of aromatic compounds (Prpich and Daugulis 2006). The solid NAPs modify the underlying mechanism in TPPB from extraction/stripping to adsorption/desorption which completely eliminates the problems of phase dispersion, while sequestering the bulk of the substrate in the solid phase. The disadvantage of using solid NAP is the lower diffusivity of the molecules in solids, which can result in low mass transfer rates, eventually resulting in poor biodegradation rates (Zhao *et al.* 2009). Moreover, these polymeric adsorbents have often been observed to exhibit low adsorption capacities and if the regeneration is not effective, the long-term operation of the solid/liquid TPPBs can be jeopardized. In addition, these TPPBs, in the current configuration, are difficult to operate in a continuous mode due to the adsorbent regeneration problems. For the same reason, these bioreactors cannot offer sustainable simultaneous adsorption and biodegradation, as well.

Although phase dispersion-associated problems during two-phase processes such as liquid/liquid extraction are often alleviated using membrane-based technologies (Bocquet *et al.* 2006; González-Muñoz *et al.* 2003), these have seldom been explored

in the context of a TPPB, certainly not in the alleviation of substrate inhibition in biodegradation. In the membrane-based extraction/stripping approach, the aqueous and the organic phases are physically separated using hollow fiber membranes. If the membranes are hydrophobic, a higher pressure is applied on the aqueous side to immobilize the aqueous/organic interface into the membrane pores and prevent the solvent from leaking into the aqueous solution. While this configuration results in a non-dispersive operation, the hollow fiber membrane contactor also offers the advantage of compact design, independent phase flow rates, high specific interfacial area and flexible configuration (Shen *et al.* 2009). The drawback of this technology is the additional resistance to mass transfer due to the presence of the membrane between the two phases, although this can easily be negated through an increase in the number of membrane fibers.

A membrane contactor based hollow fiber membrane bioreactor (HFMB) can thus be a viable alternative to direct-contact biphasic biodegradation and wastewater treatment systems. The dispersive-free mass transfer between the phases in the HFMB can prevent foaming and emulsification, while the solvent can be easily recycled and reused. Furthermore, the cell growth environment in the aqueous phase will be devoid of organic solvent and resemble that in the single-phase biodegradation systems. The HFMB will also ease some of the stringent requirement regarding solvent selection such as density and biocompatibility (Quijano *et al.* 2009). The modular design of the HFMB can also provide easier scale-up opportunities and operational flexibility, which can be harnessed to achieve simultaneous extraction and biodegradation.

Another possibility is the application of hollow fiber supported liquid membranes (HFSLM) in two-phase biodegradation systems. The HFSLMs are prepared by creating a thin layer of an organic solvent onto hydrophobic hollow fiber membranes

(San Roman *et al.* 2010). In this configuration, the feed and the receiving solutions flow on either side of the membranes to attain concomitant extraction and stripping, while the solvent wetted hollow fiber membranes serve as the organic phase. The HFSLMs have the advantages of compact design, high specific interfacial area, low cost, low solvent and low energy requirements (Sengupta *et al.* 1988). Moreover, the HFSLM facilitated separation exhibits low mass transfer resistance which results in high diffusion rates between the two phases. The drawback of this technology is its instability during long-term operation, arising from the gradual evaporation or dissolution of the liquid membrane from the fibers into either of the aqueous phases (Kocherginsky *et al.* 2007). However, the instability concerns can be alleviated by resorting to a semi-dispersive approach, wherein a small amount of the organic phase is dispersed into the feed solution to create uniform solvent droplets. When the shear forces strip solvent from the hollow fibers, the solvent droplets in the feed solution readily attach to the hydrophobic membranes, resulting in a dynamic exchange that regenerates the liquid membrane (Ren *et al.* 2009; Ren *et al.* 2007) and imparts long-term stability to the HFSLM.

By substituting stripping with biodegradation, the HFSLM technology can be applied in two-phase biodegradation. In such a semi-dispersive hollow fiber supported liquid membrane bioreactor (HFSLMB), the mass transfer of substrate from feed solution to the organic solvent will be dispersive, whereas the movement of substrate from the solvent to the cell culture will be non-dispersive. Consequently, the cell growth environment will remain solvent-free and many of the dispersion associated problems, for example foaming, will be alleviated. It is anticipated that the low mass transfer resistance of the HFSLM will result in better substrate availability in the culture medium, yielding higher cell growth and biodegradation rates during concomitant

extraction and biodegradation of aromatics in wastewater. Although phase dispersion in the feed tank may result in emulsion formation, the medium can easily be de-emulsified in the absence of any emulsion-promoting biosurfactants through gravity settling.

The hollow fiber membranes find extensive use in solvent extraction but their application in membrane-based adsorption/desorption systems is rather scarce, even though these membranes have the potential to be good adsorbents due to a flexible geometry and high specific interfacial area. In fact, adsorption of phenol has been observed on polysulfone (PSF) (Li and Loh 2005) and polypropylene (Chung *et al.* 2004) hollow fiber membranes during membrane bioreactor operations. Although the adsorption capacities of these fibers were low, it has been suggested that the impregnation of conventional adsorbents such as granular activated carbon (GAC) in hollow fiber membranes can improve their sorption performance (Li and Loh 2006). Recently, several studies have been reported on the encapsulation of organic extractants in polymeric capsules (Gong *et al.* 2006; Whelehan *et al.* 2010; Yin *et al.* 2010). These liquid-core microcapsules are easier to synthesize and offer the advantages of both solvent extraction and adsorption. These microcapsules have mainly been used in the adsorption of organics and metals from wastewater but recently, these have been used as NAPs in TPPBs (Sarma *et al.* 2011; Wyss *et al.* 2006). Unfortunately, these adsorbents exhibit low sorption capacity and the long-term stability of organic solvent in hydrophobic encapsulation is a major concern (Zhao *et al.* 2010). In addition, the preparation of these adsorbents requires complex polymerization and a significant amount of extractant is lost during the encapsulation process.

So far, while designing membrane-based adsorbents or even liquid membranes, the focus had been on the use of liquid extractants with low volatility. The use of solid extractants has also been reported in some cases (Outokesh *et al.* 2011; Teresa *et al.* 2007), but these require dissolving them into another non-volatile carrier solvent. On the contrary, we envisage the use of volatile carrier solvent with solid extractants to develop high performance hollow fiber membrane-based adsorbents. The strategy is to prepare HFSLM with a solid extractant such as trioctylphosphine oxide (TOPO) by dissolving it in a highly volatile carrier solvent such as dichloromethane, and subsequently allow the carrier solvent to evaporate. TOPO, being a crystalline solid (Cichy and Szymanowski 2002), could be trapped inside the membrane pores if the pores size is smaller than the size of the TOPO crystals. The resulting extractant-impregnated hollow fiber membranes (EIHFMs) will retain all the advantages of hollow fiber membranes, along with an enhanced adsorption capacity for organic aromatics phenol due to the presence of the impregnated TOPO.

The use of EIHFMs as the partitioning phase in a TPPB can offer several benefits. The most important advantage is the simple design of these adsorbents which does not require any polymerization and needs only very small quantity of the carrier solvent. The EIHFMs are expected to be easy to regenerate, have high adsorption rates, high adsorption capacity and long-term stability, which are all important requisites to achieve sustained high performance during biodegradation in the resulting extractant-impregnated hollow fiber membrane bioreactor (EIHFMB). In addition, the modular bioreactor can be operated for simultaneous adsorption and biodegradation, which is impossible to attain in conventional solid/liquid two-phase biodegradation systems.

Phenol was chosen as the model pollutant in this research as phenol and its derivatives are commonly found contaminants in industrial wastewater. These chemicals are of

high commercial importance as these are used as precursors to manufacture a wide variety of useful products. As a result, these are present in the resulting effluents. These aromatics are also released from the petrochemical industries and coal conversion processes where their concentration can be up to 7 g/L, while the discharge limit is less than 1 mg/L (González-Muñoz *et al.* 2003).

Phenol is a highly toxic chemical. Even at a low concentration of 5-25 mg/L, phenol is lethal for fish, while a high concentration of phenol in natural water bodies can be detrimental for the aquatic life (Loh *et al.* 2000). Phenol can also cause several health-related problems for humans. It is rapidly absorbed in the body through inhalation, ingestion and upon skin contact, affects several organs adversely and can even cause death at high concentrations (Busca *et al.* 2008). Phenol is also recalcitrant and persists in water, thereby endangering aquatic life. Under favorable conditions, phenol is capable of undergoing various substitution reactions which can generate even more harmful compounds such as chlorophenols, with mutagenic or carcinogenic properties (Michałowicz and Duda 2007). In Singapore, the National Environment Agency mandates a discharge limit for phenolic compounds of less than 0.2 mg/L. The removal of phenol and its derivatives from the industrial wastewater is, therefore, crucial for environmental protection.

1.2 Research Objectives and Scope

The overall objective of this thesis was to apply hollow fiber membrane-based technology to design novel membrane bioreactors to alleviate the problems in conventional liquid/liquid or solid/liquid two-phase partitioning bioreactors, using phenol as the model pollutant.

The specific research objectives included:

1. Design an HFMB for dispersion-free two-phase biodegradation of phenol and compare the biodegradation performance with that of conventional TPPB;
2. Study the kinetics of simultaneous extraction and biodegradation of phenol in the HFMB;
3. Enhance the two-phase biodegradation of phenol in a semi-dispersive hollow fiber supported liquid membrane bioreactor;
4. Develop extractant impregnated hollow fiber membranes as novel adsorbents for phenol removal from wastewater and study the adsorption kinetics and isotherms; and
5. Perform solid/liquid two-phase biodegradation of phenol in the extractant impregnated hollow fiber membrane bioreactor.

A schematic layout of the research program and the specific objectives has been presented in Fig. 1.1.

This research demonstrates the suitability of hollow fiber membranes in alleviating the problems associated with TPPBs. While the hollow fiber membranes act as the semi-permeable physical barrier to facilitate non-dispersive mass transfer of phenol from the organic phase in HFMB and HFSLMB, these membranes serve as the support of the organic phase in the EIHFMB. The hollow fiber membranes are finding increasing application in bioprocesses now-a-days, but this research is the first ever application of the HFSLM technology in bioprocesses, to the best of our knowledge. In addition, the EIHFM is a new technology which was developed during the course of this research.

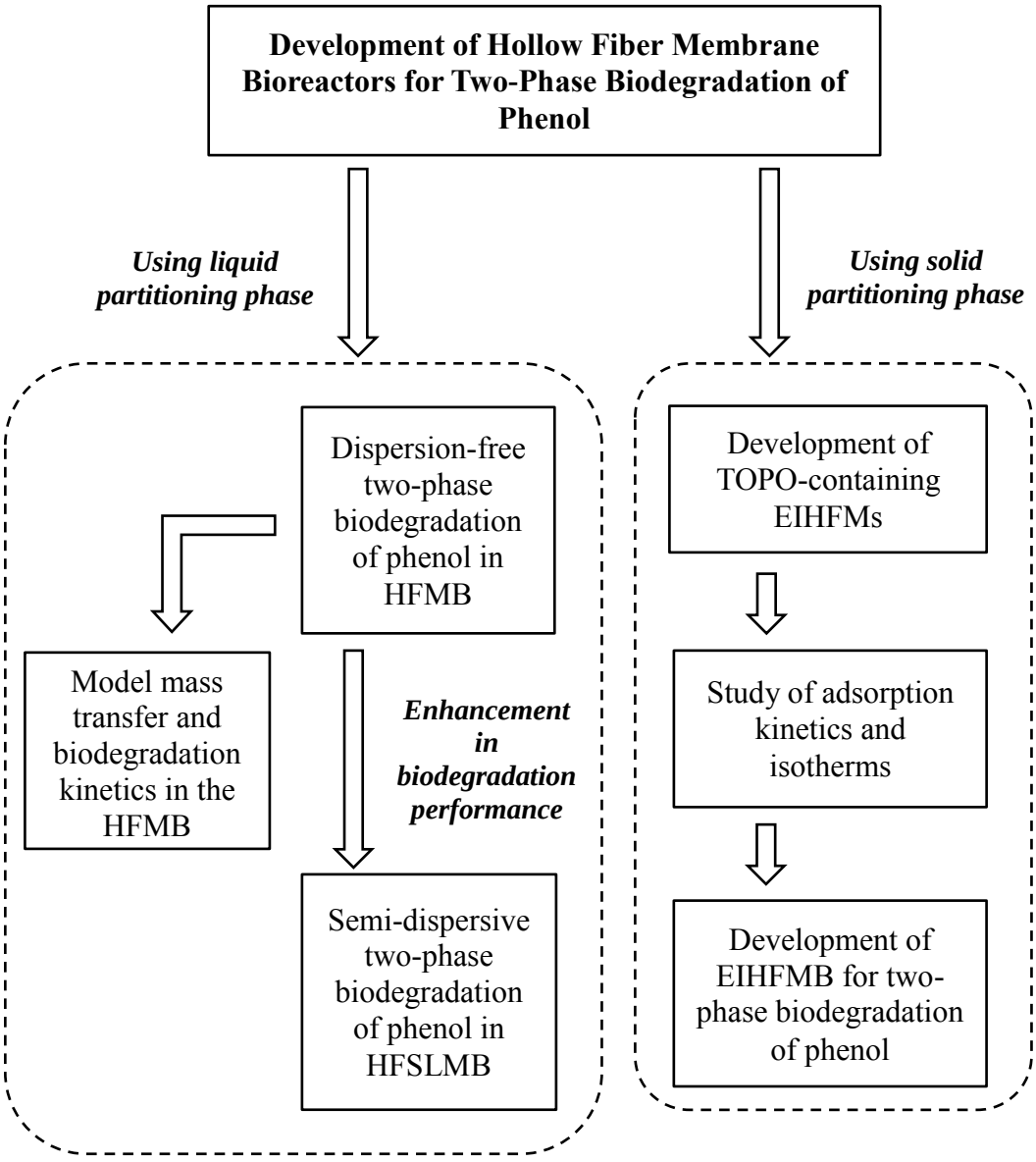

Figure 1.1 Schematic layout of the research program and the specific objectives

1.3 Thesis Organization

This thesis comprises of nine chapters. Chapter 1 outlines the research background, motivations and objectives. A detailed review of the relevant literature on TPPB, solvent extraction and membrane bioreactors in biodegradation is presented in Chapter 2. Chapter 3 describes the materials and methods used in designing and executing the experiments performed in this research. Chapter 4 presents the baseline studies on single-phase and conventional two-phase biodegradation systems and, results on two-phase biodegradation of phenol in the HFMB, along with the performance comparison of the three systems. The two-phase biodegradation kinetics of phenol in the HFMB is modeled in Chapter 5. Chapter 6 describes the two-phase biodegradation of phenol in the HFSLMB, along with the effects of bioreactor operating parameters and the study on the long-term stability of the bioreactor. The development of EIHFM is described in Chapter 7, which also contains the results on the adsorption kinetics and isotherms during removal of phenol from aqueous solutions using EIHFM. In Chapter 8, the EIHFMs are used to develop EIHFMB for solventless two-phase biodegradation of phenol. Finally, all the research findings are summarized in Chapter 9, along with some suggestions and recommendations for future work.

2 Literature Review

This section reviews the recent relevant literature pertaining to the TPPBs, the membrane-based solvent extraction and the application of hollow fiber membrane bioreactors in biodegradation.

2.1 Two-Phase Partitioning Bioreactors

During biodegradation in a TPPB, the aqueous phase is the cell culture medium, while the NAP is either an organic solvent in which the substrate has a high solubility, or a polymeric adsorbent having high sorption capacity for the substrate. Due to the high affinity for the NAP, most of the substrate gets sequestered into the NAP upon equilibration, resulting in a sub-inhibitory substrate concentration in the aqueous phase. The equilibrium is disrupted when the microorganisms metabolize the substrate, which triggers the diffusion of the substrate from the NAP to the cell culture (Quijano *et al.* 2009). But the increasing microbial population in the aqueous phase with gradual metabolism of the substrate ensures that the disequilibrium prevails in the bioreactor which is critical to ensure the unidirectional transport of the substrate from the NAP to the aqueous phase, and the complete removal of the substrate from both the phases. The TPPBs resemble extraction/stripping systems with two important differences: (1) the substrate removal in TPPBs is carried out by biodegrading microorganisms; and, (2) TPPB operation is aimed at destroying the xenobiotics and not recovering them, as is the case with solvent extraction.

2.1.1 Design Considerations

Two-phase biodegradation is typically carried out in stirred-tank bioreactors, often in commercial fermenters. Fig. 2.1 shows the schematic diagram of an aqueous/organic TPPB. In this configuration, the substrate laden organic solvent is added to the cell

culture medium and the two phases are dispersed in the fermenter at high agitation speed. The purpose of agitation is also to facilitate the aeration of the aqueous phase. The key steps in designing TPPBs are – selection of appropriate NAP, adequate mixing to prevent nutrient limitation and efficient aeration to prevent oxygen limitation (Quijano *et al.* 2009).

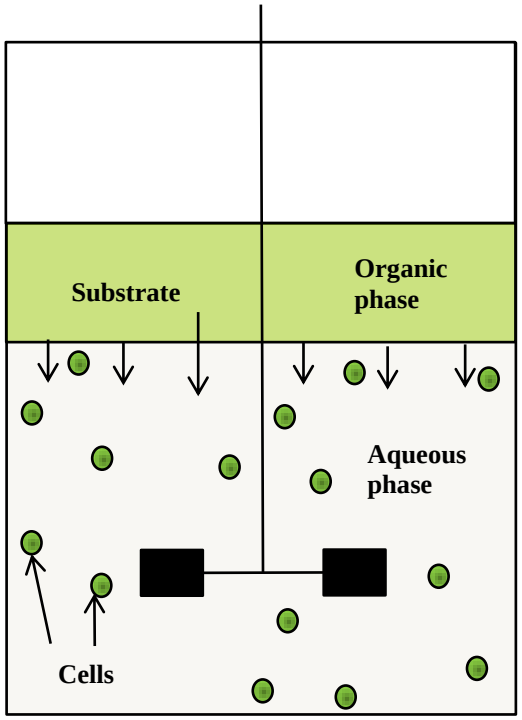

Figure 2.1 Schematic diagram of an aqueous/organic TPPB

The selection of an appropriate solvent is critical for the stability and efficacy of two-phase biodegradation and the guidelines for NAP selection is listed in Table 1.1. This process is influenced by several factors, including the physical properties of the substrate and the NAP, initial substrate concentration, and the growth characteristics of the microorganisms. The most important NAP selection criteria are the biocompatibility and non-bioavailability of the NAPs. While toxic NAPs can retard cell growth, biodegradable solvents could result in alternative carbon source to the bacteria which could result in incomplete biodegradation (Chikh *et al.* 2011).

The biocompatibility of organic solvents is related to their octanol/water partition coefficient (Malinowski 2001). It has been reported that organic solvents with octanol/water (O/W) partition coefficients below a critical level are toxic for

Table 2.1 NAP selection criteria in TPPBs

Characteristics	Reference
High distribution coefficient High selectivity for the substrate Insoluble in water Chemical and thermal stability Low emulsion forming tendency Non-biodegradable, biocompatible Non-hazardous, inflammable Inexpensive	(Bruce and Daugulis 1991)
Low vapor pressure Low viscosity High mass transport characteristics	(Munoz *et al.* 2008)

microorganisms. This critical value depends on the nature of the microorganism and it may differ from one bacterial strain to another. For example, Collins and Daugulis (1997) estimated the critical log of O/W partition coefficient for *Pseudomonas putida* ATCC 11172 as 3.2. The biocompatibility issue usually does not arise with solid NAPs, as these polymeric adsorbents are typically non-toxic (Amsden *et al.* 2003). The affinity of the substrate to the NAP is also crucial in NAP selection. The use of NAPs with high distribution coefficient is usually preferred as they result in high

mass transfer flux (Bruce and Daugulis 1991), and greatly reduce the amount of NAPs required to alleviate substrate inhibition. A flammable or hazardous NAP is not preferred due to safety reasons, while the NAP should have low vapor pressure to minimize any loss due to evaporation. The liquid NAPs should also have low emulsion formation tendency to simplify the downstream phase separation. Apart from these, there may be additional selection criteria depending upon the specific process. For example, Munoz and co-workers (2008) suggested that the NAP should be evaluated for substrate diffusivity, long-term biodegradability, interactions with the microorganisms, and the ability to support direct substrate uptake during biodegradation of volatile organic contaminants (VOC).

In TPPBs, mixing between the two phases is the driver for interphasic mass transfer of the substrate. Typically, phase dispersion in TPPBs are carried out at high agitation speeds but the efficiency of mixing depends on several factors: the agitation speed, the phase ratio and the physical properties of the two phases. In several studies involving biodegradation of monoaromatic compounds using liquid NAP, the impeller speed was below 300 RPM (Collins and Daugulis 1997; Collins and Daugulis 1999; Zilouei *et al.* 2008) but higher agitation rates were reported in the biodegradation of polyaromatics hydrocarbon (PAH). High speed agitation was also required when the NAP was highly viscous or had poor mass transfer characteristics (Gardin *et al.* 1999). For example, during biodegradation of pyrene by *Mycobacterium frederiksbergense* using silicone oil, the optimal agitation rate reported by Mahanty and co-workers (2008) was 600 RPM. Likewise, the agitation rate reported by Rehmann and co-workers (2008) in the biodegradation of PAH using desmopan pellets was 600 RPM. The agitation rates are also affected by phase ratio. Typically, higher phase ratio results in higher energy requirement. The study by Hamid and co-

workers (2004) suggested that the biodegradation performance in TPPB improved at lower phase ratio if the agitation rates were same. They reported the optimal phase ratio of 0.0625, at which the biodegradation time was shorter as compared to that at phase ratios of 0.25 and 0.125. Likewise, pentachlorophenol (PCP) removal rate was significantly higher at the phase ratio of 16%, as compared to that at 37% (Zilouei *et al.* 2008).

The biodegradation rates in TPPBs improves at higher agitation rates as demonstrated by Hamed and his co-workers (2004) in the biodegradation of monoaromatics by *P. putida* F1. At 150 RPM, phenol, toluene and benzene were biodegraded within 13, 12 and 32 hours, respectively, whereas the treatment time was shortened to 10, 11 and 28 hours, respectively, at 200 RPM. Similar trends were observed in the biodegradation of PCP using dioctyl sebacate as the partitioning phase (Zilouei *et al.* 2008). While the performance improvement had mainly resulted from improved mass transfer of the substrate, the increase in the agitation speed can also improve the oxygen distribution in the bioreactor. Collins and Daugulis (1997) observed oxygen limitation in phenol biodegradation using 2-undecanone as the partitioning phase. Since increasing the aeration rate resulted in severe foaming and overflowing, the efficiency of aeration was improved by increasing the agitation rate from 200 to 250 RPM.

Since the TPPBs operate at high substrate loading, a high aeration rate is required to prevent oxygen limitation. However, increasing the aeration rate in aqueous/organic TPPBs can result in foaming and overflowing (Cruickshank *et al.* 2000), which may result in the loss of the solvent and the biomass from the bioreactor. One approach to overcome this challenge is the gradual increase in the aeration rate. For example, Collins and Daugulis (1997) operated the bioreactor at 0.25 gas volume per reactor volume per minute (VVM) during phenol biodegradation at low biomass

concentrations. The aeration rate was increased to 0.5 VVM when oxygen was exhausted. But the aeration rate was again adjusted to 0.3 VVM to control excessive foaming in the bioreactor. Another approach to alleviate oxygen limitation in TPPBs is to enhance the saturation concentration of oxygen in the NAP or to select an NAP with high affinity for oxygen so that the NAP can act as a reservoir for oxygen. This could result in the transport of oxygen from the NAP to the aqueous phase under a concentration gradient, analogous to the substrate (Nielsen *et al.* 2003). The effectiveness of aeration can also be enhanced by sparging pure oxygen in the bioreactor as demonstrated by Cruickshank and co-workers (2000a) in the biodegradation of phenol.

2.1.2 Liquid/Liquid TPPB

The liquid/liquid TPPBs have been extensively exploited since the early eighties in the recovery of low-molecular weight volatile products and organic acids from fermentation broth. These studies, however, were focused on product partitioning in order to prevent product inhibition and to reduce the downstream separation costs (Malinowski 2001). The first application of this technology in the context of substrate inhibition was in the biodegradation of phenol using 2-undecanone as the NAP (Collins and Daugulis 1996; Collins and Daugulis 1997). Since then, TPPBs have been used in the biodegradation of several monoaromatics such as phenols (Collins and Daugulis 1997; Guieysse *et al.* 2004; Tomei *et al.* 2008) and benzene (Collins and Daugulis 1999; Hamed *et al.* 2004), polyaromatics such as pyrene and phenanthrene (Guieysse *et al.* 2001; Mahanty *et al.* 2008; Vandermeer and Daugulis 2007) and VOCs (Hernandez *et al.* 2012; Nielsen *et al.* 2007). Table 2.2 summarizes the application of aqueous/organic TPPBs in biodegradation.

Cell growth in TPPBs is always preceded by a lag phase which can vary from few hours (Hamed *et al.* 2004; Juang *et al.* 2010) to even one day (Guieysse *et al.* 2001; Zilouei *et al.* 2008). The lag phase can be a characteristic of the microbial growth or a result of the presence of hydrophobic solvent in cell growth medium. The lag phase duration tends to increase with the increase in substrate concentration and this trend has been attributed to the higher system loading of the substrate (Collins and Daugulis 1997). In this phenomenon which is described as phase toxicity, microorganisms can experience toxicity from the pollutant present in the NAP in the TPPB (Deziel *et al.* 1999).

Table 2.2 Summary of research on liquid/liquid TPPB

Pollutant	NAP	Micro-organism	Agitation Speed (RPM)	Reference
Phenol	2-undecanone	*P. putida*	200-250	(Collins and Daugulis 1997)
BTX	Adol 85 NF	*Pseudomonas* sp.	250	(Collins and Daugulis 1999)
Xylene	Silicon oil	Isolated	500	(Gardin *et al.* 1999)
Phenanthrene, pyrene	Slicon oil	Isolated	200	(Guieysse *et al.* 2001)
Benzene	Hexadecane	*A. xylosoxidans*	200-500	(Yeom and Daugulis 2001)
Phenanthrene, naphthalene	Dodecane	*Sphingomonas aromaticivorans*	300	(Daugulis and Janikowski 2002)
Phenol	Adol 85 NF	*P. putida*	400	(Vrionis *et al.* 2002)
Phenol	1-decanol	*P. putida*	-	(Vrionis *et al.* 2002)

Phenol	2-undecanone	*Pseudomonas* strain	-	(Guieysse *et al.* 2004)
Benzene, toluene, phenol	2-undecanone	*P. putida*	150-200	(Hamed *et al.* 2004)
Phenanthrene, pyrene	Silicon oil	*Pseudomonas* sp.	150	(Guieysse and Viklund 2005)
Hexane	Silicon oil	*Fusarium Solani*	150	(Arriaga *et al.* 2006)
Benzene	n-hexadecane	*Achromobacter xylosoxidans*	800	(Nielsen *et al.* 2007)
PAHs	Dodecane	*S. aromaticivorans*	350	(Vandermeer and Daugulis 2007)
Pyrene	Silicone oil	*M. frederiksbergense*	600	(Mahanty *et al.* 2008)
α-pinene	FC 40, silicone oil, HMN, HMS	*P. fluorescens*	300	(Munoz *et al.* 2008)
4-nitrophenol	2-undecanone	Sludge	-	(Tomei *et al.* 2008)
PCP	Dioctyl sebacate	*Sphingobium chlorophenolicum*	100-200	(Zilouei *et al.* 2008)
Phenol	Kerosene	*P. putida*	100-300	(Juang *et al.* 2010)
4-nitrophenol	2-undecanone	Mixed culture	-	(Tomei *et al.* 2010)
Toluene	Hexadecane	Sludge	300	(Chikh *et al.* 2011)
Hexane	Silicon oil	Mixed culture	200-500	(Hernandez *et al.* 2012)

During biodegradation of toxic aromatics in TPPBs, the bioreactor performance could be improved dramatically by resorting to a sequential feeding strategy as demonstrated by Collin and Daugulis ((1999) in the biodegradation BTX. In this approach, only toluene was added into the TPPB at first, and the addition of the other two substrates was delayed until most of the toluene had been metabolized. This strategy resulted in an improved biodegradation rates due to the alleviation of substrate inhibition. In another study, 28 g of phenol was biodegraded within 165 hours in fed-batch mode at a volumetric removal rate of 175 mg/L-hr, while the maximum removal rate in the batch mode was only 135 mg/L-hr (Collins and Daugulis 1997). It has also been reported that microorganisms in fed-batch mode gradually acquire enhanced tolerance to high concentration of the substrate and the growth is sustained even if the substrate concentration exceeds the inhibitory limit during sequential substrate spiking into the bioreactor (Vrionis *et al.* 2002).

TPPBs have several advantages in the biodegradation of poorly soluble pollutants such as PAHs. These include improved bioavailability of the PAHs due to a high mass transfer rate between the two phases, and improved biodegradation due to the direct uptake of the substrate from the organic phase by the bacteria presence at the aqueous/organic interface (Guieysse *et al.* 2001). Recently, Vandermeer and Daugulis (2007) demonstrated biodegradation of a mixture of low and high molecular weight PAHs by a microbial consortium using dodecane as the NAP. PAH degradation rates of 1200-1500 mg/L-day were reported which are among the highest reported till date. In biodegradation of pyrene using silicone oil, Mahanty and co-workers (2008) reported a maximum specific growth rate of 0.154 hr^{-1} at 400 g/L pyrene, whereas the corresponding degradation rate was 139 mg/L-day. PAH biodegradation has also been conducted in a pilot scale TPPB at 150 L volume, where the biodegradation rates

were quite high at 238 mg/L-hr (Daugulis and Janikowski 2002). Further performance enhancement in TPPBs has been attained by improving the oxygen supply to the microorganisms by improving the solubility of oxygen in the organic phase (Nielsen *et al.* 2003). Recently, Hernandez and co-workers (2012) assessed the effects of microbial characteristics on TPPB performance in VOC degradation, and they concluded that hydrophobic microorganisms gave better performance in the hydrophobic growth environment in TPPBs.

Overall, the aqueous/organic TPPB is an excellent technology in preventing substrate inhibition in biodegradation systems and improving bioavailability of poorly soluble pollutants. However, phase dispersion and emulsion formation are serious issues which must be addressed before this technology can be considered for industrial application. Other challenges that need to be considered are the availability of cheap, biocompatible, non-biodegradable and non-volatile solvents, along with the suitable means to recycle and reuse them. While exploring an alternative to these challenges in the past few years, the research on TPPBs has shifted from the use of liquid NAPs to the solid NAPs. The recent developments in this new bioreactor configuration have been described in the next section.

2.1.3 Solid/liquid TPPB

The use of polymeric adsorbents in TPPBs provides a biocompatible, non-biodegradable, non-volatile, easily-recyclable and low-cost alternative to the organic solvents. The use of solid NAPs in TPPB was first demonstrated by Amsden and his co-workers (2003) in the biodegradation of phenol using poly(ethylene-co-vinylacetate) (EVA) as the partitioning phase. The EVA beads exhibited a sorption capacity of 14 mg phenol/mg EVA, and 2000 mg/L phenol was biodegraded within

60 hours using 104 g/L of the solid phase. In another study, more than 1 g/L benzene could be metabolized within 40 hours by *Alcaligenes xylosoxidans* using EVA beads (Daugulis *et al.* 2003). These were followed by several other studies on two-phase biodegradation of several mono- and polyaromatic compounds. A summary of the research on solid/liquid TPPBs is presented in Table 2.3.

Table 2.3 Summary of research on solid/liquid TPPB

Pollutant	NAP	Micro-organism	Agitation Speed (RPM)	Reference
Phenol	EVA	*P. putida*	400	(Amsden *et al.* 2003)
Benzene	EVA	*A. xylosoxidans*	450	(Daugulis *et al.* 2003)
Phenol	EVA	Microbial Consortium	400	(Prpich and Daugulis 2005)
Atrazine	Liquid-core capsule	*Pseudomonas sp.*	200	(Wyss *et al.* 2006)
Phenols	HYTREL	Microbial Consortium	180	(Prpich and Daugulis 2006)
BTEX	Silicone rubber	Bacterial consortium	800	(Littlejohns and Daugulis 2008)
PCBs	HYTREL	Pseudomonas strain	500	(Rehmann and Daugulis 2008)
PAH	Desmopan	Microbial Consortium	600	(Rehmann *et al.* 2008)
Phenol	OMMT-PSF	Mixed culture	180	(Zhao *et al.* 2009)
Phenanthrene	Desmopan 9370A	Microbial Consortium	600	(Isaza and Daugulis 2010)
4-nitrophenol	Hytrel	Mixed culture	-	(Tomei *et al.* 2010)
4-nitrophenol	Hytrel	Mixed culture	-	(Tomei *et al.* 2010)

PAH	Alginate/PVA	*M. frederiksbergense*	180	(Sarma *et al.* 2011)
Substituted phenols	Hytrel	Mixed culture	-	(Tomei *et al.* 2011)

Unlike organic solvents, the solid NAPs are usually non-toxic and do not affect cell growth adversely. This has facilitated the use of mixed cultures in these TPPBs, which exhibit enhanced tolerance to toxic substrates, resulting in better growth and biodegradation rates (Prpich and Daugulis 2005). The flexibility in preparing the microbial cocktail has been harnessed to use microbes with high metabolic diversity, which could simplify the metabolism of a mixture of different pollutants via different metabolic pathways. This was demonstrated by Prpich and Daugulis (2006) in the concomitant biodegradation of phenol, o-cresol and 4-chlorophenol using a microbial consortium consisting of *Pseudomonas*, *Klebsiella*, *Citrobacter*, *Salmonella* and *Enterobacter* species. TPPBs operating with Hytrel beads have also been used in conjugation with sequencing batch bioreactors in the biodegradation of phenolic compounds using activated sludge (Tomei *et al.* 2010; Tomei *et al.* 2011).

The use of polymeric adsorbents is also very attractive in the removal of pollutants from contamination sites. In this approach, pollutants are first adsorbed on the solid phases and subsequently biodegraded in a TPPB, resulting in the removal of the pollutant and the regeneration of the solid phase, as demonstrated by Rehmann and co-authors (2008) in the bioremediation of PAHs and PCBs. More than 80% of the PAH mixture at a concentration of 900 mg/Kg could be recovered from the soil within 48 hours using Hytrel, and approximately 78%, 62% and 36% of phenanthrene, pyrene and fluoranthene, respectively, were biodegraded within 14 days.

The solid/liquid TPPB technology is relatively new and so far very few polymeric adsorbents with high adsorption rates and capacity have been exploited. In fact, most of the research on these bioreactors has been carried out using Hytrel beads, which exhibits excellent affinity for phenolic compounds (Prpich and Daugulis 2006). In the recent years however, several new adsorbents such as desmopan, polyethylene and nylon have been investigated for their application in the biodegradation of PAH (Rehmann *et al.* 2007), whereas the use of automobile tyres has been proposed in the removal of hydrocarbons from wastewater (Prpich *et al.* 2008). The use of automobile tyres, in particular, is very attractive, as these are cheap and easily available source. In addition, their use in TPPB will also result in a more effective management of solid waste from auto industry. Furthermore, there are numerous adsorbents available in the literature with high adsorption capacities for different pollutants. As the research is solid/liquid TPPB progresses further and the conventional adsorbents are tested for their applicability in TPPBs, it will lead to a surge in the availability of these NAPs.

An alternative to the conventional adsorbents in TPPBs is the use of solvent encapsulated microcapsules. These are prepared by encapsulating organic solvents/extractants into a polymeric matrix. These novel adsorbents facilitate dispersion-free extraction of solutes into the encapsulated solvent, whereas the high partition coefficient of the solvent results in high removal rate and high adsorption capacity (Gong *et al.* 2006; Wyss *et al.* 2006; Yang *et al.* 2007; Zhao *et al.* 2010). The microcapsules have been commonly used in the adsorption of pollutants from wastewater, but recently their use has also been reported in two-phase biodegradation. For example, Wyss and co-workers (2005) impregnated dibutyl sebacate in cross-linked alginate/polyacrylamide membrane for two-phase biodegradation of pesticides. In another study, Sarma and co-authors (2010) encapsulated silicone oil in chitosan-

coated alginate-PVA beads for biodegradation of pyrene. One important observation in these studies was the absence of lag phase for the bacteria, which indicated that the solvent encapsulation could prevent the bacteria from the phase toxicity, and could facilitate the use of non-biocompatible solvents in TPPB. Using organic modified montmorillonite (OMMT-PSF) containing PSF microcapsules, Zhao and co-workers (2009) reported a volumetric consumption rate of 342 mg/L-hr at a phenol concentration of 2000 mg/L, which is one of the highest reported in the literature.

The use of solid NAPs in TPPBs offers high operational superiority over liquid NAPs and further improves the scope of the applicability of this technology, i.e., *in situ* soil remediation. The solid adsorbents are inexpensive, easy to regenerate and recycle, and their use does not give rise to secondary contamination. In addition, the use of liquid-core microcapsules combines the advantages of both extraction and adsorption resulting in high cell growth and biodegradation rates. On the other hand, liquid NAPs have the advantages of easy handling, high partition coefficient, high interfacial area, high mass transfer rates, and high substrate diffusivity. But improving the applicability of liquid NAPs requires dispersion-free bioreactor configurations, which can eliminate the problem of emulsion formation, and facilitate more efficient solvent recovery.

2.2 Membrane Enhanced Solvent Extraction

The introduction of a semi-permeable membrane between an aqueous and an organic phase for non-dispersive solvent extraction has been a widely investigated research area (Ana Maria and Anil Kumar 2008; Asimakopoulou and Karabelas 2006; Cichy and Szymanowski 2002; González-Muñoz *et al.* 2003; Kosaraju and Sirkar 2007; Lazarova and Boyadzhieva 2004; Liu and Shi 2009; Pierre *et al.* 2001; Souchon *et al.*

2004; Younas *et al.* 2008). This technology has been applied in the extraction of metals and organics using different solvents and membranes. The solute movement here is based on the concentration gradient across the membrane (Bocquet *et al.* 2006), while the aqueous/organic interface is stabilized within the membrane pores.

The use of membrane contactors in solvent extraction offers several advantages: large surface area to volume ratio, absence of emulsions or phase entrainment; easy downstream separation; easy solvent recovery; independent phase flow rates; no density difference requirement between phases; compact design, flexible configuration and relative ease of scale-up (Gawronski and Wrzesinska 2000; Kosaraju and Sirkar 2007; Shen *et al.* 2009). The membrane based extraction technologies can be broadly classified into two categories: (1) non-dispersive solvent extraction, where the organic solvent comprises one of the bulk liquid phases; and, (2) hollow fiber supported liquid membrane (HFSLM), where the presence of the solvent is limited to the membranes.

2.2.1 Non-Dispersive Solvent Extraction

The performance of membrane contactors in solvent extraction can be affected by the membrane specifications and orientation. Membrane resistance to mass transfer is low when the solute prefers the phase that wets the membrane, i.e., the solute prefers the organic phase during extraction using hydrophobic fibers, while a low distribution coefficient is desirable during back-extraction (Kosaraju and Sirkar 2007). In many cases, membrane orientation is also decided by the nature of the incoming feed. For example, if the feed contains large particulates which can block the membrane capillaries, it cannot be pumped into the lumen side. On the other hand, very large particulates can also create dead zones in the shell side (Gabelman and Hwang 1999).

Under these circumstances, one strategy could be the filtration of the particulates prior to the feed wastewater circulation in the membrane contactors.

Solute recovery in extraction/stripping is also affected by the partition coefficient of the solute, the physical properties of the aqueous and organic liquids, and the operating conditions. The two criteria that mainly govern the selection of the solvents in membrane based extraction are: high distribution coefficient and low solubility in water (González-Muñoz *et al.* 2003). When the distribution coefficient is low, the degree of extraction can be improved by dissolving a reactive extractant in the solvent. Some of the commonly used extractants are alkylamines, tributyl phosphate (TBP), trioctylphosphine oxide (TOPO), trialkylphosphine oxide and trialkylphosphine sulfide (Cichy and Szymanowski 2002; González-Muñoz *et al.* 2003; Kujawski *et al.* 2004). TBP and TOPO are basic solvating agents and these are widely used in the extraction of phenol, while the commonly used organic solvent in phenol extraction are kerosene, octanol, decanol, methyl isobutyl ketone, benzene, heptanes, toluene, isopropyl ether and isopropyl acetate (Cichy and Szymanowski 2002; Kosaraju and Sirkar 2007; Lazarova and Boyadzhieva 2004; Shen *et al.* 2009).

The distribution coefficient depends on the pH, temperature and salt concentration in the aqueous phase, and any changes in these conditions can affect extraction performance (Hossain and Maisuria 2008; Rzeszutek and Chow 1998). During extraction of lactic acid using trioctylamine (TOA) dissolved in sunflower oil, Hossain and Maisuria (2008) observed a significant decrease in the distribution coefficient when pH was increased from 4 to 6, while the distribution coefficient increased by increasing the temperature from 8-40°C. But these changes cannot be generalized for all the extractants. For example, Rzeszutek and Chow (1998) did not observe any change in the distribution coefficient at acidic pH, whereas the

distribution coefficient decreased significantly upon the addition of bases. The recovery of solutes during extraction can also benefit from the ionic strength of the aqueous solution. It has been reported that some solutes can form "ion pairs" at high salt concentration, which could enhance the extraction efficiency significantly (Correia and de Carvalho 2005).

The overall mass transfer rate during solvent extraction in membrane contactors depends on the resistances in the boundary layers and that in the membranes (Basu *et al.* 1990). The membrane resistance depends on the membrane properties of porosity, tortuosity, thickness and the diffusivity of the solute in the solvent-wetted membranes. Therefore, the membrane resistance can be minimized by appropriate selection of the membrane, by improving the solute diffusivity, and by changing the temperature or the pH (Prasad and Sirkar 1988). On the contrary, the thickness of the boundary layer is determined by the flow rates in the lumen and the shell side. Usually, the flow in the lumen side is laminar and the mass transfer resistance depends on the dimensions of the membranes, the liquid properties and the solute diffusivity (Gabelman and Hwang 1999). Apart from these, mass transfer on the shell side also depends on the fiber packing density.

In a recent study, Shen and co-workers (2009) investigated the extraction of phenol in TBP dissolved in kerosene with concomitant stripping in sodium hydroxide using two polypropylene hollow fiber membrane contactors. The experiments were performed with the aqueous phase in the lumen side and the organic solvent on the shell side, and the overall mass transfer coefficients were calculated using the resistance-in-series approach. It was reported that the fractional mass transfer resistance in the lumen side boundary layer was highest during extraction and contributed 64-70% of the total resistance, whereas the fractional resistances in the shell side and in the

membranes were 15% and 20%, respectively. Therefore, the diffusion through the lumen side boundary layer was the rate determining step and the separation performance improved by increasing the aqueous phase flow rate. On the contrary, membranes contributed 60-72% of total resistance during stripping, and changes in flow rates did not have significant effects on the stripping performance. When membrane diffusion is the rate limiting step, the separation performance could be enhanced by increasing the porosity to tortuosity ratio, but changes in membrane specifications do not affect the extraction efficiency when mass transfer is controlled by the boundary layer resistances (Bocquet *et al.* 2005). Therefore, the determination of the rate controlling step is critical to improve the extraction performance in membrane contactors.

Membrane contactor based non-dispersive solvent extraction has several advantages over the conventional mixed settlers. While it can eliminate the problems of phase dispersion, it also facilitates simultaneous extraction and stripping in coupled membrane modules. With the emergence of the supported liquid membranes (SLM), the membrane based extraction can be made more efficient and economical. The recent development in hollow fiber supported liquid membrane (HFSLM) technology has been described next.

2.2.2 Hollow Fiber Supported Liquid Membranes

In HFSLM, an organic solvent is embedded into the pores of hydrophobic hollow fiber membranes, and is retained there by capillary forces. If the solvent is immiscible in water, the HFSLM can be used to separate two aqueous liquids, i.e., the feed solution and the stripping solution, and it can facilitate concomitant extraction and recovery of solutes in a single membrane contactor (Kocherginsky *et al.* 2007). The

HFSLM offers several advantages: low solvent volume, high separation factors, low energy requirement, low capital and operating costs, simple operation and easy scale-up. In addition, separation using liquid membranes may not be limited by the equilibrium constrains which could result in a higher mass transfer flux during the separation (Venkateswaran and Palanivelu 2006).

The relatively small volume of the organic solvent required in the HFSLM processes provides high flexibility in the selection of the solvent as the cost concerns are largely alleviated. Often, the use of organic extractants is recommended as these extractants can help in adjusting the physical properties of the organic phase, increase the stability of the liquid membrane, and enhance the distribution coefficient of the solute manifold (Zidi *et al.* 2011). By careful selection of the organic phase in the liquid membranes, the extraction performance can be dramatically improved. For example, Zidi and co-workers (2010) reported an optimal extraction efficiency of 90% with 20% TBP in kerosene and the extraction was completed within 3 minutes. The extraction efficiency dropped significantly when using pure TBP or pure kerosene as the organic phase.

Despite attaining high separation performance and operational superiority, the HFSLM technology has not resulted in industrial application because of its instability. Although the exact reason for the instability is not known, it mainly arises from: (1) the loss of the organic phase from the polymeric support due to gradual evaporation or dissolution of the solvent into either of the aqueous solutions; (2) progressive wetting of the support pores as more and more aqueous phase displaces the organic liquid in the membrane; (3) emulsion formation in the liquid membrane phase; and (3) the displacement of the liquid/liquid interface due to high differential pressure created by the flowing liquid (San Roman *et al.* 2010). The stability of the SLM can be sustained

from few hours to several months depending on the nature of the solute, the solvent, the membrane and the operating conditions. But eventually the performance deteriorates, and regeneration of the liquid membrane is required for high-performance separation.

Over the past few years, several strategies have been suggested to improve the stability of the liquid membranes. These include careful choice of the membrane, the solvent as well as the compositions of the feed and the stripping liquids and a precise control on the operating conditions, especially on the trans-membrane pressure. Gelation of the liquid membrane on the polymer surface and interfacial polymerizations have also been suggested as the potential remedial techniques (Kocherginsky *et al.* 2007). Some recent studies have also investigated the potential of using ionic liquids as liquid membrane (Malik *et al.* 2011). Since the ionic liquids have negligible vapor pressure and high viscosity, their retention is membranes pores is expected to be more stable as compared to the organic solvents. In addition, several new HFSLM configurations with higher stability have been explored including hollow fiber contained liquid membrane (HFCLM) (Sengupta *et al.* 1988; Yang *et al.* 2003), pseudo-emulsion-based hollow fiber strip dispersion (PEHFSD) (Raghuraman and Wiencek 1993; Sonawane *et al.* 2007) and hollow fiber renewal liquid membranes (HFRLM) (Ren *et al.* 2009; Ren *et al.* 2007).

A. Hollow Fiber Contained Liquid Membrane

In HFCLM, simultaneous extraction and stripping is carried out in a single membrane contactor containing two sets of fibers: one for extraction and another for stripping. The organic solvent is contained in the interstices of the fibers on the shell side (Guha *et al.* 1994) whereas the aqueous liquids flow in the lumen sides. To stabilize the

aqueous/organic interface, the pressure of the two phases are adjusted depending whether the membrane is hydrophilic or hydrophobic (Sengupta *et al.* 1988). In HFCLM, the solute is first extracted from the feed to the liquid membrane at the feed/membrane interface, and then back-extracted into the strip phase at the strip-membrane interface. Since the shell side is connected to a constant pressure source, any loss in the liquid membrane is automatically replenished from the reservoir, which results in high stability.

The HFCLM configuration was proposed by Sengupta and co-workers (1988) in the extraction of phenol and acetic acid. The extraction performance remained unchanged for 72 hours with decanol as the organic phase. First-order mass transfer models were developed and it was observed that the overall mass transfer coefficients were independent of CLM thickness or the fiber packing density. HFCLM stability claims were corroborated by Guha and co-workers (1994) in the extraction of heavy metals over extended periods of time without any observed loss in the liquid membrane. The high stability of the HFCLM was also acknowledged by Yang and co-workers (2003) in the comparison between SLM and HFCLM, although the mass transfer resistance in the SLM was lower.

Even though the HFCLM was a significant step towards improving the stability and operation of SLMs, its application in liquid membrane separation has been quite limited. This is mainly because of the complex design of these membrane contactors which are difficult to fabricate in laboratory, and are not available commercially. The HFCLM configuration also requires a much higher quantity of the organic solvents as compared to the HFSLM, with very precise control over the phase pressure. In addition, the mass transfer resistance in HFCLM was much higher as compared to HFSLM.

B. Pseudo-Emulsion-based Hollow Fiber Strip Dispersion

The PEHFSD technology is also known as 'SLM with strip dispersion', and it is a combination of two other liquid membrane configurations, the emulsion liquid membrane (ELM) and the SLM. By combining the two techniques, the individual limitations associated with each of them can be eliminated. For example, the PEHFSD can minimize ELM swelling, while providing high stability to the SLM (Ho and Poddar 2001). In this technology, the aqueous strip solution is dispersed into the organic membrane phase to create a water-in-oil emulsion. The dispersion is then pumped into the shell side of a hollow fiber membrane contactor for non-dispersive contact with the feed solution flowing in the lumen side. The continuous organic phase of the dispersion wets the hydrophobic fibers, resulting in the formation of SLM, which is stabilized by the constant supply of the organic phase in the shell side.

The advantages of PEHFSD were first demonstrated in the extraction of metals by Raghuraman and Wiencek (1993), in a Liqui-Cel hollow fiber membrane contactor. The authors reported high extraction efficiency of more than 95%, while using low stability emulsions. A low surfactant concentration resulted in limited swelling, and easy de-emulsification. The PEHFSD configuration also allowed the option of not using any surfactant for stabilizing the emulsion, without adversely affecting extraction efficiency or the SLM stability (Hu and Wiencek 1998). The surfactant-free extraction of chromium using PEHFSD has been demonstrated by several researchers, emphasizing on the simplification of the phase separation process and reduction in the separation costs (Bringas *et al.* 2006; Ho and Poddar 2001; Ortiz *et al.* 2003).

Recently, Sonawane and his co-workers (2007) investigated recovery of gold (Au(I)) through PEHFSD in a polypropylene hollow fiber membrane contactor. Au (I) was

concentrated from a 17 L feed of 10 mg/L strength within 100 min, and the resulting concentration in the stripping phase was about 15 times higher. The separation performance was affected by the conditions of pH, feed composition, stripping solution concentration, partition coefficient, volumes of the three phases and hydrodynamic conditions. A precise control on the aqueous flow rate was found to be crucial for stable operation, as very high flow rates could still result in the loss of the liquid membrane, whereas very low flow rate could result in an unstable interface.

The use of PEHFSD technology is quite promising in alleviating the instability concerns of HFSLMs. However, it compromises the non-dispersive nature of the HFSLM due to emulsification of the stripping phase, and requires additional treatment for phase separation. Furthermore, PEHFSD also requires larger volume of the organic solvent as compared to the HFSLM. Nevertheless, this technology has the advantages of the SLM and ELM processes, and is a significant step towards the development of stable liquid membranes.

C. Hollow Fiber Renewal Liquid Membranes

In PEHFSD, the aqueous/organic dispersion consisted mainly of the organic phase and the volume of the stripping phase was small. It required large solvent volume and the mass transfer resistance was higher than that in HFSLM. The HFRLM proposed by Ren and co-workers (2007) was analogous to the semi-dispersive configuration of the PEHFSD, but the liquid membrane regeneration here was based on the surface renewal theory and the HFRLM offered comparatively lower mass transfer resistance.

The HFRLM are prepared by pre-wetting hydrophobic hollow fiber membranes with the organic solvent so that the membrane pores are filled with the solvent. The aqueous/organic dispersion is prepared by mixing either of the aqueous phases

(usually stripping phase) with the solvent. Unlike PEHFSD, the amount of solvent used in the HFRLM is very small and no surfactant is required. The aqueous/organic dispersion is stirred to create organic droplets uniformly dispersed into the aqueous solution. The aqueous phase is circulated in the shell side whereas the dispersion is pumped into the lumen side. When the aqueous/organic dispersion flows in the lumen side, the shear forces due to the flow tend to remove the solvent from the membranes. Consequently, the solvent forms droplets at the liquid membrane interface and peels off into the flowing liquid in the lumen side. On the other hand, the organic droplets in the lumen side have strong affinity for the SLM and they tend to attach to and fill the hydrophobic surface. This results in a dynamic exchange of the organic phase which facilitates liquid membrane regeneration and provides high stability to the liquid membrane. Furthermore, the dynamic exchange of the organic droplets from the dispersion to the SLM introduces turbulence in the boundary layer, which can reduce the mass transfer resistance in the boundary layer significantly.

During copper extraction from wastewater using HFRLM, Ren and co-authors (2007) demonstrated high stability of the HFRLM by carrying out the process for 17 hours in continuous mode. The HFRLM stability was also demonstrated in the extraction of penicillin G (Ren *et al.* 2009) and citric acid (Ren *et al.* 2009). Although the mass transfer resistance in the HFRLM was comparatively low, the separation performance could be further enhanced using organic extractants (Ren *et al.* 2010; Zhang *et al.* 2010).

Although the HFRLM technology compromises the dispersion-free operation of the HFSLM, it retains most of the other advantages offered by the HFSLM, including high mass transfer rates, low solvent requirement, and operational flexibility. The preparation of aqueous/organic dispersion is not very energy intensive as the purpose

of agitation is to generate uniform solvent droplets, and not create stable emulsions. Therefore, the use of HFRLM in solvent extraction is quite promising.

2.3 Hollow Fiber Membrane Bioreactors in Biodegradation

The use of membrane bioreactors is very common in domestic wastewater treatment (Wang *et al.* 2009; Zhang *et al.* 2006), and these bioreactors have been the subject of numerous review papers in the past (Judd 2008; Le-Clech 2010; Reij *et al.* 1998). However, the role of the membranes in most of these studies was limited to biomass retention and ultrafiltration. Here, we discuss only those novel hollow fiber membrane bioreactor configurations which have demonstrated excellent performance in the biodegradation of toxic organic pollutants, while protecting the microorganisms from severe substrate inhibition.

The alleviation of substrate inhibition in HFMB is usually achieved by cell immobilization in membrane pores or biofilm formation on the membrane walls. The membrane wall in anisotropic hollow fiber membranes is usually a porous spongy structure which can be engineered to obtain desired pore size and thickness. If the pores are larger than the bacteria, the bacteria can diffuse into the membrane walls and hide into the membrane pore to survive substrate toxicity (Vick Roy *et al.* 1983). Depending on the cell surface properties, bacteria readily attach to the membranes to form biofilms. Usually hydrophobic isotropic membranes are used in biofilm formation, wherein the presence of the microorganisms is limited to the membrane surface, and not in the porous wall. The EPS-bacteria complex in the biofilms has enhanced tolerance to substrate toxicity and can be used to mitigate substrate inhibition (Singh *et al.* 2006).

In a very interesting study, Chung and co-workers (1998) developed asymmetric PSF hollow fiber membranes of 0.2-0.7 μm pore size for immobilizing *P. putida* in biodegradation of phenol. SEM analysis showed that the bacteria diffused into the porous spongy area of the membranes on prolonged contact and were retained inside. These immobilized cells could biodegrade inhibitory phenol concentrations in a relatively shorter time. Cell immobilization in the membranes matrix was natural and was not stabilized using any chemical agent. As a result, the immobilization was partial, i.e., the bacteria remained hidden in membrane pores when phenol concentration in solution was toxic, but diffused out of the membranes when phenol concentration dropped to sub-inhibitory levels. The immobilized microorganisms could biodegrade phenol concentrations as high as 3500 mg/L (Loh *et al.* 2000).

Due to the leakage of the microorganisms from the membranes, and the subsequent biodegradation by suspended cells, Li and Loh (2005) proposed a two stage biodegradation in these bioreactors. The first stage was slow wherein the substrate was metabolized mainly by the immobilized cells, while biodegradation in the second stage was dominated by the suspended cells and the biotransformation rates were higher. The second stage was responsible for the high performance of the immobilized cell HFMB. The change in the biodegradation trend could be witnessed from the biodegradation profile which was linear in the beginning and exponential in later stages (Li and Loh 2005; Li and Loh 2006; Zhu *et al.* 2000). It was also reported that the bacteria hidden in the membranes could acquire higher substrate tolerance. For example, *P. putida* in the biodegradation of 2000 mg/L phenol in the HFMB started leaking out in suspension at phenol concentration of 1200 mg/L which was inhibitory for the suspended cells (Loh *et al.* 2000).

While the membranes for cell immobilization can be hydrophilic or hydrophobic, biofilm formation in HFMB is usually carried out on hydrophobic support. Chung and co-authors (2004) used polypropylene fibers for the biofilms formation and subsequent biodegradation of phenol in commercial membrane contactors. The authors proposed four steps in biodegradation: phenol sorption on fibers, phenol diffusion through the membrane walls, biofilm formation on the membrane, and biodegradation. It was also estimated that the contribution of biofilm in biodegradation was less than 50%, and majority of phenol was metabolized by suspended cells which leaked from the biofilms into suspension at sub-inhibitory phenol concentrations (Juang and Kao 2009). It was also observed that the biofilm thickness was crucial to prevent substrate toxicity and a higher thickness was required at higher phenol concentrations (Chung *et al.* 2005). Since thick layers of extracellular polymeric substance (EPS) could impede the mass transfer of phenol, biofilm thickness was optimized using a dispersion agent tetrasodium pyrophosphate (TSP).

The hydrophobic membrane in the HFMBs could adsorb phenol as observed on PSF , polyvinylidene fluoride (PVDF) and polypropylene membranes (Chung *et al.* 2004). This phenomenon resulted in a lower solution concentration of the substrate, which was harnessed to alleviate competitive inhibition between phenolic compounds during cometabolism of 4-chlorophenol using phenol as the growth substrate (Li and Loh 2005). The adsorption capacity of the hollow fibers could be improved by impregnating GAC in the membranes (Li and Loh 2006). The GAC incorporated PSF fibers exhibited more porous structure and better adsorption rates, which resulted in a higher biotransformation rates of 4-chlorophenol. The concentration of the adsorbents in the polymer and their regeneration properties were critical in designing

the hybrid membranes. When desorption was not rapid, the biodegradation rates were limited by the mass transfer of phenol (Wang and Li 2007).

Apart from the high cell growth and biodegradation rates, these HFMB also exhibited high stability during long-term operation. Li and Loh (2005) carried out repeated batch runs at high concentrations of phenolic compounds, and no appreciable change in the biodegradation performance was observed in the 600 hours of operation. In addition, the high stability of the HFMB was also demonstrated in the 400 hours of continuous operation (Li and Loh 2006). The performance of the HFMB was found to be stable during nine months of continuous operation in the cometabolism of trichloroethylene (TCE) using toluene as the growth substrate and PVDF as support material (Zhao *et al.* 2011).

Previously, membrane contactors have been used in the alleviation of product inhibition in extractive fermentations. In these bioreactors, the product from the fermentation broth was continuously extracted and recovered in an appropriate organic solvent. This configuration had the advantages of high product recovery and low downstream separation costs (Malinowski 2001). Recently, this concept was applied in biological wastewater treatment for the biodegradation of aromatics from highly saline and acidic industrial wastewater using membrane bioreactors (Juang and Huang 2008; Juang *et al.* 2009). Phenol was extracted from the saline/acidic solution into kerosene and then back-extracted into a cell culture medium, thereby preventing the inhibitions arising from the high salinity/acidity of the wastewater, as well as that from high concentrations of phenol.

The hollow fiber membranes have shown excellent performance in various separation processes, some of which can be highly useful in environmental applications such as

biodegradation. The flexibility in HFMB configurations allows biodegradation using suspended or immobilized cells, or biofilms. However, there are several challenges such as clogging of the fiber lumen due to the high cell concentration or the presence of particulates in feed wastewater, membrane rupture due to excessive cell growth and biofouling, which should be addressed to make the industrial application of these bioreactors more viable. Significant progress has been made in all these fronts and the future of the HFMB in biodegradation is quite promising.

2.4 Conclusions

The TPPBs are unique combinations of the high growth potential and metabolic diversity of biodegrading microorganisms, and the high separation efficiency and rapid removal rate of solvent extraction. While the merger of these technologies has significantly enhanced the prospects of biological treatment of toxic organics, it has also given rise to new set of challenges which should be addressed to further improve the bioreactor performance, economy, and sustainability. We believe that a combination of biodegradation, solvent extraction and hollow fiber membrane based separation can result in innovative hollow fiber membrane bioreactor designs which can mitigate the challenges in conventional TPPBs, while facilitating high performance biodegradation of xenobiotics.

3 Materials & Methods

3.1 Microorganisms, Culture Conditions, and Chemicals

Pseudomonas putida ATCC 11172 was used throughout this research. Stock cultures were maintained on nutrient agar (Oxoid, Hampshire, UK) slants by periodic sub-transfer and were stored at 4°C.

The microorganisms were grown in a chemically defined mineral medium supplemented with phenol in a 500 mL Erlenmeyer flask on a shaking water bath (GFL 1092, Burgwedel, Germany) at 30 °C and 150 RPM. The composition of the mineral medium is listed in Table 3.1. All media (except phenol and the organic solvents), pipette tips, and Erlenmeyer flasks fitted with cotton plugs were autoclaved at 121 °C for 20 min before use. Prior to inoculation, cells were induced by transferring stock culture from the nutrient agar slant to the mineral medium containing 200 mg/L phenol as the sole carbon source. Activated cells in the late exponential growth phase were used as inoculum for all the experiments.

All the chemicals used in this research were of analytical grade and purchased either from Merck (Darmstadt, Germany) or Sigma-Aldrich (St. Louis, United States), unless otherwise stated. Phenol was dissolved in 0.02M sodium hydroxide to prepare a stock solution of 10,000 mg/L. Phenol was also dissolved in 2-undecanone to prepare another stock solution of 50,000 mg/L, which was used in preparing the phenolic feed for the TPPB and the HFMB. For EIHFM fabrication, TOPO stock solution of 400 g/L was prepared in dichloromethane (DCM).

Table 3.1 Composition of mineral medium

Component	Concentration (g/L)
K_2HPO_4	0.65
KH_2PO_4	0.19
$NaNO_3$	0.5
$MgSO_4.7H_2O$	0.1
$FeSO_4.7H_2O$	0.00556
$(NH_4)_2SO_4$	0.5
$(CH_2)_3N(COOH)_3$	0.015
$MnSO_4.H_2O$	0.005
$CoCl_2.6H_2O$	0.001
$CaCl_2$	0.001
$ZnSO_4.7H_2O$	0.001
$CuSO_4.5H_2O$	0.0001
H_3BO_3	0.0001
$Na_2MoO_4.2H_2O$	0.0001

3.2 Solvent Selection

3.2.1 Determination of Distribution Coefficients

To determine the distribution coefficient of phenol in the organic phase, phenol solutions of concentrations 100-2000 mg/L were prepared. To 5 mL of each of these solutions in 50 mL Falcon tubes, 5 mL of the organic solvent was added and the two phases were agitated on a thermomixer (MKR11, HLC Biotech, Germany) operating at 30 °C and 200 RPM. After 12 hours of equilibration, the aqueous and the organic

phases were separated by centrifugation and phenol concentrations in the two phases were determined by gas chromatography (GC). A plot of phenol concentrations in the organic phase versus the corresponding concentration in the aqueous phase resulted in a straight line and the distribution coefficient was the slope of the straight line.

3.2.2 Biodegradation of Organic Solvents

To examine the biodegradability of the organic solvents using *P. putida*, experiments were carried out in 500 mL Erlenmeyer flask with 200 mL of mineral medium containing 200 mg/L of the organic solvent as the sole carbon source. Solvent was not added to one of the flasks which served as the control. The flasks were inoculated and cell growth in each of the flasks was monitored periodically for two days. At the end of 48 hours, cell growth rate and biomass yields in the test experiments were compared with those in the control experiment. A change in cell density less than or equal to that seen in the control was an evidence that the solvent was not consumed by the cells (Collins and Daugulis 1997). On the other hand, a change in the biomass concentration higher than that in the control implied that the solvent was biodegradable and it was unsuitable for use in the TPPB.

3.2.3 Biocompatibility of Organic Solvents

To examine the biocompatibility of the organic solvents with *P. putida*, experiments were carried out in 500 mL Erlenmeyer flask with 200 mL of mineral medium and containing 500 mg/L of glucose as the sole carbon source. Prior to inoculation, 20 mL of the organic solvent was added to each of the flasks, except the control flask. The flasks were inoculated and the cell growth was monitored periodically for two days. At the end of 48 hours, cell growth rates and biomass yields in the test flasks were compared with that in the control. A change in the cell density comparable to that

seen in the control was an indication that the solvent was biocompatible and suitable for use in the TPPB.

3.3 Membrane Contactor Fabrication

The membrane contactors used to set up the HFMB, HFSLMB and EIHFMB were fabricated by potting polypropylene hollow fiber membranes (Accurel PP 50/280, Membrana GmbH, Germany) into a glass module using epoxy resins (Araldite, England). Specifications for the hollow fiber membranes and the membrane contactors are given in Table 3.2 and 3.3, respectively. Membrane contactors with two different specifications – A and B, were used in this research. Although the glass casing and the membrane used were same in both the cases, the two contactors were of different packing density. Membrane contactor A was packed with 120 fibers with a packing density of 0.27, whereas membrane contactor B had 150 fibers and the packing density was 0.33.

Table 3.2 Specifications for the hollow fiber membranes

Membrane Characteristics	Values
Internal diameter (μm)	280
Wall thickness (μm)	50 ± 10
Outer diameter (μm)	380 ± 35
Average pore diameter (μm)	0.2
Porosity	0.6
Tortuosity	3

The membranes were chosen based on their mass transfer performance during liquid/liquid extraction and the compatibility of the membrane material with the selected organic solvent 2-undecanone. Polypropylene membrane was preferred because it exhibited high stability during prolonged contact with 2-undecanone and the extraction performance remained stable for long periods of time.

Table 3.3 Specifications for the two membrane contactors

Characteristics	Contactor A	Contactor B
Material	Glass	Glass
Internal Diameter (cm)	0.7	0.7
Outer Diameter (cm)	1	1
Effective Length (cm)	30	30
Number of Fibers	120	150
Packing density	0.27	0.33

The preparation of the membrane contactors with fragile hollow fiber membranes was very difficult and required high skills to keep the membrane integrity intact during the process. The hollow fiber membranes were first unwound from the spool and cut into 40 cm length pieces. An extra 10 cm fiber was necessary for the packing. The small pieces of the membrane were then bundled together at one end using parafilms, each bundle contained 20 fibers. The bundles were fastened gently about 0.5 cm away from the end. A small amount of fast setting epoxy was applied at the fastened end to secure the bundle. The parafilms were then unfastened from each bundle, and all the bundles were grouped together to form a bigger bundle using parafilms. At both the ends of the big bundle, the areas on which the epoxy resins were to be applied were

marked in such a way that at least 2 cm of the membrane length were free at both the ends of the bundle. The bundle was then gently inserted into the glass casing mounted vertically on a retort stand such that the parafilm-fastened end of the bundle was at the top whereas the free end was at the bottom. A thread was tied at the upper end of the bundle and the position of the bundle in the casing was adjusted so that the area marked for the adhesive application at the lower end of the bundle was protruding out of the glass casing. Slow setting epoxy resin was then gently applied on the marked region of the lower end of the bundle, ensuring that the adhesive reached in between all the fibers and the surfaces. This step was critical because any lapse in the adhesive application could result in leakage during bioreactor operation. It was also important to control the amount of the adhesive applied as it increased the thickness of the bundle. After adhesive application, that end of the bundle was secured using parafilms and the epoxy resins were allowed to polymerize for 3 hours. The glass casing with the fibers was then inverted and the same procedure was followed at the other end of the bundle. Once the fibers were secured at both the ends of the bundle, the position of the bundle in the glass casing was again adjusted in such a way that the epoxy free length of the bundle spanned 30 cm from the inlet to the outlet on the shell side of the module. The empty space between the bundle and the glass casing at both the ends were then filled with fast-setting epoxy resins. Once the membrane contactor was ready, it was dried at 60 °C in a hot air oven for 6 hours. After drying, the integrity of the membrane contactor was investigated by pumping water into the lumen and the shell side separately for one hour. If no leakage was observed, the membrane contactor was ready for use.

3.4 Preparation of the EIHFMs

The polypropylene hollow fiber membranes were cut into small pieces of 6 cm each and bundles of 20 pieces were prepared using epoxy resins. For immobilization, TOPO/DCM stock solution was diluted with DCM to the desired concentration and the bundles were added to it. The solution was then stirred on the shaking water bath for an hour at 150 RPM to allow the solvent to penetrate the fibers. The solvent wetted fibers were then removed and rinsed twice with ultrapure water to remove DCM present on the outer surface of the fibers. Finally, the fibers were dried under dry air stream for 24 hours to evaporate DCM, leaving TOPO inside the fibers. The resulting EIHFMs were washed thoroughly to remove loosely held extractant on the outer surface of the fibers. Four sets of EIHFMs were prepared with initial TOPO concentrations of 50, 100, 200 and 400 g/L. The fibers were characterized using a scanning electron microscope (SEM) (JEOL JSM-5600LV) after sputtering with platinum.

3.5 EIHFM Contactor Fabrication

Polypropylene membrane contactors with specifications B shown in Table 3.3 were transformed into EIHFM contactors by impregnating the hollow fibers membranes with TOPO. The TOPO/DCM solution of concentration 400 g/L was pumped into the shell side of the membrane contactor for one hour at a flow rate of 3 mL/min, while the lumen side was blocked at both the ends in order to trap solid TOPO in the lumen side. After one hour, the solvent was removed from the contactor and the shell side was washed with water for 10 minutes to remove any residual solvent. Dry air was then blown into the shell side for 24 hours to evaporate DCM and impregnate TOPO into the membranes. After drying, the shell side was washed twice with water for 10

minutes each to remove any TOPO loosely attached to the outer surface of the membranes or the glass.

3.6 Membrane Contactor Sterilization

The membrane contactors could not be sterilized by autoclaving as the thin layer of epoxy between the fiber bundle and the glass wall was susceptible to damage by the wet heat, which could result in a leakage during bioreactor operation. Therefore, the membrane contactors were sterilized by washing the shell and the lumen side with 2 M sodium hydroxide for 2-3 hours. The alkaline washing was followed by at least three washings with sterilized ultrapure water to completely remove sodium hydroxide from the contactors. This sterilization technique was effective and no contamination was observed during the entire operation of the HFMB, the HFSLMB and the EIHFMB. At the end of each experimental run in these bioreactors, the lumen or the shell side through which cell culture medium was circulated was washed with 1 M sodium hydroxide solution. It was followed by two washings of one hour each with sterilized ultrapure water. The main purpose of these washings was to remove the loosely bound cells on the membranes and the tubing, but it also ensured sterilization of the bioreactor setup for the next run.

3.7 Experimental Setup

3.7.1 TPPB Operation

The TPPB operations were conducted in 500 mL Erlenmeyer flasks in a shaking water bath operating at 30°C and 200 RPM. A silicone bung with tubes inserted for air inlet and outlet was used to stopper the flask. Purified air was sparged into the contents at 2 VVM based on the aqueous phase volume. Collection of samples from the emulsion was quite difficult. Therefore, 10 mL of the liquid was collected from the flasks and centrifuged at 1000 RPM for one minute to separate the two phases.

Samples of 100 μL and 3 mL were collected from the top and the bottom phases, respectively, for phenol analysis, while another 1.5 mL of the aqueous phase was required to estimate the biomass concentration. The remaining liquid was returned back into the bioreactor.

During TPPB operation, the aqueous and the organic phases comprised of 200 mL of mineral medium and 40 mL of 2-undecanone, respectively. Stock phenol dissolved in 2-undecanone was diluted with the same solvent to prepare the organic phase. Phenol concentrations in the organic phase investigated were 3000, 5000 and 10,000 mg/L. Since the volume ratio of organic to aqueous phases was 1:5, these concentrations were equivalent to 600, 1000 and 2000 mg/L, respectively, in aqueous phase concentration terms. The TPPB operations were conducted in 500 mL Erlenmeyer flasks. The aqueous phase was inoculated with 3 mL of preculture and the absorbance of the resulting solution was measured. The organic phase was then added to the solution and the mixture was agitated in a shaking water bath. Samples from both the phases were periodically withdrawn for analyzing biomass and phenol concentrations. The pH of the aqueous phase was frequently monitored and maintained in the range of 6.5-7.0. Each experiment was performed in triplicates.

3.7.2 HFMB Operation

Fig. 3.1 shows the schematic diagram of the experimental setup. Two peristaltic pumps (L/S modular pump with PTFE-tubing pump head, Masterflex, USA) were used to pump the aqueous and the organic phases from Erlenmeyer flasks to the HFMB. Phenol containing solvent was circulated in the shell side at 1 mL/min whereas *P. putida* suspended in mineral medium was circulated in the lumen side at 10 mL/min. Air was sparged into the aqueous flask at 2 VVM. All the shell side

connections were made using polytetrafluoroethylene (PTFE) material as other tubing materials were not compatible with 2-undecanone, while the lumen side was connected using silicone tubings. The experiments were carried out in triplicates for reproducibility.

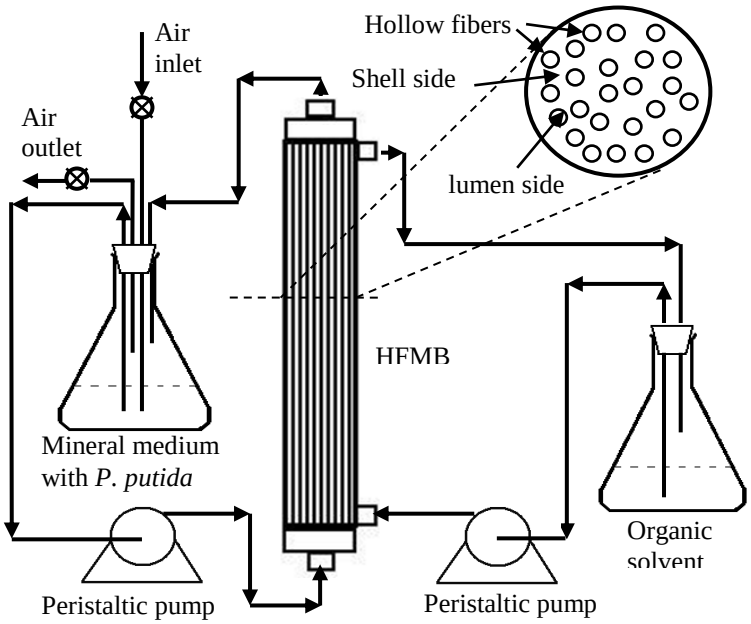

Figure 3.1 Schematic diagram of the HFMB

Prior to bioreactor operation, the polypropylene hollow fiber membranes were wetted with 2-undecanone in the shell-side for one hour. It was followed by washing of the tube side with ultrapure water to remove any solvent leaked into the lumen side during the wetting process. The volumes for the organic and the aqueous phases used were 50 and 250 mL, respectively. The HFMB was operated at initial phenol concentrations of 3000, 5000 and 10,000 mg/L in the organic phase. Samples were collected from both the phases to determine biomass and phenol concentrations. The pH of the aqueous phase was periodically measured and maintained in the range of 6.5-7.0. Membrane contactors of specification A (Table 3.2) were used here but for all the other experiments in this research, contactors with specification B were used.

During simultaneous extraction and biodegradation of phenol, two membrane contactors were required – one for extraction of phenol from the feed wastewater to the organic solvent and another for back-extraction of phenol from the organic solvent the cell culture medium. The bioreactor setup is shown in Fig. 3.2. The aqueous phases were circulated in the lumen side of the respective modules at a flow rate of 6 mL/min, whereas the organic solvent was pumped into the shell side at a flow rate of 4 mL/min.

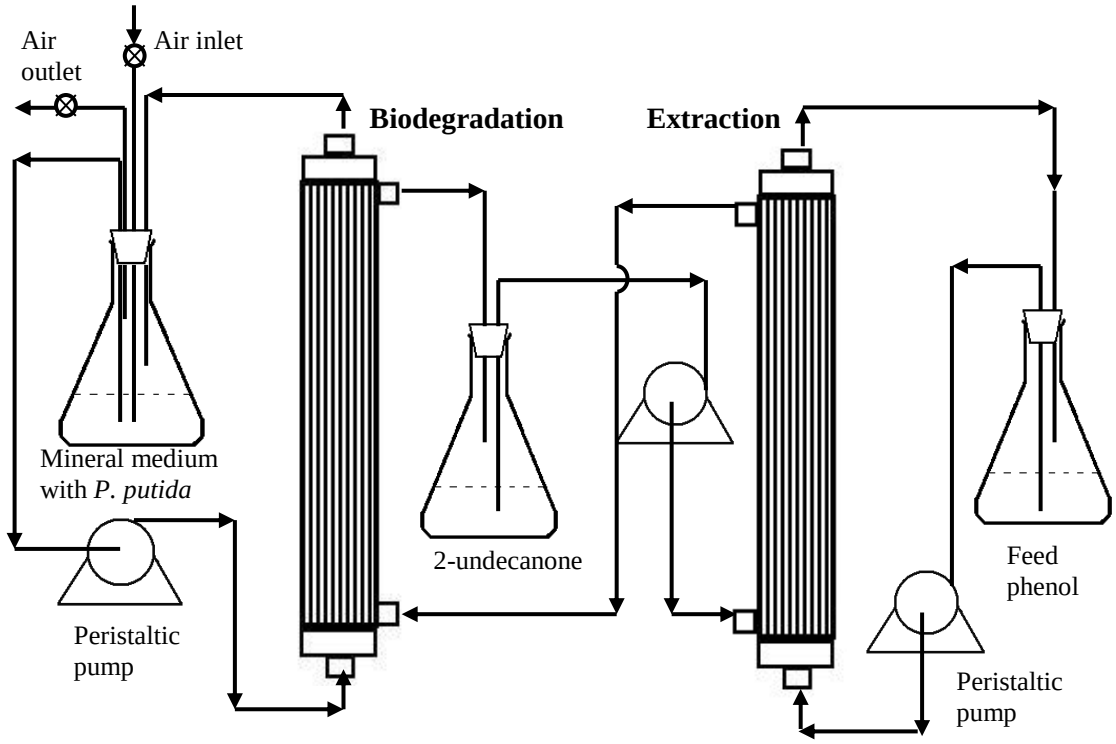

Figure 3.2 Schematic diagram of the HFMB in simultaneous extraction and biodegradation

The operation of the HFMB during simultaneous extraction and biodegradation was similar to the bioreactor shown in Fig. 3.1. Once the polypropylene membranes were wetted with 2-undecanone, the three phases were pumped into the bioreactor at fixed flow rates. The volumes for the organic and the aqueous phase used were 40 and 200 mL, respectively. The volumes of the two phases were decreased in these studies to enhance the effective membrane area per unit liquid volume and improve the mass

transfer flux in the bioreactor. The HFMB was operated at feed phenol concentrations of 1000, 1500 and 2,000 mg/L. The organic solvent was recycled at the end of each operation and reused after topping up the volume to make up for the loss due to sample collection during the experiments.

3.7.3 HFSLMB Operation

Fig. 3.3 shows the schematic diagram of the experimental setup. The solvent was uniformly dispersed into the feed phenol solution by mixing using a magnetic stirrer. Two peristaltic pumps were used to pump the aqueous/organic dispersion and the cell culture from 500 mL Erlenmeyer flasks to the shell and the lumen side, respectively. Purified air was sterilized by filtration through a 0.45 µm filter and then passed into a humidification tank. The saturated air was then sparged into the cell culture at 2 VVM. All shell side connections were made using PTFE material, whereas the lumen side was connected using silicone tubings as was the case in the HFMB.

The HFSLM was prepared by pre-wetting the hydrophobic hollow fiber membranes with 2-undecanone for one hour by pumping the solvent into the shell side of the membrane contactor. It was followed by a short washing of 10 minutes with sterilized ultrapure water to wash away any solvent leakage into the lumen. In all the experiments, 200 mL of mineral medium was inoculated with 3 mL of *P. putida* in late exponential growth phase from the preculture and the initial cell density was measured. The feed phenol solution of 200 mL volume was prepared by diluting phenol stock solution to the required concentration. The organic solvent 2-undecanone was then added to the feed solution and the mixture was stirred at 200 RPM to create uniform dispersion. Both fluids were contacted in cocurrent mode and the aqueous/organic interface was immobilized into the membrane pores by applying

a positive pressure on the lumen side. Samples were periodically collected from the bioreactor to determine biomass concentration in the cell culture medium and phenol concentrations in all the three liquid phases. The pH of the cell culture medium was frequently measured and adjusted in the range of 6.5-7.0.

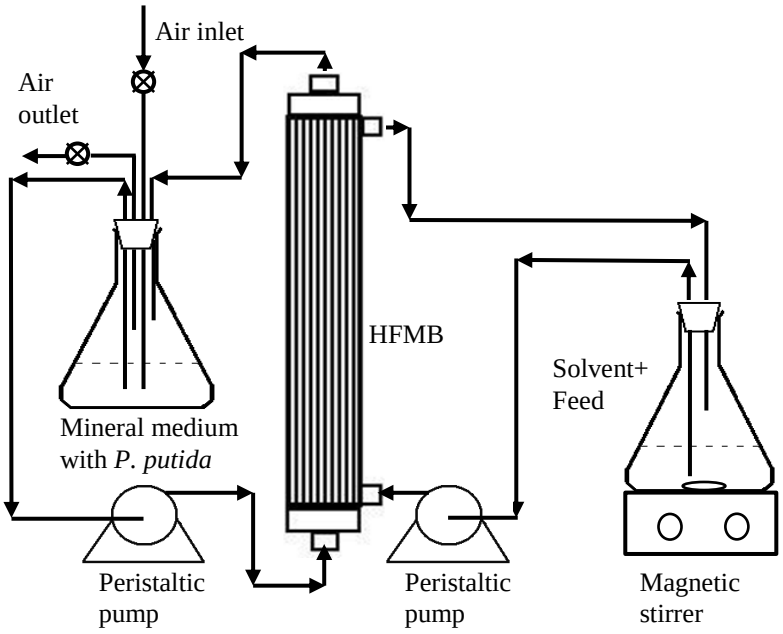

Figure 3.3 Schematic diagram of the HFSLMB

3.7.4 Adsorption/Desorption of Phenol on EIHFMs

The adsorption/desorption experiments were carried out in batch mode in a 50 mL Falcon tube with 40 mL of solution on a thermomixer (MKR11, HLC Biotech, Germany) operating at 30 °C and 200 RPM. A total of 15 bundles of EIHFMs weighing 0.5g with four different concentrations of TOPO were used to investigate the adsorption of 500, 1000, 1500 and 2000 mg/L phenol. Samples were collected from these tubes periodically to measure phenol concentration in the liquid phase, while the amount of phenol adsorbed on the EIHFMs was calculated by material balance. Desorption of phenol was carried out in 0.2 M sodium hydroxide solution. Each experiment was repeated three times for reproducibility.

Biodegradation of 1000 and 2000 mg/L phenol in the solid/liquid TPPB was carried out in batch mode in a 500 mL flask with total volume of 150 mg/L. Sixty bundles of EIHFMs prepared using 400 g/L TOPO were added to the phenol solution and the two phases were allowed to equilibrate on a shaking water bath at 30 °C and 150 RPM. After half an hour, the TPPB was inoculated with *P. putida* from the preculture and the bioreactor was aerated with sterile humidified air at a rate of 2 VVM. Samples were collected periodically to measure biomass and phenol concentrations.

3.7.5 EIHFMB Operation

Fig. 3.4 shows the schematic diagram of the experimental setup. A peristaltic pumps (L/S modular pump with Easy-Load II pump head, Masterflex, USA) was used to pump the aqueous medium from a 500 mL Erlenmeyer flask to the shell side of the EIHFMB. Purified air saturated with water was sparged into the bioreactor at 2 VVM.

The EIHFMB operation was started by circulating the synthetic phenolic wastewater of 200 mL volume into the shell side at a fixed flow rate. During this period, phenol was adsorbed from the aqueous solution on to the EIHFMs under abiotic conditions. After one hour of equilibration, the wastewater was inoculated with 3 mL of *P. putida* in late exponential growth phase from the preculture. The initial cell density and the phenol concentration at the time of inoculation were measured. Samples were periodically drawn to determine the biomass and phenol concentrations in the EIHFMB. The pH of the aqueous phase was frequently measured and adjusted in the range of 6.5-7.0. At the end of each run, the attached cells on the membrane and the tubings were removed by washing the shell side first with 1M sodium hydroxide, and then twice with sterilized ultrapure water.

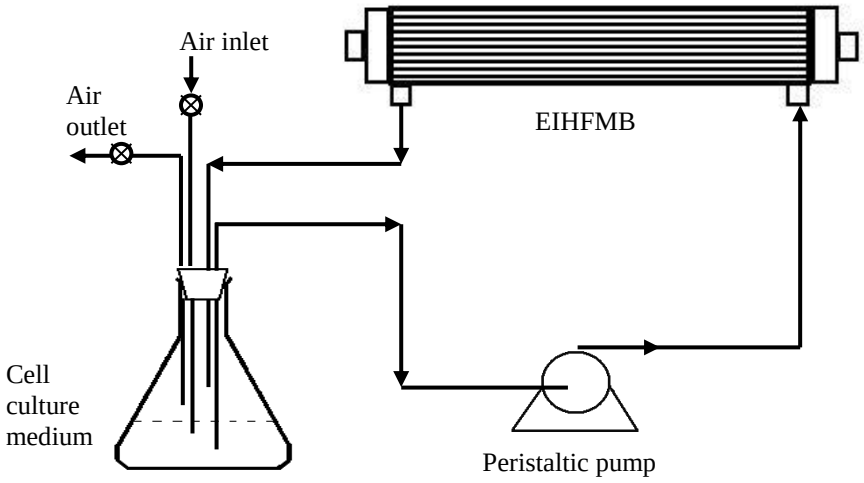

Figure 3.4 Schematic diagram of the EIHFMB

3.8 Analytical Methods

Cell density was determined by measuring the optical density (OD) of the aqueous medium at 600 nm using an ultraviolet-visible spectrophotometer (UV-1240, Shimazdu, Japan). The OD was used to compute the biomass concentration by the formula: dry cell weight (mg/L) = 385.1*OD_{600}.

Phenol concentrations during the abiotic experiments were determined by measuring the OD at 270 nm. For determining phenol concentration during the biotic experiments, 3 mL of the cell culture was filtered through 0.45 µm syringe filter (Millex, Millipore, USA) and extracted into an equal volume of DCM containing 100 mg/L *o*-cresol as internal standard. Phenol in the extract was analyzed by GC equipped with a flame ionization detector (Clarus 600, Perkin Elmer, USA). Phenol concentration in 2-undecanone and TOPO concentration in DCM was directly analyzed by GC.

Since the volumes of the aqueous and the organic phases were different, the concentration of phenol in the organic phase was normalized to the aqueous phase volume to compute the equivalent concentration in the aqueous phase. Total phenol concentration in the bioreactor at any time was the sum of the phenol concentrations in each of the aqueous phases, and the aqueous phase equivalent of the organic phase phenol concentration. Average biodegradation rate was calculated by dividing the net amount of biodegraded phenol for the time period when phenol was about 10% and 90% of the initial phenol by the corresponding elapsed time as suggested by Loh and Wang (1998). Biomass yield refers to the ratio of maximum cell concentration observed during biodegradation divided by the initial total phenol concentration.

4 Two-phase Biodegradation of Phenol in a Hollow Fiber Membrane Bioreactor

4.1 Introduction

In this section, the feasibility of non-dispersive two-phase biodegradation of phenol in an HFMB was examined. The objectives of this research were:

1. Elucidate the effects of substrate inhibition on suspended cells of *P. putida* during biodegradation of phenol in suspension;
2. Screen for a suitable organic solvent to be used as the partitioning phase in the two-phase biodegradation of phenol;
3. Investigate two-phase biodegradation of phenol in a dispersion-based aqueous/organic TPPB;
4. Develop an HFMB for two-phase biodegradation of phenol at inhibitory concentrations; elucidate the effects of interfacial area;
5. Compare the performances of the HFMB and the TPPB based on the cell growth environment, biodegradation rates, operating costs and the challenges pertaining to the operating conditions; and
6. Operate the HFMB for simultaneous extraction and biodegradation of phenol from wastewater.

The suspension studies were carried out to characterize cell growth under substrate inhibition conditions and to determine the inhibitory limit of phenol for *P. putida* ATCC 11172. The information gathered from these experiments was used to design the experiments during the HFMB operation, in order to showcase the effectiveness of the HFMB under severe substrate inhibition at phenol concentrations 3-4 times higher than the inhibitory limit for the bacteria.

The design of a two-phase biodegradation hinges upon the selection of a suitable organic phase. Although numerous solvents have been used in membrane-based extraction/stripping of phenol (González-Muñoz *et al.* 2003; Nanoti *et al.* 1997; Shen *et al.* 2009), these solvents must be evaluated for their biocompatibility and biodegradability before these can be used in a TPPB. The additional criteria serve to protect the microorganisms from an additional toxic solvent which could affect cell growth adversely, as well as to prevent the metabolism of the organic phase which could incur additional operating costs and may also result in incomplete biodegradation (Daugulis 2001).

Prior to the design and operation of the HFMB, baseline studies on conventional aqueous/organic TPPBs was carried out in order to gain a first-hand experience on the operating challenges encountered in these bioreactors. These experiments were also important to understand the cell growth and substrate removal trends in the two-phase systems, which were quite different from those in single-phase systems. The biodegradation results from the TPPB were subsequently used for comparison with those obtained in the HFMB.

When all the baseline studies have been concluded, the HFMB was operated at inhibitory phenol concentrations using the bioreactor setup shown earlier in Fig. 3.1. During the several experimental runs in the HFMB, the effects of increasing substrate concentration on the specific growth rate, biomass yield, biodegradation rate and biodegradation time were investigated. Further experiments were carried out to evaluate the HFMB performance at higher interfacial mass transfer area. In addition, two-phase biodegradation in the HFMB was compared with that in the TPPB, based on the mass transfer rates, biodegradation performance and the operating conditions.

Finally, the flexibility in configuration and operation of the HFMB was demonstrated by operating the HFMB for simultaneous extraction and biodegradation of phenol from synthetic wastewater. Our results here were significant as they demonstrate the advantages of dispersion-free operation in the HFMB, which are impossible to perform in the TPPBs.

4.2 Results and Discussions

4.2.1 Single-phase Biodegradation of Phenol

Fig. 4.1 shows the effects of increasing phenol concentration on cell growth. It can be seen that cell growth gradually slowed down at higher phenol concentrations. The specific growth rate which was observed to be 0.63 hr^{-1} at 100 mg/L decreased monotonically to 0.1 hr^{-1} at the maximum phenol concentration of 600 mg/L. The same trend was observed for the biomass yield, which decreased from 0.65 g/g to 0.41 g/g when phenol concentration was increased from 100 to 600 mg/L. For phenol concentrations below 400 mg/L, microorganisms did not exhibit any lag phase. But at 500 mg/L phenol, a 3 hour lag phase was observed. The lag phase duration increased at 600 mg/L and the rates of cell growth and substrate removal were very slow. No cell growth was observed at phenol concentrations above 600 mg/L, which was determined to be the inhibitory limit for *P. putida* ATCC 11172.

These results are consistent with the findings reported in the literature and the variations in the cell growth rates and biomass yields have been attributed to the increase in the severity of substrate inhibition at high phenol concentrations. The variations in biomass yield could also be caused by the accumulation of toxic metabolic intermediates during biodegradation of the phenol (Wang and Loh 1999).

(a)

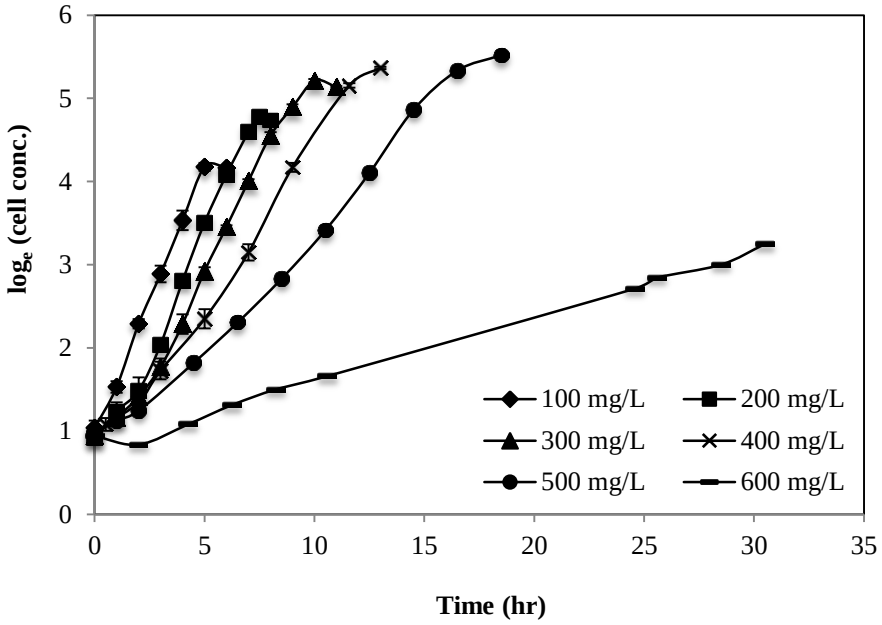

(b)

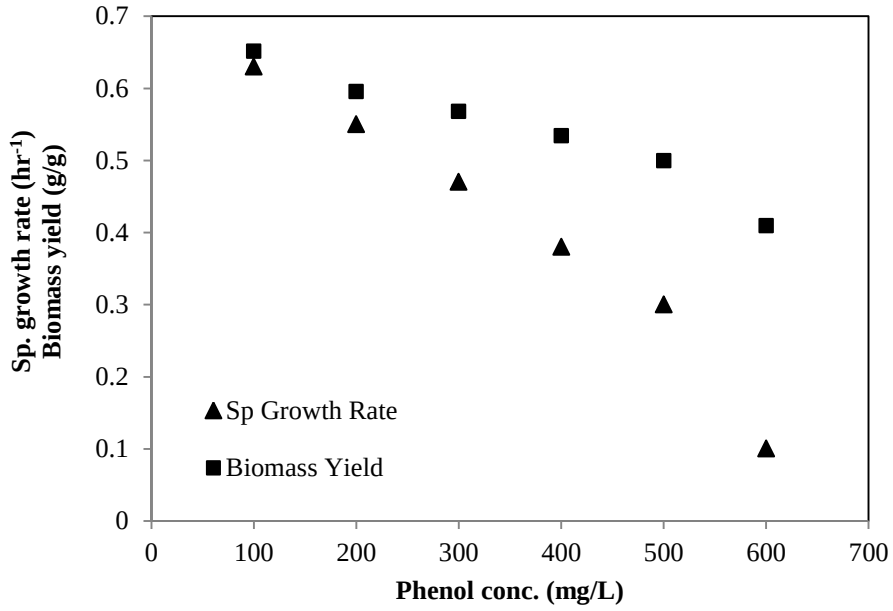

Figure 4.1 Effects of substrate inhibition on: (a) cell growth; (b) specific growth rate and biomass yield, during biodegradation of phenol in single-phase

4.2.2 Solvent Selection

Organic solvents – kerosene, 2-undecanone and 1-decanol, which are commonly used solvents in the removal of phenol from wastewater in solvent extraction or two-phase biodegradation (González-Muñoz *et al.* 2003; Tomei *et al.* 2008; Vrionis *et al.* 2002; Zidi *et al.* 2010), were screened for their suitability in the HFMB. Each of these solvents was tested for their biocompatibility, biodegradability and the distribution coefficient of phenol. The results are summarized in Table 4.1. Other factors that were considered during the screening were the hazardous nature of the solvents, their vapor pressure (obtained from the respective Material Safety Data Sheets (MSDS)), solubility in water (obtained from the respective MSDS) and the ease of analyzing phenol concentration in the solvent using GC.

Table 4.1 Solvent screening for the selection of organic phase in two-phase biodegradation of phenol

Attributes	Organic solvents		
	Kerosene	2-undecanone	1-decanol
Biodegradable	×	×	✓
Biocompatible	✓	✓	✓
Hazardous	✓	×	✓
Water soluble	×	×	×
Ease of analysis	×	✓	✓
Mechanical problems	✓	✓	×
Vapor Pressure (hPa at 20°C)	0.31	> 1	> 0.01
Distribution coefficient	0.11	33	14

While 1-decanol was found to be biodegradable by *P. putida*, kerosene and 2-undecanone met most of the criteria (Quijano *et al.* 2009). Since the distribution coefficient of kerosene was very low, its use in the TPPB would have required a large quantity of the solvent or another supplementary extractant. In addition, being a mixture of hydrocarbons, kerosene also interfered with the detection of phenol in GC. On the contrary, 2-undecanone did not interfere with phenol analysis and exhibited high affinity for phenol. The biocompatibility and biodegradability of 2-undecanone for *P. putida* are quite established and it has been widely used in two-phase biodegradation of phenolic compounds (Collins and Daugulis 1997; Hamed *et al.* 2004; Tomei *et al.* 2008).

4.2.3 TPPB Operation

Fig. 4.2 shows the temporal profile of cell growth and biodegradation for initial total phenol concentration of 1000 mg/L. When the two immiscible liquid phases were shaken together in a 500 mL Erlenmeyer flask, phenol rapidly diffused from the organic to the aqueous phase to achieve equilibrium distribution between the two phases. After three hours, phenol concentration in the aqueous phase was recorded as 128 mg/L while there was an equivalent decrease in phenol concentration in the organic phase. After 8 hours of slow growth, *P. putida* multiplied rapidly with a maximum specific growth rate of 0.71 hr^{-1}. Cell growth continued for 19 hours and about 900 mg/L phenol was metabolized during that period with an average biodegradation rate of 66.7 mg/L-hr. A negative cell growth period ensued when phenol was exhausted in the aqueous phase and the diminishing flux of phenol from the organic phase could not sustain high biomass concentration in the aqueous phase. Phenol was removed from the organic phase within 31 hours. Similar cell growth and

substrate removal trends were observed during biodegradation of 600 and 2000 mg/L phenol, the results of which are summarized in Table 4.2.

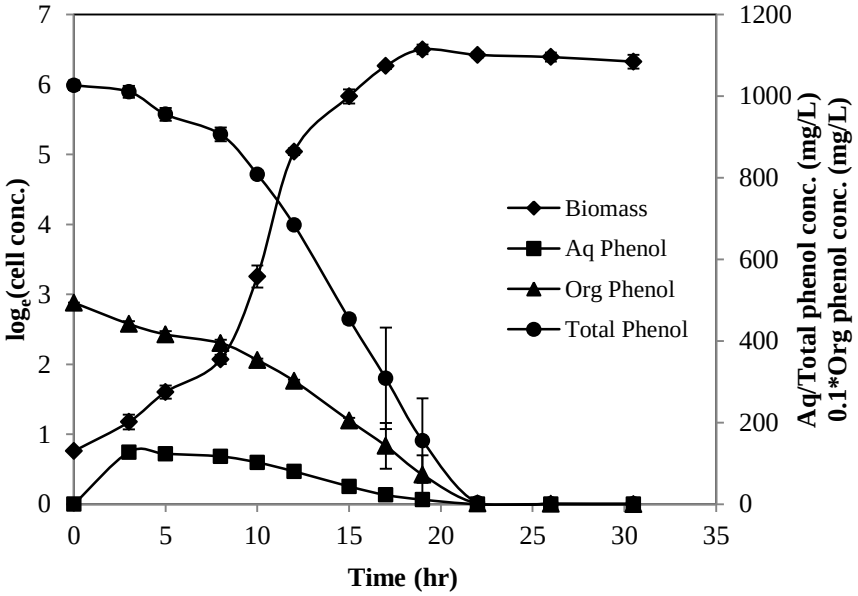

Figure 4.2 Temporal concentration profiles of biomass and phenol during biodegradation of 1000 mg/L phenol in TPPB

Typically, biphasic biodegradation of phenol in the TPPB occurred in three stages starting with a lag phase that lasted 8-10 hours. Lag phase is commonly observed in TPPBs as a result of toxic inhibition due to higher system loading of phenol, which exerts substrate inhibition on the microorganisms. It has been reported that the lag phase duration increases with substrate concentration in the organic phase (Collins and Daugulis 1997). Lag phase was followed by an exponential growth phase in which *P. putida* exhibited high growth and biodegradation rates. Most of the substrate was removed during this period and the biomass concentration reached a maximum. The remaining phenol in the organic phase was removed during the third stage, which was characterized by negative cell growth rates.

Phenol metabolism by *P. putida* usually proceeds with the accumulation of a reaction intermediate 2-hydroxymuconic semialdehyde (2-HMSA), which imparts a greenish-

yellow color to the nutrient medium (Wang and Loh 1999). This color change is often accompanied by a pH change in the medium due to the acidic nature of 2-HMSA. Since pH change affects cell growth adversely, the pH of the aqueous phase in the TPPB was monitored and maintained at 6.5 - 7. Emulsification of the aqueous-organic dispersion was another growth associated phenomenon in the TPPB. Emulsions were first spotted in the bioreactor during the exponential growth phase and the degree of emulsification as well as emulsion stability increased with biomass concentration. This growth-linked emulsification has been reported earlier during TPPB operation and it has been attributed to the production of emulsion promoting biosurfactants by the microorganisms (Quijano *et al.* 2009).

Table 4.2 Effects of phenol concentration on biodegradation parameters in TPPB

Parameters	Phenol concentration (mg/L)		
	600	1000	2000
Lag phase (hr)	7	8	10
Specific growth rate (hr^{-1})	0.72	0.72	0.69
Biomass yield (g/g)	0.53	0.65	0.58
Biodegradation time (hr)	24	31	51
Average biodegradation rate (mg/L-hr)	48	67	100

4.2.4 HFMB Operation

A. Cell Growth and Phenol Metabolism

To investigate biphasic biodegradation of phenol in the HFMB, batch experiments were performed at a volume ratio of organic to aqueous phase of 1:5. Apart from preventing phase dispersion, polypropylene fibers used in the HFMB served two

additional purposes: (a) the low pore size prevented cell immobilization into the porous matrix of the fibers, and (b) the fibers served as a physical barrier to prevent any contact between the organic solvent and the cells. Since the hydrophobic fibers were wetted with 2-undecanone, a higher pressure was maintained on the aqueous side to forcibly immobilize the aqueous/organic interface into the membrane pores and prevent any solvent leak into the lumen. These arrangements prevented the direct contact of *P. putida* with 2-undecanone which could result in a lag phase during biodegradation.

Fig. 4.3 shows the representative temporal profiles of biomass and phenol concentrations during biodegradation of 1000 mg/L phenol. Phenol removal in the HFMB occurred in three stages. The quick drop in the total phenol concentration in the first hour was mainly due to the sorption of phenol on the polypropylene fibers. The amount of phenol sorbed on the fibers depends on the volume of the fibers as well as the concentration of the feed solution (Chung *et al.* 2004). Initial sorption was immediately followed by an exponential removal phase during which phenol was rapidly metabolized by suspended cells of *P. putida*. About half of the initial substrate was removed during that period whereas the second half was removed during an equally prominent third stage wherein biodegradation was limited by mass transfer of phenol from the organic to the aqueous phase.

The exponential growth phase lasted 12 hours with *P. putida* growing at a maximum specific growth rate of 0.49 hr^{-1}. During that period, phenol concentration was reduced to 485 mg/L and the corresponding biomass yield was 0.53 g/g. Both cell growth and substrate removal rates diminished when *P. putida* completely exhausted phenol in the aqueous phase. Although cells continued to grow for 34 hours, the observed overall biomass yield was much lower at 0.36 g/g. Phenol was completely

removed from the organic phase after 46 hours. Compared to the TPPB, aqueous phase phenol concentration in the HFMB after 4 hours of operation was 20% lower at 105 mg/L. This suggests that the mass transfer rate and consequently redistribution of phenol in the HFMB was comparatively slower. Lower aqueous phase phenol concentration could also be a result of a change in the distribution coefficient of phenol due to the triphasic distribution of phenol in the HFMB, with polypropylene fibers being the third phase.

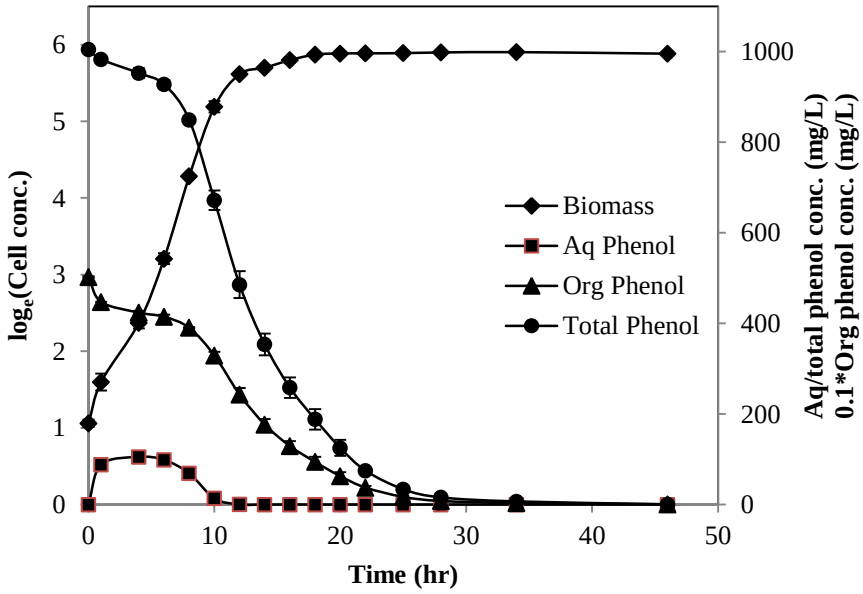

Figure 4.3 Temporal concentration profiles of biomass, aqueous phenol, organic phenol and total phenol in biodegradation of 1000 mg/L phenol in HFMB

While *P. putida* in the HFMB did not exhibit any lag phase when the initial total phenol concentration was increased from 600 to 2000 mg/L, gradual decrease in the maximum specific growth rate and the biomass yield were observed (Table 4.3). This trend is consistent with single-phase biodegradation reported in literature under the influence of substrate inhibition (Wang and Loh 1999). The specific growth rates observed in the HFMB were also comparable with those observed in monophasic biodegradation of phenol at equivalent aqueous phenol concentrations. This suggests that the cell growth environment in the HFMB was free from any solvent interference

and resembled that in aqueous cultures. The lower computed biomass yields in the HFMB were mainly a consequence of microbial attachment on the polypropylene fibers and the silicone tubing which resulted in a lower suspended cell concentration.

Table 4.3 Effects of phenol concentration on biodegradation parameters in HFMB

Parameters	Phenol concentration (mg/L)		
	600	1000	2000
Lag phase (hr)	0	0	0
Specific growth rate (hr^{-1})	0.52	0.48	0.43
Biomass yield (g/g)	0.48	0.37	0.31
Biodegradation time (hr)	39	46	60
Average biodegradation rate (mg/L-hr)	42	58	77

Two-phase biodegradation is analogous to an extraction-stripping process. However, unlike stripping agents, biomass concentration during substrate removal does not remain constant but increases with time. With gradual increase in the biomass density, substrate is removed faster, which in turn, adds more biomass to the system. On the other hand, when substrate is metabolized, the concentration gradient across the phase boundary diminishes which results in lower diffusion rates. At some point, substrate removal rate equals the flux from the organic to the aqueous phase and mass transfer limitation is imposed on biodegradation. Fig. 4.4a shows phenol distribution between the two phases in the HFMB as the ratio of organic to aqueous phase phenol concentrations during biodegradation. Initially, phenol moved from the organic to the aqueous phase to attain equilibrium distribution. During the first few hours after inoculation, biomass concentrations were low but concentration gradients across the

membrane were high. Therefore, equilibrium distribution of phenol was maintained in the HFMB. However, at higher biomass concentration, when phenol removal was faster from the aqueous phase, the equilibrium was perturbed and a gradual increase in the organic to aqueous phenol concentration ratio was observed. This concentration ratio kept increasing with biomass concentration until all the phenol was left sequestered in the organic phase. At higher phenol concentrations, specific growth rates were low but the concentration gradient between the two immiscible phases was high, resulting in higher mass transfer rates and slower changes in equilibrium conditions. After aqueous phenol was completely exhausted, the removal of phenol was linear with time (Fig. 4.4b) and the rates observed during this period were lower than the average biodegradation rates. This suggests that the biodegradation was limited by the mass transfer of substrate across the membrane (Li and Loh 2005).

B. Effects of Interfacial Area

In two-phase partitioning bioreactors, biodegradation performance is inextricably linked with the mass transfer of substrate between the two-phases and can be enhanced by increasing the interfacial mass transfer area. When the phases are dispersed, interfacial area is enhanced by using higher agitation rates (Zilouei *et al.* 2008) whereas mass transfer area in membrane contactors increases with the area of the membranes. A common practice to increase the efficiency of membrane-based processes is to connect several membrane modules in series (Gabelman and Hwang 1999).

To enhance the two-phase biodegradation performance of the HFMB, the bioreactor setup in Fig. 3.1 was modified by connecting another identical membrane contactor in series with the existing unit. The effective fiber length thus was increased to 60 cm

(a)

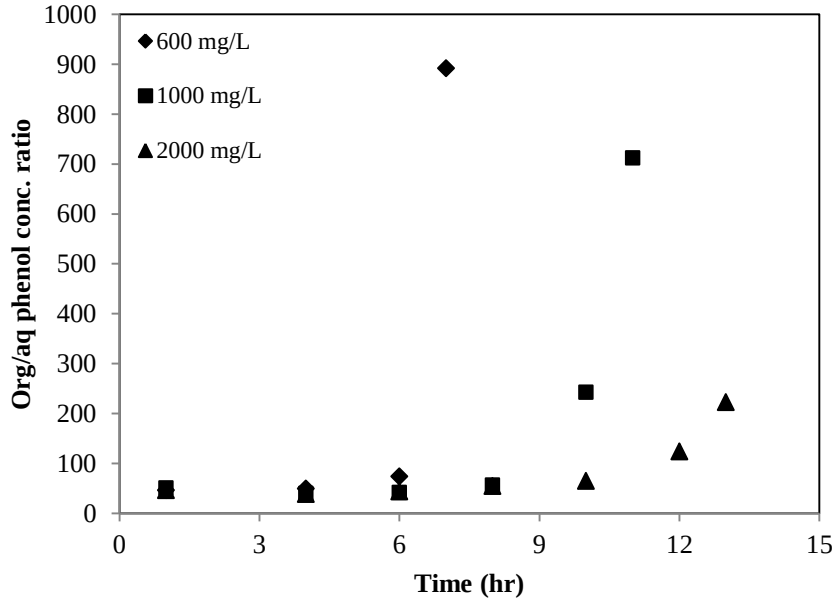

(b)

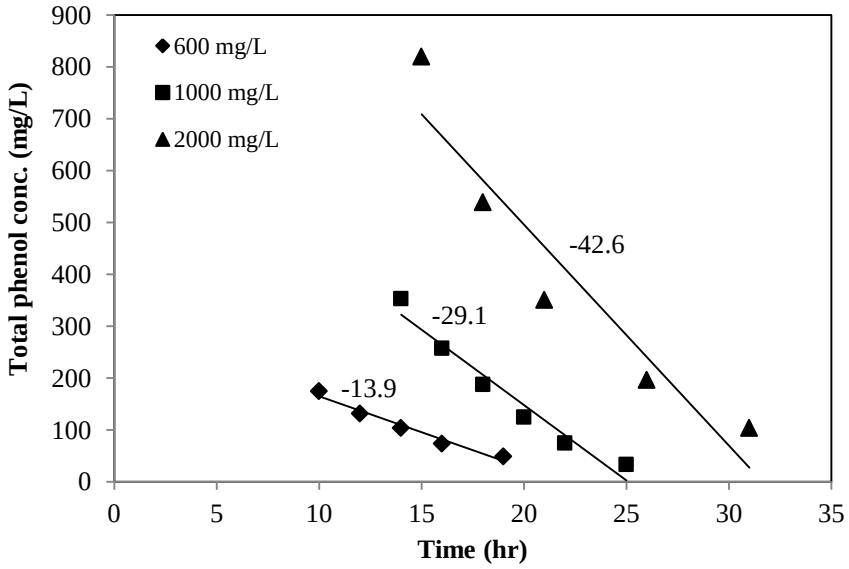

Figure 4.4 Effects of substrate concentration on: (a) phenol distribution between two-phases and (b) effect of mass transfer limitation on biodegradation, for initial phenol concentrations of 600, 1000, and 2000 mg/L

and consequently, the interfacial mass transfer area was doubled. Although cell growth and phenol removal trends in the HFMB remained unchanged with the increase in the interfacial area, there was a substantial increase in the biodegradation rate and 2000 mg/L phenol was removed from both the phases within 43 hours of operation as shown in Fig. 4.5.

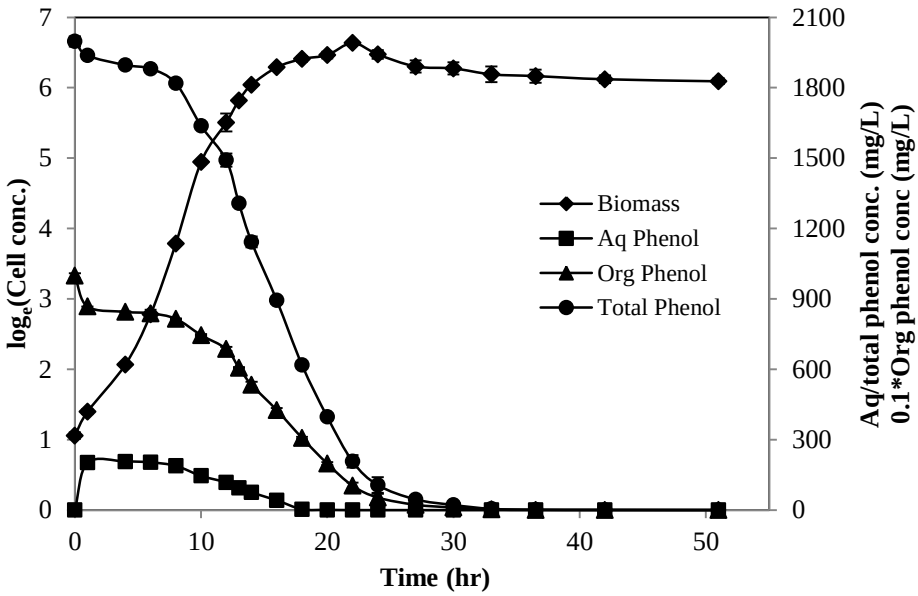

Figure 4.5 Temporal concentration profiles of biomass and phenol in HFMB with twin modules at initial substrate concentration of 2000 mg/L

Under improved mass transfer rates, the replenishment of substrate consumed by the microorganisms was quicker and the presence of phenol in the aqueous phase was prolonged to to 20 hours (Fig. 4.6a). Most of the initial substrate was biodegraded during this period and less than 10% of initial phenol remained in the organic phase during the realm of diffusion limitation (Fig. 4.6b). The maximum specific growth rate improved slightly to 0.47 hr^{-1} whereas average biodegradation rate increased by more than 60% to 123.1 mg/L-hr and resulted in shortening of the biodegradation time by 17 hours (Table 4.4). The biomass yield too increased from 0.3 to 0.35 g/g. These results are significant because of two reasons: (1) a prolonged exponential

(a)

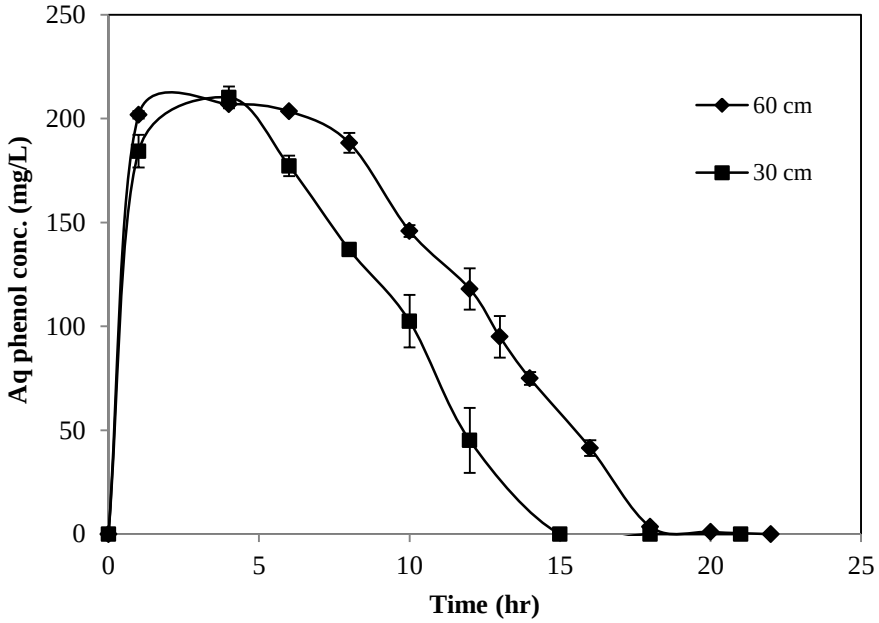

(b)

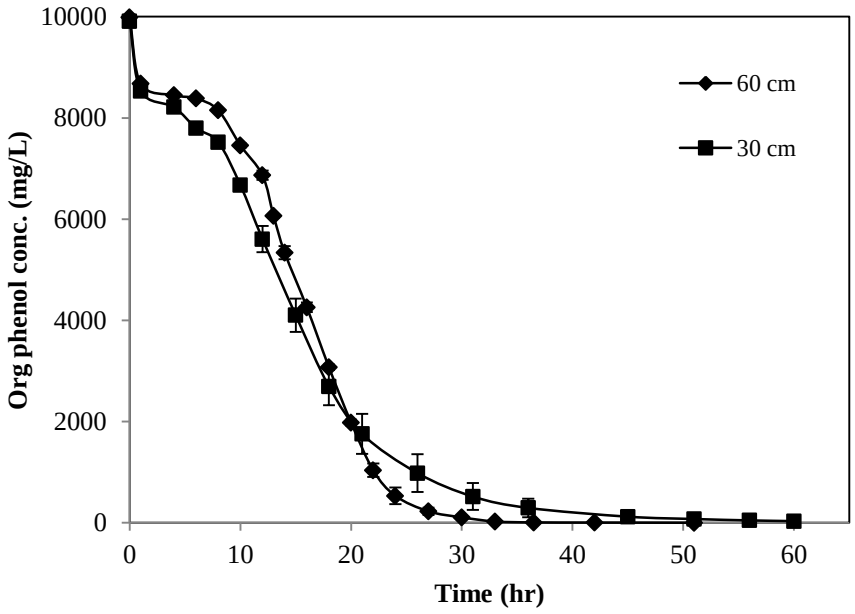

Figure 4.6 Effects of the membrane length on (a) aqueous phenol concentration; and (b) phenol removal rate

growth phase and the consequent improvement in the biodegradation rate at higher interfacial membrane area corroborate the hypothesis that the biodegradation of phenol in HFMB was limited by the mass transfer of phenol towards the end of the experimental runs; and, (2) the mass transfer limitation could be easily subsided and the performance can be improved by increasing the membrane area without any increase in the agitation speed and the operating costs.

Table 4.4 Effects of membrane length on two-phase biodegradation of phenol in the HFMB

Parameters	Single module (30 cm)	Double module (60 cm)
Specific growth rate (hr^{-1})	0.43	0.47
Biodegradation time (hr)	60	43
Avg biodegradation rate (mg/L-hr)	76.2	123.1
Biomass Yield (g/g)	0.30	0.35

The biodegradation performance of the HFMB was better than some of the recently reported membrane bioreactors in which an equivalent amount of phenol was mineralized in 75 hours using biofilms (Chung *et al.* 2004), 110 hours using immobilized cells (Loh *et al.* 2000) and 270 hours using suspended cells (Juang *et al.* 2009). The biodegradation performance of the HFMB was also comparable to that in the conventional TPPBs using either liquid or solid NAPs. Table 4.5 lists the performance of TPPBs in biodegradation of phenol. Unlike conventional TPPB configurations where lag phase was inevitable and varied from 8-12 hours, microorganisms in the HFMB were segregated and protected from the solvent by

polypropylene membranes and did not exhibit any lag phase. Another advantage was the low agitation rate in the HFMB, whereas the agitation rates required to disperse the two phases in conventional TPPBs was much higher. It is anticipated that the biodegradation performance of the HFMB could be further improved by optimizing the hydrodynamics in the bioreactor.

Table 4.5 Performance comparison of TPPBs in biodegradation of phenol

NAP	Micro-organism	Lag phase	Phenol conc. (mg/L)	Removal time (hr)	Agitation rate (RPM)	Ref.
2-undecanone	*P. putida* 11172	12	4000	60	200	(Collins and Daugulis 1997)
2-undecanone	*P. putida* F1	8	500	28	200	(Hamed *et al.* 2004)
EVA	*P. putida* 11172	13	2000	60	400	(Amsden *et al.* 2003)
EVA	Microbial consortium	10	2000	30	600	(Prpich and Daugulis 2005)
Kerosene	*P. putida* 14365	10	1800	80	300	(Juang *et al.* 2012)
2-undecanone	*P. putida* 11172	0	2000	43	150	This study

4.2.5 Comparison between HFMB and TPPB

In two-phase biodegradation systems, a high biotransformation rate is obtained by controlling the rate of diffusion of the substrate between the two phases. Usually, better mass transfer characteristics within the bioreactor result in higher biodegradation performance. During biodegradation of 2000 mg/L phenol, phenol

distribution between the aqueous and organic phases for the TPPB and the HFMB with twin modules are compared in Fig. 4.7a. It can be seen that the distribution was more stable for the TPPB in which phenol could be sustained in the aqueous phase for 28 hours. However, the microorganisms in the TPPB also exhibited a lag phase of 10 hours and after netting the lag phase duration, substrate distribution profiles for the two bioreactors were nearly identical. Even the substrate removal profiles for the two bioreactors ran parallel to each other for most of the biodegradation duration, only separated by a time difference of approximately 10 hours (Fig. 4.7b).

Apart from the biodegradation kinetics, the HFMB also has several operational advantages over the dispersion-based TPPBs. These are summarized in Table 4.6. The non-dispersive operation of the HFMB provided a solvent-free growth environment for *P. putida*, and the resulting cell growth kinetics was similar to that observed in single-phase biodegradation systems. This indicates that the membrane barrier had protected the microorganisms from any adverse effects of the solvent. This advantage can be harnessed for the application of other organic solvents which are not biocompatible but offer higher distribution coefficient for phenol. Moreover, the solventless growth environment in the HFMB can also pave the way for the application of mixed microbial consortium in aqueous/organic two-phase biodegradation. Mixed cultures have been shown to exhibit better growth and substrate metabolism potential as compared to pure cultures and is often used in solid/liquid TPPBs (Prpich and Daugulis 2005; Tomei *et al.* 2011).

During the entire operation of the HFMB, no foaming or emulsions were detected in the cell culture medium. While the absence of emulsions simplified the collection and analysis of the samples, it also facilitated organic solvent recycling and reuse without

(a)

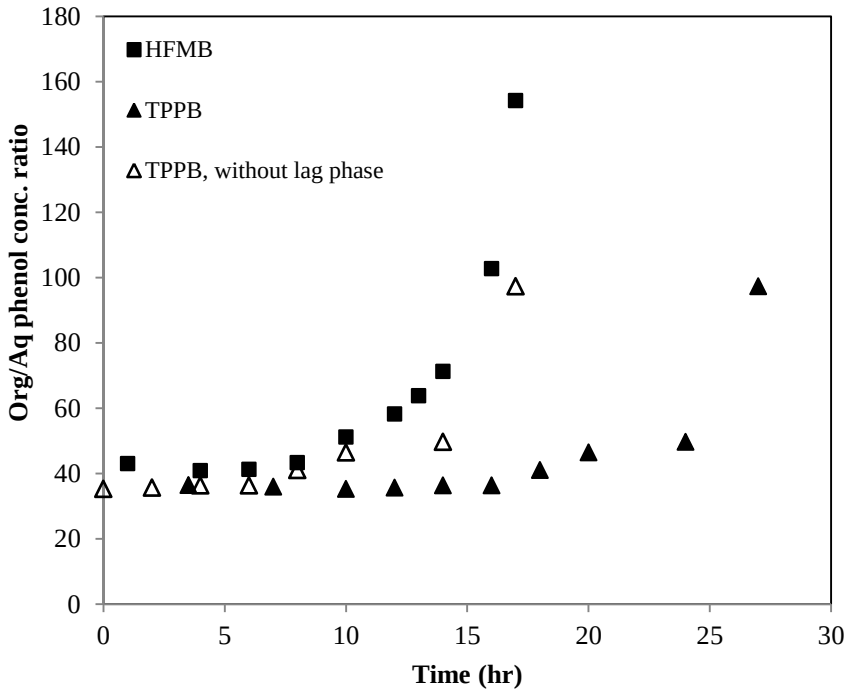

(b)

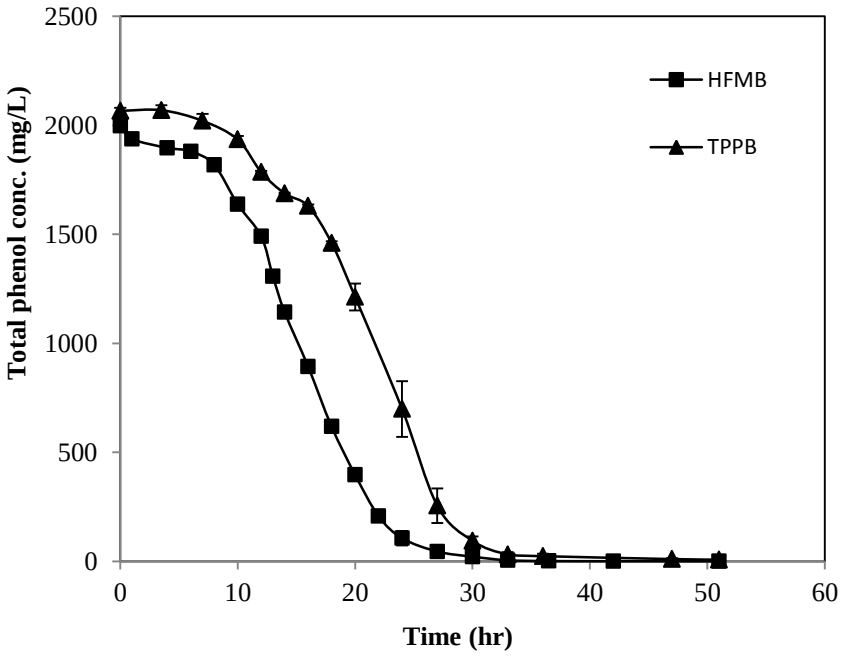

Figure 4.7 Comparison of the TPPB and HFMB of 60 cm effective length: (a) substrate distribution between the aqueous and organic phases, and the distribution in TPPB after offsetting the lag phase; (b) total phenol removal profiles

generating any secondary waste. In the absence of foaming, it was easier to aerate the aqueous phase without losing the solvent to the environment, unlike the possibility of this happening in the TPPB operation. Furthermore, the mass transfer performance of the HFMB was independent of the agitation rate which implies that there was no need for high-energy agitation for the mixing and aeration of the cell culture medium. The low agitation rates in association with total solvent recycling make the HFMB highly cost-effective as compared to the traditional aqueous/organic TPPB. The modular design of the HFMB is easier to scale-up and offers the possibility of continuous operation.

Table 4.6 Comparison of TPPB and HFMB based on the operating problems typically observed during two-phase biodegradation of phenol

Observation	TPPB	HFMB
Emulsion	Unavoidable, emulsion stability improved with cell growth	None
Foaming	Unavoidable, severe at high aeration rates	None
Phenol/Biomass analysis	Emulsions interfere with sample collection	No issue
Solvent recovery	Difficult, de-emulsification required centrifugation	Easy recycle and reuse
Mixing/Agitation rate	Intensive, depending on the solvent	Low mixing/agitation rate, optimum for cell growth
Waste handling	Sent for incineration	Organic phase recycled, aqueous phase autoclaved and discharged

4.2.6 Simultaneous Extraction and Biodegradation

Having established the operational superiority of the HFMB over conventional TPPB at comparable cell growth and biodegradation rates, the HFMB was operated for simultaneous extraction and biodegradation of phenol from the wastewater. In this

unique configuration, the organic solvent was concomitantly contacted with synthetic feed wastewater and the cell culture medium using two hollow fiber membrane contactors. Phenol was extracted from the aqueous feed to the organic solvent and simultaneously back-extracted from the solvent to the cell culture medium. The bioreactor setup is shown in Fig. 3.2. Since phenol metabolism by the microorganisms disrupted the equilibrium distribution of phenol between the three phases, a unidirectional transport of phenol from the feed to the cell culture via 2-undecanone was obtained in the HFMB, which was sustained until phenol was completely removed from both the phases.

Fig. 4.8 shows the cell growth and phenol removal profiles during simultaneous extraction and biodegradation of 1000 mg/L phenol. During the extraction and back-extraction in the first hour, phenol was distributed from the feed phase to the organic phase and the cell culture medium. The concentration of phenol in cell culture medium after one hour was about 100 mg/L. At such low phenol concentration, *P. putida* exhibited exponential growth at a specific growth rate of 0.48 hr^{-1}. The exponential growth continued for 10 hours until phenol was completely exhausted from the culture medium. During this period, about 40% of the initial substrate was metabolized with a corresponding biomass yield of 0.53 g/g. It was followed by a period of diffusion limitation, wherein cell growth and phenol removal rates slowed down significantly. The biodegradation of phenol was completed in 28 hours when feed phenol concentration dropped below 1 mg/L. The average biodegradation rate during biodegradation was 57.1 mg/L-hr, while the final biomass yield was 0.43 g/g.

Similar cell growth and phenol removal trends were observed at different phenol concentrations in the HFMB. The effects of initial phenol concentration on the biodegradation parameters in the HFMB are summarized in Table 4.7. Since the

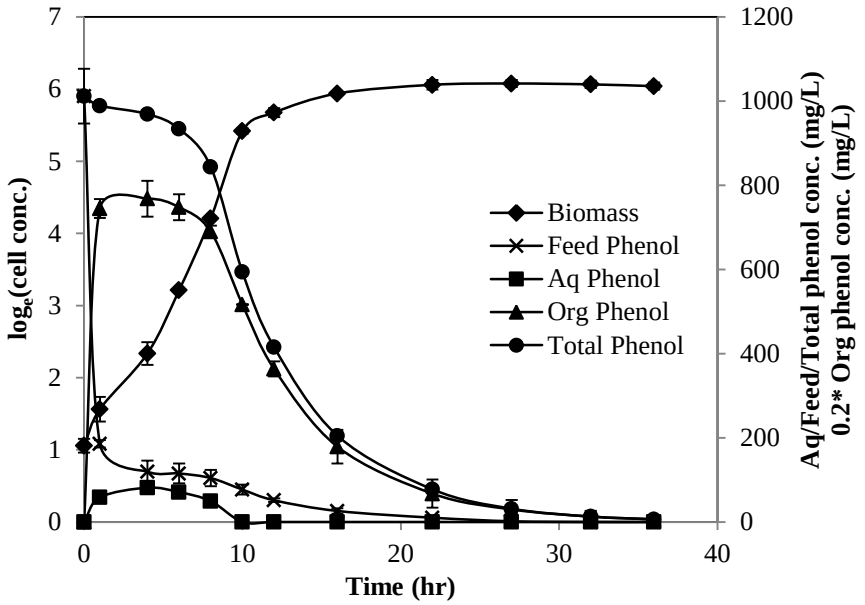

Figure 4.8 Temporal concentration profiles of biomass, aqueous phenol, organic phenol, feed phenol and total phenol in the HFMB during simultaneous extraction and biodegradation of 1000 mg/L phenol

Table 4.7 Effects of phenol concentration on biodegradation parameters in simultaneous extraction and biodegradation of phenol in the HFMB

Parameters	Phenol concentration (mg/L)		
	1000	1500	2000
Specific growth rate (hr^{-1})	0.51	0.49	0.49
Biodegradation time (hr)	28	36	43
Avg. biodegradation rate (mg/L-hr)	57.1	66.7	78.3
Biomass yield (g/g)	0.43	0.39	0.35

maximum aqueous phenol concentration was below 250 mg/L during each of these experiments, the specific growth rates remained almost constant, while the biodegradation time increased with higher phenol loading.

Although TPPBs have been explored extensively for wastewater treatment, these bioreactors were mostly operated with substrate laden organic solvent, assuming that the substrate had already been extracted into the solvent from the wastewater. In reality however, the extraction of substrate from the wastewater into the solvent and the subsequent separation of the two phases can be quite challenging. In a stirred tank, the mixing of two immiscible phases can be quite energy-intensive and it may require a large quantity of the solvent. If the solvent has a tendency to form strong emulsions, downstream separation of the two phases cannot be carried out by gravity settling and it may require another energy intensive step such as centrifugation. It is also likely that the phase separation efficiency may not be 100% and some of the emulsions with dissolved phenol could be released into the environment as secondary waste. Furthermore, phenol cannot be extracted completely from the wastewater due to the equilibrium constraints. Two-phase biodegradation in conventional TPPBs however, seldom accounts for the time and energy spent during the extraction of the substrate into the solvent which can increase the bioreactor operating cost and treatment time significantly. Recently, Juang and co-workers (2010) investigated simultaneous extraction and biodegradation of phenol in conventional stirred-tank TPPBs and they identified emulsion-formation as the biggest operational challenge. The extraction/back-extraction was carried out at low agitation speed of 100 RPM to suppress emulsion formation and to sustain the bioreactor operation. However, the low agitation speed resulted in poor mass transfer and biodegradation rates. For example, a feed of 500 mg/L phenol was treated in about 80 hours. The low agitation

rates in conventional TPPBs could reduce emulsion formation, but it resulted in poor oxygen transfer rates and oxygen limitation in the bioreactor (Nielsen *et al.* 2003). On the contrary, mass transfer in the non-dispersive HFMB was independent of the agitation speed and depended on the interfacial contact area. Aeration of the cell culture medium in single-phase was straight-forward and oxygen transfer in the HFMB did not require high agitation speeds. In addition, the absence of emulsions greatly simplified the recycling and reuse of the organic solvent.

4.3 Conclusions

A HFMB was fabricated and operated with *P. putida* to biodegrade inhibitory phenol concentrations. The equilibrium distribution of the substrate between the two-phases averted any substrate inhibition, while the hollow fiber membranes shielded the cells from the organic solvent which resulted in a better growth environment, analogous to that in the single-phase. Non-dispersive operation of the HFMB offered several operational advantages over conventional TPPBs which made the bioreactor more economical as well as eco-friendlier. Substrate removal rates in biphasic biodegradation were found to be related to the mass transfer characteristics of the bioreactor and could be easily enhanced by increasing the interfacial membrane area.

The performance of the HFMB was compared against that of conventional TPPBs. Apart from several operational advantages such as the absence of foaming and emulsion formation, it was also demonstrated that the biodegradation performance of the HFMB was better than that of the TPPB at comparable mass transfer rates. The HFMB could also ease some of the stringent criteria applied in the selection of the organic phase in TPPBs. The use of HFMB can also bring down the operating costs of

TPPBs and can facilitate the use of mixed microbial consortium which exhibit better growth and biodegradation performance.

The flexibility in the configuration and operation of the HFMB was demonstrated during simultaneous extraction and biodegradation of phenol wherein 1000-2000 mg/L phenol was extracted from the wastewater into a carrier solvent, then back-extracted into cell culture medium for biodegradation. The dispersion-free operation of the HFMB facilitated complete recycling of the solvent, while obviating the need for any energy-intensive separation processes. It can thus be concluded that the application of hollow fiber membranes in two-phase biodegradation systems is highly promising, not only to enhance the performance and effectiveness of two-phase biodegradation but also to achieve improved bioreactor economy and sustainability.

5 Kinetic Modeling of Two-Phase Biodegradation in a Hollow Fiber Membrane Bioreactor

5.1 Introduction

During two-phase biodegradation of phenol in the HFMB described in Chapter 4, biodegradation rates in the later stages of biodegradation were limited by the mass transfer of phenol which resulted in prolonged biodegradation time. Mass transfer rates in the HFMB depend on several factors including liquid flow rates in lumen and shell, interfacial area, packing density, diffusivity of the substrate in the two phases and membrane properties of porosity, tortuosity and thickness. The effects of diffusion limitation on two-phase biodegradation in the HFMB can be minimized by optimizing these parameters to achieve better mass transfer rates between the two phases.

Another important observation during HFMB operation was the attachment of *P. putida* on the polypropylene fibers and the silicone tubing which resulted in the lower observed biomass yield in suspension. Biofilm formation is inevitable in membrane bioreactors. However, the nett effect of biofilms during biodegradation of toxic pollutants in membrane bioreactors is advantageous as biofilms impart higher substrate tolerance to the microorganisms (Juang and Kao 2009; Rainer Gross 2007; Splendiani *et al.* 2003). On the other hand, it is also important to limit the biofilm thickness on the membranes because biofilms impede the transfer of the substrate from the organic to the aqueous phase. Furthermore, cell growth and substrate removal kinetics of biofilms may not be the same as that of the suspended cells. Slow biodegradation kinetics by the biofilms may result in poor bioreactor performance.

In order to enhance the two-phase biodegradation performance of the HFMB, a deeper insight into the mass transfer mechanisms and cell growth kinetics in the

HFMB is required. For HFMB stability, on the other hand, it is imperative that the effects of biofilm on the biodegradation kinetics and HFMB operation are elucidated. In this chapter, a kinetics model was developed to investigate the kinetics of simultaneous extraction and biodegradation of phenol in the HFMB. The objectives of this research were:

1. Estimate the overall mass transfer coefficients in the HFMB for the transfer of phenol from the aqueous to the organic phase and vice versa;
2. Evaluate the cell growth kinetics under substrate inhibition using the Haldane model, estimate the model parameters using experimental data, and determine the effects of biofilms on cell growth and biodegradation kinetics;
3. Model the kinetics of simultaneous extraction and two-phenol biodegradation of phenol in the HFMB;
4. Validate the model against the experimental data obtained during HFMB operation;
5. Determine the model sensitivity to the changes in the adjustable parameters; and
6. Run simulations to investigate the effects of feed phenol concentrations, lumen and shell side flow rates, interfacial mass transfer area and packing density on overall HFMB performance

Kinetics of solvent extraction in hollow fiber membrane modules have been extensively studied by several researchers (Cichy and Szymanowski 2002; Gawronski and Wrzesinska 2000; González-Muñoz *et al.* 2003; Prasad and Sirkar 1988; Shen *et al.* 2009). The common approach in these studies was the determination of overall mass transfer coefficients using experimental data or suitable empirical correlations, which were used to simulate the extraction and subsequent stripping profile of the solute. A similar approach can be followed in modeling the mass transfer of substrate

in the HFMB by substituting stripping with biodegradation. To obtain the overall mass transfer coefficients in the HFMB, the individual mass transfer resistances during extraction and back-extraction were identified, and the resistances in each step was estimated using suitable empirical correlations obtained from the literature. These local resistances were then summed up following a resistance-in-series approach to calculate the overall mass transfer coefficient.

In an extraction/stripping system used in the recovery of solutes from aqueous solutions, the concentration of the stripping solution is quite high and usually does not change significantly during the separation. On the contrary, the substrate removal rate during biodegradation depends on the biomass concentration in the bioreactor which increases with substrate metabolism. The cell growth rate may depend on many factors including temperature, pH and dissolved oxygen concentrations. If the substrate is toxic, for example phenol, the cell growth rate also depends on the initial substrate concentration. The cell growth kinetics here was modeled using the Haldane equation and the model parameters were determined using the experimental data on cell growth at different initial phenol concentrations in suspension. The Haldane model was then used to predict the specific growth rates in the HFMB.

The mass transfer of phenol from the feed wastewater to the cell culture medium via the organic solvent in the HFMB was driven by the concentration gradient between these phases, depending on the distribution coefficient of phenol. The disequilibrium in the HFMB resulted due to the metabolism of phenol in the cell culture medium, which was the driver for the unidirectional transport of phenol from the feed wastewater to the cell culture medium. Based on these, the model equations for the rate of change of phenol and cell concentrations in the three phases were formulated and solved using ode45 in MATLAB.

The kinetics model was validated against the experimental data obtained during the simultaneous extraction and biodegradation of phenol at a feed phenol concentration of 1000 mg/L, and the adjustable parameters in the model equations were determined. The model sensitivity to the fluctuations in these adjustable parameters was then examined by varying these parameters within ±20% interval. Finally, the kinetics model was used to predict the HFMB performance at various initial phenol concentrations, flow rates, effective membrane lengths and fiber packing density.

5.2 Theory

5.2.1 Cell Growth Kinetics

The cell growth kinetics on phenol biodegradation is often modeled using the Haldane equation (Wang and Loh 1999):

$$\mu = \frac{\mu_m C_{aq}}{K_s + C_{aq} + \frac{(C_{aq})^2}{K_I}} \tag{5.1}$$

where μ is the specific growth rate (hr^{-1}), μ_m is the maximum specific growth rate (hr^{-1}), K_s is the substrate affinity constant (mg/L), K_I is the substrate inhibition constant (mg/L), and C_{aq} is the phenol concentration in the cell culture medium. The values of the model parameters μ_m, K_s and K_I were estimated from the experimental data.

In the HFMB, cell growth took place partly in suspension and partly immobilized on the fibers. Therefore, the cell growth rates and biomass yields observed in suspension were not the actual biomass present in the bioreactor at any time. To account for the loss of biomass on the membrane surfaces, an adjustable parameter b was used to estimate the observed specific growth rate and biomass yield such that:

$$\mu_{obs} = (1 - b)\mu \tag{5.2}$$

The cell death rate and the maintenance requirements were assumed to be negligible. The yield coefficient (Y_{xs}) used here was 0.5 ± 0.05 g/g. During substrate inhibition, the yield coefficient decreases with increasing phenol concentrations (Wang and Loh 1999). However, for the concentration range studied in the HFMB, phenol concentration in the cell culture medium varied in the range of 100-250 mg/L, at which substrate inhibition was not very severe and Y_{xs} was nearly constant. It should also be emphasized that Y_{xs} in this model refers to the maximum biomass yield in the HFMB, and not the final biomass yield which was much lower.

5.2.2 Overall Mass Transfer Coefficients

During simultaneous extraction and biodegradation of phenol in the HFMB, the feed wastewater and the cell culture medium were transported in the lumen of the respective membrane contactors, whereas the organic solvent 2-undecanone was circulated in the shell side of both the contactors as shown in Fig. 3.2. The model for the mass transfer of phenol from feed to the solvent, and from solvent to the cell culture is based on the following assumptions (Bocquet *et al.* 2005; Gabelman and Hwang 1999; Shen *et al.* 2009; Younas *et al.* 2008):

- Equilibrium was reached at the fluid/fluid interface;
- Fluids were immiscible;
- Organic solvent wetted the pores and the aqueous/organic interface was immobilized in the membrane pores;
- Pore size and wetting characteristics were uniform throughout the membrane;
- Curvature of the fluid/fluid interface did not affect the rate of diffusion, partition coefficient or interfacial area significantly;
- No solute transport occurred through the non-porous parts of the membrane;

- Distribution coefficient of the solute was constant in the concentration range studied;
- Mass transfer was correctly described by the boundary layer conditions; and
- Liquid flow in the lumen was laminar.

Fig. 5.1 shows a schematic diagram of the transfer of phenol between the aqueous feed and the organic solvent phase. The transfer of phenol from the aqueous feed in the lumen to the organic solvent in the shell through the solvent wetted hydrophobic hollow fiber membranes in the HFMB can be described by:

$$J_{feed} = K_{aq} A_{in} \left(C_{feed} - C^*_{feed} \right) \tag{5.3}$$

where J_{feed} is the flux of phenol from the feed solution to the solvent, C_{feed} is the phenol concentration in the aqueous phase, C^*_{feed} is a hypothetical phenol concentration in the aqueous phase that is in equilibrium with the phenol concentration in the solvent phase, A_{in} is the interfacial area on the lumen side and K_{aq} is the overall mass transfer coefficient on the aqueous side. Likewise, the flux in the back-extraction of phenol from the solvent to the culture medium can be expressed as:

$$J_{org} = K_{org} A_{out} \left(C_{org} - C^*_{org} \right) \tag{5.4}$$

where C_{org} is the phenol concentration in the organic phase, C^*_{org} is a hypothetical phenol concentration in the organic phase that is in equilibrium with the phenol concentration in the aqueous phase, A_{in} is the interfacial area on the shell side and K_{org} is the overall mass transfer coefficient on the solvent side.

The overall mass transfer coefficients can be determined experimentally using the relationship between the flux and the concentration gradient. Alternatively, K_{org} and K_{aq} can also be determined using a theoretical approach, using suitable empirical

correlations obtained from literature. Both of these strategies are based on the resistance in series approach.

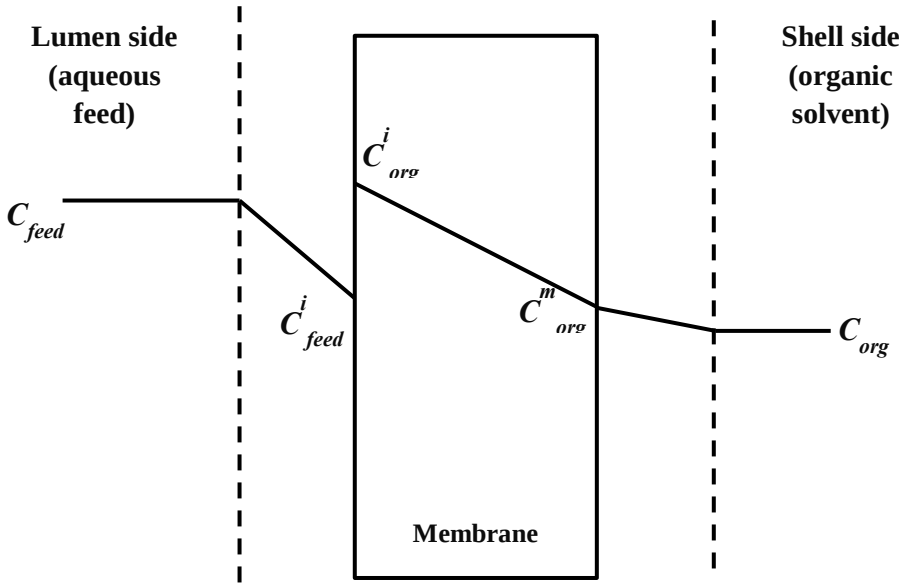

Figure 5.1 Schematic diagram of mass transfer process in extraction of phenol from feed solution to the organic solvent

5.2.3 Resistance in Series Model

With reference to Fig. 5.1, the movement of phenol from the aqueous to the organic phase through solvent wetted hydrophobic membranes takes place in four steps (Gabelman and Hwang 1999):

1. Phenol diffusion through the aqueous boundary layer;
2. Equilibrium distribution of phenol at the aqueous/membrane interface with solvent-filled membrane pores;
3. Phenol diffusion through the pores filled with the organic solvent; and
4. Phenol diffusion through the organic boundary layer.

At steady state, the flux of phenol at each of the abovementioned steps should be the same and it should be equal to the net gain of the solute in the organic phase. The mass transfer flux, *J* for each of the consecutive stages can be written as:

$$J_1 = k_t A_{in}\left(C_{feed} - C^i_{feed}\right) \tag{5.5}$$

$$J_2 = k_m A_{lm}\left(C^i_{org} - C^m_{org}\right) \tag{5.6}$$

$$J_3 = k_s A_{out}\left(C^m_{org} - C_{org}\right) \tag{5.7}$$

where k_t, k_m and k_s are the local mass transfer coefficient of the lumen side, membrane and shell side, respectively; C^i_{feed} and C^i_{org} are the phenol concentrations at the aqueous and organic side of the interface, respectively; C^m_{org} is the phenol concentration in the solvent filled membrane pores, and; A_{lm} is the log mean area of the membrane. Analogous equations can be written for the transfer of phenol from the organic phase to the aqueous cell culture medium.

Based on the detailed derivations by Bocquet and co-workers (2005), the resulting total resistance is the sum of the three individual resistances:

$$R = R_{aq} + R_m + R_{org} \tag{5.8}$$

which can be written as,

$$R = \frac{1}{\pi L}\left(\frac{1}{d_{in}k_t} + \frac{1}{d_{lm}k_m P} + \frac{1}{d_{out}k_s P}\right) \tag{5.9}$$

The overall mass transfer coefficient K_{aq}, based on the aqueous phase in the lumen side can then be calculated as:

$$\frac{1}{K_{aq}} = \frac{1}{k_t} + \frac{d_{in}}{d_{lm}k_m P} + \frac{d_{in}}{d_{out}k_s P} \tag{5.10}$$

where d_{in}, d_{out} and d_{lm} are the inside, outside and log mean diameter of the hollow fiber membranes. P is the distribution coefficient of phenol and L is the effective length of the membrane fibers. The log mean diameter is calculated as:

$$d_{lm} = \frac{(d_{out} - d_{in})}{\ln\left(\frac{d_{out}}{d_{in}}\right)} \tag{5.11}$$

The movement of substrate from the organic phase to the cell culture medium takes place in an analogous manner and the overall mass transfer coefficient K_{org}, in the shell side can be calculated as:

$$\frac{1}{K_{org}} = \frac{P}{k_t} + \frac{d_{in}}{d_{lm}k_m} + \frac{d_{in}}{d_{out}k_s} \tag{5.12}$$

5.2.4 Estimation of Mass Transfer Coefficients

A. Estimation of k_m

The local mass transfer coefficient k_m is a function of membrane properties such as porosity (ε), tortuosity (τ), thickness (δ) and solute diffusivity in the solvent-filled pores (D_{org}) and was calculated from (Prasad and Sirkar 1988):

$$k_m = \frac{\epsilon D_{org}}{\tau\delta} \tag{5.13}$$

The values of porosity, tortuosity and thickness were obtained from the manufacturer, whereas the diffusivity of phenol in 2-undecanone was estimated from the Wilke-Chang correlation as:

$$D_{org} = \frac{7.4 \times 10^{-8}(\psi_B M_B)^{0.5} T}{\eta V_A^{0.8}} \tag{5.14}$$

where D_{org} is the diffusivity (cm^2/s) of phenol in 2-undecanone, T is the absolute temperature (K), V_A is the molar volume (cm^3/mol) of phenol as liquid at its normal

boiling point, ψ_B is the association parameter for 2-undecanone, M_B is the molecular weight of 2-undecanone and η is the viscosity of 2-undecanone. Since ψ_B for 2-undecanone could not be found in literature, it was treated as an adjustable parameter.

B. Estimation of k_t

The mass transfer coefficients in membrane contactors could be predicted using several empirical correlations available in the literature, in terms of the Sherwood number (*Sh*), the Schmidt number (*Sc*) and the Reynolds number (*Re*). A general form of the equation is:

$$Sh \propto Sc^a Re^b f \tag{5.15}$$

where *a*, *b* are constants and *f* is some function of the geometry.

The flow of the aqueous phase in the lumen side was laminar. The most well-known Leveque equation (Gabelman and Hwang 1999) was used to estimate of the lumen side mass transfer coefficient, k_{aq}:

$$Sh = 1.62\left[\frac{d_{in}}{L}\, Sc\, Re\right]^{0.33} \tag{5.16}$$

The expression for the Sherwood, the Schmidt and the Reynolds numbers are given by:

$$Sh = \frac{k_t d_{in}}{D_{aq}} \tag{5.17}$$

$$Sc = \frac{\eta_{aq}}{\rho_{aq} D_{aq}} \tag{5.18}$$

$$Re = \frac{\rho_{aq} v_{aq} d_{in}}{\eta_{aq}} \tag{5.19}$$

where ρ_{aq} is the density of the aqueous phase, v_{aq} is the velocity in the lumen side, η_{aq} is the viscosity of the aqueous medium; D_{aq} is the diffusivity of phenol in the aqueous medium.

C. Estimation of k_s

The determination of the shell side mass transfer coefficient is the most challenging task in obtaining the overall mass transfer coefficient in membrane contactors. The challenges arise mostly because of the flexible and irregular distribution of the hollow fibers in the shell side which results in changes in the flow pattern from one module to another, and even in the same module during different runs. Over the years, several empirical correlations have been proposed for determining k_s, each of which result in a different Sherwood number. The correlation proposed by Prasad and Sirkar (1988) is applicable for the operating conditions ($0<Re<500$, $0.04<\varphi<0.4$) in the HFMB and it was used to predict k_s in this research:

$$Sh = \beta(1-\varphi)\frac{d_h}{L}\,Sc^{0.33}Re^{0.6} \tag{5.20}$$

where φ is the packing density of the membrane module, d_h is the hydraulic diameter and β is constant. The value of β for hydrophobic membranes was 5.85.

5.3 Model Equations

The models equations were formulated based on four material balances around the HFMB. The balances were made for cell concentration in the aqueous phase and phenol concentrations in the feed solution, the organic solvent and the cell culture medium.

$$\frac{dX}{dt} = (1-b)\mu X \tag{5.21}$$

$$\frac{dC_{feed}}{dt} = -\frac{K_{aq}A_{in}}{V_{aq}}\left(C_{feed} - \frac{C_{org}}{P}\right) \quad (5.22)$$

$$\frac{dC_{org}}{dt} = \frac{K_{aq}A_{in}}{V_{org}}\left(C_{feed} - \frac{C_{org}}{P}\right) - \frac{K_{org}A_{out}}{V_{org}}\left(C_{org} - PC_{aq}\right) \quad (5.23)$$

$$\frac{dC_{aq}}{dt} = \frac{K_{org}A_{out}}{V_{aq}}\left(C_{org} - PC_{aq}\right) - \frac{\mu X}{Y_{XS}} \quad (5.24)$$

where X is biomass concentration (mg/L) in the culture medium, and V_{aq} and V_{org} are the volume of the aqueous and the organic phases, respectively. Based on the equations set out in the preceding pages, the adjustable parameters were identified: the association parameter ψ_B [Eqn. (5.14)] and the loss of suspension biomass concentration, b [Eqn. (5.2)].

5.4 Results & Discussion

5.4.1 Parameter Estimation

In order to determine the Haldane model parameters, batch suspended cell culture experiments at different phenol concentrations were conducted. The model parameters μ_m, K_S and K_I were obtained as 1.29 hr^{-1}, 46.0 mg/L and 169.5 mg/L, respectively, by curve-fitting using non-linear least-square techniques (Fig. 5.2). The correlation between the experimental and estimated values of the specific growth rates was found to be excellent (R^2 = 0.99).

For determination of D_{org} using the Wilke-Chang correlation [Eqn. (5.14)], the values for M_B and η were obtained as 170.33 and 1.61 cP, respectively, from the Material Safety Data Sheet (MSDS) of 2-undecanone. The molar volume of phenol at its normal boiling point, V_A, was obtained from literature as 84.7 cm^3/mol (Juang *et al.* 2012). The real challenge was the estimation of the association parameter ψ_B which is usually assumed unity for organic solvents (Juang *et al.* 2012; McCabe *et al.* 2005;

Shen *et al.* 2009). However, assuming ψ_B = 1 for 2-undecanone overestimated the K_{org} and K_{aq} values, which resulted in poor correlation with the experimental data. Through a mathematical fit of Eqns. (5.21) to (5.24) to the experimental data for operation in the HFMB at 1000 mg/L feed phenol concentration, ψ_B was estimated to be 0.3, and the corresponding D_{org} value was 2.76 x 10^{-10} m^2/s. From literature, the diffusivity of phenol in organic solvents have been reported to be in 10^{-9}-10^{-10} m^2/s range (Juang *et al.* 2010; Shen *et al.* 2009; Teresa *et al.* 2007) and the calculated D_{org} was within the acceptable range.

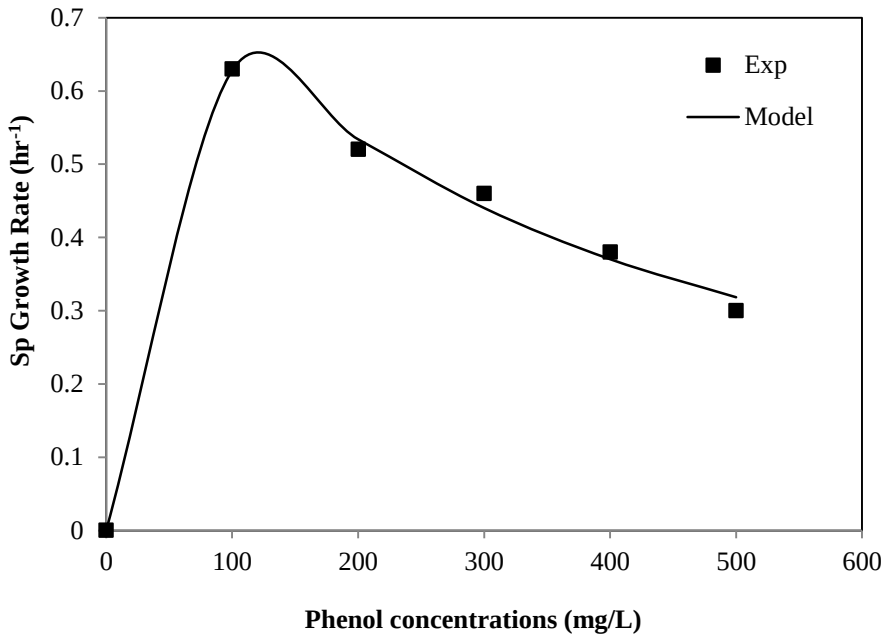

Figure 5.2 Specific growth rate of *P. putida* (ATCC 11172) on phenol

The parameter *b*, which accounts for the attachment of *P. putida* on the polypropylene fibers and tubing, was estimated by trial and error. It was observed that the specific growth rates in the HFMB was about 20% lower than the predicted growth rates using the Haldane equation for suspension cell culture at the maximum phenol concentration observed in the cell culture medium. Therefore, *b* was initially assumed

0.2. A better fit between the experimental and modeled cell growth profiles was obtained at b = 0.18, which represented the fraction of biomass attached to the fibers and the silicone tubings.

5.4.2 Model Validation and Analysis

Fig. 5.3 shows the experimental and modeled biomass and phenol concentration profiles during simultaneous extraction and biodegradation of 1000 mg/L phenol in the HFMB. It can be seen that the model corroborate the experimental data very well. The regression coefficients (R^2) for the experimental and modeled concentration profiles of biomass, feed phenol, organic phenol and aqueous phenol were 0.98, 0.96, 0.98 and 0.93, respectively.

The physical properties of the aqueous and the organic phases, the equilibrium parameters and the membrane module characteristics used to determine the local mass transfer coefficients are listed in Table 5.1. The membrane characteristics from Table 3.2 were used to compute the packing density, interfacial areas and superficial velocity. The physical properties of the aqueous and organic liquids were mostly obtained from the literature. The diffusivity of phenol in aqueous phase was obtained from Shen *et al.* (2009).

The values of the local mass transfer coefficients were determined at shell side flow rate (Q_{org}) of 4 mL/min and lumen side flow rate (Q_{aq}) of 6 mL/min. Using Eqns. (5.11), (5.14) and (5.18), the local mass transfer coefficients k_m, k_t and k_s were estimated as 9.2 x 10^{-7}, 8.32 x 10^{-6}, and 5.03 x 10^{-8} m/s, respectively. These values were substituted in Eqns. (5.8) and (5.10), and the overall mass transfer coefficients K_{aq} and K_{org} were calculated as 1.51 x 10^{-6} and 4.58 x 10^{-8} m/s, respectively. The

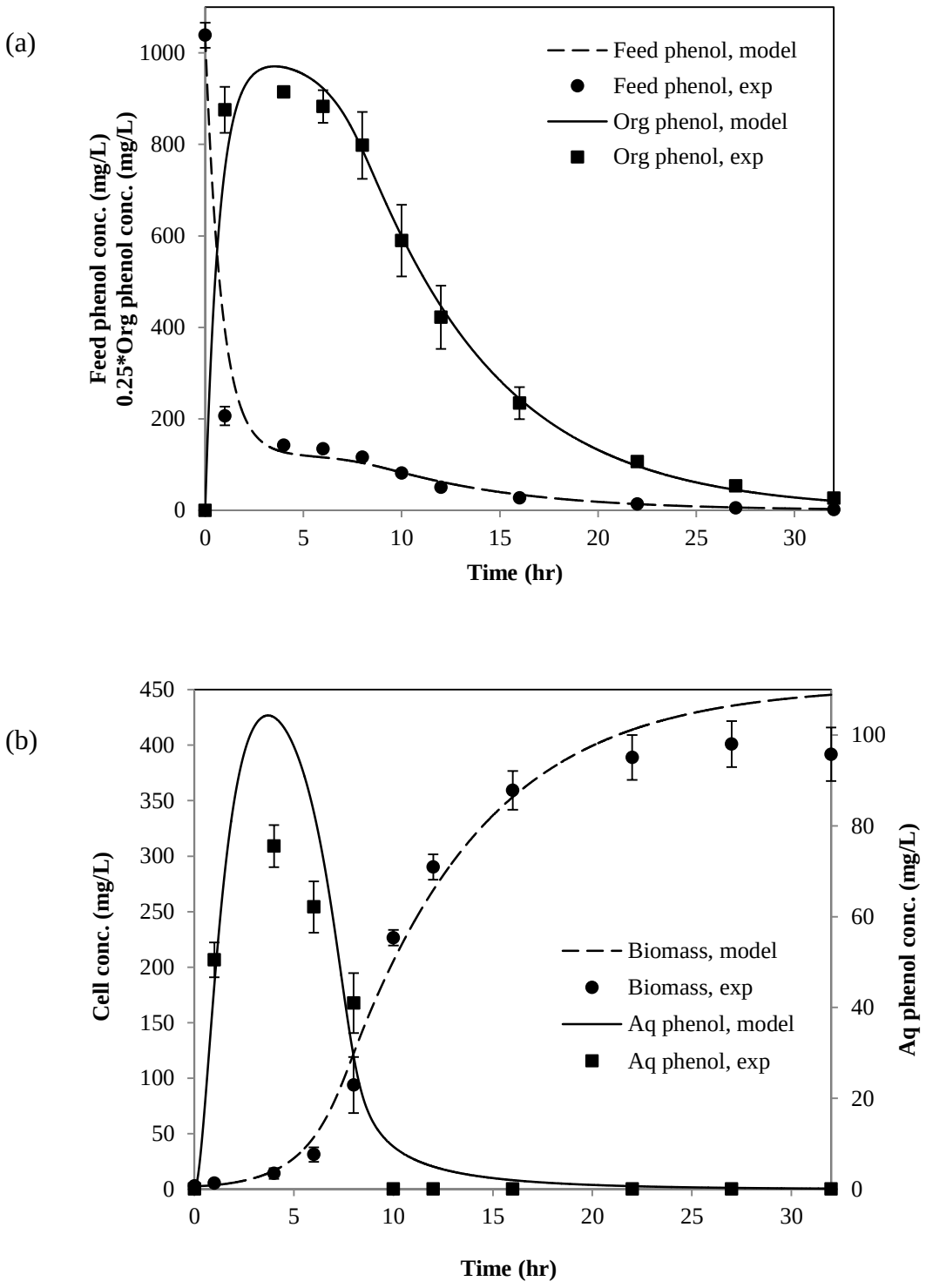

Figure 5.3 Two-phase biodegradation of 1000 mg/L of phenol in the HFMB: (a) feed and organic phenol concentration profile; and, (b) biomass and aqueous phenol concentration profile

Table 5.1 Physical properties, equilibrium parameters and membrane characteristics used for simultaneous extraction and biodegradation in HFMB

Characteristics	Values
Packing density, φ	0.3333
Interfacial area, lumen (m^2)	0.0396
Interfacial area, shell (m^2)	0.0466
Porosity, ε	0.5
Tortuosity, τ	3
Viscosity, aqueous phase (cP)	0.8
Viscosity, organic phase (cP)	1.61
Density, aqueous phase (kg/m^3)	1000
Density, organic phase (kg/m^3)	830
Phenol diffusivity, aqueous phase (m^2/s)	1.03×10^{-9}
Phenol diffusivity, organic phase (m^2/s)	2.76×10^{-10}
Distribution coefficient, P	33
Hydraulic diameter (m)	6.6×10^{-4}

fractional mass transfer in each step was calculated and these are listed in Table 5.2, along with the mass transfer coefficients.

The overall mass transfer coefficient K_{aq} was of the same order of magnitude as those reported in recent studies in phenol extraction using kerosene/TBP (Shen *et al.* 2009), decanol (González-Muñoz *et al.* 2003) and Cyanex 923 (Cichy *et al.* 2005; Teresa *et al.* 2007) as the organic phase. On the other hand, the value of K_{org} calculated here was lower than those reported in other studies which could be due to the low flow rate

of the organic solvent in the HFMB or due to the difference in the correlations used for k_s estimation. Shen and co-workers (2009) reported that the Eqn. (5.20) underestimated the K_{org} value and to obtain a better fit to their experimental data, they had modified the β value from 5.85 to 43.5.

Table 5.2 Mass transfer coefficients at the operating conditions in the HFMB

Mass transfer coefficient	Values (m/s)	Percentage resistance
k_{aq}	8.32×10^{-6}	18
k_m	9.20×10^{-7}	5
k_{org}	5.03×10^{-8}	77
K_{aq}	1.51×10^{-6}	-
K_{org}	4.58×10^{-8}	-

The value of k_m in the HFMB was lower than those reported in other polypropylene membrane contactors with comparable porosity and tortuosity but higher thickness (Teresa *et al.* 2007). Therefore, it is possible that the low K_{org} could have resulted from the lower diffusivity of phenol in 2-undecanone. The overall volumetric mass transfer coefficients $K_{org}A = 5.34 \times 10^{-8}$ sec^{-1} and $K_{aq}A = 2.99 \times 10^{-7}$ sec^{-1} in the HFMB were also lower than those reported in conventional TPPBs. For example, Juang and co-workers (2012) reported the volumetric mass transfer coefficient $K_{org}A$ and $K_{aq}A$ as 9.8×10^{-5} and 1.6×10^{-3} sec^{-1}, respectively, using kerosene as the organic phase at an agitation rate of 300 RPM. Since the mass transfer coefficients in agitated two-phase systems depend on the rate of agitation, Juang and his co-workers (2010) reported a lower K_{org} of 7.83×10^{-6} m/s, for the same system at a lower agitation speed of 120 RPM. In another study, Cruickshank and co-workers (2000a) reported

$K_{org}A$ of 0.069 sec^{-1} in a commercial fermenter operating at 250 RPM using 2-undecanone as the organic phase. Our low values of the mass transfer coefficients could be the reason for the presence of diffusional limitations in the HFMB, which is usually not observed in conventional TPPB.

The fractional resistance to mass transfer was highest in the organic side boundary layer and contributed about 77% of the total resistance. The resistance in the aqueous boundary layer was comparatively smaller at 18%, while the resistance in the solvent-filled membrane pores was negligible, and barely contributed 5% of the total resistance. These results indicate that the movement of phenol from the organic side boundary layer was the slowest and it was also the rate-controlling step.

During biodegradation of 1000 mg/L phenol in the HFMB, the maximum phenol concentration observed in the cell culture medium and the organic phase were lower than those predicted using the developed kinetics model. This difference could have resulted from the adsorption of phenol on the polypropylene fibers. The results in Chapter 4 have shown that up to 10% of the total phenol initially supplied to the HFMB could be adsorbed on the polypropylene fibers. Since the model did not account for the adsorption, a higher total phenol concentration was modeled as compared to that in the experimental profile. Fig. 5.4 shows the total phenol concentration profile (experimental and model validation, R^2 = 0.99) for the biodegradation of 1000 mg/L phenol in the HFMB. A sharp drop in the total phenol concentration can be seen after one hour of HFMB operation due to the adsorption of phenol on the fibers. On the other hand, there was little change in phenol concentration in the modeled profile for the same time period. This difference between the experimental and predicted values of total phenol is also reflected in the predicted organic and aqueous phenol concentrations in the HFMB.

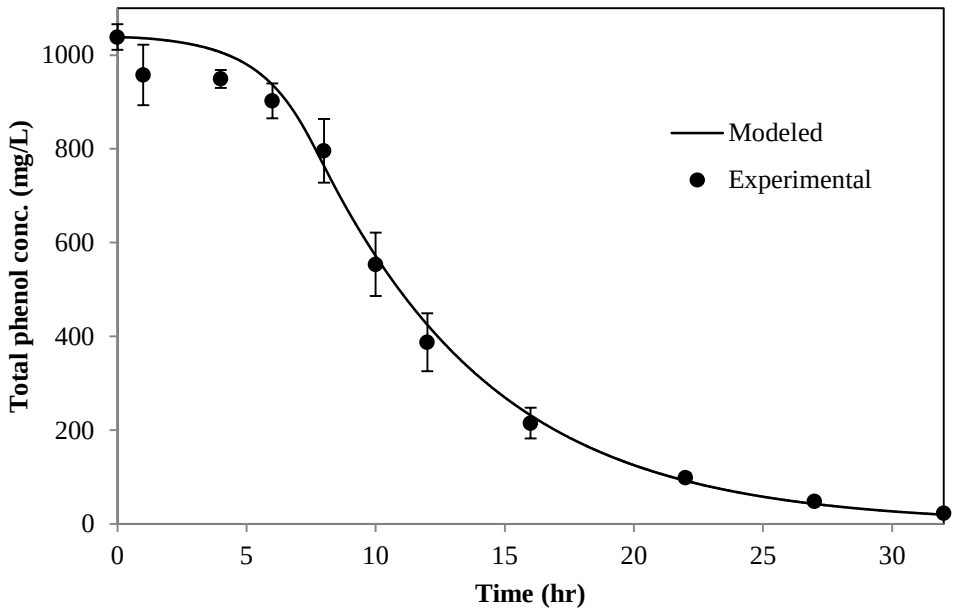

Figure 5.4 Experimental and modeled total phenol concentration profiles in the biodegradation of 1000 mg/L phenol in the HFMB

5.4.3 Parameter Sensitivity Analysis

The sensitivity of the kinetics model to the adjustable parameters ψ_B and *b* was examined by varying these parameters in the range of ±20%, and assessing their effects on cell growth and phenol removal profiles in the HFMB. It is evident from Eqns. (5.21) to (5.24) that parameter *b* did not affect the mass transfer coefficients. The changes due to variations in *b* were reflected only in the suspended cell concentration. Since cell growth and biodegradation kinetics of the biofilms and the suspended cells were not different, the parameter *b* did not affect the total cell concentration and the biodegradation rates. Fig. 5.5a shows the effects of parameter *b* on suspended cell concentration in the bioreactor. It can be seen that the increase in *b* by 20% resulted in a slower cell growth rate and lower biomass yield in suspension, while the contrary was true when *b* was reduced by 20%. These changes in *b* had no effect on phenol concentration profiles (data not shown), which shows that the HFMB

performance was relatively unaffected by the presence of cell attachment on the membranes and the silicone tubings.

In contrast, parameter ψ_B and the resulting D_{org} directly affected the mass transfer resistance of the solvent-wetted membrane pores. Consequently, changes in ψ_B had significant effects on the overall mass transfer coefficients K_{aq} and K_{org}, and the biodegradation rates. Fig. 5.5b shows the effects of the fluctuations in the association parameter ψ_B on organic phase phenol concentration at feed phenol concentration of 1000 mg/L. At ψ_B = 1, which is the most common value of ψ_B used in literature for many solvents, D_{org} was quite high and mass transfer resistance was low. As a result, diffusion of phenol through the membranes was faster and the deviation between the experimental and modeled data was large. The best fit was obtained at ψ_B = 0.3, when R^2 between the experimental and modeled biodegradation profiles was higher than 0.98.

5.4.4 Model Simulations

Having validated the model against experimental data at 1000 mg/L phenol and the values of the adjustable parameters ψ_B and b determined, the model was used to simulate the HFMB performance at 1500 and 2000 mg/L feed phenol concentrations. Fig. 5.6 and 5.7 show a comparison of the model simulations against the experimental data. It can be seen that the model predictions matched the experimental data excellently. A few interesting noteworthy points observed were: (a) at higher phenol loading, the microorganisms experienced higher substrate inhibition and the specific growth rates and the biomass yields were comparatively low; (b) with the increase in feed phenol concentration, a higher amount of phenol was also adsorbed on the polypropylene fibers. As a result, the difference between the maximum phenol

(a)

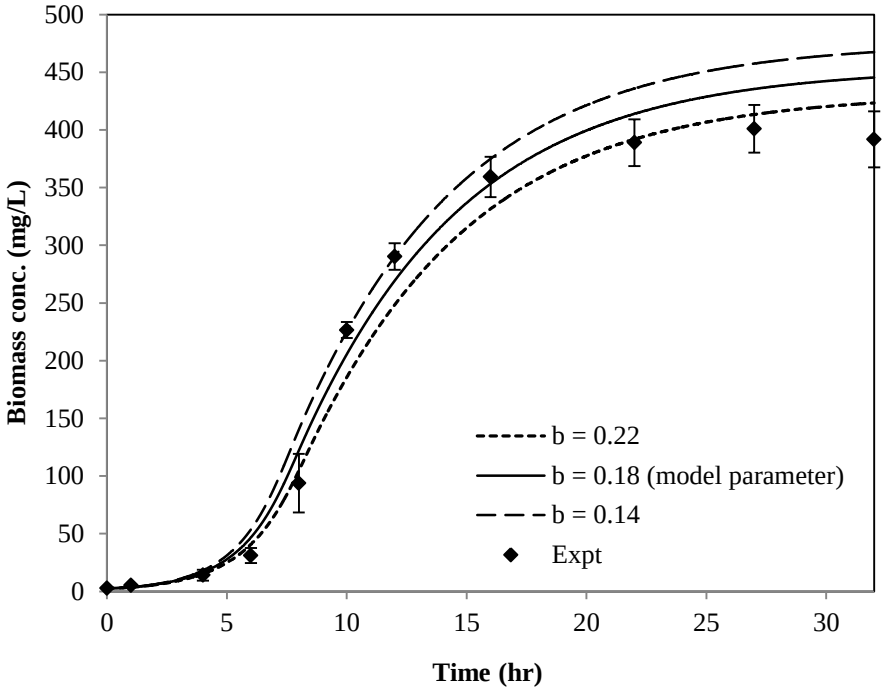

(b)

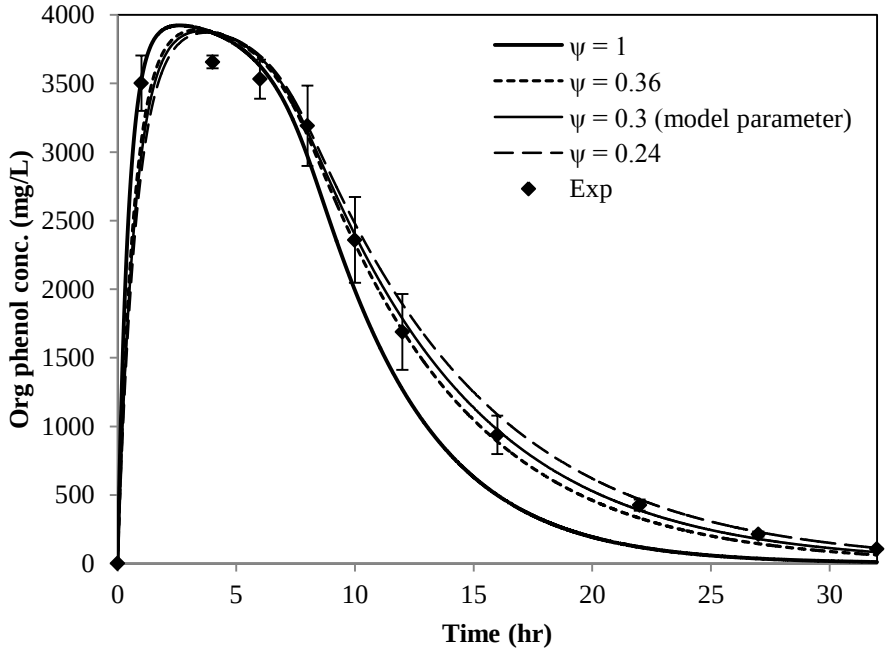

Figure 5.5 Parameter sensitivity: (a) effects of *b* on the cell growth; and, (b) effects of ψ_B on the organic phase phenol concentration

concentrations in the aqueous and the organic phases obtained experimentally and those predicted by the model differed quite discernibly. Apart from these, all the other effects of increase in the substrate concentrations were reflected by the model predictions. It can therefore be concluded that the kinetics model developed could predict the performance of the HFMB at different feed phenol concentrations with reasonable accuracy.

The biodegradation rates in two-phase biodegradation systems depend mainly on the mass transfer rates of the substrate from the NAP to the aqueous medium. If the flux of the substrate from the organic phase is lower than the substrate consumption rate of the cells, the cell growth and the biodegradation rates are limited by the slower mass transfer rate of the substrate. During two-phase biodegradation at high agitation rates in conventional TPPBs, the mass transfer coefficients are higher and the substrate is depleted concomitantly in the aqueous and the organic phases, which signifies the absence of diffusion limitation (Collins and Daugulis 1997; Zilouei *et al.* 2008). In the HFMB, however, C_{aq} was depleted much quicker than C_{org} and C_{feed}, which resulted in diffusion limitation. For example, during simultaneous extraction and biodegradation of 1000 mg/L phenol in the HFMB, C_{aq} dropped to zero in about 12 hours, at which C_{org} was 1688 mg/L, while X was 290 mg/L. The calculation of flux using Eqn. (5.4) at that time gave J_{org} = 13 mg/hr, whereas the phenol consumption rate at such high cell concentration would be close to 60 mg/hr. At these conditions, even if only 25% of the cells were viable, biodegradation rates would be controlled by the slower rate of diffusion. In order to alleviate the occurrence of this nutrient limitation in the HFMB, two strategies are proposed: (1) improvement in the overall mass transfer coefficients, K_{aq} and K_{org}, through changing the bioreactor

(a)

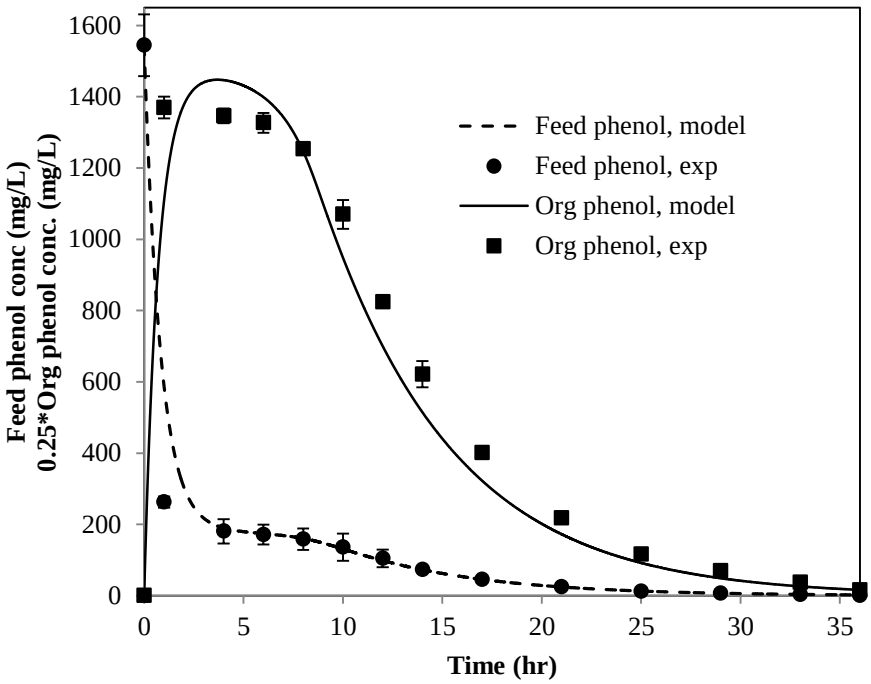

(b)

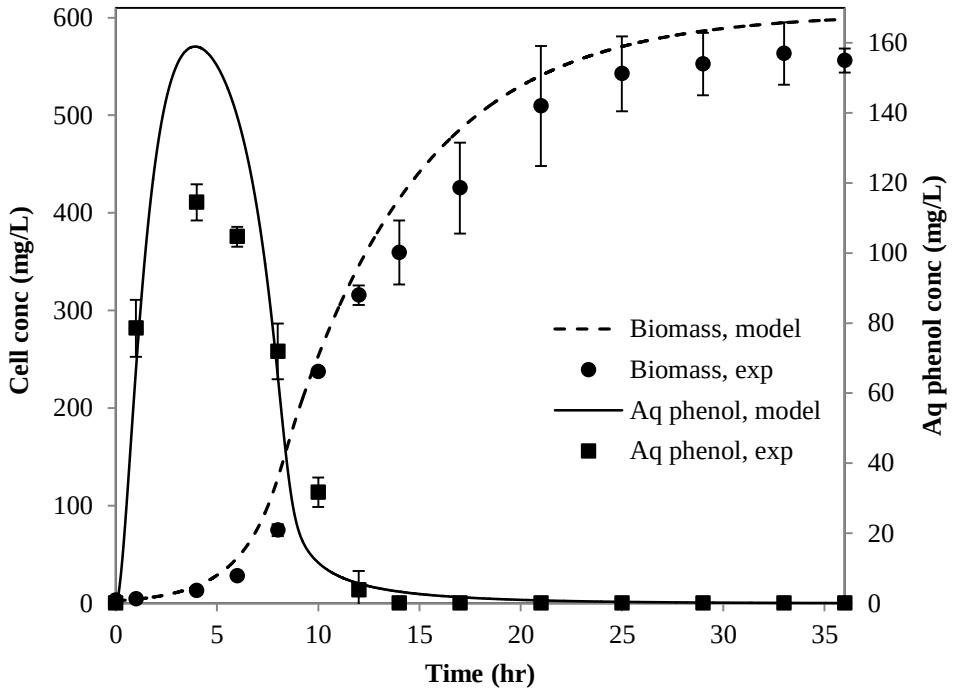

Figure 5.6 Comparison of the experimental data and model simulations at feed phenol concentration of 1500 mg/L: (a) feed and organic phenol concentration; and, (b) aqueous phenol and biomass concentrations

(a)

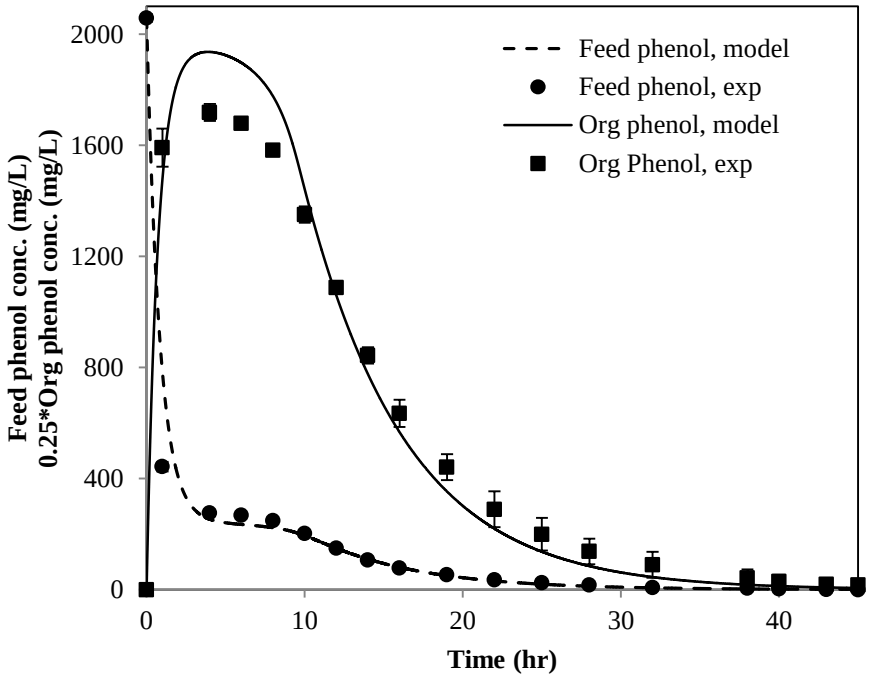

(b)

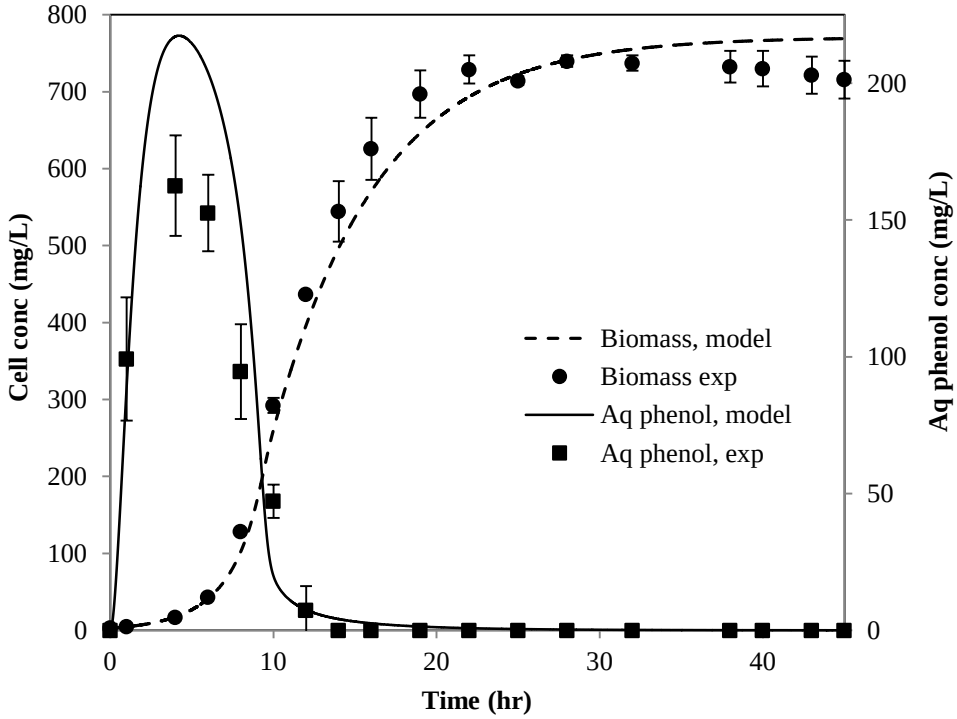

Figure 5.7 Comparison of the experimental data and model simulations at feed phenol concentration of 1500 mg/L: (a) feed and organic phenol concentration; and, (b) aqueous phenol and biomass concentrations

hydrodynamics or membrane properties, and (2) increase the interfacial membrane area by changing the length or the number of fibers in the membrane contactors. The mass transfer coefficients, K_{aq} and K_{org}, have been calculated based on the resistances in series approach, and lowering these resistances either by operating the HFMB at higher flow rates or higher interfacial area could significantly improve the biodegradation performance of the HFMB.

The efficacy of the kinetics model in predicting the HFMB performance at different operating conditions was demonstrated by carrying out simulations at different flow rates, packing density and membrane area. Fig. 5.8a shows the effects of Q_{aq} on cell growth and phenol removal profiles at C_{feed} = 1000 mg/L in the HFMB. In this simulation, Q_{aq} was doubled from 6 mL/min to 12 mL/min, while Q_{org} was kept constant at 4 mL/min. A higher Q_{aq} resulted in only marginal increase in K_{aq} and K_{org}, to 4.76 x 10^{-8} and 1.57 x 10^{-6} m/s, respectively, and the effects on cell growth and biodegradation were negligible. On the other hand, when Q_{org} was increased from 4 to 8 mL/min at a fixed Q_{aq} of 6 mL/min, K_{aq} and K_{org} increased to 6.21 x 10^{-8} and 2.05 x 10^{-6} m/s, respectively. This resulted in a significant improvement in the biodegradation performance of the HFMB as can be seen in Fig. 5.8b. These results evinced that the maximum resistance to the mass transfer of phenol was present in the organic boundary layer on the shell side and the diffusion of phenol through the organic boundary layer was the rate limiting step.

Contrary to the effects of the flow rates, increasing the length of the fibers (L) to 60 cm resulted in lower K_{aq} and K_{org} values of 2.52 x 10^{-8} and 8.3 x 10^{-7} m/s, respectively. However, the change in L also doubled the interfacial mass transfer area, which could offset the effects of the low mass transfer coefficients. The overall effect

(a)

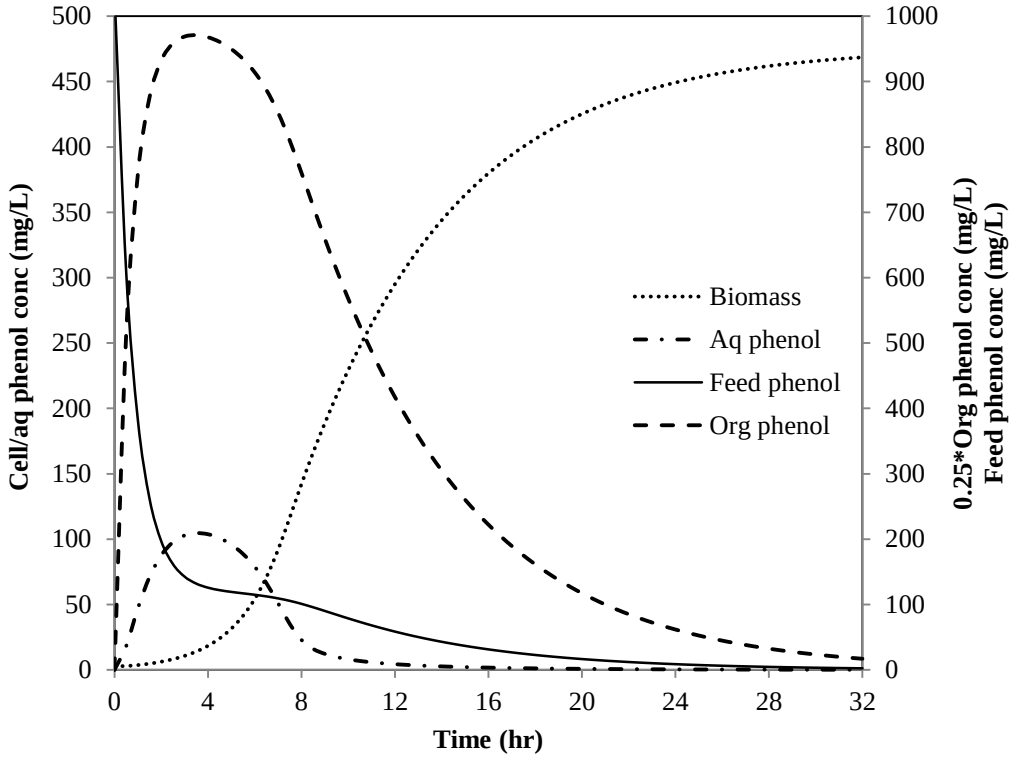

(b)

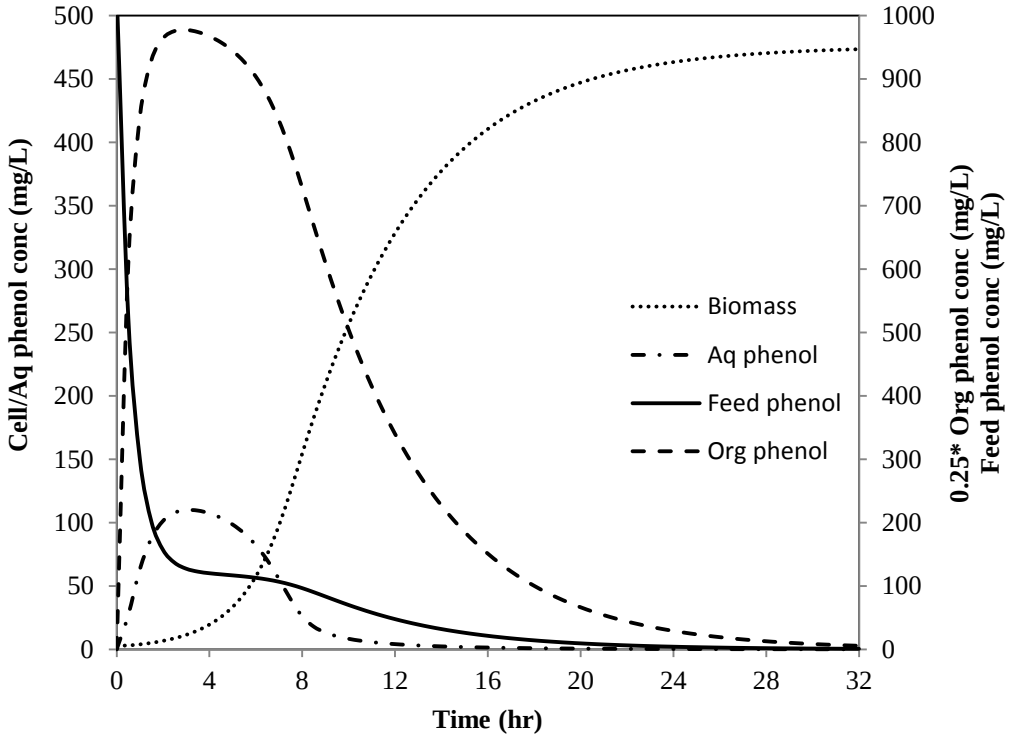

Figure 5.8 Effects of flow rate on HFMB performance: (a) lumen side flow rate of 12 mL/min; and (b) shell side flow rate of 8 mL/min

of changing the membrane length was enhanced mass transfer rate of phenol. Fig. 5.9a shows rapid equilibrium between the aqueous and the organic phases at L = 60 cm. The membrane length did not have any significant effects on the cell growth rate or biomass yield, but initial equilibration was attained faster. In addition, the duration of diffusion limitation at L = 60 cm was shorter and phenol biodegradation was achieved within 24 hours.

At higher packing density φ of 0.4, K_{aq} and K_{org} increased to 4.75 x 10^{-8} and 1.57 x 10^{-7} m/s, respectively, and there was a significant increase in the interfacial mass transfer area as well. These changes had a positive effect on the cell growth and biodegradation in the HFMB as can be seen in Fig. 5.9b. It should also be noted that higher packing density resulted in low Q_{aq}. However, there was an increase in Q_{org}, which could have contributed towards an improved K_{aq} and K_{org}.

In summary, biodegradation of toxic pollutants in TPPBs have been widely investigated using various substrates, organic solvents, polymeric adsorbents and single and mixed culture, which has helped provide better insights into the effects of the operating parameters and the cell growth environment in TPPBs. On the theoretical front, the biodegradation kinetics in two-phase biodegradation has been examined by several researchers (Cruickshank *et al.* 2000; Cruickshank *et al.* 2000; Juang *et al.* 2012; Nielsen *et al.* 2003; Nielsen *et al.* 2007; Quijano *et al.* 2010; Tomei *et al.* 2008). These models were based on the combination of the extraction kinetics of the substrate and the growth kinetics of the microorganisms. Cell growth kinetics in TPPB is usually studied using the Haldane model, but other models which account for the effects of dissolved oxygen concentration on cell growth have also been reported (Cruickshank *et al.* 2000). On the other hand, several strategies have been suggested for the estimation of the overall mass transfer coefficients. For example, Cruickshank

(a)

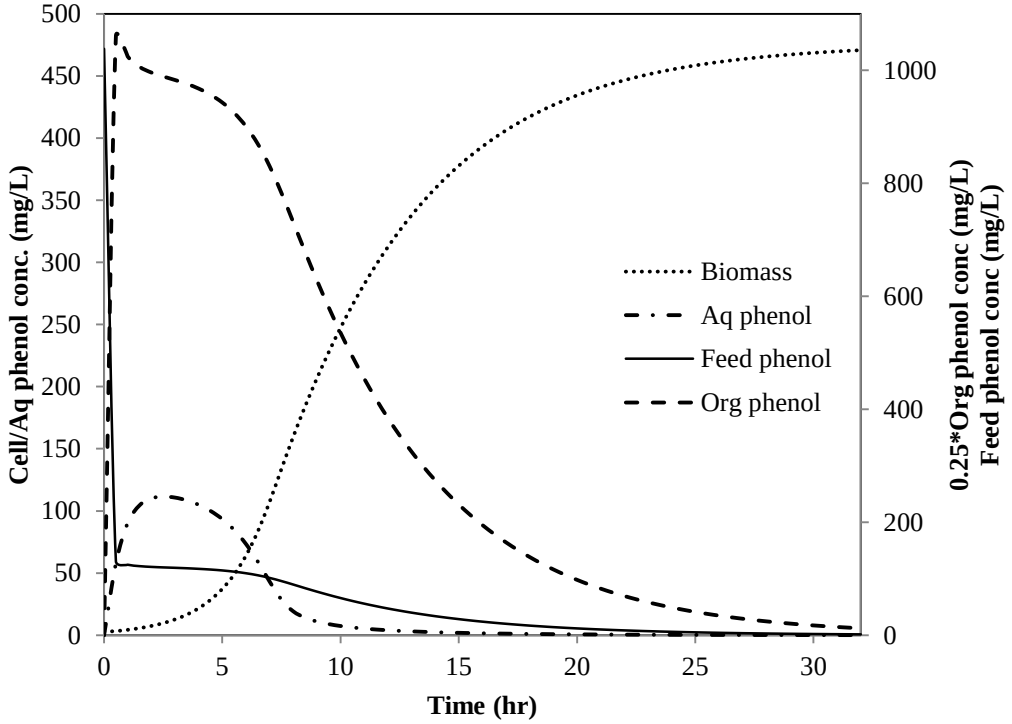

(b)

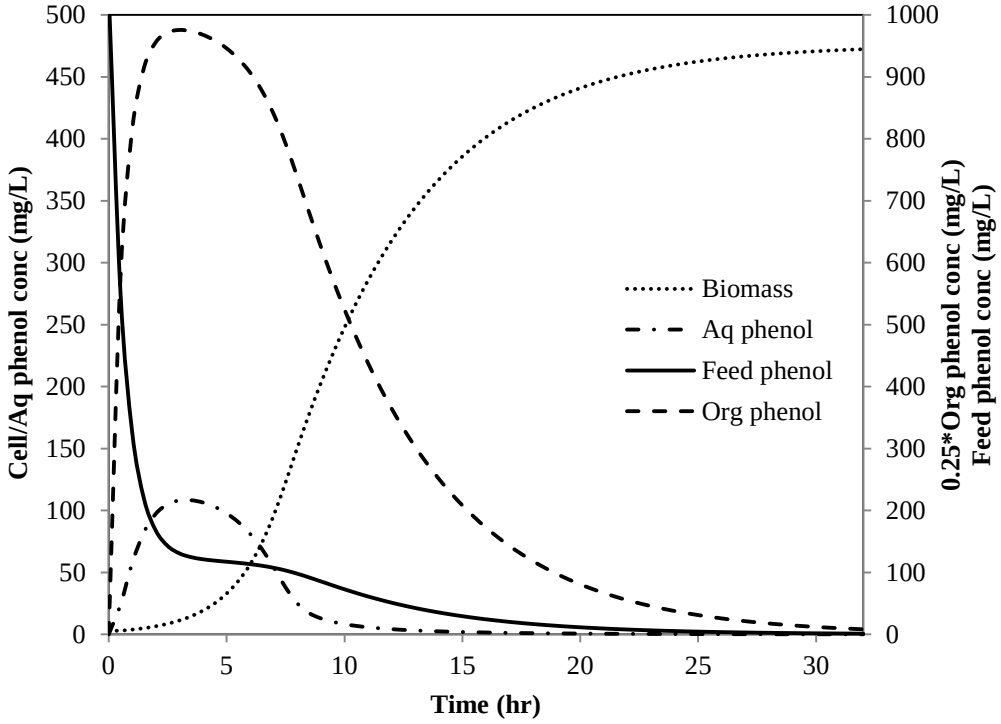

Figure 5.9 Model simulations to study: (a) effects of effect membrane length; and, (2) effects of fiber packing density

and co-workers (2000a) treated the overall mass transfer coefficient as an adjustable parameter, which was determined by trial and error using the experimental data. In a separate approach, Juang and co-workers (2012) determined the volumetric mass transfer coefficients in simple abiotic diffusion experiments in agitated vessels. Although these approaches could lead to suitable K_{org} and K_{aq} values, the mass transfer coefficients had no practical significance. They could not provide further insight into the mass transfer mechanisms of the substrate; neither could they simulate the bioreactor performance at varying operating conditions.

On the contrary, the kinetics model developed in this research describes the mass transfer and subsequent biodegradation of phenol in a holistic manner. The model provides a deeper understanding of the mass transfer of phenol from the feed to the cell culture medium, through the organic solvent. The model was also sensitive to the changes in the operating parameters of the HFMB, and it could predict the HFMB performance at varying feed concentrations, flow rates, membrane length and packing density, which would facilitate further advancement in the application of this technology.

5.5 Conclusions

A kinetics model, which combines the steady state mass transfer equations and dynamic cell growth kinetics, was developed for simultaneous extraction and biodegradation of phenol in the HFMB. The overall mass transfer coefficients have been determined using suitable empirical correlations following a resistance in series approach. It was found that the diffusion of phenol through the organic boundary layer was the rate limiting step. The model parameters have been determined and validated against the experimental data obtained at feed phenol concentration of 1000

mg/L. The diffusivity of phenol in the organic phase was estimated as 2.76 x 10^{-10} m^2/s, and biofilms constituted about 18% of the total biomass in the HFMB. The performance of the HFMB has also been simulated at higher feed phenol concentrations of 1500 and 2000 mg/L, which corroborated the experimental data excellently.

The effects of operating conditions on the overall mass transfer coefficients, and the biodegradation performance of the HFMB has been examined by performing model simulations at different flow rates, interfacial area and packing density. The results indicate that the HFMB performance could be enhanced by changing the organic solvent flow rate, the membrane length and the packing density.

6 Simultaneous Extraction and Biodegradation of Phenol in a Hollow Fiber Supported Liquid Membrane Bioreactor

6.1 Introduction

A liquid membrane can be defined as a thin layer of organic solvent that separates two aqueous phases and facilitates the transport of a solute from one aqueous phase to another. In practice, liquid membranes are often found imbedded in the pores of hydrophobic hollow fiber membranes and are held there by capillary force. This form of liquid membranes are known as hollow fiber supported liquid membranes (HFSLM) and they offer several advantages: high separation factor, high surface area, easy scale-up, low solvent volume, low energy requirement, and low capital and operating costs (Kocherginsky *et al.* 2007). The most interesting aspect of the HFSLMs is that they can perform simultaneous extraction and back-extraction in a single hollow fiber membrane contactor, which results in a simple, efficient and economical separation process (San Roman *et al.* 2010).

The HFSLM technology has been extensively investigated in the extraction/stripping of metals (Guha *et al.* 1994; Hu and Wiencek 1998) and organic compounds (Nanoti *et al.* 1997; Teresa *et al.* 2007; Zidi *et al.* 2010) from wastewater. However, there has been few large scale application of this technology despite offering numerous advantages over conventional separation processes. The main reason for the limited application of the HFSLM is its instability which arises due to the loss of the solvent from the supporting membrane pores. Although the exact cause for the solvent loss is not known, it has been attributed to the gradual dissolution or evaporation of the organic phase into either of the adjacent aqueous phases.

Over the past few years, several strategies have been suggested to enhance the stability of the HFSLMs. While most of these strategies are based on careful selection of the membrane, the organic solvent and the operating conditions, others are based on membrane engineering or the use of alternative HFSLM configurations (San Roman *et al.* 2010). In one such configuration, the organic phase is dispersed into the feed wastewater for extraction, while stripping is carried out non-dispersively using hollow fiber membranes. This semi-dispersive configuration has been deemed stable and it has been described as hollow fiber renewal liquid membrane (HFRLM). In HFRLM, hydrophobic fibers are pre-wetted with an organic solvent to create a very thin liquid film on the membrane surface. During HFRLM operation, the shear force due to the aqueous liquid flowing over the film causes the film to break and peel off from the membrane. At the same time, organic droplets dispersed in the aqueous phase fill the surface of the liquid film due to their wetting affinity for the fibers. This process results in the exchange of solvent between the aqueous phase and the liquid membrane which compensates the loss of liquid membrane. This dynamic process results in the renewal of the liquid membrane and provides long-term stability to the HFSLM as has been demonstrated in the recovery of copper and citric acid from dilute solutions (Ren *et al.* 2009; Ren *et al.* 2007).

In this section, a semi-dispersive hollow fiber supported liquid membrane bioreactor (HFSLMB) was developed for simultaneous extraction and biodegradation of phenol from wastewater. Since the microorganisms were separated from the solvent by the hollow fiber membranes, this bioreactor configuration eliminated many of the dispersion-associated problems, such as foaming and emulsion formation in the cell culture medium. On the other hand, the dispersion-based extraction of phenol from wastewater to 2-undecanone resulted in high mass transfer rates between the two

phases, which improved the overall biodegradation performance of the HFSLMB. The objectives of this research were:

1. Design and operate the HFSLMB for two-phase biodegradation of inhibitory concentrations of phenol;
2. Examine the effects of phenol concentration on cell growth and biodegradation in the HFSLMB;
3. Determine the effects of organic to aqueous phase volume ratio on cell growth and biodegradation rates in the HFSLMB;
4. Investigate the effects of operating conditions such as flow rates and the interfacial mass transfer area on the biodegradation performance of the HFSLMB; and
5. Evaluate the long-term stability of the HFSLMB during repeated batch operations at high phenol concentrations

The HFSLMB setup is shown in Fig. 3.3 and its operation is described in detail in Section 3.7.3. A summary of all the experiments performed using HFSLMB are listed in Table 6.1. Experiment set A was carried out to study the cell growth and phenol removal trends in the HFSLMB. The results were analyzed to elucidate the effects of increasing phenol concentrations on suspended cells of *P. putida* in the HFSLMB.

In liquid membrane based processes, the volume of the organic phase is important for the mass transfer of substrate. In addition, the amount of organic solvent also regulates substrate concentration in the aqueous phase. In the context of TPPBs, solvent volume plays an important role in mitigating substrate inhibition. In experiment set B, the effects of the organic to aqueous phase volume ratio on cell growth and biodegradation were investigated.

Table 6.1 Summary of the experimental runs in the HFSLMB

Exp. set	Feed conc. (mg/L)	Org/aq phase ratio	Fiber length (cm)	Flow rates (mL/min)		Study the effects of
				Shell	Lumen	
A1	1000	1:10	60	4	6	Initial phenol concentration
A2	1500	1:10	60	4	6	
A3	2000	1:10	60	4	6	
A4	4000	1:10	60	4	6	
B1	4000	1:10	60	4	6	Phase ratio
B2	4000	1:6.7	60	4	6	
C1	1000	1:10	60	4	4	Lumen side flow rate
C2	1000	1:10	60	4	6	
C3	1000	1:10	60	4	10	
D1	1000	1:10	60	2	6	Shell side flow rate
D2	1000	1:10	60	4	6	
D3	1000	1:10	60	6	6	
D4	1000	1:10	60	8	6	
E1	1000	1:10	30	4	10	Interfacial area
E2	1000	1:10	60	4	10	
F1	1000	1:10	60	8	10	Bioreactor sustainability
F2	1000	1:10	60	8	10	
F3	1000	1:10	60	8	10	

Experiment sets C and D were carried out to investigate the effects of lumen and shell side flow rates on HFSLMB performance. In membrane based processes, mass transfer rates of solutes are retarded due to the presence of boundary layers of limited turbulence in the vicinity of the membranes. An increase in the flow rates of the

aqueous and the organic liquids can change the thickness of the boundary layer and minimize the mass transfer resistances.

The effects of interfacial area on two-phase biodegradation in the HFSLMB were evaluated in experiment set E. Since the mass transfer flux at the interface is proportional to the interfacial mass transfer area, the biodegradation performance was expected to improve with the increasing interfacial area. In the HFSLMB, the interfacial area was same as the area of the hollow fiber membranes, which was changed by varying the effective length of the fibers.

Finally, repeated batch runs were carried out in the HFSLMB at 1000 mg/L phenol concentration under identical conditions to evaluate the long-term stability of the bioreactor in the backdrop of the instability concerns of the HFSLM as well as the biofilm formation on the hollow fiber membranes. During the experiment set F, the HFSLMB was operated for more than 400 hours with intermittent washing to demonstrate that the HFSLMB performance can be sustained for prolonged periods of time.

6.2 Results & Discussion

6.2.1 Two-phase biodegradation of phenol

To investigate two-phase biodegradation in the HFSLMB, batch experiments A1-A4 were performed at inhibitory phenol concentrations ranging from 1000-4000 mg/L. The polypropylene fibers which were used as support for the liquid membranes prevented any physical contact between the organic solvent and the cells, while preventing the microorganisms from immobilizing into the membrane pores due to the low pore size of the membranes. Thus, the fibers helped in retaining *P. putida* in suspension, away from 2-undecanone, which could result in a lag phase during

biodegradation. Prior to circulation in the shell side of the HFSLMB, the phenol wastewater was mixed with 2-undecanone in an organic to aqueous phase volume ratio of 1:10 using a magnetic stirrer at 200 RPM. While mixing of the two-phases facilitated redistribution of phenol between the solvent and the feed solution, it also generated organic droplets uniformly dispersed in the feed solution. These droplets were required to stabilize the HFSLM by the dynamic solvent renewal process as well as to transport phenol from the feed solution to the HFSLM.

Fig. 6.1 shows the temporal profile of cell growth and phenol removal for 1000 mg/L phenol concentration in the HFSLMB. Upon addition of the solvent into the feed solution, phenol was transported from the aqueous feed to 2-undecanone to attain an equilibrium distribution between the two-phases. The substrate laden 2-undecanone then contacted the mineral medium flowing in the lumen through the HFSLM and phenol was transported into the cell culture medium. The rapid redistribution process lowered the feed phenol concentration from 1000 mg/L to 190 mg/L within one hour of operation, while the corresponding increase in phenol concentrations in the organic phase and the cell culture medium were about 6000 mg/L and 110 mg/L, respectively. Since the biomass concentration at that point in the HFSLMB was low and phenol metabolism was negligible, the rapid decrease in total phenol concentration during the first hour can be attributed to the sorption of phenol onto the polypropylene fibers.

P. putida growing in the solvent-free medium did not exhibit any lag phase and an exponential growth phase ensued with cells multiplying at a rate of 0.53 hr^{-1}. The high cell growth rate stems from the fact that the microorganisms in the mineral medium experienced only a small fraction of the total phenol in the bioreactor. The maximum phenol concentration observed in the cell culture medium was only 120 mg/L, a

concentration at which substrate inhibition was negligible. The exponential growth continued for 10 hours during which more than half of the initial phenol was metabolized. Growth rate retardation coincided with the exhaustion of phenol in the culture medium, which could have been caused by nutrition limitation resulting from the high biomass density and a diminishing mass transfer flux across the HFSLM. Cell growth continued for 10 more hours at lower growth and biodegradation rates while phenol was completely removed from the feed solution within 24 hours with an average biodegradation rate of 47 mg/L-hr and the overall biomass yield was 0.40 g/g.

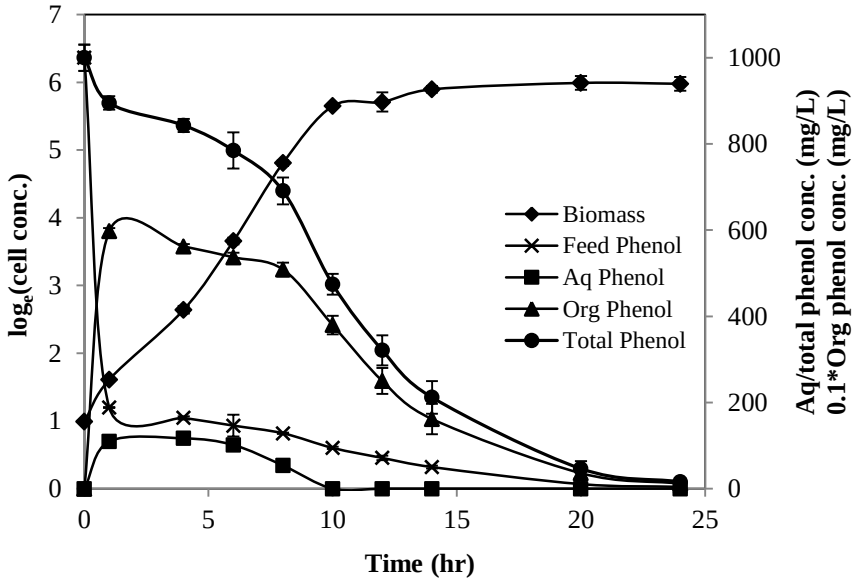

Figure 6.1 Temporal concentration profiles of biomass and phenol concentrations during two-phase biodegradation of 1000 mg/L phenol in the HFSLMB

Phenol removal in the HFSLMB occurred in three stages as shown in Fig. 6.2a. During the first hour, the biomass concentration was very low and the amount of phenol metabolized was insignificant; the quick removal of approximately 10% phenol during this period was mainly due to the sorption of phenol on to the polypropylene fibers. Sorption of phenolic compounds on hollow fibers has been reported earlier and this phenomenon has been used to mitigate various inhibitions

encountered during biodegradation of aromatic compounds (Chung *et al.* 2004; Li and Loh 2005). Initial sorption in the HFSLMB was immediately followed by biodegradation by exponentially growing cells, wherein phenol was rapidly metabolized by suspended cells of *P. putida*. During the exponential growth phase, about half of the initial phenol was metabolized. The remaining half of the substrate was removed during the third stage, which was characterized by slower cell growth and biodegradation rates. Phenol removal during this stage was almost linear with time, and biodegradation rate was limited by the mass transfer of phenol (Li and Loh 2005).

The availability of the substrate to the microorganisms in the HFSLMB depended on the balance between the mass transfer rates from the organic to the aqueous phase and the biodegradation rates. In the beginning of the HFSLMB operation, the mass transfer flux was high owing to a high concentration gradient across the HFSLM, while the cell density and the biodegradation rates were low. Therefore, the changes in phenol concentration in the cell culture medium due to metabolism could be easily nullified and the ratio of phenol concentration in 2-undecanone to that in cell culture remained at a lower value as shown in Fig. 6.2b. However, as more phenol was metabolized, the biomass density gradually increased, resulting in higher biodegradation rates. On the other hand, the mass transfer rate decreased due to a diminishing concentration gradient across the HFSLM. At some point, biodegradation rate exceeded the mass transfer rate and phenol was removed faster from the culture medium. This resulted in a sharp rise in the organic to aqueous phenol concentration ratio for the culture medium. This concentration ratio kept increasing until phenol was completely exhausted from the cell culture. Thereafter, phenol removal in the cell culture medium was limited by the mass transfer of phenol from the organic phase to

(a)

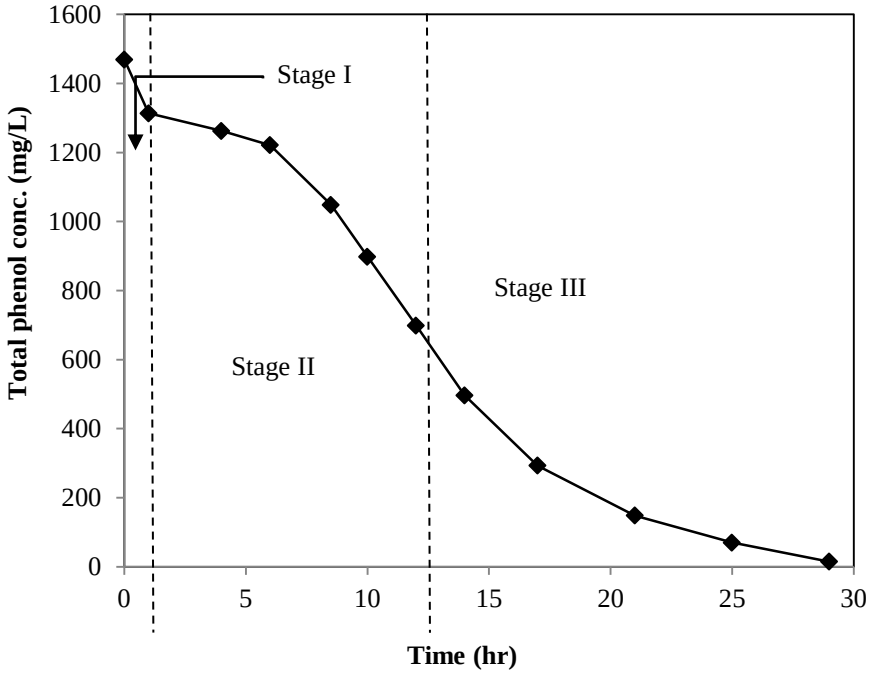

(b)

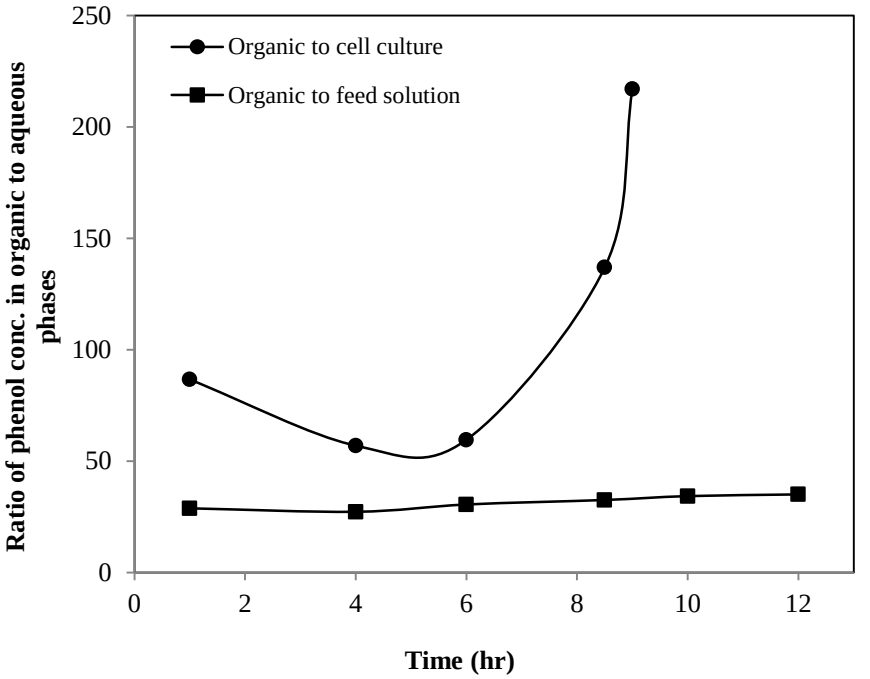

Figure 6.2 Two-phase biodegradation of 1500 mg/L phenol in the HFLMB: (a) three different stages of phenol removal; (b) changes in the distribution of phenol between the organic and the two aqueous phases during biodegradation

the cell culture. In contrast, the ratio of phenol concentration between the feed solution and 2-undecanone was quite stable during biodegradation. This constant concentration ratio can be attributed to the absence of microorganisms in the feed solution and a higher mass transfer rate between the dispersed phases where equilibrium was achieved quicker than that in a membrane-based system (Ren *et al.* 2007).

6.2.2 Effects of substrate concentration

During two-phase biodegradation in the HFSLMB, majority of the substrate fed to the bioreactor remained sequestered in the organic phase due to the high affinity of phenol for 2-undecanone. As a result, phenol concentration in the aqueous phase remained low and the maximum substrate concentration available to the microorganisms was only 10-12% of the initial phenol concentration in the feed solution (Fig. 6.3a). The maximum phenol concentration experienced by the cells increased proportionately with initial feed concentration. The minimum concentration observed was 120 mg/L for experiment A1, while the maximum was 470 mg/L for experiment A4. Although these concentrations were sub-inhibitory, the microorganisms experienced a higher degree of substrate inhibition at rising phenol concentrations. Consequently, there was a gradual decrease in the specific growth rate and biomass yield at higher phenol concentrations as can be seen in Table 6.2. For experiments A1-A3, the changes in the specific growth rates were not very significant as substrate inhibition up to phenol concentrations of 200 mg/L was not very severe. However, phenol concentration in the cell culture medium at 4000 mg/L feed wastewater was approximately 500 mg/L which was inhibitory and resulted in a large drop in the specific growth rate to 0.31 hr^{-1} whereas the biomass yield was reduced to 0.26 g/g.

Table 6.2 Effects of initial phenol concentration on two-phase biodegradation in the HFSLMB

Parameters	Experiments			
	B1	**B2**	**B3**	**B4**
Specific growth rate (hr^{-1})	0.53	0.51	0.51	0.31
Biomass yield (g/g)	0.40	0.38	0.33	0.26
Avg. biodegradation rate (mg/L-hr)	47	60	84.2	110.3
Biodegradation time (hr)	24	29	36	76

Cell growth in the HFSLMB was independent of the total phenol concentration and the growth rates depended only on the phenol concentration in the mineral medium as evinced from the growth trends. These growth trends were also consistent with those observed in single-phase biodegradation. The specific growth rates observed in the HFSLMB were also comparable to those obtained during the single-phase biodegradation experiments. It can therefore be concluded that the growth environment in the HFMB was free from solvent (2-undecanone) interference and it resembled that in the single-phase aqueous culture. The lower biomass yield in the HFSLMB, on the other hand, can be attributed mainly to the microbial attachment onto the polypropylene fibers and the silicone tubing which resulted in a lower detected biomass concentration in suspension. The low biomass yield can also be a result of the early onset of diffusion limitation which resulted in nutrient deprivation for the microorganisms and could have led to cell death. While the mass transfer limited removal phase accounted for the metabolism of about half of the initial total phenol provided in the bioreactor, it resulted in a nominal increase in the biomass concentration.

(a)

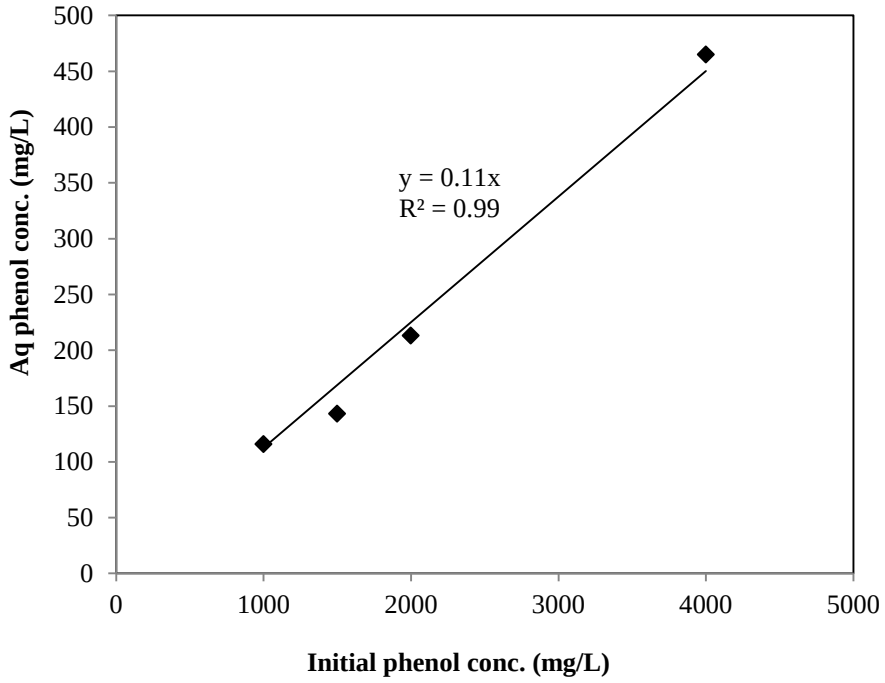

(b)

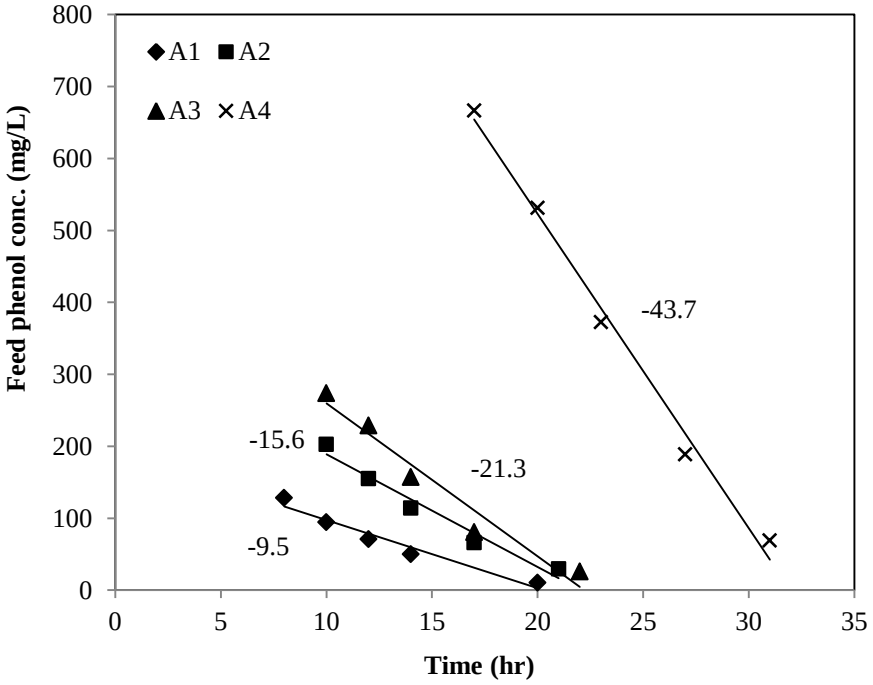

Figure 6.3 Effects of initial phenol concentration on two-phase biodegradation in the HFLMB: (a) aqueous phase phenol concentration in the cell culture; (b) removal rates under diffusion limitation

During two-phase biodegradation in the HFSLMB, the first 10% phenol was removed primarily by sorption whereas the last 10% was removed under severe nutrient limitation. Therefore, the average phenol biodegradation rates in the HFSLMB were calculated based on the removal of only 80 % of the total phenol. From Table 6.2, it can be seen that the average biodegradation rate increased with initial phenol concentration and the highest rate of 110 mg/L-hr was observed during the biodegradation of 4000 mg/L phenol. On the contrary, despite the high biodegradation rates, the biodegradation time increased with the feed phenol concentration. This could be attributed to the slow removal of the final 10% of the phenol under diffusion limitation. Notwithstanding this, the biodegradation time in the HFSLMB was still shorter than those reported in other membrane bioreactors in which 2000 mg/L phenol was mineralized in 75 (Chung *et al.* 2004), 110 (Loh *et al.* 2000) and 270 hours (Juang *et al.* 2009) using either immobilized cells or biofilms. Two-phase biodegradation performance in the HFSLMB was also comparable to other TPPBs using solid (Amsden *et al.* 2003) or liquid (Collins and Daugulis 1997) NAPs.

While phenol removal from the HFSLMB during the exponential growth phase depended on the specific growth rate of the microorganisms, substrate removal during diffusion limitation was controlled by the mass transfer flux of phenol from the organic solvent to the cell culture. The removal of phenol under mass transfer limitation was linear with time as shown in Fig. 6.3(b). The removal rate increased with increasing phenol concentration (from 9.5 mg/L-hr to 43.7 mg/L-hr, corresponding to phenol concentrations of 1000 mg/L to 4000 mg/L, respectively), possibly due to a higher concentration gradient. Since the duration of the diffusion limitation depended on the mass transfer rates of phenol, it was anticipated that a

change in the operating conditions or the interfacial mass transfer area could improve the biodegradation performance, as we discussed further below.

6.2.3 Effects of Phase Ratio

Having established that cell growth in the HFSLMB was independent of the total phenol concentration and the variations in the specific growth rate were caused by the changes in the aqueous phase phenol concentrations, experiments B1-B2 were performed to study the effects of organic to aqueous phase volume ratio on biodegradation performance in the HFSLMB. Fig. 6.4 shows the cell growth and phenol removal profile for experiment B2. While the trends in cell growth and phenol removal remained unchanged at the higher phase ratio, lower phenol concentrations were observed in the two aqueous phases. Compared to B1, the maximum substrate concentration experienced by the microorganisms in experiment B2 was 20% lower at 390 mg/L. The direct consequence of the low phenol concentration was the alleviation of substrate inhibition, resulting in a higher specific growth rate of 0.38 hr^{-1}. The change in the phase ratio also resulted in a modest increase in the biomass yield and the duration of mass transfer limitation was shortened. Phenol wastewater under these circumstances could be treated within 60 hours at an average biodegradation rate of 114 mg/L-hr (Table 6.3).

Unlike immobilized cell bioreactors, TPPBs enable suspended cells to degrade inhibitory substrate concentrations. However, the direct contact between the microorganisms and the organic solvent in conventional TPPBs results in the loss of substrate and cells due to foaming. At higher organic to aqueous phase ratio, poor oxygen mass transfer may also limit biodegradation rate and adversely affect cell growth (Collins and Daugulis 1997). In contrast, these problems were not observed in

the current HFSLMB where the cell growth environment was free of the organic solvent. This eliminated any aeration-associated problems and the positive advantageous effect of the increase in the phase ratio was the lowering of the severity of substrate inhibition and the consequent increase in the growth and biodegradation rates. An independent control on the phase ratio therefore can help in expedited removal of the substrate at very high concentrations.

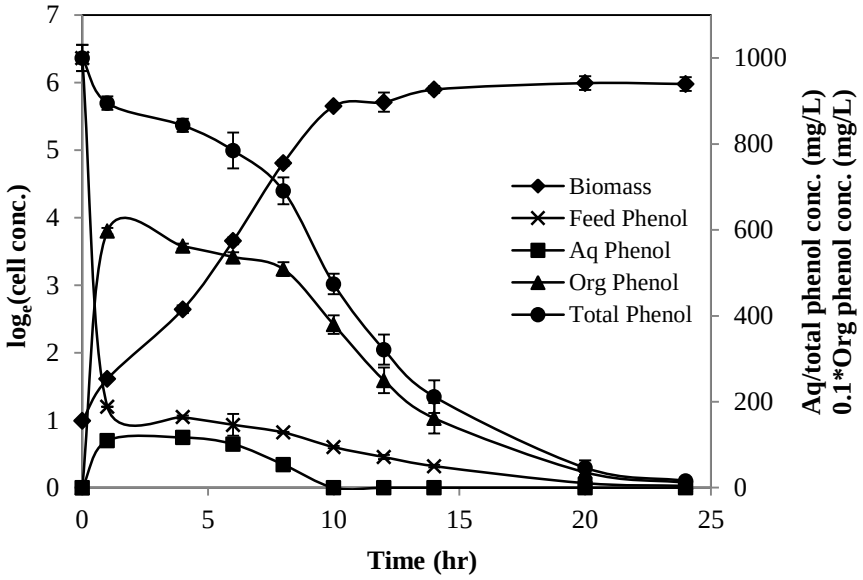

Figure 6.4 Temporal concentration profiles of biomass and phenol concentrations during two-phase biodegradation of 4000 mg/L phenol in the HFSLMB at organic to aqueous phase ratio of 1:6.67

6.2.4 Effect of flow rates

In membrane based solvent extraction, a solute moving from the organic to the aqueous phase through hydrophobic membranes usually encounters three resistances in series: the organic phase boundary layer, the solvent-filled membrane and the aqueous phase boundary layer (Gabelman and Hwang 1999). At increasing flow rates, the thickness of the boundary layer is reduced, which results in lower mass transfer resistances and the mass transfer flux across the membrane improves (Shen *et al.* 2009; Zidi *et al.* 2010). To investigate the effects of flow rates on the biodegradation

kinetics in the HFSLMB, experimental sets C and D were carried out. For experiments C1-C3, the shell side flow rate was kept constant at 4 mL/min while the lumen side flow rate was varied from 4 to 10 mL/min. On the other hand, for experiments D1-D4, the shell side flow rate was varied from 2 to 8 mL/min while keeping the lumen side flow rate at 6 mL/min.

Table 6.3 Effects of organic to aqueous phase ratio on two-phase biodegradation in the HFSLMB

Parameters	Experiments	
	C1	C2
Max. aqueous phenol concentration (mg/L)	464	395
Specific growth rate (hr^{-1})	0.31	0.38
Biomass yield (g/g)	0.26	0.28
Avg. biodegradation rate (mg/L-hr)	52.6	75.5
Biodegradation time (hr)	76	53

Fig. 6.5 shows phenol removal profiles obtained for experiments C1-C3. The changes in the total phenol concentration profiles in the HFSLMB during sorption and exponential growth phase were nearly identical at different flow rates, and deviations were observed only after 8-10 hours when biodegradation was limited by mass transfer of phenol. During this period, phenol removal rates increased from 6.8 to 15.4 mg/L-hr when flow rate was increased from 4 to 10 mL/min. The higher biodegradation rates resulted from lowering of mass transfer resistances in the aqueous boundary layer. The increase in the mass transfer rates shortened the period of diffusion limitation which had a direct impact on the biodegradation time. The biodegradation time for metabolism of 1000 mg/L phenol at lumen side flow rates of

(a)

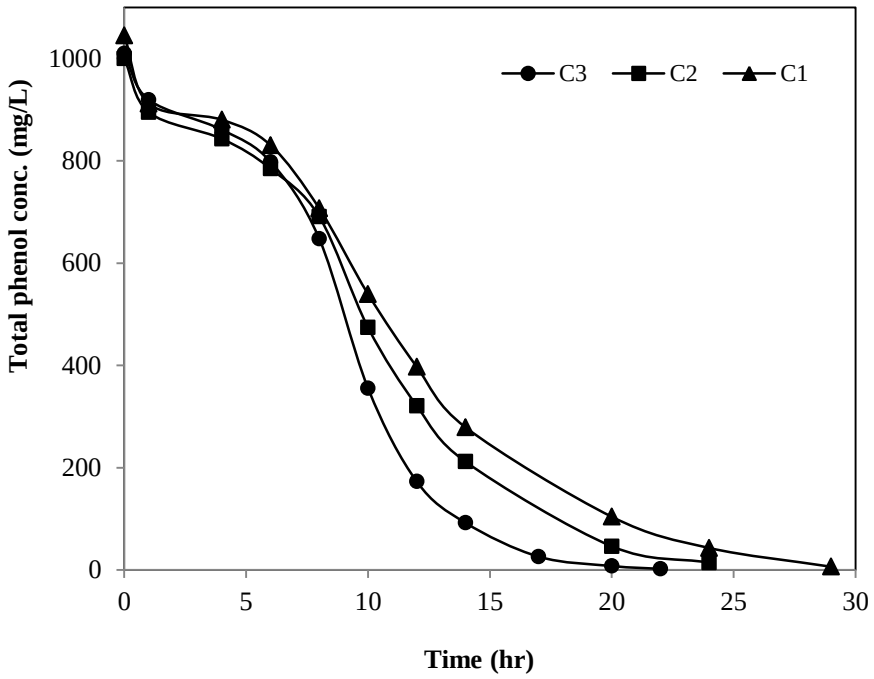

(b)

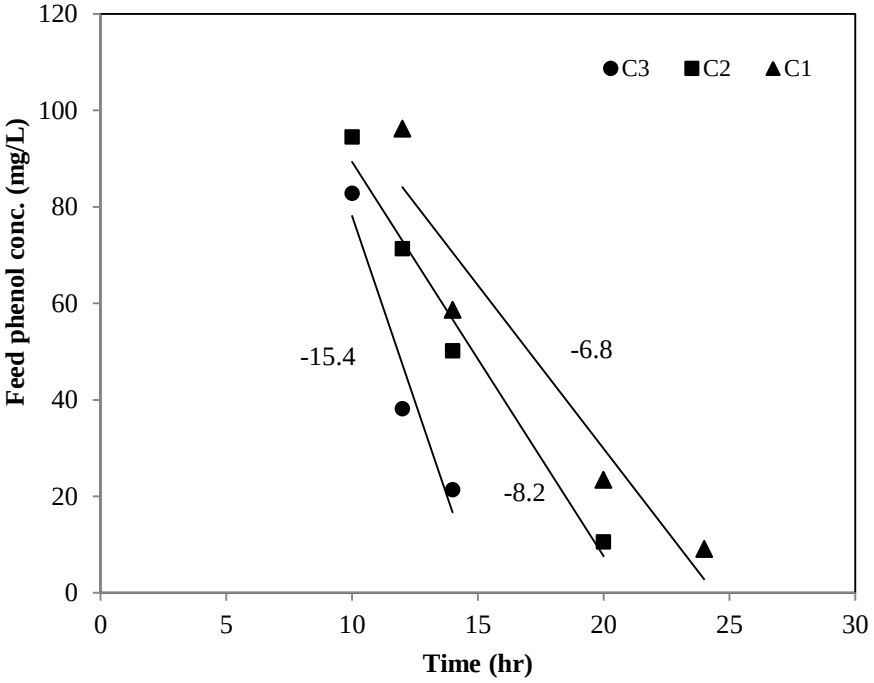

Figure 6.5 Effects of lumen side flow rate on two-phase biodegradation of phenol in the HFSLMB: (a) total phenol concentration profiles; (b) removal rates under mass transfer limitation

10, 6 and 4 mL/min were 20, 24 and 29 hours, respectively, which implies that a shorter time was required for phenol metabolism at higher lumen side flow rate. In contrast, the effects of the changes in the shell side flow rate on biodegradation were insignificant as shown in Fig. 6.6. Biodegradation profiles for experiments D2-D4 were identical and phenol was completely metabolized within 20 hours. For experiment D1, phenol removal rate was marginally smaller the biodegradation was completed within 22 hours.

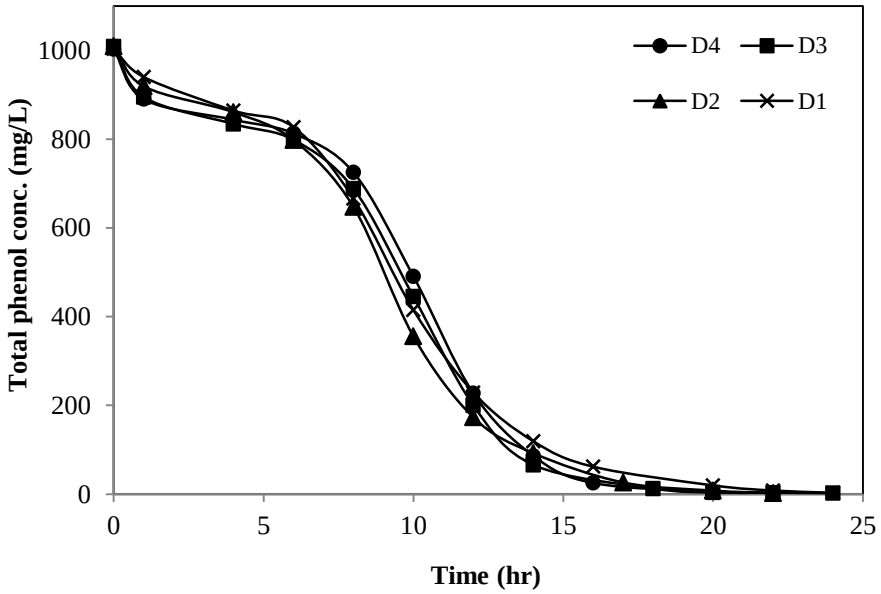

Figure 6.6 Effects of shell side flow rate on two-phase biodegradation of phenol in the HFSLMB

For hydrophobic membranes wetted by an organic solvent having high affinity for the solute, the mass transfer resistance lies primarily on the aqueous side (Shen *et al.* 2009). In the HFSLMB, the aqueous phase hydrodynamics in the lumen side resulted in a significant change in the removal rate whereas the changes in the bioreactor performance due to the increase in the shell side flow rates were marginal. Therefore, it can be inferred that the mass transfer of phenol in the HFSLMB was controlled by the aqueous phase boundary layer resistance in the lumen.

6.2.5 Effects of interfacial area

In TPPBs, biodegradation performance is inextricably linked to the mass transfer rates of the substrate between the immiscible phases. One approach to increase the mass transfer flux in these bioreactors is to enhance the interfacial contact area between the two-phases. The interfacial mass transfer area in a dispersion-based system depends on the agitation rates (Zilouei *et al.* 2008), while the contact area in membrane contactor is same as the surface area of the membranes. A common practice to increase the efficiency of membrane-based processes is to increase the effective length of the membranes by connecting several membrane modules in series (Gabelman and Hwang 1999).

The effects of interfacial mass transfer area on HFSLMB performance was investigated in experiments E1- E2 by varying the effective length of the hollow fiber membranes. Since extraction of phenol from feed wastewater to 2-undecanone was independent of the membrane area, the increase in the organic phase phenol concentration during equilibration was same for the two experiments. On the other hand, the redistribution of phenol from 2-undecanone to the cell culture was facilitated by the HFSLM and a higher diffusion rate was observed at higher interfacial area in experiment E2. This resulted in a quicker lowering of organic phase phenol concentration and a rapid increase in phenol concentration in the cell culture as shown in Fig. 6.7a and 6.7b. Since the experiments were carried out under identical conditions, the equilibrium parameters were not affected by increasing the fiber length and the maximum phenol concentration in the cell culture medium was same for experiments E1-E2 at about 110 mg/L. It can also be observed that at improved mass transfer rate, the decrease in phenol concentration in the culture medium was slower and phenol could be sustained in the culture medium for a longer time. The effects of

(a)

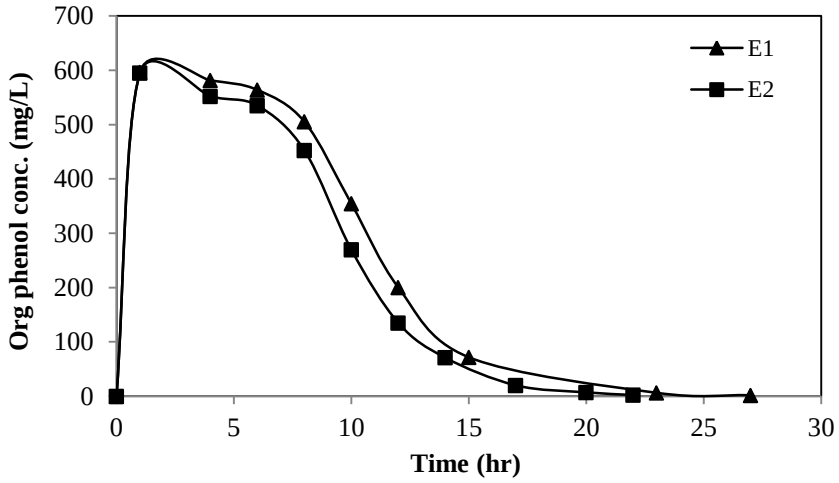

(b)

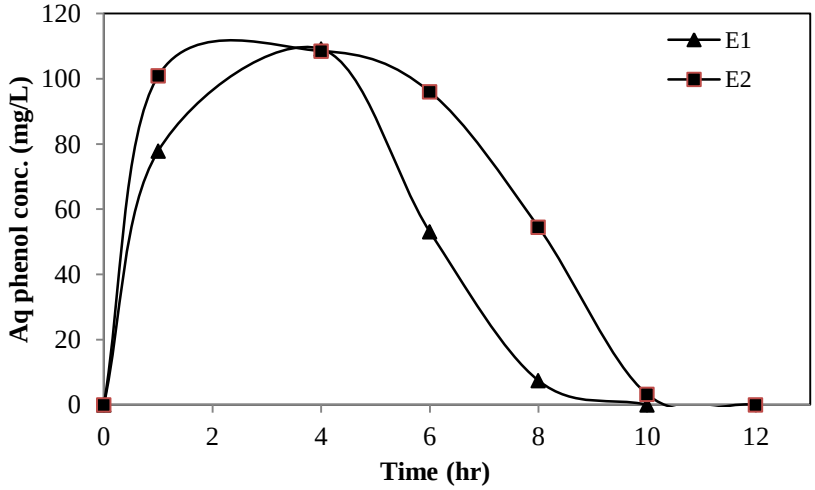

(c)

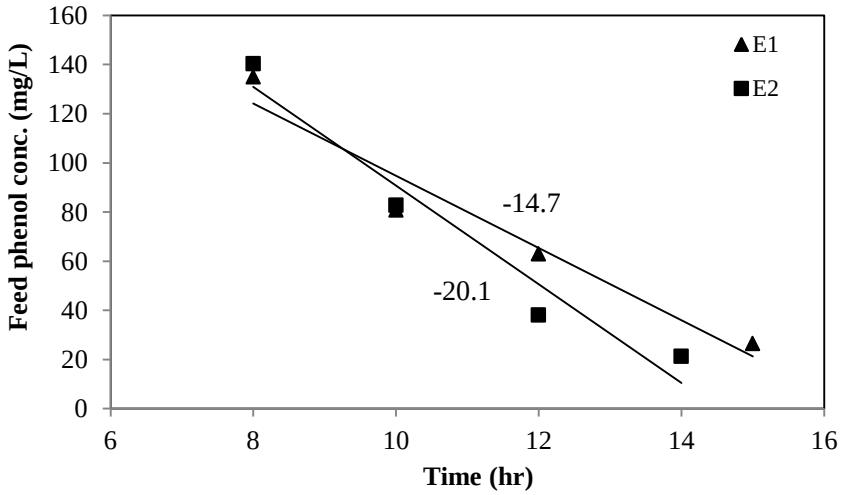

Figure 6.7 Effects of interfacial area on two-phase biodegradation of phenol in the HFSLMB: (a) phenol concentration in the organic phase; (b) phenol concentration in the cell culture; (c) removal rates under diffusion limitation

the improvement in mass transfer flux were most evident during diffusion limitation as shown in Fig. 6.7c. The linear removal rate observed for experiment E2 was 20 mg/L-hr, whereas that for experiment E1 was 20% lower at 14.7 mg/L-hr. From the bioreactor parameters listed in Table 6.4, it can also be seen that the prolonged exponential growth phase in experiment E2 had no effect on the specific growth rate but it resulted in about 20% increase in the biomass yield and the biodegradation time was shortened by 20%.

Table 6.4 Effects of interfacial surface area on two-phase biodegradation in the HFSLMB

Parameters	Experiments	
	E1	E2
Specific growth rate (hr^{-1})	0.52	0.51
Biomass yield (g/g)	0.32	0.40
Avg. biodegradation rate (mg/L-hr)	57.1	64.0
Biodegradation time (hr)	25	20

Two conclusions can be drawn from these results: (1) higher interfacial mass transfer area can expedite substrate removal by prolonging the exponential growth period when biodegradation rates were higher; and (2) improved flux at higher interfacial area leads to higher removal rate under mass transfer limitation and consequently a shorter biodegradation time. The effects of increasing the interfacial area in the HFSLMB were analogous to the effects of lumen side hydrodynamics. It can, therefore, be concluded that the cell growth and biodegradation rates during the exponential cell growth phase could be controlled by changing the organic to aqueous

phase ratio, while the flow rates and interfacial area could boost the bioreactor performance during diffusion limitation by achieving higher removal rates.

The HFSLMB thus presents itself as an ideal bioreactor for two-phase biodegradation of aromatic compounds. Not only did the liquid membrane-based bioreactor achieve simultaneous extraction and biodegradation from wastewater, it also prevented solvent dispersion into the culture medium. In the aqueous cell growth environment in the HFSLMB, microorganisms achieved high growth and biodegradation rates and cell growth kinetics was regulated by phenol concentration in the aqueous phase only. The bioreactor also offered flexibility of operation by providing independent control of the liquid flow rates, the agitation rate, the interfacial area and the solvent volume. The two major removal phases observed in the HFSLMB operation could be easily controlled by changing these parameters to achieve very high biodegradation rates. Conventional TPPBs on the other hand, have seldom been used for simultaneous extraction and biodegradation using either an organic solvent or a polymeric solid. Recently, simultaneous extraction and biodegradation of phenol has been reported from saline solutions using kerosene as the organic phase in a dispersion-based bioreactor (Juang *et al.* 2010). Although severe emulsification of the feed solution could be prevented by gentle mixing of the two-phases, the microorganisms exhibited lag phase at feed phenol concentrations less than 2500 mg/L and cell growth was not observed at 3000 mg/L phenol. The agitation rates required to aerate the cell culture were quite high and the biodegradation rates were low. Phenol concentration of 1160 mg/L could be metabolized only after 60 hours.

6.2.6 Bioreactor Sustainability

Hydrophobic hollow fiber membranes such as polypropylene or polyvinylidene fluoride (PVDF) have been used as support materials for biofilm formation during biodegradation of aromatic compounds (Chung *et al.* 2004; Zhao *et al.* 2011). Unlike other separation processes, the presence of biofilms in these bioreactors enhanced the biotransformation. However, biofilms impede mass transfer flux of substrate across the membrane in the long run and are often detrimental for membrane-based processes (Meng *et al.* 2009). During HFSLMB operation, the specific growth rates of the microorganisms at different initial phenol concentrations correlated well with the corresponding maximum phenol concentration in the aqueous phase. However, the observed biomass yield in the HFSLMB was only 50-60% of the theoretical value. The theoretical biomass yield was calculated based on the maximum phenol concentration exposed to the cells. For example, if the maximum phenol concentration in the mineral medium was 200 mg/L for feed concentration of 1000 mg/L, the biomass yield should be 0.6 g/g, i.e., the biomass yield obtained on 200 mg/L phenol in the single-phase suspension cultures. Apart from nutrient deprivation under diffusion limitation, the reason for the low biomass yield in the HFSLMB was the adhesion of the microorganisms onto the hydrophobic membranes and the silicone tubings. The biofilms on the tubings were often visible towards the end of the biodegradation experiments and these could be easily sloughed off into the bioreactor during subsequent runs when the mineral medium was circulated in the membrane module.

To investigate the HFSLMB stability over long periods of operation time and to elucidate the effects of biofilm formation on biodegradation, repeated batch runs were conducted at feed phenol concentration of 1000 mg/L without biofilm removal

between consecutive runs. The shell and lumen side flow rates were chosen to be 8 and 10 mL/min, respectively, while the organic to aqueous phase ratio was 1:10. Fig. 6.8 shows the feed and total phenol concentration profiles during the bioreactor operation. During experiment F1, the HFSLMB was operated for 216 hours to complete 10 experimental runs. For the first 5 runs, phenol removal in the bioreactor was faster and the removal time improved from 21 hours during the first run to 19 hours for the fifth run (Fig. 6.9a). The increase in the biodegradation rate could be attributed to the increase in the inoculum size for each subsequent runs due to the increased attachment of cells on the membrane and tubing surfaces. This hypothesis is supported by the observation that the observed biomass yield during each subsequent run decreased gradually from 0.46 to 0.32 g/g (Fig. 6.9b), while the amount of phenol metabolized was same in each run. The positive impact of biofilms in the HFSLMB lasted only for the first five runs (100 hours) and the performance deteriorated from the sixth run. For runs 6-10, the biodegradation trend was reversed. While phenol was completely biodegraded during each run, lower biodegradation rates were observed resulting in longer removal times; run 10 was completed in 25 hours. The monotonic decrease in the biomass yield continued during runs 6-10 and it reached its minimum at 0.15 g/g during run 9. A spike in the biomass yield during run 10 is an outlier which could have resulted from the presence of cell aggregates in the sample during the analysis. At the end of experiment F1, a thick greenish yellow film could be seen on the silicone tubings and even the tubing weight increased due to the cell attachment. It can be seen from Fig. 6.9b that most of the biomass generated during the last five runs had accumulated on the fiber and tubing surfaces.

The loss in the biodegradation performance of the HFSLMB could be attributed to the high density biofilm formation on the polypropylene fibers. The bacteria being larger

(a)

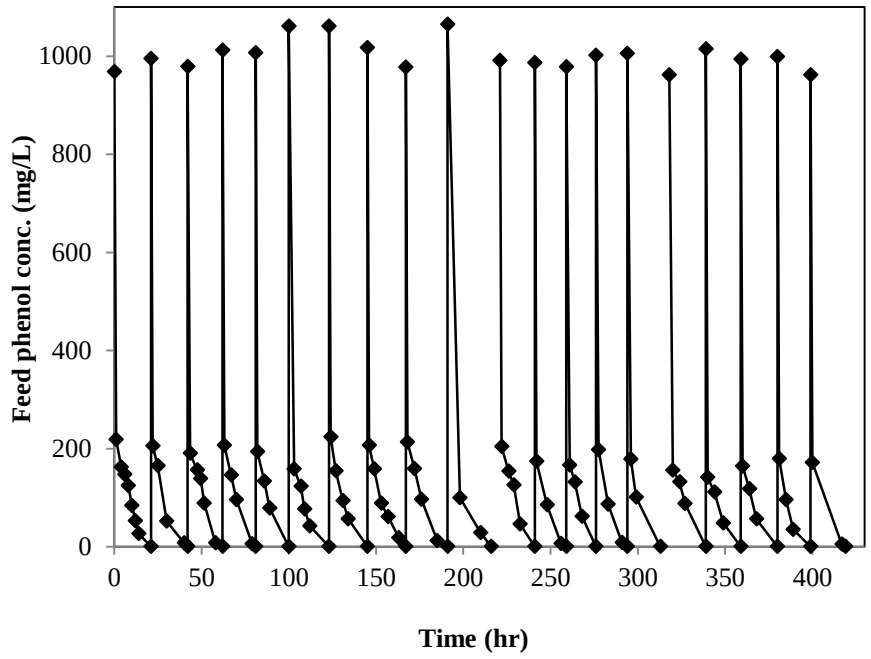

(b)

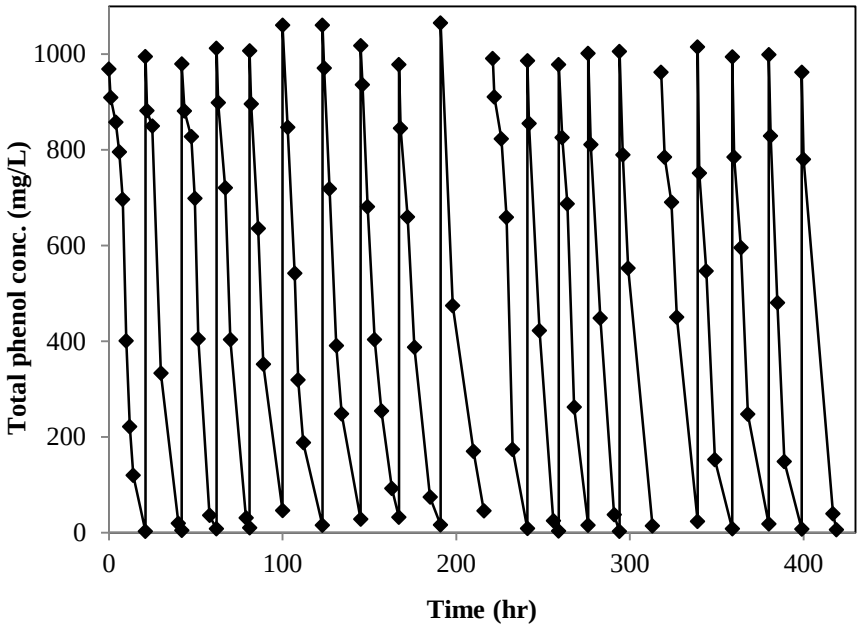

Figure 6.8 Bioreactor sustainability studies for the HFSLMB: (a) feed phenol concentration profiles; (b) Total phenol concentration profiles, for the 20 consecutive runs

(a)

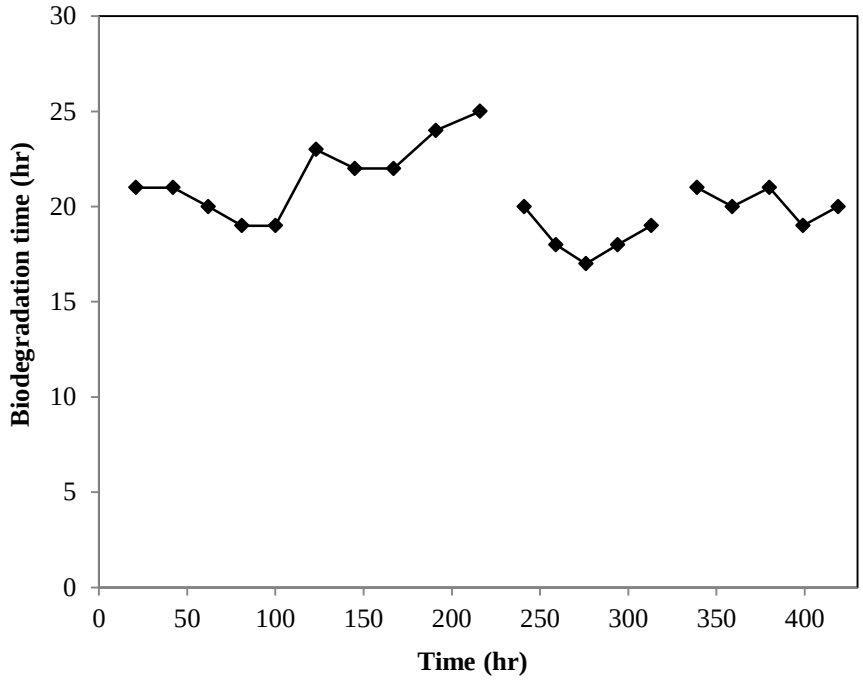

(b)

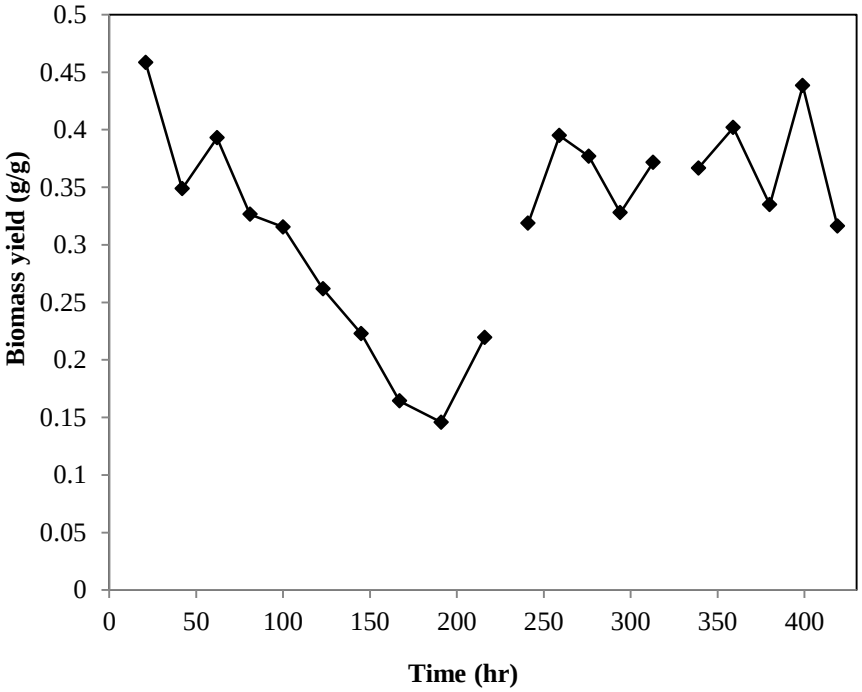

Figure 6.9. Bioreactor sustainability studies for the HFSLMB: (a) biodegradation time and; (b) biomass yields, for the 20 consecutive runs

than the membrane pores, could have blocked the pores (Meng *et al.* 2009), impeding the diffusion of phenol into the culture medium. At the end of run 10, the lumen side was washed with 1M sodium hydroxide for three hours to remove the biofilms. This was followed by two short washings with sterilized ultrapure water to remove the dislodged cells and the remaining sodium hydroxide in the HFSLMB.

Biodegradation in the HFSLMB was resumed after 5 hours of washing for experiment F2. At this stage, the HFSLMB was operated for another 92 hours in which 5 runs were completed under identical conditions as F1. The biomass yields obtained in the runs 11-15 were comparable to those observed in the first five runs of F1. Phenol was completely metabolized during each run within 17-20 hours. At the end of each five run cycle, another identical washing cycle was administered for biofilm removal, which was quite visible in the bioreactor. The final five runs for experiment F3 were completed after the washing in another 101 hours. The biomass yield for the last cycle varied in the range of 0.44-0.32, whereas the biodegradation time was relatively stable in the 19-21 hours range.

Biofilms formation during biodegradation in a membrane bioreactor is inevitable. However, by administering short washing cycles with sodium hydroxide, biofilm growth in the bioreactor could be minimized and the bioreactor operation could be sustained. The HFSLMB was operated for a total of 419 hours with two washing breaks. The results indicate that a 5 hour washing with 1M sodium hydroxide after every 100 hours of operation could prevent the biofilm-associated performance loss and sustain the bioreactor operation for a long period of time. The short washing cycles might not hamper the bioreactor operation as it took only 5% of the operation time to recover the bioreactor performance. It can also be observed that the biodegradation time for the first and last runs were identical although they were

carried out after a gap of 400 hours. This further ascertains that the HFSLM facilitating the mass transfer was stable.

6.3 Conclusions

An HFSLMB has been fabricated and operated with *P. putida* for two-phase biodegradation of phenol. In the first ever application of liquid membrane in biodegradation, simultaneous extraction and biodegradation of the toxic substrate was facilitated via hollow fiber supported liquid membranes. The semi-dispersive design stabilized the liquid membrane and facilitated dispersion free mass transfer from the solvent to the cells.

The HFSLMB provided a solvent free growth environment in which cells were exposed only to a small fraction of the total phenol, resulting in high cell growth rates. The biodegradation rates during the exponential growth phase could be controlled by the organic to aqueous phase ratio, while the same could be enhanced during diffusion limitation by increasing the flow rates and the interfacial area. In evaluating the long-tern stability of the HFSLMB, it was found that controlling the biofilms was crucial for achieving sustained high biodegradation performance. A washing strategy lasting 5% of the operation time after 100 hours of operation was suggested to remove the attached-cells and sustain biodegradation for a long time. The results of this research also demonstrate that the HFSLMB could eliminate the operating problems encountered in conventional TPPBs. The modular design is easier to scale-up and can be operated continuously. Modeling the HFSLMB will provide further insights into the mass transfer mechanisms and operation of the bioreactor.

7 Development of Extractant Impregnated Hollow Fiber Membranes for Adsorption of Phenol from Wastewater

7.1 Introduction

Aqueous/organic TPPBs are analogous to extraction/stripping systems and have conventionally been carried out using organic solvents as the sequestering phase. However, various operating problems arising due to phase dispersion and the high cost and toxicity of organic solvents have resulted in the replacement of organic solvents with solid NAPs such as polymeric adsorbents. The resulting solid/liquid TPPBs have the advantages of biocompatible and non-biodegradable NAPs, easy regeneration and recycling of NAPs, absence of foaming and emulsification, and abundant supply of the adsorbents (Amsden *et al.* 2003). However, the low diffusivity of solutes in solid phase can results in low adsorption/desorption rates and poor regeneration of the adsorbents in these TPPBs. Furthermore, many of these solid adsorbents have low adsorption capacity and some of them are quite expensive (Zhao *et al.* 2009).

Recently, polymeric microcapsules impregnated with organic solvents have been investigated for dispersion-free extraction/adsorption of metals and organic compounds. (Zhao *et al.* 2010). These microcapsules combine the advantages of both extraction and adsorption which helps them mitigate the challenges encountered in each of the individual processes. While the presence of polymer between the encapsulated solvent and the aqueous medium prevents phase dispersion and related problems, the encapsulated solvent can also enhance the adsorption capacity and the solute diffusivity within the polymeric microcapsules (Yin *et al.* 2010), resulting in better separation performance. The adsorption capacity of these novel polymers can

be further improved by the use of organic extractants with high affinity for the target compound (Gong *et al.* 2006; Outokesh *et al.* 2011).

Solvent encapsulated porous microcapsules have found application in the removal of organics (Gong *et al.* 2006; Whelehan *et al.* 2010; Yin *et al.* 2010) and metals (Illanes *et al.* 2008; Ma *et al.* 2011; Yang *et al.* 2004) from wastewater. Polysulfone is the most commonly used polymer for encapsulation, whereas TBP, TOPO, 1-nonanol and several other solvents including ionic liquids (Xiang *et al.* 2008) have been used as the extractant. These microcapsules have also found application as the partitioning phase in TPPBs in biodegradation of phenol (Zhao *et al.* 2009) and pyrene (Sarma *et al.* 2011). However, the preparation of these microcapsules requires complex polymerization and a lot of solvent/extractant is wasted during that encapsulation. Besides, the long-term stability of the organic solvent encapsulation within a hydrophobic support is a cause for concern.

In order to achieve high stability for the solvent impregnated into hydrophobic polymers, the use of solid extractants was investigated in this research. Solid organic extractants such as TOPO has been extensively studied in the extraction of metals and organic compounds using hollow fiber membranes (Cichy and Szymanowski 2002), HFSLMs (Teresa *et al.* 2007) and liquid-core microcapsules (Outokesh *et al.* 2011). The strategy here was to create HFSLM on polypropylene membranes using TOPO dissolved in a volatile carrier solvent and then evaporate the solvent to entrap TOPO in the membrane walls. Using membranes of small pore size, the extractant can be effectively confined within the porous membrane walls and the performance of the resulting extractant impregnated hollow fiber membranes (EIHFM) should be stable.

TOPO was chosen as the model extractant in EIHFM preparation as it is one of the most commonly used extractant in phenol extraction and has high affinity for phenol. At experimental conditions, TOPO exists as crystalline solids (Cichy *et al.* 2001) and it is soluble in non-polar solvents. The use of TOPO has also been reported in the extraction of phenol using liquid membranes (Cichy *et al.* 2005), although using non-volatile carrier solvents.

In this section, the feasibility of impregnating polypropylene hollow fiber membranes with TOPO was investigated. The objectives of this research were:

1. Prepare and characterize EIHFMs using TOPO as the model extractant into polypropylene hollow fiber membranes;
2. Investigate the effects of TOPO concentration, contact time and phenol concentration on the adsorption of phenol using the EIHFMs;
3. Examine the adsorption kinetics of phenol on the EIHFMs using suitable models and adsorption isotherms;
4. Evaluate the stability of the EIHFMs during long-term repeated operation; and
5. Investigate the feasibility of using the EIHFMs as the NAP in solid/liquid TPPB during the biodegradation of phenol.

A technique was developed for the impregnation of solid extractants into the pores of the hydrophobic membranes. By varying the concentration of TOPO from 50-400 g/L in the carrier solvent, four different sets of EIHFMs with varying TOPO content were prepared. The presence of TOPO in the pores and the surfaces of the EIHFMs were validated using SEM. The EIHFMs were then used for the adsorption of phenol from aqueous solutions and the effects of contact time, feed phenol concentration and

TOPO concentrations on the adsorption rate and capacity of the EIHFMs were evaluated.

In order to understand the mass transfer mechanism and determination of the rate controlling step during phenol adsorption on the EIHFMs, the adsorption kinetics was studied using pseudo-first-order, pseudo-second-order and intraparticle diffusion models. The equilibrium adsorption capacities of the four sets of EIHFMs were modeled after the Freundlich and the Langmuir isotherms.

Desorption of phenol from the EIHFMs was carried out in 0.2 M sodium hydroxide solution. To evaluate the efficacy of desorption process and long-term stability of the EIHFMs, repeated batch cycles of adsorption and desorption were conducted at a fixed phenol concentration of 1000 mg/L.

Finally, the EIHFMs were used as the partitioning phase in a TPPB for biodegradation of phenol using *P. putida*. The phenol concentrations investigated were 1000 and 2000 mg/L. In these experiments, the EIHFMs were first added into the aqueous solution to adsorb phenol and reduce its concentration to sub-inhibitory levels. The aqueous medium was then inoculated with *P. putida* for biodegradation.

7.2 Theoretical

7.2.1 Adsorption kinetics modeling

Phenol is a mildly acidic compound and it has a tendency to ionize in solutions. The adsorption of phenol on basic extractants such as TOPO involves diffusion of phenol to impregnated TOPO within the membrane followed by a chemical reaction with TOPO. Either of these processes can control the rate of reaction. To investigate the kinetics and mechanism of phenol adsorption on the EIHFMs, pseudo-first-order, pseudo-second-order and intraparticle diffusion kinetic models were used to fit the

experimental data. Lagergren's pseudo-first-order rate expression can be written as (Ho and McKay 1998):

$$\frac{dQ_t}{dt} = k_1(Q_e - Q_t) \tag{7.1}$$

where Q_t and Q_e are the amounts of phenol adsorbed on the EIHFMs at time t and at equilibrium, respectively, and k_1 is the pseudo-first-order rate constant. Eqn. (7.1) can be integrated to obtain:

$$\log_e(Q_e - Q_t) = \log_e Q_e - k_1 t \tag{7.2}$$

With experimental data of Q_t and t, Q_e and k_1 are obtained as adjustable parameters from curve fitting.

The rate of adsorption for pseudo-second-order kinetics is given by the expression:

$$\frac{dQ_t}{dt} = k_2(Q_e - Q_t)^2 \tag{7.3}$$

Eqn. (7.3) can be integrated to obtain:

$$\frac{t}{Q_t} = \frac{1}{k_2 Q_e^2} + \frac{t}{Q_e} \tag{7.4}$$

The rate constant Q_e and k_2 can be calculated from the slope and the intercept, respectively, of the straight line when experimental t/Q_t is plotted against t.

In adsorption systems where intraparticle diffusion can be a rate limiting step, the adsorption kinetics is commonly studied using the intraparticle diffusion model described by:

$$Q_t = k_i t^{0.5} \tag{7.5}$$

where k_i is intraparticle diffusion rate constant which can be calculated from the slope of the straight-line portions of Q_t vs. $t^{0.5}$ (Bahdod *et al.* 2009).

7.2.2 Adsorption isotherm

The most commonly used isotherm equations are the Langmuir and Freundlich isotherms. The Langmuir isotherm is based on the assumption of monolayer adsorption and is given by (McCabe *et al.* 2005):

$$Q_e = Q_{max}\left[\frac{k_L C_e}{1 + k_L C_e}\right] \tag{7.6}$$

Eqn. (7.6) can be rearranged as:

$$\frac{1}{Q_e} = \frac{1}{Q_{max}} + \frac{1}{k_L Q_{max} C_e} \tag{7.7}$$

where C_e is the equilibrium concentration of the solute in the solution (mg/L), k_L is the Langmuir adsorption constant (L/mg) and Q_{max} is the maximum adsorption capacity (mg/g). k_L and Q_{max} can be calculated from the slope and intercept , respectively, of the straight line when $1/Q_e$ is plotted against $1/C_e$.

Freundlich isotherm, on the other hand, assumes adsorption on heterogeneous sites with non- uniform distribution of energy levels and is given by:

$$Q_e = k_F C_e^{\frac{1}{n}} \tag{7.8}$$

which can be rearranged as,

$$\log_e Q_e = \log_e k_F + \frac{1}{n}\log_e C_e \tag{7.9}$$

where k_F and n are constants and can be estimated from the slope and intercept of the straight line obtained by plotting $\log_e Q_e$ against $\log_e C_e$, respectively.

7.3 Results and Discussion

7.3.1 Characterization of EIHFM

Fig. 7.1 shows the cross sections and external surface of polypropylene membrane as captured by SEM before and after immobilization with the extractant. The untreated fibers (Fig. 7.1a – 7.1c) exhibited smooth surfaces and cross sections, and could be easily distinguished from the EIHFMs which were characterized by white deposits of TOPO on every surface. The distribution of TOPO within the membrane was non-uniform and a higher concentration was observed towards the outer surface of the fibers. This distribution trend could have resulted from the movement of DCM during evaporation. Since the carrier solvent could only leave through the external surface of the hollow fibers, the trailing extractant could have been dragged to the outer surface and even outside the surface. That could also be the reason for TOPO deposits observed on the external surface of the EIHFMs, even though they were rinsed with water before the evaporation to remove the carrier solvent from the external surface.

Apart from TOPO deposits, SEM observation also showed changes in the fiber morphology after immobilization. The cross sections (Fig. 7.1d and 7.1e) showed irregular surfaces with fibrous morphology. This irregularity was more evident on the outer surface (Fig. 7.1f) which appeared scratchy with narrow fissures deposited with the extractant. These structural changes must have resulted from the high pressure on the membrane during carrier solvent evaporation which was accompanied by the phase change of TOPO. TOPO is a low density solid, which implies it can occupy a large volume even at a low concentration. On the other hand, the thickness of the membrane was only 50 μm and under these circumstances, membrane deformity was inevitable. For conventional membrane-based processes such as filtration and osmosis, such changes can alter membrane performance by affecting selectivity or

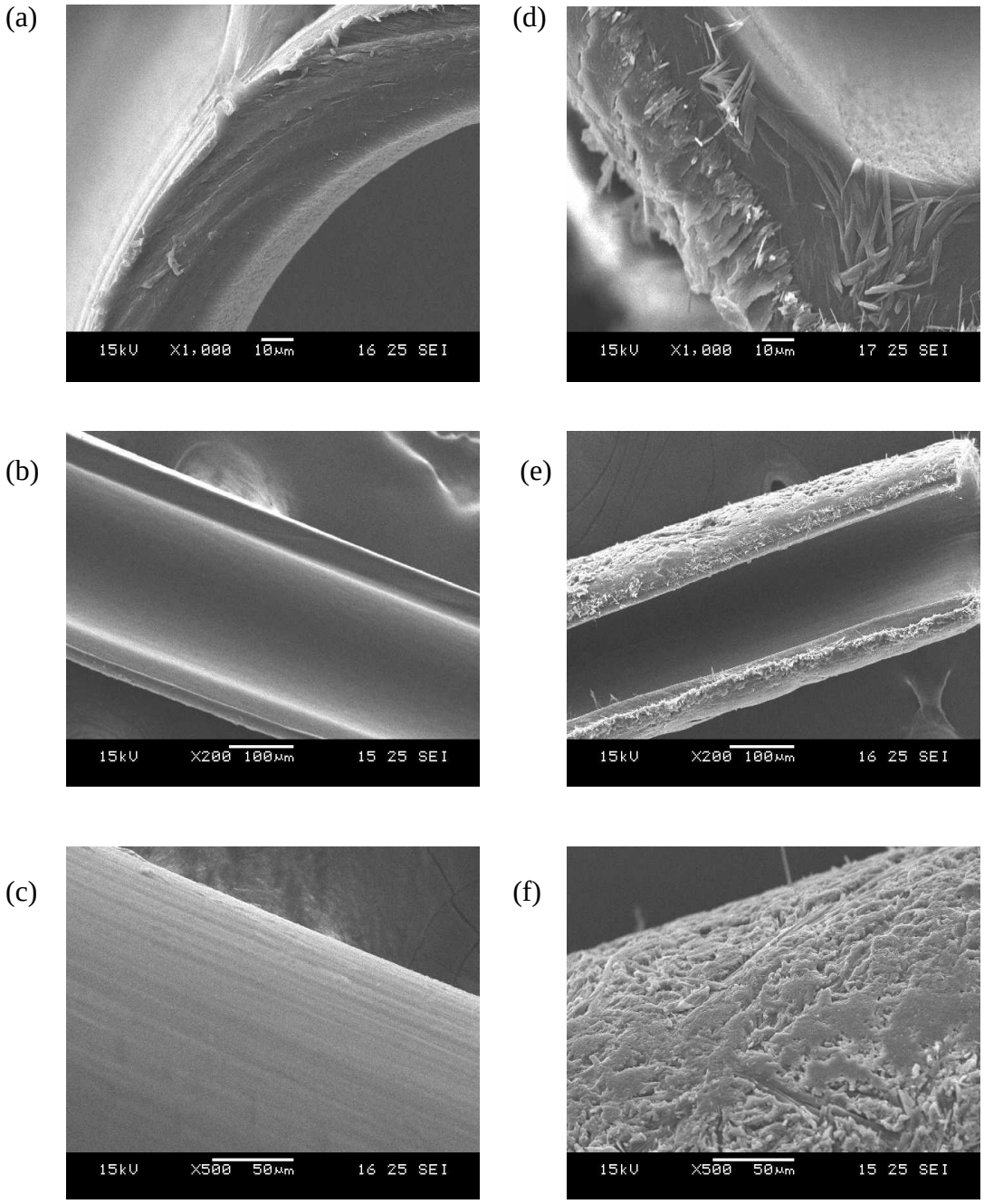

Figure 7.1 Cross-sections (a and b) and external surface (c) of untreated polypropylene membrane and; cross-sections (d and e) and external surface (f) of the EIHFMs.

mass transfer flux. However, the purpose of using hollow fibers in this research was only to provide a support for the extractant. Therefore, the physical stability of the fibers was more important.

7.3.2 Adsorption/Desorption on EIHFM

A. Effects of TOPO Concentration

To investigate the effects of increasing TOPO concentration during immobilization, adsorption experiments were carried out with four different sets of EIHFMs prepared with 50, 100, 200 and 400 g/L TOPO. Fig. 7.2 shows the adsorption profiles of 1000 mg/L phenol using different EIHFMs. The equilibrium adsorption capacity, Q_e, of the EIHFMs increased gradually with increasing concentration of TOPO within the hollow fibers. The experimental Q_e for the adsorption of 1000 mg/L phenol was lowest at 32 mg/g for 50 g/L TOPO, while a maximum of 57 mg/g was observed at 400 g/L TOPO. The increase in the adsorption capacity was not proportional to TOPO concentration, which implies that the amount of TOPO immobilized within the hollow fiber membranes was not directly proportional to the TOPO concentration in the carrier solvent. It was observed that a significant amount of TOPO was lost during evaporation of the carrier solvent during the fabrication of the EIHFMs. The loss was higher at higher TOPO concentrations as was observed from the growing thickness of TOPO deposits observed on the outer membrane after evaporation (SEM data not shown). While the sorption capacity increased by more than 20 mg/g when TOPO was increased from 50 to 200 g/L, it increased by a mere 5 mg/g for an increase in TOPO concentration from 200-400 mg/g.

The rate of adsorption on the EIHFM was quite fast and more than 70% phenol was adsorbed on the fibers (Q_t) in the first 2.5 minutes. A slower adsorption rate was

observed at higher TOPO concentration as the solute had to diffuse deeper into the membrane for the reaction when the extractant molecules closer to the outer surface were saturated. This could have resulted in a higher mass transfer resistance, resulting in a slower removal of phenol.

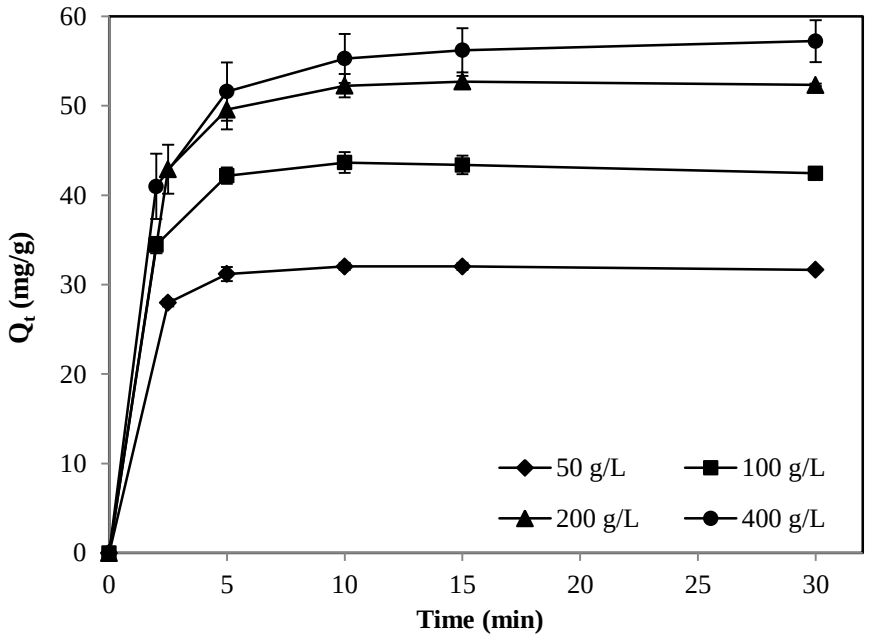

Figure 7.2 Effects of contact time on adsorption of 1000 mg/L phenol for the four sets of EIHFMs with varying TOPO concentration

B. Effects of Phenol Concentration

Fig. 7.3 shows the rate of adsorption of 500-2000 mg/L phenol on EIHFM prepared with 100 g/L TOPO. Phenol removal from the solution was rapid; Q_t reached approximately 95% of the saturation value within first 10 minutes and the equilibrium was achieved within 15 minutes in each experiment. Once again, the adsorption capacity did not increase proportionately with phenol concentration and a four times concentration increase from 500 to 2000 mg/L evoked only a three times increase in the adsorption capacity from approximately 23 to 69 mg/g. This could have happened due to a limited concentration of TOPO; however, this trend was observed for all the EIHFMs as shown in Table 7.1 and it can be concluded that the distribution

coefficient of phenol in TOPO/water system was not constant. This is consistent with the findings of Cichy and Szymanowski (2002) who reported a change in the partition coefficient of phenol at different phenol concentrations in the extraction of phenol using TOPO dissolved in kerosene.

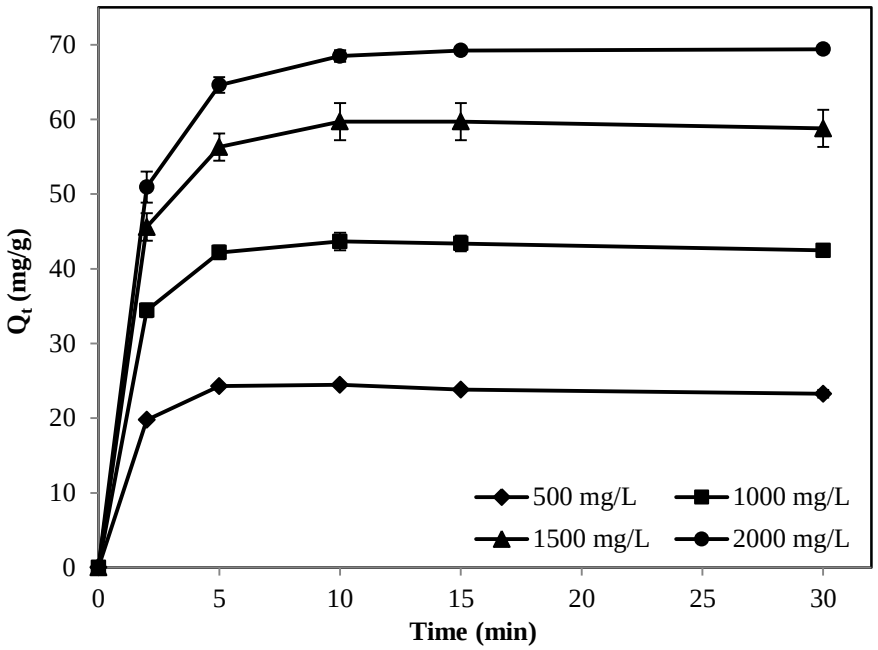

Figure 7.3 Effects of contact time on adsorption using EIHFM containing 100 g/L TOPO at varying initial phenol concentrations

Non-dispersive extraction of phenol has been carried out by several researchers in liquid-core microcapsules. Using 1-nonanol encapsulated in polysulfone (PSF), Zhao and his co-workers reported an equilibrium adsorption capacity of 20 mg/g at 2050 mg/L phenol, which required 10 hours to reach equilibrium. At different PSF to solvent ratio, adsorption rate could be enhanced but it resulted in a lower equilibrium capacity. Using tributylphosphate (TBP)/PSF microcapsules, Yin and his co-workers (2010) achieved better adsorption rates and the equilibrium capacity for 1000 mg/L phenol was 35 mg/g. The adsorption rates and capacities obtained by the EIHFMs fabricated in this research were much higher than these microcapsules as well as the conventional adsorbents such as apatites (Bahdod *et al.* 2009).

7.3.3 Adsorption kinetics

Our experimental adsorption data obtained using initial phenol concentration of 1000 mg/L was first fitted to the pseudo-first-order equation and the values of the model parameters Q_e and k_1 obtained from curve fitting has been tabulated in Table 7.2. The theoretical adsorption capacities for 50, 100, 200 and 400 g/L TOPO obtained from the model were 18, 30, 45 and 70 mg/g, with corresponding regression coefficients of 0.98, 0.99, 0.99 and 0.97, respectively. Since the theoretical Q_e values were widely different from the experimental values, pseudo-first order kinetics was not pursued any further.

Table 7.1 Experimental sorption capacities using four sets of EIHFMs for different phenol concentrations

Phenol Concentration (mg/L)	TOPO Concentration (g/L)			
	50	100	200	400
500	18	23	30	32
1000	32	42	52	57
1500	48	59	86	90
2000	54	69	106	113

In contrast, pseudo-second-order kinetic expression, when applied to the experimental data, resulted in a good fit with high regression coefficient for all the experiments. Fig. 7.4 shows pseudo-second-order adsorption kinetics for 1000 mg/L phenol using the four sets of EIHFMs. The Q_e values obtained from the plots for 50, 100, 200 and 400 g/L TOPO were 32, 43, 53 and 59, respectively, almost identical to the experimental values (Table 7.1). The rate constant, k_2 decreased with increasing TOPO concentration. Similar trends were observed for all other phenol concentrations

Table 7.2 Kinetic rate constants (k), equilibrium adsorption capacities (Q_e) and regression coefficients (R^2) obtained using different models for removal of phenol using TOPO-containing EIHFM

Kinetic model	Phenol conc.	Parameters	TOPO Conc (mg/L)			
			50	100	200	400
Pseudo-first-order	1000 mg/L	k_1 (hr^{-1})	0.551	0.647	0.586	0.702
		Q_e (mg/g)	18	30	45	70
		R^2	0.98	0.99	0.99	0.97
Pseudo-second-order	500 mg/L	k_2 (g/mg-hr)	0.432	0.382	0.264	0.04
		Q_e (mg/g)	18	23	29	33
		R^2	0.99	0.99	0.99	0.99
	1000 mg/L	k_2 (g/mg-hr)	0.239	0.138	0.052	0.02
		Q_e (mg/g)	32	43	53	59
		R^2	0.99	0.99	0.99	0.99
	1500 mg/L	k_2 (g/mg-hr)	0.048	0.058	0.012	0.007
		Q_e (mg/g)	49	60	89	94
		R^2	0.99	0.99	0.99	0.99
	2000 mg/L	k_2 (g/mg-hr)	0.066	0.026	0.007	0.008
		Q_e (mg/g)	55	71	111	120
		R^2	0.99	0.99	0.99	0.99
Intraparticle diffusion	1000 mg/L	k_i (mg/g-$hr^{0.5}$)	2.46	4.12	5.7	8.1
		R^2	0.83	0.84	0.89	0.91

as shown in Table 7.2, with regression correlation coefficients, $R^2 > 0.99$ in all the experiments. It can thus be concluded that the adsorption kinetics on the EIHFMs was pseudo-second order. This is consistent with reported studies of phenol adsorption using TBP containing PSF microcapsules wherein adsorption kinetics was best described by pseudo-second-order model (Yin *et al.* 2010).

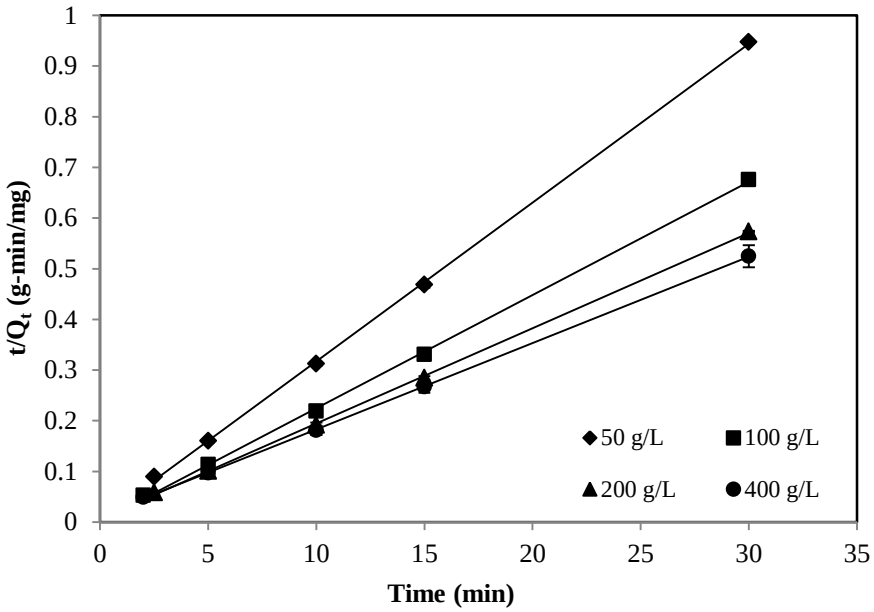

Figure 7.4 Pseudo-second-order sorption kinetics of 1000 mg/L phenol using different sets of EIHFM with varying TOPO concentration.

To determine whether intraparticle diffusion controlled the rate of adsorption, the amount of phenol adsorbed on the EIHFM were plotted against square root of elapsed time. The data could be fitted to a straight line in the first 10 minutes but with poor correlation coefficients. The rate constants were computed and listed in Table 7.2. The straight lines did not pass through the origin, implying that the intraparticle diffusion may not be the rate-controlling step although it could be an important factor influencing adsorption along with film diffusion and chemical reaction in some cases (Sun and Yang 2003)

Langmuir and Freundlich adsorption isotherms were used to model the equilibrium adsorption data obtained using all four sets of EIHFMs. Langmuir isotherm parameter Q_{max} and k_L, and Freundlich isotherm parameters k_F and n were determined from the equilibrium adsorption data along with the corresponding regression coefficients and these have been listed in Table 7.3. Both of these models described the experimental data with reasonable accuracy but the Langmuir isotherm resulted in a better fit as evident from the higher R^2 values. The maximum adsorption capacity, Q_{max} increased with increasing TOPO concentration, indicating an increase in the number of adsorption sites at higher TOPO concentration. The k_L values, too, increased at higher TOPO concentrations, resulting in more favorable adsorption isotherms (McCabe *et al.* 2005) as shown in Fig. 7.5. The k_F for Freundlich isotherm increased with TOPO concentration, showing a higher extent of adsorption at rising TOPO content within the EIHFMs.

Table 7.3 Langmuir and Freundlich isotherm parameters for the four different sets of EIHFM

TOPO Concentration	Parameters					
	Langmuir			Freundlich		
	Q_{max}	k_L	R^2	n	k	R^2
50 g/L	122	6.35×10^{-4}	0.99	1.44	0.382	0.98
100 g/L	151	8.72×10^{-4}	0.99	1.47	0.645	0.98
200 g/L	212	12.3×10^{-4}	0.99	1.33	0.748	0.99
400 g/L	217	15.8×10^{-4}	0.99	1.39	1.10	0.99

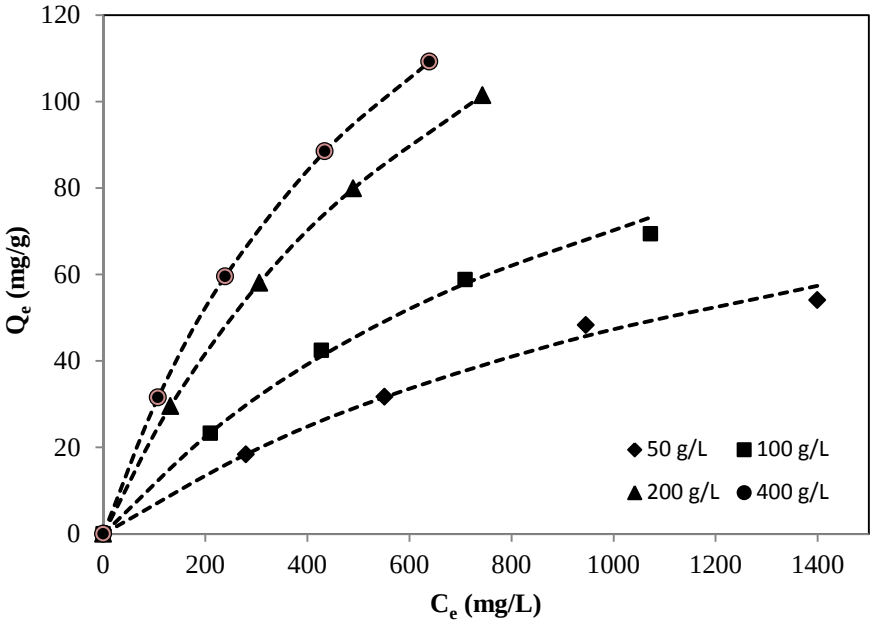

Figure 7.5 Langmuir isotherms for EIHFMs containing varying TOPO concentration (markers represent experimental values and the dotted lines represent modeled values)

7.3.4 Regeneration and Stability

Fig. 7.6 shows phenol desorption profiles from the EIHFMs after equilibrium adsorption of phenol at an initial concentration of 1000 mg/L. Compared to the adsorption profiles shown in Fig. 7.2, the desorption rates were slower and phenol removal required longer times with increasing TOPO content within the EIHFMs, especially at 400 g/L TOPO. While phenol from EIHFMs containing 50 g/L TOPO was removed within the first 30 min, approximately 2%, 4% and 14% (from mass balance calculations) of the solute remained in the other EIHFMs containing 100, 200 and 400 g/L TOPO, respectively, after the same time period. However, the amount of phenol desorbed after one hour in each set of EIHFMs was comparable to the amount initially adsorbed, implying that desorption was completed within one hour in all the experiments. The comparatively slower mass transfer rate observed during desorption versus adsorption is an indication of the strong affinity of the solute for the extractant, which resulted in a slow release of phenol into sodium hydroxide.

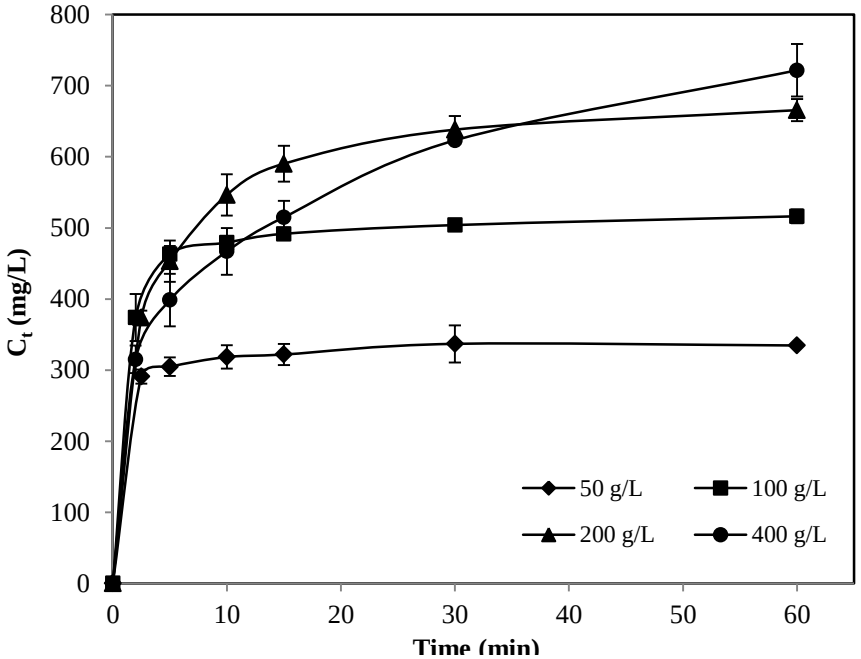

Figure 7.6 Effects of contact time on desorption of phenol using all four sets of EIHFMs with varying TOPO concentration after adsorption of phenol at 1000 mg/L

In an adsorption/desorption process, while a good adsorbent should exhibit high adsorption capacity and high mass transfer rates, regeneration and reuse of the adsorbent are critical to achieve high process economy and sustainability of operation. To investigate the stability of the EIHFMs over repeated operations, adsorption/desorption cycles were carried out with 1000 mg/L initial phenol concentration using EIHFMs containing 50 g/L and 200 g/L TOPO and the results are shown in Fig. 7.7. The amounts of phenol removed from the solution during ten consecutive batch experiments under identical conditions remained constant during each run. The average values of Q_e were computed as 32.2 ± 1.3 and 52.3 ± 0.9 mg/g for 50 and 200 g/L TOPO, respectively. Therefore, it can be concluded that the immobilization of the extractant in the polypropylene hollow fibers was stable.

Although solvent/extractant encapsulation in polymeric support has been keenly pursued in the past few years (Whelehan *et al.* 2010; Yin *et al.* 2010; Zhao *et al.*

2010), immobilization could only be carried out during membrane polymerization which is a complex process and a significant amount of the extractant is lost during encapsulation. On the other hand, EIHFM preparation is a simple technique requiring only a very small quantity of the extractant and the carrier solvent. It is even possible to recycle the fibers used during immobilization by washing the EIHFMs with the carrier solvent. Table 7.4 lists the Q_e values for adsorption of 1000 mg/L phenol on EIHFMs containing 100 mg/L TOPO after washing with pure DCM. The Q_e value dropped from 42 mg/g to 6 mg/g after first wash and to 4 mg/g after the second wash, which was almost identical to the Q_e of the original untreated fibers.

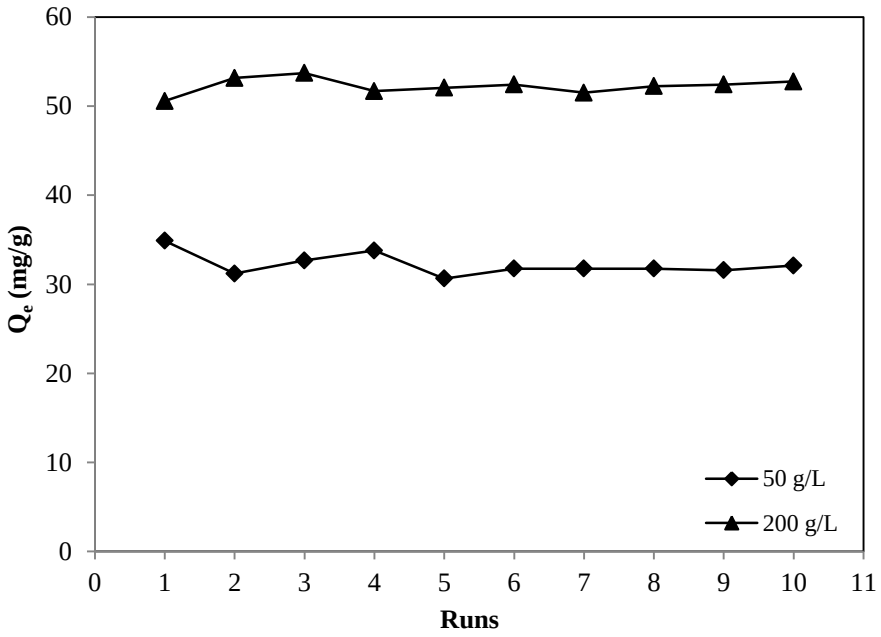

Figure 7.7 Sorption capacities of 50 and 200 g/L TOPO containing EIHFMs during consequent runs at initial phenol concentration of 1000 mg/L

These results are significant as most of the membrane-enhanced extraction processes are carried out in commercial membrane contactors or fibers (Cichy and Szymanowski 2002; González-Muñoz *et al.* 2003; Shen *et al.* 2009; Teresa *et al.* 2007). These contactors/fibers are quite expensive and will incur huge operating costs if the membranes cannot be recycled.

Table 7.4 Adsorption capacities (Q_e) of EIHFMs after washing with DCM

Condition	EIHFM	First Wash	Second Wash	Untreated fibers
Q_e (mg/g)	42	6	4	4

7.3.5 Application to TPPB

TPPBs are one of the most innovative applications of solvent extraction and have extensively been studied for the biodegradation of aromatic compounds using both organic solvents (Collins and Daugulis 1997) and polymeric adsorbents (Tomei *et al.* 2010) including liquid-core microcapsules (Sarma *et al.* 2011) as the partitioning phase. To demonstrate the applicability of our TOPO-containing EIHFMs, these were used as the partitioning phase in a solid/liquid TPPB.

Fig. 7.8a shows cell growth and substrate removal profiles for the biodegradation of 1000 mg/L phenol. During the abiotic mixing of the two phases, rapid partitioning of phenol in the EIHFMs decreased the solution phenol concentration to 130 mg/L within 30 minutes. For *P. putida*, the inhibitory phenol limit was 600 mg/L. Consequently, an exponential growth profile was observed in the absence of substrate inhibition with a specific growth rate of 0.19 hr^{-1}. Cell growth continued for 22 hours and the beginning of negative growth period coincided with the exhaustion of phenol in the aqueous phase. The slow change in the substrate removal profile was an indication of the rapid mass transfer rate which ensured that equilibrium conditions prevailed between the two phases. Phenol was completely removed within 26 hours with a biomass yield of 0.42 g/g and an average biodegradation rate of 40.2 mg/L-hr. At the end, the EIHFMs were washed with sodium hydroxide to wash away any loosely bound cells on the membrane and to analyze any residual phenol on the fibers.

(a)

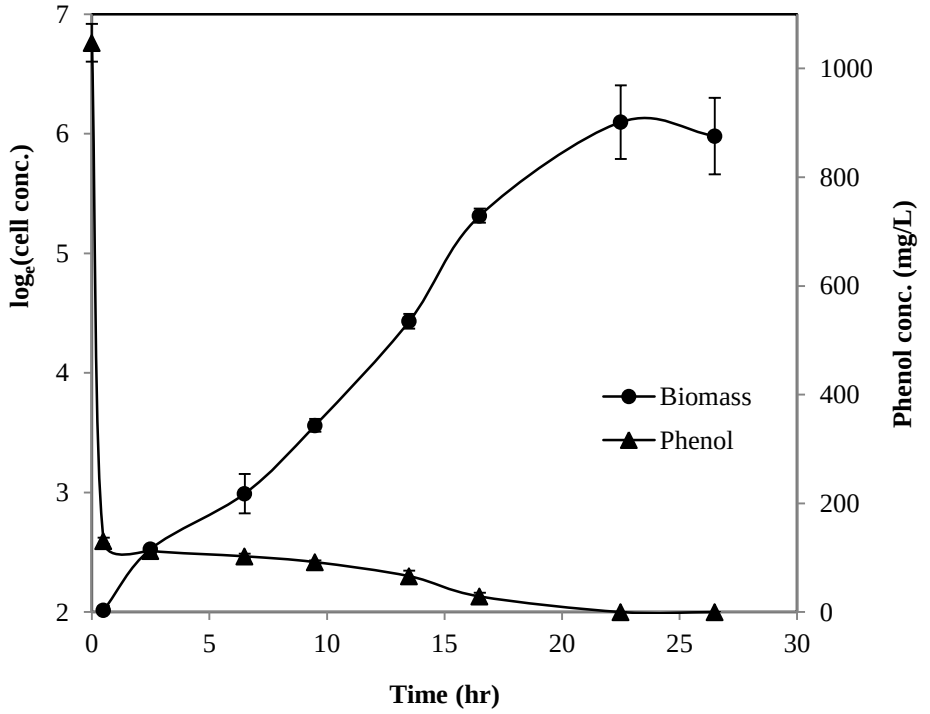

(b)

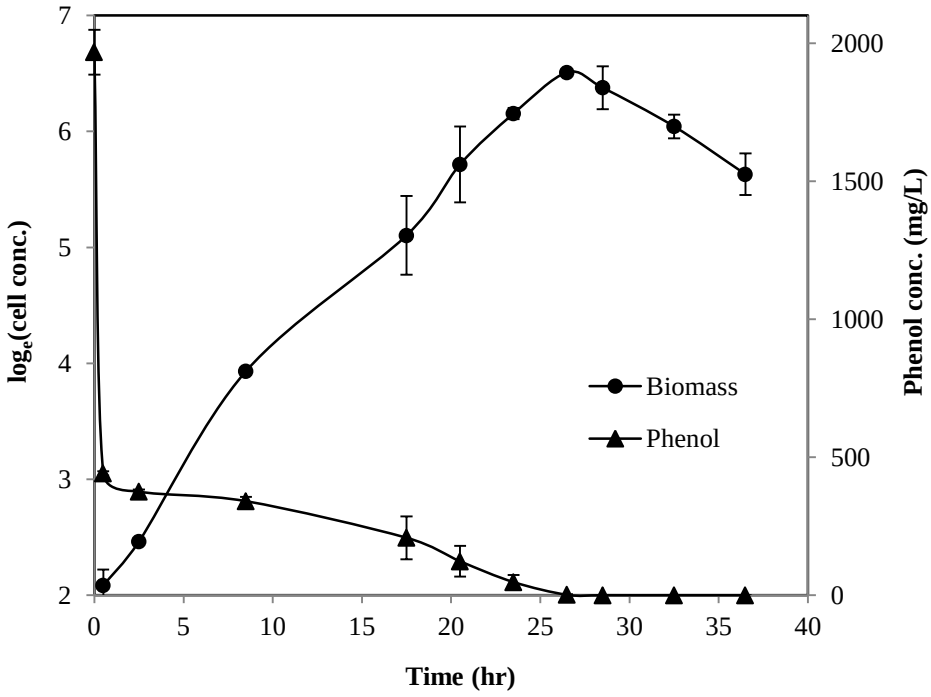

Figure 7.8 Cell growth and substrate removal profiles in the TPPB at initial phenol concentrations of: (a) 1000 mg/L and, (b) 2000 mg/L.

No phenol was detected in the alkaline solution which confirmed that phenol metabolism was completed within 26 hours.

Similar trends were observed during biodegradation of 2000 mg/L phenol as shown in Fig. 7.8b. After initial equilibration, phenol concentration in the solution was recorded as 440 mg/L. The reason for a comparatively higher solution concentration of phenol could either be a change in the distribution coefficient or a slower mass transfer rate. Nevertheless, the aqueous concentration of substrate at 440 mg/L was sub-inhibitory and microorganisms exhibited a specific growth rate of 0.17 hr^{-1}. Cell growth reached confluence after 26 hours with concomitant exhaustion of phenol in the aqueous phase. Although phenol was no longer detectable in the aqueous medium, the experiment was continued for another 10 hours to ensure that all phenol within the EIHFMs was completely desorbed and degraded. Biodegradation was deemed completed within 36 hours and the biomass yield and the average biodegradation rate were obtained as 0.34 g/g and 55.6 mg/L-hr, respectively.

Although a higher cell growth rate was expected in the TPPB in the absence of substrate inhibition, the maximum specific growth rates obtained were relatively low. It is suspected that the TOPO-containing fibers may not be quite compatible with the microorganisms due to the toxic nature of TOPO. Nevertheless, biodegradation rates achieved in the TPPB were still quite high, largely because of the high sorptioncapacity of the EIHFMs, which helped in rapid mitigation of substrate inhibition and the high desorption rate which ensured that an equilibrium distribution of phenol was maintained between the two phases and the onset of diffusion limitation was either prevented or delayed.

7.4 Conclusions

A novel technique for the immobilization of solid extractants in hollow fiber membranes was proposed and EIHFMs have been prepared using TOPO as the model extractant. TOPO impregnation within the membrane was verified using SEM and adsorption/desorption performance of the EIHFMs has been investigated. The EIHFMs exhibited high sorption rates and capacity, achieving equilibrium within 10-30 minutes. The sorption capacity could be easily enhanced by increasing TOPO content within the EIHFMs. The adsorption kinetics has been described accurately using pseudo-second-order model and fitted Langmuir and Freundlich isotherms with reasonable accuracy. Phenol desorption from the EIHFMs was effective, which facilitated its reuse without any loss of performance during consequent operations. The use of EIHFMs in the TPPB facilitated rapid alleviation of substrate inhibition, enabling *P. putida* to metabolize phenol at high biodegradation rates.

The EIHFM comes across as a hybrid technology, which combines the merits of solvent extraction, adsorption and hollow fiber membranes to extenuate the drawbacks associated with each of the individual process. With high sorption capacity, rapid equilibration and prolonged stability, EIHFM is a powerful tool for the removal of aromatic compounds from wastewater streams and can be explored as a substitute to HFSLM.

8 Two-Phase Biodegradation of Phenol in an Extractant Impregnated Hollow Fiber Membrane Bioreactor

8.1 Introduction

Solid/liquid two-phase biodegradation is usually carried out in commercial fermenters wherein the polymeric adsorbents are dispersed into the liquid medium using high agitation speeds (Prpich and Daugulis 2005). The use of solid NAPs in TPPBs has several advantages over their liquid counterparts as these are usually inexpensive, non-volatile, non-flammable, non-bioavailable and biocompatible (Daugulis *et al.* 2011). The downside of using solid NAPs is the low adsorption capacity of the polymeric adsorbents which may necessitate the use of large quantities of the NAPs for the alleviation of substrate inhibition (Zhao *et al.* 2009). The desorption characteristics of the polymeric adsorption is also critical for the process stability. If desorption is not effective, the biodegradation rates could be slow and biodegradation might not be complete. Besides, the NAPs could be unusable after only a few experimental runs. In many cases, in which the density of the polymeric adsorbents is lower than that of water, the adsorbents tend to float at the surface of the aqueous phase. This could result in poor contact between the solid and the liquid phases, leading to low mass transfer rate of the substrate between the two phases (Zhao *et al.* 2010). Furthermore, interphasic mass transfer rate of the substrate in TPPBs still depend on the rate of mixing. Agitation rate of 400 RPM has been reported during biodegradation of phenol (Amsden *et al.* 2003) and 600 RPM in the biodegradation of biphenyls (Rehmann and Daugulis 2007) in solid/liquid TPPBs. Another disadvantage of solid/liquid TPPBs is the inflexible bioreactor configuration, which limits their applicability in simultaneous adsorption and biodegradation

In previous chapter, a new technique was described for the immobilization of solid organic extractants into hollow fiber membranes, and EIHFMs were prepared by immobilizing TOPO in polypropylene support. The EIHFMs come across as a hybrid technology which combine the advantages of three different technologies in separation processes: (1) the operational and configurational flexibility, and high specific interfacial area of the hollow fiber membranes (Shen *et al.* 2009); (2) the high mass transfer rates and high capacity of the organic extractants for aromatic compounds (Hossain and Maisuria 2008), and; (3) the non-dispersive and environmentally sustainable nature of adsorption (Quijano *et al.* 2009). The EIHFMs exhibited rapid adsorption and desorption rates and high adsorption capacity, and these novel adsorbents can be used as the NAP to alleviate the challenges associated with solid/liquid TPPBs.

In this chapter, an extractant impregnated hollow fiber membrane bioreactor (EIHFMB) was developed and operated for two-phase biodegradation of phenol. In this novel membrane bioreactor, the membranes themselves acted as the partitioning phase, obviating the need for additional solvent or adsorbents for pollutant sequestration, as required in conventional TPPBs. The objectives of this research were:

1. Fabricate and operate the EIHFMB for biodegradation of high strength phenolic wastewater;
2. Investigate the effects of increasing phenol concentrations on cell growth and phenol removal in the EIHFMB;
3. Evaluate the effects of increasing EIHFM length on biodegradation performance of the EIHFMB;

4. Study the effects of aqueous flow rate on cell growth and phenol removal in the EIHFM; and
5. Examine the stability of the immobilized extractants in the presence of biodegrading microorganism in the EIHFMB.

The details of the EIHFM contactor fabrication are provided in Section 3.7.5 and the EHFMB setup is shown in Fig. 3.4. The phenolic wastewater was first circulated in the EIHFMB at a flow rate of 8 mL/min and phenol was allowed to equilibrate between the TOPO-containing fibers and the aqueous phase. Microorganisms were inoculated into the EIHFMB once phenol concentration in the aqueous phase reached sub-inhibitory levels. At the end of each experimental run, the bioreactor was washed with 1 M sodium hydroxide solution to remove the bacteria from the membranes and to ensure reproducibility of the results. All the experiments were carried out using the same EIHFM contactors.

To demonstrate the effects of substrate inhibition on cell growth and biodegradation performance in the EIHFMB, experiments were conducted at feed phenol concentrations of 800-3000 mg/L. The trends in adsorption rates, equilibrium aqueous phenol concentration, cell growth rates, biomass yields and biodegradation rates were analyzed. These results were also used to deduce the maximum phenol concentration that could be treated in the EIHFMB under the operating conditions investigated.

In hollow fiber membrane based solvent extraction, the increase in the membrane length enhances the interfacial mass transfer area. On the other hand, the extraction capacity in the NAP increases with the volume of the NAP, or with an increase in the partition coefficient of the substrate in the NAP. In the EIHFMB, however, the EIHFMs themselves were the partitioning phase and it was anticipated that an

increase in the membrane length could enhance the adsorption capacity as well as the adsorption rate in the EIHFMB. To demonstrate the effects of membrane length, the effective EIHFM length was increased from 60 to 90 cm by connecting another membrane contactor of 30 cm effective length in series with the EIHFM contactor in the bioreactor setup shown in Fig. 3.4.

In membrane contactor based separation processes, a large fraction of the mass transfer resistance lies in the boundary layers. The thickness of this boundary layer is very important as the diffusion resistance increases with the thickness, which may lead to slow adsorption and desorption of phenol in the EIHFMB. To study the effects of aqueous flow rates in the EIHFMB, the flow rate was varied between 5-12 mL/min and the consequent changes in the cell growth and phenol biodegradation were examined.

In Chapter 7, the stability of the EIHFMs was examined during repeated batch cycles of adsorption/desorption and the performance remained stable as shown in Fig. 7.7. Since these experiments were carried out in an abiotic environment, the stability of immobilized TOPO within the hollow fiber membrane was again investigated in the EIHFMB. To demonstrate the EIHFMB stability, two-phase biodegradation of 1000 mg/L phenol in the EIHFMB was repeated over a span of 400 hours, during which the EIHFMB was operated at different phenol loadings and operating conditions. The original and repeated cell growth and phenol removal profiles were also compared.

8.2 Results and Discussion

8.2.1 Cell Growth and Biodegradation

To investigate two-phase biodegradation in the EIHFMB, batch experiments were performed at inhibitory phenol concentrations ranging from 800-3000 mg/L. The

membrane contactors used for these experiments were the same as those used for two-phase biodegradation in the HFSLMB, except that the polypropylene fibers here had been impregnated with solid TOPO. The fibers therefore acted as the adsorbents to facilitate solvent-free two-phase biodegradation. Prior to inoculation, the phenolic wastewater was circulated in the shell side of the EIHFMB for one hour to facilitate the phenol adsorption on the EIHFMs. This lowered the aqueous phenol concentration to sub-inhibitory levels which were suitable for cell growth. *P. putida* in the late exponential phase from the preculture was then inoculated into the EIHFMB. Cell growth and phenol removal profiles in the EIHFMB were similar for all the phenol concentration investigated except at the highest concentration of 3000 mg/L. For discussion purposes, results obtained at 1000 mg/L and 2000 mg/L are presented here as being representative.

Fig. 8.1 shows the temporal cell growth and phenol removal profiles in the EIHFMB at feed phenol concentration of 1000 mg/L. During the first 1 hour of wastewater recirculation in the shell side, phenol was rapidly adsorbed on the EIHFMs. The equilibrium distribution of phenol between the two phases was achieved within 3 hours, and the aqueous phase phenol concentration stabilized at a sub-inhibitory concentration of 124 mg/L. The microorganisms were inoculated into the EIHFMB after one hour of operation. Although phenol concentration in the aqueous phase had decreased significantly in the first hour, it did not reach equilibrium as evident from further lowering of phenol concentration. Microorganisms in the EIHFMB exhibited a lag phase of about 5 hours, during which phenol metabolism was negligible. Therefore, it can be concluded that the changes in phenol concentration during this period was only due to the adsorption of phenol on the EIHFMs. The slow adsorption rate in the EIHFMB could be attributed to the high packing density of the fibers in the

EIHFM contactor which prevented direct contact of the aqueous phase with all of the 150 fibers. In that case, phenol was not able to diffuse into the EIHFMs immediately.

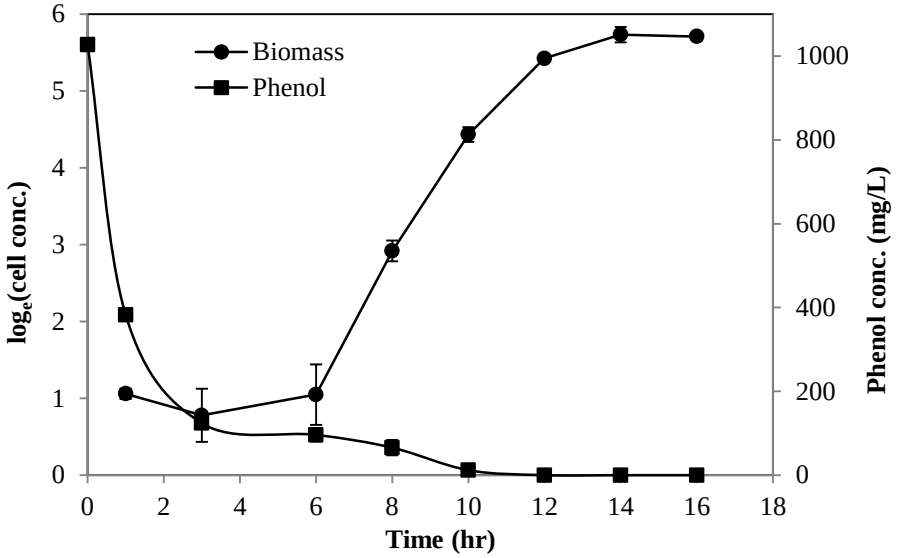

Figure 8.1 Temporal cell growth and phenol concentration profiles during biodegradation of 1000 mg/L in EIHFMB

The short lag phase exhibited by *P. putida* during biodegradation of 1000 mg/L phenol was consistent with other TPPBs reported in the literature, which has been attributed to the higher system loading of phenol (Rehmann *et al.* 2008). Since the aqueous phenol concentration in the EIHFMB at the time of inoculation was below 400 mg/L which was not inhibitory, the lag phase could also be a result of the presence of TOPO on the outer surface of the membranes. Experimentally, we have found that TOPO was slightly toxic to the cells when the cells were directly exposed to it. The lag phase in the EIHFMB was followed by an exponential growth phase in which *P. putida* exhibited a specific growth rate of 0.73 hr^{-1}. This growth rate was quite high and even better than that exhibited by the cells at an equivalent phenol concentration in suspension cultures. This high growth rate could be a result of the physiological changes in the cells during cell adaptation in the lag phase. Such high cell growth rates have also been observed during two-phase biodegradation of phenol

in the dispersion-based TPPB, as described in Chapter 4 (Fig. 4.3). Most of the phenol in the EIHFMB was metabolized within 7 hours of exponential growth phase which was a result of the rapid desorption of phenol from the fibers and high biodegradation rates of the microorganisms. Phenol was removed from the aqueous phase within 12 hours, at a volumetric removal rate of 85.6 mg/L-hr and a biomass yield of 0.31 g/g.

Similar cell growth and phenol removal trends were observed during the biodegradation of 2000 mg/L phenol as shown in Fig. 8.2. After adsorption of phenol on the EIHFMs, the equilibrium concentration of phenol observed in the bioreactor after 6 hours of operation was about 400 mg/L. The microorganisms again exhibited a short lag phase, this time of about of 6 hours. During the lag phase, cell concentration did not remain constant but decreased to lower concentrations. This change in cell concentration could be a result of phenol toxicity at high concentrations in the EIHFMB at the time of inoculation. The aqueous phenol concentration after one hour of equilibration was 532 mg/L, which was still rather toxic for the suspended cells. During exponential growth phase, the specific growth rate was determined as 0.57 hr^{-1}, which was again much higher than the specific growth rate observed at equivalent phenol concentration in suspension cultures. Phenol removal was completed within 22 hours.

The biodegradation performance of the EIHFMB was comparable to other studies on phenol biodegradation in solid/liquid TPPBs reported in literature (Table 8.1). For example, Amsden and co-workers (2005) used poly(ethylene-co-vinyl acetate) (EVA) beads to reduce phenol concentration in a TPPB from 2000 to 718 mg/L in 23 hours. Phenol was subsequently metabolized by *P. putida* in in about 35 hours, starting with a 13 hours lag phase. Prpich and Daugulis (2005) harnessed the biocompatibility of

solid NAPs to formulate a microbial consortium with better growth characteristics and the potential for phenol metabolism. Since then, most of the research on solid/liquid TPPBs had been carried out using mixed microbial consortiums (Tomei *et al.* 2010; Tomei *et al.* 2011). The biodegradation performance of the EIHFMB was also better than that reported for TPPBs using liquid partitioning phase as has been previously shown in Table 4.4.

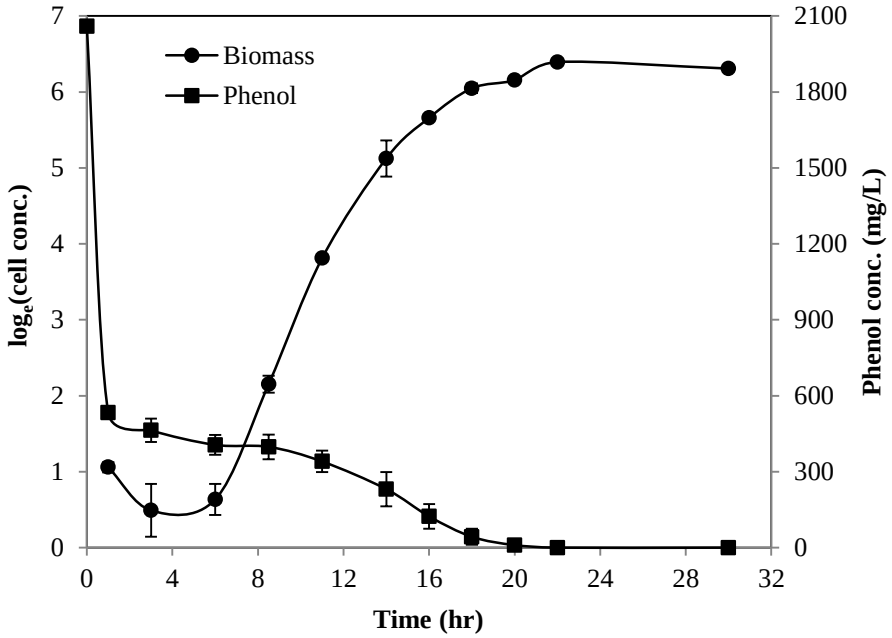

Figure 8.2 Temporal cell growth and phenol concentration profiles during biodegradation of 2000 mg/L in EIHFMB

8.2.2 Biodegradation Stages

Phenol removal in the EIHFMB occurred in three distinct stages as shown in Fig. 8.3a. During the first hour, the aqueous medium was bacteria-free and the removal of phenol was solely due to adsorption on the EIHFMs. Phenol adsorption continued for the first 3-6 hours until equilibrium with the EIHFMs was reached. At a feed phenol concentration of 1500 mg/L, the equilibrium concentration after 5 hours was close to 250 mg/L. For the first few hours after inoculation in the EIHFMB, microorganisms exhibited a lag phase and phenol metabolism was negligible (Fig. 8.3b). In many

cases, especially at feed phenol concentrations above 1500 mg/L, the biomass concentration in the bioreactor decreased during the lag phase. It was possible that at high feed phenol concentrations, the aqueous concentration of phenol did not reach sub-inhibitory levels at the time of inoculation. Consequently, the microorganisms were exposed to toxic concentrations of phenol which could have led to cell death.

Table 8.1 Performance of conventional TPPBs in two-phase biodegradation of phenol

Phenol conc. (mg/L)	NAP	Micro-organism	Lag phase (hr)	Biodegradation time (hr)	Agitation Speed (RPM)	Reference
2000	EVA	*P. putida* 11172	13	60	400	(Amsden *et al.* 2003)
2000	EVA	Microbial Consortium	10	30	400	(Prpich and Daugulis 2005)
1000	HYTREL	Microbial Consortium	3	12	180	(Prpich and Daugulis 2006)
4800	OMMT-PSF	Mixed culture	8	32	180	(Zhao *et al.* 2009)

The lag phase was immediately followed by an exponential growth phase, which was characterized by high cell growth and biodegradation rates. At the onset of exponential growth, phenol distribution between the two phases was at equilibrium. When the microorganisms started metabolizing phenol, the equilibrium was disrupted and phenol was desorbed from the EIHFMs to sustain the equilibrium in the EIHFMB. In the beginning, the biomass concentration and the consequent biodegradation rate were low, whereas the desorption rate was high due to a higher concentration gradient. As a result, the removal of aqueous phenol was quickly

(a)

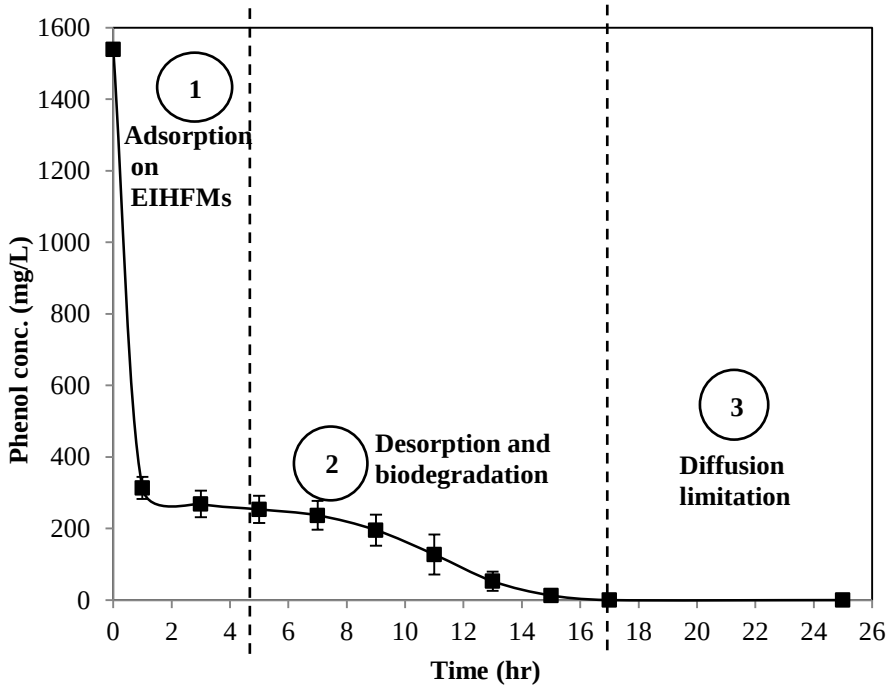

(b)

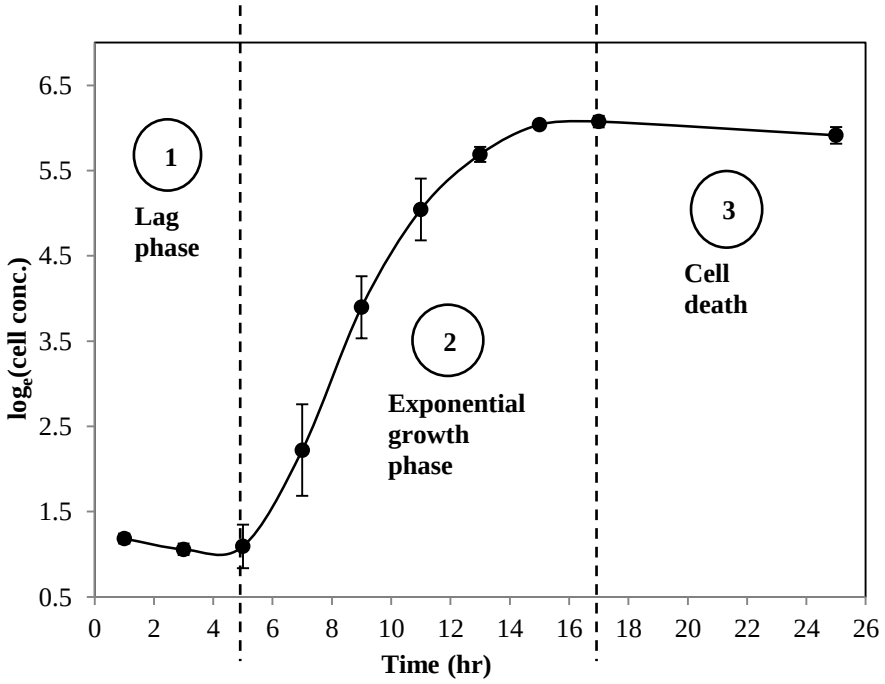

Figure 8.3 Two-phase biodegradation of 1500 mg/L phenol in the EIHFMB: (a) different stages of phenol removal; (b) different stages of cell growth

replenished. However, with gradual metabolism of more phenol and generation of new biomass, the biodegradation rates increases, whereas the desorption rates decreased due to the falling concentration gradient. When the biodegradation rate of phenol surpassed the desorption rate of phenol, phenol was rapidly depleted from the aqueous medium, which eventually led to phenol depletion in the aqueous phase. The exhaustion of aqueous phenol coincided with the beginning of the negative cell growth period. Any remaining phenol on the EIHFMs was metabolized under nutrient limitation during the third stage.

Since there was no way to determine the concentration of phenol in the solid phase during biodegradation, the EIHFMB was operated for an additional 7-10 hours, to ensure that all the phenol from the EIHFMs had desorbed and subsequently biodegraded. At the end of each experimental run, the EIHFMB was washed with 1 M sodium hydroxide solution, which was later analyzed by GC for any presence of phenol. No phenol was detected in the alkaline solution in any of the experiments, which indicated that phenol had been completely mineralized in the EIHFMB.

8.2.3 Effects of Substrate Concentration

During EIHFMB operation, majority of phenol dissolved in the feed wastewater was adsorbed on the TOPO impregnated fibers in the first few hours. As a result, phenol concentration in the aqueous phase remained low and the maximum phenol concentration available to the microorganisms was only 10-20% of the initial phenol concentration. When phenol concentration in the feed solution was increased to higher concentrations, there was a corresponding increase in the equilibrium phenol concentration in the aqueous phase, as well as in the severity of substrate inhibition experienced by the microorganisms. The microorganisms were exposed to a minimum

phenol concentration of 87 mg/L at feed phenol concentration of 800 mg/L, whereas the equilibrium concentration at feed phenol concentration of 3000 mg/L was close to 1000 mg/L, at which no cell growth or phenol metabolism was observed. The equilibrium concentrations during other experiments were all below 600 mg/L, and their effects on cell growth and phenol biodegradation in the EIHFMB are summarized in Table 8.2.

Table 8.2 Effects of substrate inhibition on two-phase biodegradation of phenol in EIHFMB

Feed conc. (mg/L)	Equilibrium conc. (mg/L)	Lag phase (hr)	Specific growth rate (hr^{-1})	Biomass yield (g/g)	Removal time (hr)	Removal rate (mg/L-hr)
800	87	5	0.6	0.31	12	73.9
1000	110	5	0.73	0.31	12	85.6
1500	253	5	0.6	0.29	17	90.6
2000	406	7	0.57	0.3	22	98
2500	540	7	0.34	0.24	28	91.4
3000	970	-	-	-	-	-

The gradual increase in the equilibrium phenol concentrations at increasing feed concentration from 800-2500 mg/L heightened the severity of the substrate inhibition on the microorganisms. As a result, there was a gradual lowering in the specific growth rates of the microorganisms as can be seen in Table 8.2. The maximum specific growth rate observed at phenol concentration of 1000 mg/L was 0.73 hr^{-1}, which decreased to 0.34 hr^{-1} at a feed of 2500 mg/L phenol. At 3000 mg/L, however, the aqueous phenol concentration was detrimental for the cells, and neither cell

growth nor biodegradation was observed in the bioreactor. This growth trends in the EIHFMB was consistent with those observed earlier in Chapter 4, in which phenol biodegradation was accomplished by suspension culture. Even the lag phase duration in the bioreactor was quite consistent in every experimental run, which was constant at around 5-7 hours. Since the lag phase duration did not change much with phenol concentrations, and there was a lag phase at innocuous aqueous phenol concentrations as low as 100-200 mg/L, it is possible that the lag phase was a result of the microbes acclimatizing to the presence of TOPO embedded on the outer surface of the hollow fiber membranes. The biodegradation time and the biodegradation rate increased with phenol loading, except at 2500 mg/L of initial phenol. The lower biodegradation at 2500 mg/L could have been a result of the slow growth rate of the microorganisms.

Analogous to the HFMB and the HFSLMB, the cell growth in the EIHFMB was independent of the total phenol concentration as evident from the high cell growth rates, which exceeded the growth rates in single-phase cultures. The biomass yields in the EIHFMs however, were lower than those in the single-phase cultures at equivalent aqueous phenol concentrations. It was also observed that the biomass yields were constant at 0.29-0.31 g/g at initial phenol concentrations up to 2000 mg/L. However, the biomass yield decreased significantly at a higher concentration of 2500 mg/L, which could be attributed to the high toxicity of phenol at concentrations above 500 mg/L. Nevertheless, these biomass yields which were determined based on suspended cell densities, were really rather subjective because a significant amount of biomass have been observed to be attached on the membranes and the silicone tubing.

8.2.4 Effects of Interfacial Area

Unlike conventional TPPBs, where the substrate partitioning in the NAP could be enhanced by improving the NAP to aqueous phase volume ratio while the mass transfer rates were improved by increasing the interfacial mass transfer area, the adsorption capacity and rates in the EIHFMB could be enhanced by increasing the length of the EIHFMB. The effects of interfacial mass transfer area on EIHFMB performance was investigated in the biodegradation of 3000 mg/L phenol, by increasing the effective EIHFM length to 90 cm, by connecting an additional EIHFM contactor in the existing bioreactor setup.

Fig. 8.4 shows the cell growth and biodegradation profile during biodegradation of 3000 mg/L phenol at the increased interfacial area of the EIHFMs. Phenol concentration in the aqueous phase dropped to 600 mg/L in the first two hours of operation and the equilibrium concentration of 480 mg/L was reached within 4 hours. Since it was anticipated that the phenol concentration could not reach sub-inhibitory levels within one hour, the microorganisms were inoculated in the bioreactor after two hours of equilibration. The microorganisms exhibited an exponential growth profile after 7-8 hours of lag phase. The specific growth rate at this concentration was 0.49 hr^{-1} and phenol was completely removed from the aqueous phase within 35 hours at an average removal rate of 84.1 mg/L-hr, while the final biomass yield was 0.3 g/g.

For the increased EIHFM length, phenol in the aqueous feed was rapidly lowered to sub-inhibitory concentrations, whereas there was a huge improvement in the adsorption capacity of the EIHFMB. The low equilibrium concentration in the aqueous phase was accompanied by high cell growth rate and biomass yield, which were higher than those observed earlier in the biodegradation of 2500 mg/L phenol.

These results are significant as they demonstrate that the EIHFMB can achieve an improvement in the adsorption capacity and adsorption rates by changing just one of the bioreactor parameters, while the same is achieved by changing two bioreactor parameters namely the interfacial area and the phase ratio in conventional TPPBs. It can also be concluded that the increase in the length of the EIHFMs did not affect cell growth adversely because no significant changes were observed in lag phase duration, while the specific growth rates and biomass yields were still quite high.

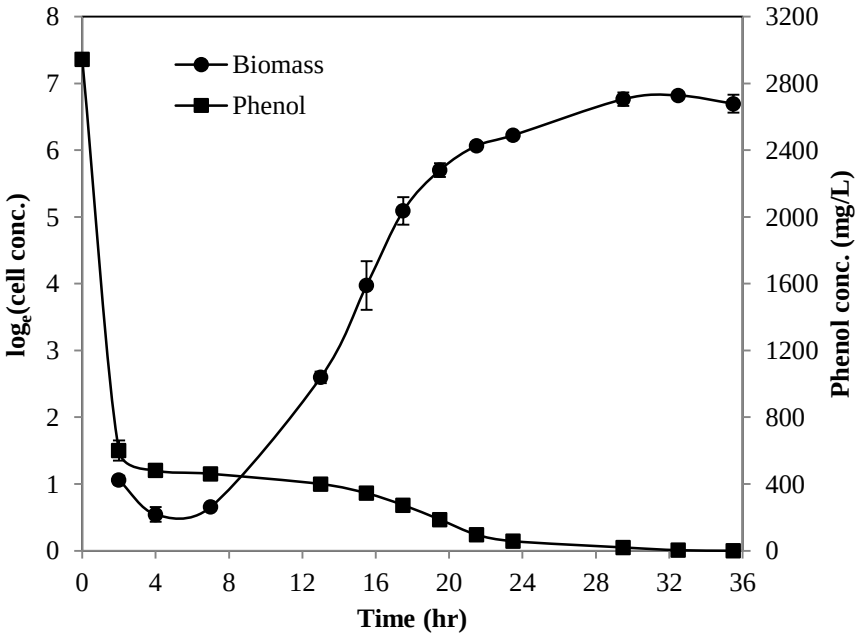

Figure 8.4 Cell growth and phenol removal profiles during biodegradation of 3000 mg/L phenol at effective EIHFM length of 90 cm in the EIHFMB

8.2.5 Effects of Flow Rate

To investigate the effects of flow rates on biodegradation kinetics in the EIHFMB, the flow rates in the EIHFMB was varied from 5 mL/min to 11.5 mL/min. Fig. 8.5 shows the phenol removal profiles obtained from these experiments. It can be seen that the equilibrium phenol concentration in all the three experiments were almost the same at 125 mg/L, although equilibrium was reached at different times in each of the three experiments. At a flow rate of 11.5 mL/min, equilibrium concentration was reached in

about one hour, while the same was achieved within 3 hours at a flow rate of 8 mL/min. The adsorption rate was slowest at the flow rate of 5 mL/min, wherein equilibrium was attained only after 4 hours of operation.

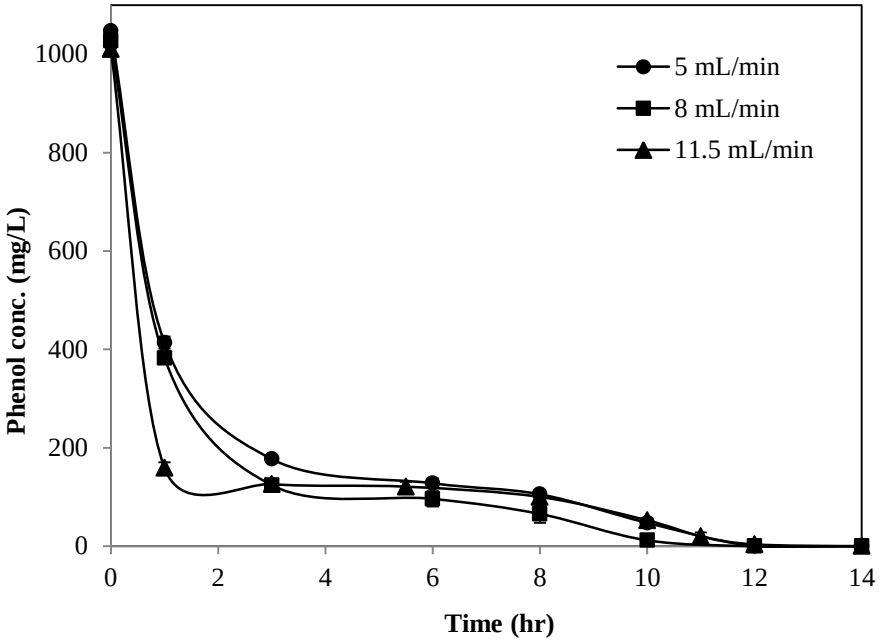

Figure 8.5 Effects of aqueous flow rate on the removal of 1000 mg/L phenol in the EIHFMB

In membrane based separation processes, solutes moving from the aqueous phase to the membrane encounter resistance to mass transfer in the boundary layer at the solid/liquid interface. The boundary layer is a stagnant region of poor or no mixing at the solid/liquid interface, through which the mass transfer is quite slow (Gabelman and Hwang 1999). Often, during liquid/liquid extraction using hollow fiber membranes, solute diffusion through the aqueous boundary layer is the rate-limiting step (Lazarova and Boyadzhieva 2004). An increase in the flow rate introduces more turbulence of the flow area which results in better mixing at the interface and the thickness of boundary layer increases. Consequently, the mass transfer resistance decreases and the rate of diffusion of the substrate to and from the membrane are enhanced.

The cell growth and biodegradation trends at different flow rates in the EIHFMB have been summarized in Table 8.3. It can be seen that phenol concentration in the EIHFMB at the time of inoculation varied between 159-414 mg/L, but these had marginal effects on cell growth and biodegradation rates. The lag phase duration in the three experiments was 5-6 hours, while the specific growth rates were constant at 0.71-0.73 hr^{-1}. This was anticipated as the changes in the flow rates had no effects on the adsorption capacity of the EIHFMs, and the equilibrium phenol concentrations that the microorganisms were exposed to during exponential phase were the same in all the three experiments. Since the flow rates did not have any significant effect on the biodegradation time, it can be concluded that phenol biodegradation in the EIHFMB was not limited by the mass transfer of phenol.

Table 8.3 Effect of aqueous flow rate on bioreactor parameters during biodegradation of 1000 mg/L phenol

Flow rate (mL/min)	Specific growth rate (hr^{-1})	Biomass yield (g/g)	Removal Time (hr)	Lag phase duration (hr)
5	0.71	0.21	12	5
8	0.73	0.31	12	5
11.5	0.73	0.29	13	6

8.2.6 Bioreactor Stability

In order to achieve sustainable high performance biodegradation in solid/liquid TPPBs, the regeneration of the adsorbents should be rapid and effective. When the adsorbents are prepared by immobilizing extractants into polymers, as is the case of polymeric microcapsules or the EIHFMs, the extractants should not be lost from the polymers over time. Although the stability of the EIHFMs was demonstrated earlier in

Chapter 5, during repeated adsorption/desorption cycles of phenol, the conditions in the EIHFMB were quite different from the abiotic experimental conditions during adsorption. Instability in EIHFMB could arise from: (1) the presence of biodegrading bacteria; (2) the long periods of operation; (3) changing operating conditions and the changes in the physical properties of the solution during biodegradation; and (4) the alkaline washing of the EIHFMB at the end of each experimental run.

In this research, the same sets of membrane contactors were used during all the experiments after repeated washing and cleaning with alkaline solutions after each run. The experimental runs were started with the biodegradation of 1000 mg/L phenol, which was followed by at least ten more sets of experiments with multiple runs, at different phenol loadings or operating conditions. It was estimated that the total number of hours the EIHFMB was operated during this period including the washing cycles exceeded 400 hours. To examine the stability of the EIHFMB, biodegradation of 1000 mg/L phenol in the EIHFMB was repeated under identical conditions after a gap of approximately 400 hours.

Fig. 8.6 shows the comparison of the original and repeated experiments at feed phenol concentration of 1000 mg/L. It can be seen that the cell growth and biodegradation profiles for the two sets of data were almost identical. The lag phase durations in the original and after 400 hours of repeated operations were the same and the equilibrium aqueous phenol concentration in both the cases stabilized at nearly the same concentration. Since the equilibrium phenol concentration in both the cases were comparable, the specific growth rate during the repeated run was also the same as that observed earlier (0.73 hr^{-1}), while the biomass yield was slightly lower at 0.28 g/g. Biodegradation was completed within 12 hours in both the cases.

These results indicate that the adsorption capacity of the EIHFMs remained unchanged over 400 hours of operation and therefore it can be concluded that the immobilization of TOPO within the polypropylene support was stable and no TOPO was lost during the entire EIHFMB operation. These results are significant because: (1) they reaffirm the high stability of the EIHFMs and show that the EIHFMB can be operated over long periods of time, without any loss in the adsorption capacity or biodegradation performance; (2) the cell growth in the EIHFMB was not affected by the age of the EIHFMs and immobilized TOPO was not degraded or transformed under microbial action, and; (3) biofilm formation on the EIHFMs and the subsequent washing at high alkalinity does not affect the mass transfer performance of the EIHFMs.

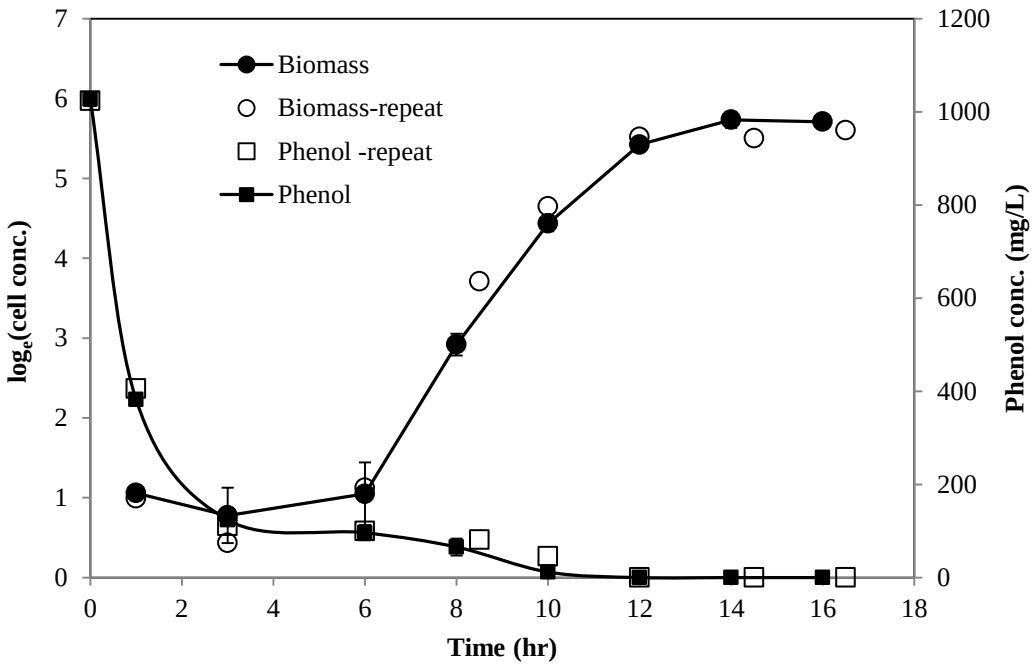

Figure 8.6 Comparison of cell growth and biodegradation profiles at initial phenol concentration of 1000 mg/L, carried out after an interval of 400 hours of operation in the EIHFMB. Solid shapes represent original profiles whereas open shapes represent the profiles after 400 hours of repeated operation

8.3 Conclusions

EIHFMs with high TOPO content have been used to develop an EIHFMB, which was operated for biodegradation of inhibitory phenol concentrations. Phenol concentrations at 800-2500 mg/L were completely mineralized in the bioreactor during solid/liquid two phase biodegradation, with the EIHFMs serving as the partitioning phase. The cell growth was characterized by a short lag phase, which was followed by an exponential growth phase at high specific growth rate. The maximum specific growth rate of 0.73 hr^{-1} was observed during biodegradation of 1000 mg/L phenol. The specific growth rates in the EIHFMB were for better than those observed in suspension cultures of correspondingly similar phenol concentrations. It was also found that cell growth was independent of the total phenol concentration in the EIHFMB.

The adsorption capacity and the adsorption rates in the EIHFMB could be enhanced by increasing the effective length of the EIHFMs. At the higher EIHFM length, biodegradation of 3000 mg/L phenol could be achieved within 36 hours. The effects of aqueous flow rate on phenol removal from the EIHFMB were also examined and it was observed that the mass transfer and consequent biodegradation rates in the EIHFMB improved at higher flow rates. Finally, the stability of the EIHFMB over long periods of operation was demonstrated. It was observed that the EIHFMB performance was stable for over 400 hours. These results indicate that the EIHFMB can be a promising alternative to conventional TPPBs. Further research on EIHFMB should be focused on simultaneous extraction and biodegradation of phenol from the wastewater.

9 Conclusions and Recommendations for Future Work

9.1 Conclusions

In this research program, hollow fiber membrane technology was applied to the realm of two-phase biodegradation to develop novel hollow fiber membrane bioreactor configurations which were capable of mitigating various operational issues and ameliorating the contact between the aqueous and the non-aqueous phases. The overall challenge was to accomplish more effective, economical and sustainable two-phase biodegradation of phenol in wastewater. The strategy of the non-dispersive HFMB and the semi-dispersive HFSLMB configurations, both based on the use of organic solvents, was to segregate the aqueous cell culture medium from the organic phase using hydrophobic polypropylene hollow fiber membranes. On the other hand, the EIHFMB configuration was based on the use of solid extractants impregnated into the polypropylene membranes. In this approach, the extractant-containing hollow fibers membranes themselves acted as the partitioning phase.

During biodegradation in the HFMB, the mass transfer between the aqueous and the organic phases was dispersion-free and the phases were physically separated. As a result, *P. putida* in the aqueous phase was protected from the adverse effects of phenol laden 2-undecanone and did not exhibit any lag phase. The cell growth kinetics in the solvent-free growth environment was analogous to that observed in single-phase biodegradation systems, and the cell growth rates were independent of the total phenol concentration in the HFMB. The bacteria metabolized phenol concentrations as high as 2000 mg/L, achieving high cell growth and biodegradation rates. Phenol removal in the HFMB took place in three stages: initial sorption, biodegradation by exponentially growing bacteria, and biodegradation under nutrient limitation. The duration of the exponential growth phase could be prolonged by

increasing the interfacial area, which resulted in improved biodegradation performance. Compared to the conventional TPPB, the HFMB operation was devoid of foaming, emulsions or downstream separation problems, and facilitated complete solvent recycle. Biodegradation rate in the HFMB was also higher than that in TPPB at comparable mass transfer flux of phenol from the organic to the aqueous phase. In addition, the HFMB offered high operational flexibility, which was harnessed to facilitate simultaneous extraction and biodegradation of phenol directly from the feed wastewater. A kinetics model was developed to examine the mass transfer and biodegradation kinetics of phenol in the HFMB. The results indicate that mass transfer through the shell side boundary layer was the slowest and it was the rate limiting step. From model simulations, it was predicted that the HFMB performance could be enhanced by increasing the packing density, the membrane length and the shell side flow rate. The kinetics model also predicted that about 18% of the total biomass in the HFMB was present as biofilm on the membranes and the silicone tubings surfaces. Furthermore, the biodegradation kinetics of the biofilms was analogous to that of the suspended cells, and the presence of biofilms on the membranes did not pose additional resistance to the mass transfer of phenol.

Simultaneous extraction and biodegradation, which were performed in two hollow fiber membrane contactors in the HFMB, were carried out in the HFSLMB using a single membrane contactor. In this semi-dispersive configuration, the transfer of phenol from the feed wastewater to the organic solvent was based on phase dispersion, but the movement of phenol from the organic phase to the cell culture was dispersion-free. In the membrane protected growth environment, cell growth in the HFSLMB was analogous to that in the HFMB. The microorganisms experienced only 10% of the total phenol concentration in the HFSLMB and biodegraded phenol

concentrations of 1000-4000 mg/L. The high diffusion rates resulting from the low mass transfer resistance during extraction and the presence of the liquid membrane on the shell side effected higher biodegradation rates as compared to the TPPB and the HFMB. The biodegradation performance of the HFSLMB could be further improved by varying the operating conditions of phase ratio, flow rates and the interfacial mass transfer area. The HFSLMB was operated for more than 400 hours to examine the long-term sustainability of the bioreactor operation during repeated batch runs at 1000 mg/L phenol. While the supported liquid membrane remained intact throughout the HFSLMB operation, the biodegradation performance deteriorated after 100 hours of operation due to the growing thickness of the biofilms on the membrane surface. The HFSLMB performance could be recovered by administrating a 5 hour washing cycle with 1 M sodium hydroxide after every 100 hours of biodegradation in HFSLMB.

The HFSLMB had the advantages of higher mass transfer rates, lower solvent volume and lower energy requirement, as compared to the HFMB. In addition, the HFSLMB facilitated concomitant extraction and biodegradation in a single hollow fiber membrane contactor. The use of HFSLMB resulted in low installation and operating costs, but it also compromised the non- dispersive characteristic of the HFMB and an additional phase separation step was required before the treated wastewater could be discharged. Therefore, we recommend the use of HFSLMB for the organic solvents with low emulsion formation tendency and high distribution coefficients. The use of the HFSLMB is also advisable for very expensive solvents which could not be availed in large quantities. On the other hand, the HFMB is more suited for the use of organic solvents with low distribution coefficients and high emulsion-forming tendency.

While the HFMB and the HFSLMB were developed to alleviate the operational concerns in aqueous/organic two-phase biodegradation, the development of the

EIHFMB was aimed at addressing the concerns pertaining to the solid/liquid two-phase biodegradation process in conventional TPPBs. The EIHFMs were prepared by impregnating polypropylene fibers with the solid extractant TOPO. The EIHFMs were characterized using SEM, whereas the adsorption capacity and adsorption rates of the EIHFMs were investigated at various phenol and TOPO concentrations. The adsorption isotherms were modeled after the Langmuir and the Freundlich isotherms, while the adsorption rates were described by pseudo-second-order kinetics. The EIHFMs exhibited high stability and their performance during repeated batch adsorption/desorption cycles remained unchanged for 10 cycles. The use of EIHFMs as NAP in the EIHFMB resulted in a short lag phase for the bacteria, which was followed by a high cell growth rate. Feed phenol concentrations of 800-2500 mg/L in the EIHFMB were rapidly lowered to sub-inhibitory concentrations, which were subsequently metabolized by *P. putida* at high biodegradation rates. The phenol loading capacity and the biodegradation rate in the EIHFMB could be enhanced by increasing the effective length of the EIHFMs as demonstrated in the biodegradation of 3000 mg/L phenol. The mass transfer rate of phenol from the aqueous to membrane phase in the EIHFMB could be accelerated by increasing the flow rate, but it did not affect the biodegradation rate significantly, and it was concluded that the biodegradation rate in the EIHFMB was not limited by the mass transfer of phenol. The EIHFMB performance was stable for over 400 hours of the bioreactor operation, which corroborated the stability of the impregnated extractants in the membranes.

The results in this research manifest the benefits of the hollow fiber membrane bioreactors in the context of two-phase biodegradation. These advantages include the low solvent and low energy demand, high operational and configurational flexibility, absence of emulsions and consequent downstream separation and long-term

sustainability, while retaining the advantages of high cell growth and biodegradation rates of TPPBs. The development of EIHFM, in particular, has immense potential in the fields of both solvent extraction and two-phase biodegradation. This research also provides a better insight into the mass transfer and biodegradation mechanisms of phenol in two-phase biodegradation, which could be harnessed to further improve the kinetics of two-phase biodegradation.

The hollow fiber membrane bioreactors developed in this research were based on the principles in solvent extraction, adsorption, biodegradation and hollow fiber membranes based separation, and the flexibility in the design of these bioreactors allows synchronization with any relevant development in these technologies to further improve the performance of these bioreactors in wastewater treatment. To further improve the biodegradation performance and augment the applicability of these bioreactors, some recommendations for future work are suggested below.

9.2 Recommendations for Future Work

The application of hollow fiber membranes in two-phase biodegradation opens several new frontiers for the advancement of this technology. We have identified four potential avenues for further exploration of this technology:

1. One of the primary challenges in designing aqueous/organic TPPBs is the selection of the organic solvent. The solvent selection criteria are quite stringent and most of the commonly used organic solvents in solvent extraction are not favored as they do not meet all the criteria. The membrane-protected cell growth environment in the HFMB may help dilute some of these stringent guidelines, especially the biocompatibility requirement. Studies may be carried out to evaluate the feasibility of using non-biocompatible organic phases with high

distribution coefficient and better mass transfer characteristics in the HFMB and the HFSLMB. The pure culture used in this research may also be substituted by a mixed microbial consortium with better biodegradation potential. Furthermore, two-phase biodegradation in TPPBs has always been carried out in batch or fed-batch mode, while continuous operation of these bioreactors has not been investigated due to NAP regeneration/de-emulsification problems. But the bioreactors developed here are suited for continuous operation, and experiments may be performed to investigate the biodegradation rate, substrate loading capacity, effects of operating conditions and the long-term sustainability of these novel bioreactors in continuous mode. In addition, the biodegradation kinetics in the HFSLMB may be modeled to better understand the mass transfer of the substrate through the liquid membrane, identify the rate controlling step and optimize the operating conditions.

2. The bioreactors developed in this research show excellent performance in phenol biodegradation. To demonstrate the usefulness of these bioreactors further, experiments can be carried out for biodegradation of high concentration of other aliphatic and aromatic pollutants which are highly toxic and exert severe substrate inhibition on biodegrading microorganisms. Since phenol represents monoaromatics, in general, it will be interesting to study the biodegradation of polyaromatics compounds. Furthermore, the usefulness of these membrane bioreactors can also be assessed in the biodegradation of a mixture of toxic pollutants, which will require very careful selection of the organic phase and microorganisms.
3. The development of the EIHFMs is still in the nascent stage and further studies are required to establish this technology in the realm of wastewater treatment.

Experiments may be performed to design EIHFMs using different extractants, carrier solvents and hollow fiber membranes which may be used in the extraction of different organic compounds. Moreover, the SEM images of the EIHFM cross-sections in Chapter 7 showed that distribution of TOPO in the membranes was not uniform, and the extractant was more concentrated on the outer membrane surface through which the carrier solvent was evaporated. The EIHFM fabrication technique may be optimized for more uniform distribution of the extractant in the membrane walls which has the potential to enhance the adsorption capacity and the adsorption rate, as well as the reproducibility of the experimental data from one bioreactor system to another. Furthermore, the lumen side of the EIHFMs was not used in this research. Further studies are required to demonstrate simultaneous adsorption and desorption/biodegradation of phenol in EIHFMBs, which hitherto have not been performed in conventional solid/liquid TPPBs. Finally, the kinetics of adsorption/desorption of phenol may be elucidated through a mathematical model to understand the mass transfer mechanisms in EIHFMB.

4. Both solvent extraction and two-phase biodegradation are widely used in wastewater treatment. In solvent extraction, the main objective is to recover and concentrate the organic compound from the wastewater using a stripping solution. But the stripping efficiency is never 100% and the effluent concentration may not reach the discharge limit. On the other hand, the focus in two-phase biodegradation is the destruction of the pollutants from wastewater but the microorganisms suffer from substrate inhibition. In both of these techniques, the substrate must be extracted from the wastewater to the organic phase prior to stripping or biodegradation. One approach to enhance the efficacy of the wastewater treatment could be the concomitant stripping and biodegradation of

the pollutant from the wastewater. For example, during recovery of the pollutant from the feed wastewater, the wastewater can be inoculated when the pollutant concentration drops to sub-inhibitory levels. Alternatively, stripping and biodegradation can be carried out in tandem, with stripping preceding biodegradation. While this approach can lead to a more effective and efficient wastewater treatment, some of the treatment costs could be offset by recycling the recovered chemicals. The coupling of stripping and biodegradation is quite challenging in conventional TPPBs, and cannot be carried out simultaneously. It could, however, be quite straight-forward in either of the bioreactor configurations developed in this research.

REFERENCES

Amsden, B. G., Bochanysz, J. and Daugulis, A. J. (2003). "Degradation of xenobiotics in a partitioning bioreactor in which the partitioning phase is a polymer." Biotechnology and Bioengineering **84**(4): 399-405.

Ana Maria, S. and Anil Kumar, P. (2008). Hollow Fiber Membrane-Based Separation Technology. Solvent Extraction and Liquid Membranes, CRC Press**:** 91-140.

Arriaga, S., Munoz, R., Hernandez, S., Guieysse, B. and Revah, S. (2006). "Gaseous hexane biodegradation by Fusarium solani in two liquid phase packed-bed and stirred-tank bioreactors." Environmental Science & Technology **40**(7): 2390-2395.

Asimakopoulou, A. G. and Karabelas, A. J. (2006). "A study of mass transfer in hollow-fiber membrane contactors--The effect of fiber packing fraction." Journal of Membrane Science **282**(1-2): 430-441.

Bahdod, A., El Asri, S., Saoiabi, A., Coradin, T. and Laghzizil, A. (2009). "Adsorption of phenol from an aqueous solution by selected apatite adsorbents: Kinetic process and impact of the surface properties." Water Research **43**(2): 313-318.

Basu, R., Prasad, R. and Sirkar, K. K. (1990). "Nondispersive membrane solvent back extraction of phenol." AIChE Journal **36**(3): 450-460.

Bocquet, S., Gascons Viladomat, F., Muvdi Nova, C., Sanchez, J., Athes, V. and Souchon, I. (2006). "Membrane-based solvent extraction of aroma compounds: Choice of configurations of hollow fiber modules based on experiments and simulation." Journal of Membrane Science **281**(1-2): 358-368.

Bocquet, S., Torres, A., Sanchez, J., Rios, G. M. and Romero, J. (2005). "Modeling the mass transfer in solvent-extraction processes with hollow-fiber membranes." AIChE Journal **51**(4): 1067-1079.

Bringas, E., San Román, M. F. and Ortiz, I. (2006). "Separation and Recovery of Anionic Pollutants by the Emulsion Pertraction Technology. Remediation of Polluted Groundwaters with Cr(VI)." Industrial & Engineering Chemistry Research **45**(12): 4295-4303.

Bruce, L. J. and Daugulis, A. J. (1991). "Solvent selection strategies for extractive biocatalysis." Biotechnology Progress **7**(2): 116-124.

Busca, G., Berardinelli, S., Resini, C. and Arrighi, L. (2008). "Technologies for the removal of phenol from fluid streams: A short review of recent developments." Journal of Hazardous Materials **160**(2-3): 265-288.

Cao, B. and Loh, K. C. (2008). "Catabolic pathways and cellular responses of Pseudomonas putida P8 during growth on benzoate with a proteomics approach." Biotechnol Bioeng **101**(6): 1297-1312.

Chikh, R., Couvert, A., Amar, H. A. and Amrane, A. (2011). "Toluene Biodegradation in a Two Phase Partitioning System-Use of a Biodegradable Solvent." Environmental Progress & Sustainable Energy **30**(3): 303-308.

Chung, T.-P., Wu, P. C. and Juang, R. S. (2005). "Use of microporous hollow fibers for improved biodegradation of high-strength phenol solutions." Journal of Membrane Science **258**(1-2): 55-63.

Chung, T. P., Wu, P. C. and Juang, R. S. (2004). "Process development for degradation of phenol by Pseudomonas putida in hollow-fiber membrane bioreactors." Biotechnology and Bioengineering **87**(2): 219-227.

Cichy, W., Schlosser, S. and Szymanowski, J. (2001). "Recovery of phenol with CYANEX((R)) 923 in membrane extraction-stripping systems." Solvent Extraction and Ion Exchange **19**(5): 905-923.

Cichy, W., Schlosser, S. and Szymanowski, J. (2005). "Extraction and pertraction of phenol through bulk liquid membranes." Journal of Chemical Technology and Biotechnology **80**(2): 189-197.

Cichy, W. and Szymanowski, J. (2002). "Recovery of phenol from aqueous streams in hollow fiber modules." Environmental Science & Technology **36**(9): 2088-2093.

Collins, L. D. and Daugulis, A. J. (1996). "Use of a two phase partitioning bioreactor for the biodegradation of phenol." Biotechnology Techniques **10**(9): 643-648.

Collins, L. D. and Daugulis, A. J. (1997). "Biodegradation of phenol at high initial concentrations in two-phase partitioning batch and fed-batch bioreactors." Biotechnology and Bioengineering **55**(1): 155-162.

Collins, L. D. and Daugulis, A. J. (1999). "Benzene/toluene/p-xylene degradation. Part II. Effect of substrate interactions and feeding strategies in toluene/benzene and toluene/p-xylene fermentations in a partitioning bioreactor." Applied Microbiology and Biotechnology **52**(3): 360-365.

Correia, P. and de Carvalho, J. M. R. (2005). "Salt effects on the recovery of phenol by liquid-liquid extraction with Cyanex 923." Separation Science and Technology **40**(16): 3365-3380.

Cruickshank, S. M., Daugulis, A. J. and McLellan, P. J. (2000). "Dynamic modeling and optimal fed-batch feeding strategies for a two-phase partitioning bioreactor." Biotechnology and Bioengineering **67**(2): 224-233.

Cruickshank, S. M., Daugulis, A. J. and McLellan, P. J. (2000). "Modelling of a continuous two-phase partitioning bioreactor for the degradation of xenobiotics." Process Biochemistry **35**(9): 1027-1035.

Daugulis, A. J. (2001). "Two-phase partitioning bioreactors: a new technology platform for destroying xenobiotics." Trends in Biotechnology **19**(11): 457-462.

Daugulis, A. J., Amsden, B. G., Bochanysz, J. and Kayssi, A. (2003). "Delivery of benzene to Alcaligenes xylosoxidans by solid polymers in a two-phase partitioning bioreactor." Biotechnology Letters **25**(14): 1203-1207.

Daugulis, A. J. and Janikowski, T. B. (2002). "Scale-up performance of a partitioning bioreactor for the degradation of polyaromatic hydrocarbons by Sphingomonas aromaticivorans." Biotechnology Letters **24**(8): 591-594.

Daugulis, A. J., Tomei, M. C. and Guieysse, B. (2011). "Overcoming substrate inhibition during biological treatment of monoaromatics: recent advances in bioprocess design." Applied Microbiology and Biotechnology **90**(5): 1589-1608.

Deziel, E., Comeau, Y. and Villemur, R. (1999). "Two-liquid-phase bioreactors for enhanced degradation of hydrophobic/toxic compounds." Biodegradation **10**(3): 219-233.

Gabelman, A. and Hwang, S. T. (1999). "Hollow fiber membrane contactors." Journal of Membrane Science **159**(1-2): 61-106.

Gardin, H., Lebeault, J. M. and Pauss, A. (1999). "Biodegradation of xylene and butyl acetate using an aqueous-silicon oil two-phase system." Biodegradation **10**(3): 193-200.

Gawronski, R. and Wrzesinska, B. (2000). "Kinetics of solvent extraction in hollow-fiber contactors." Journal of Membrane Science **168**(1-2): 213-222.

Gong, X. C., Luo, G. S., Yang, W. W. and Wu, F. Y. (2006). "Separation of organic acids by newly developed polysulfone microcapsules containing triotylamine." Separation and Purification Technology **48**(3): 235-243.

González-Muñoz, M. J., Luque, S., Álvarez, J. R. and Coca, J. (2003). "Recovery of phenol from aqueous solutions using hollow fibre contactors." Journal of Membrane Science **213**(1-2): 181-193.

Guha, A. K., Yun, C. H., Basu, R. and Sirkar, K. K. (1994). "Heavy metal removal and recovery by contained liquid membrane permeator." AIChE Journal **40**(7): 1223-1237.

Guieysse, B., Autem, Y. and Soares, A. (2004). Biodegradation of phenol at low temperature using two-phase partitioning bioreactors. 4th World Water Congress of the International-Water-Association, Marrakesh, MOROCCO, I W a Publishing.

Guieysse, B., Cirne, M. and Mattiasson, B. (2001). "Microbial degradation of phenanthrene and pyrene in a two-liquid phase-partitioning bioreactor." Applied Microbiology and Biotechnology **56**(5-6): 796-802.

Guieysse, B. and Viklund, G. (2005). "Sequential UV-biological degradation of polycyclic aromatic hydrocarbons in two-phases partitioning bioreactors." Chemosphere **59**(3): 369-376.

Hamed, T. A., Bayraktar, E., Mehmetoglu, U. and Mehmetoglu, T. (2004). "The biodegradation of benzene, toluene and phenol in a two-phase system." Biochemical Engineering Journal **19**(2): 137-146.

Hernandez, M., Quijano, G. and Munoz, R. (2012). "Key Role of Microbial Characteristics on the Performance of VOC Biodegradation in Two-Liquid Phase Bioreactors." Environmental Science & Technology **46**(7): 4059-4066.

Ho, W. S. W. and Poddar, T. K. (2001). "New membrane technology for removal and recovery of chromium from waste waters." Environmental Progress **20**(1): 44-52.

Ho, Y. S. and McKay, G. (1998). "Sorption of dye from aqueous solution by peat." Chemical Engineering Journal **70**(2): 115-124.

Hossain, M. M. and Maisuria, J. L. (2008). "Effects of organic phase, fermentation media, and operating conditions on lactic acid extraction." Biotechnology Progress **24**(3): 757-765.

Hu, S. Y. B. and Wiencek, J. M. (1998). "Emulsion-liquid-membrane extraction of copper using a hollow-fiber contactor." AIChE Journal **44**(3): 570-581.

Illanes, C. O., Ochoa, N. A. and Marchese, J. (2008). "Kinetic sorption of Cr(VI) into solvent impregnated porous microspheres." Chemical Engineering Journal **136**(2-3): 92-98.

Isaza, P. A. and Daugulis, A. J. (2010). "Enhanced Degradation of Phenanthrene in a Solid-Liquid Two-Phase Partitioning Bioreactor via Sonication." Biotechnology and Bioengineering **105**(5): 997-1001.

Jain, R. K., Kapur, M., Labana, S., Lal, B., Sarma, P. M., Bhattacharya, D. and Thakur, I. S. (2005). "Microbial diversity: Application of microorganisms for the biodegradation of xenobiotics." Current Science **89**(1): 101-112.

Juang, R.-S., Chung, T.-P., Wang, M.-L. and Lee, D.-J. (2008). "Experimental observations on the effect of added dispersing agent on phenol biodegradation

in a microporous membrane bioreactor." Journal of Hazardous Materials **151**(2-3): 746-752.

Juang, R.-S. and Huang, W.-C. (2008). "Use of membrane contactors as two-phase bioreactors for the removal of phenol in saline and acidic solutions." Journal of Membrane Science **313**(1-2): 207-216.

Juang, R.-S. and Kao, H.-C. (2009). "Estimation of the contribution of immobilized biofilm and suspended biomass to the biodegradation of phenol in membrane contactors." Biochemical Engineering Journal **43**(2): 122-128.

Juang, R. S., Huang, W. C. and Hsu, Y. H. (2009). "Treatment of phenol in synthetic saline wastewater by solvent extraction and two-phase membrane biodegradation." Journal of Hazardous Materials **164**(1): 46-52.

Juang, R. S., Kao, H. C. and Tseng, K. J. (2010). "Kinetics of phenol removal from saline solutions by solvent extraction coupled with degradation in a two-phase partitioning bioreactor." Separation and Purification Technology **71**(3): 285-292.

Juang, R. S., Kao, H. C. and Zhang, Z. (2012). "A simplified dynamic model for the removal of toxic organics in a two-phase partitioning bioreactor." Separation and Purification Technology **90**: 213-220.

Judd, S. (2008). "The status of membrane bioreactor technology." Trends in Biotechnology **26**(2): 109-116.

Khan, T. R. and Daugulis, A. J. (2011). "Medium composition effects on solute partitioning in solid - liquid two-phase bioreactors." Journal of Chemical Technology and Biotechnology **86**(1): 157-160.

Kocherginsky, N. M., Yang, Q. and Seelam, L. (2007). "Recent advances in supported liquid membrane technology." Separation and Purification Technology **53**(2): 171-177.

Kosaraju, P. B. and Sirkar, K. K. (2007). "Novel solvent-resistant hydrophilic hollow fiber membranes for efficient membrane solvent back extraction." Journal of Membrane Science **288**(1-2): 41-50.

Kujawski, W., Warszawski, A., Ratajczak, W., Porebski, T., Capala, W. and Ostrowska, I. (2004). "Removal of phenol from wastewater by different separation techniques." Desalination **163**(1-3): 287-296.

Lazarova, Z. and Boyadzhieva, S. (2004). "Treatment of phenol-containing aqueous solutions by membrane-based solvent extraction in coupled ultrafiltration modules." Chemical Engineering Journal **100**(1-3): 129-138.

Le-Clech, P. (2010). "Membrane bioreactors and their uses in wastewater treatments." Applied Microbiology and Biotechnology **88**(6): 1253-1260.

Li, Y. and Loh, K.-C. (2006). "Activated carbon impregnated polysulfone hollow fiber membrane for cell immobilization and cometabolic biotransformation of 4-chlorophenol in the presence of phenol." Journal of Membrane Science **276**(1-2): 81-90.

Li, Y. and Loh, K. C. (2005). "Cometabolic Transformation of High Concentrations of 4-Chlorophenol in an Immobilized Cell Hollow Fiber Membrane Bioreactor." Journal of Environmental Engineering **131**(9): 1285-1292.

Li, Y. and Loh, K. C. (2006). "Continuous Cometabolic Transformation of 4-Chlorophenol in the Presence of Phenol in a Hollow Fiber Membrane Bioreactor." Journal of Environmental Engineering **132**(3): 309-314.

Littlejohns, J. V. and Daugulis, A. J. (2008). "Response of a solid-liquid two-phase partitioning bioreactor to transient BTEX loadings." Chemosphere **73**(9): 1453-1460.

Liu, Y. and Shi, B. (2009). "Interaction Parameter Method for Investigating BTEX Extraction Using the Hollow-Fiber Microporous Membrane Liquid/Liquid Extraction Technique." Chemical Engineering & Technology **32**(6): 926-931.

Loh, K.-C. and Cao, B. (2008). "Paradigm in biodegradation using Pseudomonas putida--A review of proteomics studies." Enzyme and Microbial Technology **43**(1): 1-12.

Loh, K. C., Chung, T. S. and Ang, W. F. (2000). "Immobilized-Cell Membrane Bioreactor for High-Strength Phenol Wastewater." Journal of Environmental Engineering **126**(1): 75-79.

Loh, K. C. and Liu, J. (2001). "External loop inversed fluidized bed airlift bioreactor (EIFBAB) for treating high strength phenolic wastewater." Chemical Engineering Science **56**(21-22): 6171-6176.

Lovley, D. R. (2003). "Cleaning up with genomics: applying molecular biology to bioremediation." Nat Rev Micro **1**(1): 35-44.

Ma, X., Li, Y., Li, X., Yang, L. and Wang, X. (2011). "Preparation of novel polysulfone capsules containing zirconium phosphate and their properties for Pb2+ removal from aqueous solution." Journal of Hazardous Materials **188**(1-3): 296-303.

Mahanty, B., Pakshirajan, K. and Dasu, V. V. (2008). "Biodegradation of pyrene by Mycobacterium frederiksbergense in a two-phase partitioning bioreactor system." Bioresource Technology **99**(7): 2694-2698.

Malik, M. A., Hashim, M. A. and Nabi, F. (2011). "Ionic liquids in supported liquid membrane technology." Chemical Engineering Journal **171**(1): 242-254.

Malinowski, J. J. (2001). "Two-phase partitioning bioreactors in fermentation technology." Biotechnology Advances **19**(7): 525-538.

McCabe, W. L., Smith, J. C. and Harriott, P. (2005). Unit operations of chemical engineering. New York, McGraw-Hill.

Meng, F., Chae, S.-R., Drews, A., Kraume, M., Shin, H.-S. and Yang, F. (2009). "Recent advances in membrane bioreactors (MBRs): Membrane fouling and membrane material." Water Research **43**(6): 1489-1512.

Michałowicz, J. and Duda, W. (2007). "Phenols – Sources and Toxicity." Polish J. of Environ. Stud. **16**(3): 347-362.

Munoz, R., Chambaud, M., Bordel, S. and Villaverde, S. (2008). "A systematic selection of the non-aqueous phase in a bacterial two liquid phase bioreactor treating alpha-pinene." Applied Microbiology and Biotechnology **79**(1): 33-41.

Nanoti, A., Ganguly, S. K., Goswami, A. N. and Rawat, B. S. (1997). "Removal of Phenols from Wastewater Using Liquid Membranes in a Microporous Hollow-Fiber-Membrane Extractor." Industrial & Engineering Chemistry Research **36**(10): 4369-4373.

Nielsen, D. R., Daugulis, A. J. and McLellan, P. J. (2003). "A novel method of simulating oxygen mass transfer in two-phase partitioning bioreactors." Biotechnology and Bioengineering **83**(6): 735-742.

Nielsen, D. R., Daugulis, A. J. and McLellan, P. J. (2007). "Dynamic simulation of benzene vapor treatment by a two-phase partitioning bioscrubber. Part 1:

Model development, parameter estimation, and parametric sensitivity." Biochemical Engineering Journal **36**(3): 239-249.

Ortiz, I., San Román, M. F., Corvalán, S. M. and Eliceche, A. M. (2003). "Modeling and Optimization of an Emulsion Pertraction Process for Removal and Concentration of Cr(VI)." Industrial & Engineering Chemistry Research **42**(23): 5891-5899.

Outokesh, M., Tayyebi, A., Khanchi, A., Grayeli, F. and Bagheri, G. (2011). "Synthesis and characterization of new biopolymeric microcapsules containing DEHPA–TOPO extractants for separation of uranium from phosphoric acid solutions." Journal of Microencapsulation **28**(4): 248-257.

Paul, D., Pandey, G., Pandey, J. and Jain, R. K. (2005). "Accessing microbial diversity for bioremediation and environmental restoration." Trends in Biotechnology **23**(3): 135-142.

Perez-Pantoja, D., De la Lglesia, R., Pieper, D. H. and Gonzalez, B. (2008). "Metabolic reconstruction of aromatic compounds degradation from the genome of the amazing pollutant-degrading bacterium Cupriavidus necator JMP134." Fems Microbiology Reviews **32**(5): 736-794.

Pierre, F. X., Souchon, I. and Marin, M. (2001). "Recovery of sulfur aroma compounds using membrane-based solvent extraction." Journal of Membrane Science **187**(1-2): 239-253.

Prasad, R. and Sirkar, K. K. (1988). "Dispersion-free solvent extraction with microporous hollow fiber modules." AIChE Journal **34**(2): 177-188.

Prpich, G. P. and Daugulis, A. J. (2005). "Enhanced biodegradation of phenol by a microbial consortium in a solid-liquid two phase partitioning bioreactor." Biodegradation **16**(4): 329-339.

Prpich, G. P. and Daugulis, A. J. (2006). "Biodegradation of a phenolic mixture in a solid-liquid two-phase partitioning bioreactor." Applied Microbiology and Biotechnology **72**(3): 607-615.

Prpich, G. P., Rehmann, L. and Daugulis, A. J. (2008). "On the use, and reuse, of polymers for the treatment of hydrocarbon contaminated water via a solid-liquid partitioning bioreactor." Biotechnology Progress **24**(4): 839-844.

Quijano, G., Chavez-Avila, R., Munoz, R., Thalasso, F. and Ordaz, A. (2010). "K(L)a measurement in two-phase partitioning bioreactors: new insights on potential errors at low power input." Journal of Chemical Technology and Biotechnology **85**(10): 1407-1412.

Quijano, G., Hernandez, M., Thalasso, F., Munoz, R. and Villaverde, S. (2009). "Two-phase partitioning bioreactors in environmental biotechnology." Applied Microbiology and Biotechnology **84**(5): 829-846.

Raghuraman, B. and Wiencek, J. (1993). "Extraction with emulsion liquid membranes in a hollow-fiber contactor." AIChE Journal **39**(11): 1885-1889.

Rainer Gross, B. H., Katja Otto, Andreas Schmid, (2007). "Microbial biofilms: New catalysts for maximizing productivity of long-term biotransformations." Biotechnology and Bioengineering **98**(6): 1123-1134.

Rehmann, L. and Daugulis, A. J. (2007). "Biodegradation of biphenyl in a solid-liquid two-phase partitioning bioreactor." Biochemical Engineering Journal **36**(3): 195-201.

Rehmann, L. and Daugulis, A. J. (2008). "Biodegradation of PCBs in two-phase partitioning bioreactors following solid extraction from soil." Biotechnology and Bioengineering **99**(5): 1273-1280.

Rehmann, L., Prpich, G. P. and Daugulis, A. J. (2008). "Remediation of PAH contaminated soils: Application of a solid-liquid two-phase partitioning bioreactor." Chemosphere **73**(5): 798-804.

Rehmann, L., Sun, B. and Daugulis, A. J. (2007). "Polymer selection for biphenyl degradation in a solid-liquid two-phase partitioning bioreactor." Biotechnology Progress **23**(4): 814-819.

Reij, M. W., Keurentjes, J. T. F. and Hartmans, S. (1998). "Membrane bioreactors for waste gas treatment." Journal of Biotechnology **59**(3): 155-167.

Ren, Z., Zhang, W., Li, H. and Lin, W. (2009). "Mass transfer characteristics of citric acid extraction by hollow fiber renewal liquid membrane." Chemical Engineering Journal **146**(2): 220-226.

Ren, Z., Zhang, W., Lv, Y. and Li, J. (2009). "Simultaneous extraction and concentration of penicillin G by hollow fiber renewal liquid membrane." Biotechnology Progress **25**(2): 468-475.

Ren, Z. Q., Zhang, W. D., Liu, Y. M., Dai, Y. and Cui, C. H. (2007). "New liquid membrane technology for simultaneous extraction and stripping of copper(II) from wastewater." Chemical Engineering Science **62**(22): 6090-6101.

Ren, Z. Q., Zhang, W. D., Meng, H. L., Liu, J. T. and Wang, S. G. (2010). "Extraction separation of Cu(II) and Co(II) from sulfuric solutions by hollow fiber renewal liquid membrane." Journal of Membrane Science **365**(1-2): 260-268.

Rieger, P. G., Meier, H. M., Gerle, M., Vogt, U., Groth, T. and Knackmuss, H. J. (2000). Xenobiotics in the environment: present and future strategies to obviate the problem of biological persistence. Biotechnology 2000 Meeting, Berlin, Germany, Elsevier Science Bv.

Rzeszutek, K. and Chow, A. (1998). "Extraction of phenols using polyurethane membrane." Talanta **46**(4): 507-519.

San Roman, M. F., Bringas, E., Ibanez, R. and Ortiz, I. (2010). "Liquid membrane technology: fundamentals and review of its applications." Journal of Chemical Technology and Biotechnology **85**(1): 2-10.

Saravanan, P., Pakshirajan, K. and Saha, P. (2008). "Biodegradation of phenol and m-cresol in a batch and fed batch operated internal loop airlift bioreactor by indigenous mixed microbial culture predominantly Pseudomonas sp." Bioresource Technology **99**(18): 8553-8558.

Sarma, S. J., Pakshirajan, K. and Mahanty, B. (2011). "Chitosan-coated alginate–polyvinyl alcohol beads for encapsulation of silicone oil containing pyrene: a novel method for biodegradation of polycyclic aromatic hydrocarbons." Journal of Chemical Technology & Biotechnology **86**(2): 266-272.

Sengupta, A., Basu, R. and Sirkar, K. K. (1988). "Separation of solutes from aqueous solutions by contained liquid membranes." AIChE Journal **34**(10): 1698-1708.

Shen, S. F., Smith, K. H., Cook, S., Kentish, S. E., Perera, J. M., Bowser, T. and Stevens, G. W. (2009). "Phenol recovery with tributyl phosphate in a hollow fiber membrane contactor: Experimental and model analysis." Separation and Purification Technology **69**(1): 48-56.

Singh, R., Paul, D. and Jain, R. K. (2006). "Biofilms: implications in bioremediation." Trends in Microbiology **14**(9): 389-397.

Sonawane, J. V., Pabby, A. K. and Sastre, A. M. (2007). "Au(I) extraction by LIX-79/n-heptane using the pseudo-emulsion-based hollow-fiber strip dispersion (PEHFSD) technique." Journal of Membrane Science **300**(1-2): 147-155.

Souchon, I., Athès, V., Pierre, F.-X. and Marin, M. (2004). "Liquid-liquid extraction and air stripping in membrane contactor: application to aroma compounds recovery." Desalination **163**(1-3): 39-46.

Splendiani, A., Nicolella, C. and Livingston, A. G. (2003). "A novel biphasic extractive membrane bioreactor for minimization of membrane-attached biofilms." Biotechnology and Bioengineering **83**(1): 8-19.

Sun, Q. and Yang, L. (2003). "The adsorption of basic dyes from aqueous solution on modified peat–resin particle." Water Research **37**(7): 1535-1544.

Tepe, O. and Dursun, A. Y. (2008). "Combined effects of external mass transfer and biodegradation rates on removal of phenol by immobilized Ralstonia eutropha in a packed bed reactor." Journal of Hazardous Materials **151**(1): 9-16.

Teresa, M., Reis, A., de Freitas, O. M. F., Rosinda, M., Ismael, C. and Carvalho, J. M. R. (2007). "Recovery of phenol from aqueous solutions using liquid membranes with Cyanex 923." Journal of Membrane Science **305**(1-2): 313-324.

Timmis, K. N. and Pieper, D. H. (1999). "Bacteria designed for bioremediation." Trends in Biotechnology **17**(5): 201-204.

Tomei, M. C., Annesini, M. C., Piemonte, V., Prpich, G. P. and Daugulis, A. J. (2010). "Two-phase reactors applied to the removal of substituted phenols: comparison between liquid-liquid and liquid-solid systems." Water Science and Technology **62**(4): 776-782.

Tomei, M. C., Annesini, M. C., Rita, S. and Daugulis, A. J. (2008). "Biodegradation of 4-Nitrophenol in a two-phase sequencing batch reactor: concept demonstration, kinetics and modelling." Applied Microbiology and Biotechnology **80**(6): 1105-1112.

Tomei, M. C., Annesini, M. C., Rita, S. and Daugulis, A. J. (2010). "Two-Phase Partitioning Bioreactors Operating with Polymers Applied to the Removal of Substituted Phenols." Environmental Science & Technology **44**(19): 7254-7259.

Tomei, M. C., Rita, S., Angelucci, D. M., Annesini, M. C. and Daugulis, A. J. (2011). "Treatment of substituted phenol mixtures in single phase and two-phase solid-liquid partitioning bioreactors." Journal of Hazardous Materials **191**(1-3): 190-195.

Vandermeer, K. D. and Daugulis, A. J. (2007). "Enhanced degradation of a mixture of polycyclic aromatic hydrocarbons by a defined microbial consortium in a two-phase partitioning bioreactor." Biodegradation **18**(2): 211-221.

Venkateswaran, P. and Palanivelu, K. (2006). "Recovery of phenol from aqueous solution by supported liquid membrane using vegetable oils as liquid membrane." Journal of Hazardous Materials **131**(1-3): 146-152.

Vick Roy, T. B., Blanch, H. W. and Wilke, C. R. (1983). "Microbial hollow fiber bioreactors." Trends in Biotechnology **1**(5): 135-139.

Vrionis, H. A., Kropinski, A. M. and Daugulis, A. J. (2002). "Enhancement of a two-phase partitioning bioreactor system by modification of the microbial catalyst: Demonstration of concept." Biotechnology and Bioengineering **79**(6): 587-594.

Vrionis, H. A., Kropinski, A. M. and Daugulis, A. J. (2002). "Expanded application of a two-phase partitioning bioreactor through strain development and new feeding strategies." Biotechnology Progress **18**(3): 458-464.

Wang, C. and Li, Y. (2007). "Incorporation of granular activated carbon in an immobilized membrane bioreactor for the biodegradation of phenol by Pseudomonas putida." Biotechnology Letters **29**(9): 1353-1356.

Wang, S. J. and Loh, K. C. (1999). "Modeling the role of metabolic intermediates in kinetics of phenol biodegradation." Enzyme and Microbial Technology **25**(3-5): 177-184.

Wang, Z., Chu, J. S., Song, Y., Cui, Y. J., Zhang, H., Zhao, X. Q., Li, Z. H. and Yao, J. M. (2009). "Influence of operating conditions on the efficiency of domestic wastewater treatment in membrane bioreactors." Desalination **245**(1-3): 73-81.

Whelehan, M., von Stockar, U. and Marison, I. W. (2010). "Removal of pharmaceuticals from water: Using liquid-core microcapsules as a novel approach." Water Research **44**(7): 2314-2324.

Wyss, A., Boucher, J., Montero, A. and Marison, I. (2006). "Micro-encapsulated organic phase for enhanced bioremediation of hydrophobic organic pollutants." Enzyme and Microbial Technology **40**(1): 25-31.

Xiang, Z. Y., Lu, Y. C., Zou, Y., Gong, X. C. and Luo, G. S. (2008). "Preparation of microcapsules containing ionic liquids with a new solvent extraction system." Reactive and Functional Polymers **68**(8): 1260-1265.

Yang, W. W., Lu, Y. C., Xiang, Z. Y. and Luo, G. S. (2007). "Monodispersed microcapsules enclosing ionic liquid of 1-butyl-3-methylimidazolium hexafluorophosphate." Reactive and Functional Polymers **67**(1): 81-86.

Yang, W. W., Luo, G. S., Wu, F. Y., Chen, F. and Gong, X. C. (2004). "Di-2-ethylhexyl phosphoric acid immobilization with polysulfone microcapsules." Reactive and Functional Polymers **61**(1): 91-99.

Yang, X. J., Fane, A. G. and Soldenhoff, K. (2003). "Comparison of liquid membrane processes for metal separations: Permeability, stability, and selectivity." Industrial & Engineering Chemistry Research **42**(2): 392-403.

Yeom, S.-H. and Daugulis, A. J. (2001). "Development of a novel bioreactor system for treatment of gaseous benzene." Biotechnology and Bioengineering **72**(2): 156-165.

Yin, J. J., Chen, R., Ji, Y. S., Zhao, C. D., Zhao, G. H. and Zhang, H. X. (2010). "Adsorption of phenols by magnetic polysulfone microcapsules containing tributyl phosphate." Chemical Engineering Journal **157**(2-3): 466-474.

Younas, M., Bocquet, S. D. and Sanchez, J. (2008). "Extraction of aroma compounds in a HFMC: Dynamic modelling and simulation." Journal of Membrane Science **323**(2): 386-394.

Zhang, J., Chua, H. C., Zhou, J. and Fane, A. G. (2006). "Factors affecting the membrane performance in submerged membrane bioreactors." Journal of Membrane Science **284**(1-2): 54-66.

Zhang, W. D., Cui, C. H., Ren, Z. Q., Dai, Y. and Meng, H. L. (2010). "Simultaneous removal and recovery of copper(II) from acidic wastewater by hollow fiber renewal liquid membrane with LIX984N as carrier." Chemical Engineering Journal **157**(1): 230-237.

Zhang, Y., Wu, J.-F., Zeyer, J., Meng, B., Liu, L., Jiang, C.-Y., Liu, S.-Q. and Liu, S.-J. (2009). "Proteomic and molecular investigation on the physiological adaptation of Comamonas sp. strain CNB-1 growing on 4-chloronitrobenzene." Biodegradation **20**(1): 55-66.

Zhao, G. H., Li, Y. F., Liu, X. X. and Liu, X. L. (2010). "Preparation of capsules containing 1-nonanol for rapidly removing high concentration phenol from aqueous solution." Journal of Hazardous Materials **175**(1-3): 715-725.

Zhao, G. Z., Zhou, L. C., Li, Y. F., Liu, X. X., Ren, X. J. and Liu, X. L. (2009). "Enhancement of phenol degradation using immobilized microorganisms and organic modified montmorillonite in a two-phase partitioning bioreactor." Journal of Hazardous Materials **169**(1-3): 402-410.

Zhao, Y., Liu, Z. J., Liu, F. X. and Li, Z. Y. (2011). "Cometabolic degradation of trichloroethylene in a hollow fiber membrane reactor with toluene as a substrate." Journal of Membrane Science **372**(1-2): 322-330.

Zhu, G. H., Chung, T. S. and Loh, K. C. (2000). "Activated carbon-filled cellulose acetate hollow-fiber membrane for cell immobilization and phenol degradation." Journal of Applied Polymer Science **76**(5): 695-707.

Zidi, C., Tayeb, R., Ali, M. B. and Dhahbi, M. (2010). "Liquid-liquid extraction and transport across supported liquid membrane of phenol using tributyl phosphate." Journal of Membrane Science **360**(1-2): 334-340.

Zidi, C., Tayeb, R. and Dhahbi, M. (2011). "Extraction of phenol from aqueous solutions by means of supported liquid membrane (MLS) containing tri-n-octyl phosphine oxide (TOPO)." Journal of Hazardous Materials **194**: 62-68.

Zilouei, H., Guieysse, B. and Mattiasson, B. (2008). "Two-phase partitioning bioreactor for the biodegradation of high concentrations of pentachlorophenol using Sphingobium chlorophenolicum DSM 8671." Chemosphere **72**(11): 1788-1794.

LIST OF PUBLICATIONS AND PRESENTATIONS

1. Praveen P, Loh K-C., Simultaneous extraction and biodegradation of phenol in a hollow fiber supported liquid membrane bioreactor. *Journal of Membrane Science* (2013), 430(0):242-251.
2. Praveen P, Loh K-C., Two-phase biodegradation of phenol in a hollow fiber membrane bioreactor, *Journal of Environmental Engineering* (2013), 139(5). *(In Press)*
3. Praveen P, Loh K-C., Trioctylphosphine oxide-impregnated hollow fiber membranes for removal of phenol from wastewater, *Journal of Membrane Science* (2013), 10.1016/j.memsci.2013.02.057.
4. Praveen P, Loh K-C., Kinetic modeling of two-phase biodegradation in a hollow fiber membrane bioreactor, *Water Research* (2013) *(Under review).*
5. Praveen P, Loh K-C., Two-phase biodegradation of phenol in an extractant impregnated hollow fiber membrane bioreactor, *Journal of Hazardous Materials* (2013) *(Under review).*
6. Praveen P, Loh K-C., Solventless extraction of phenol using trioctylphosphine oxide-impregnated hollow fiber membranes, *Environmental Science & Technology* (2013) *(In preparation).*
7. Praveen P, Loh K-C., Two-phase biodegradation kinetics of phenol in a hollow fiber supported liquid membrane bioreactor, *Separation & Purification Technology* (2013) *(In preparation).*
8. Praveen P, Loh K-C., Two-phase biodegradation of phenol in a hollow fiber membrane bioreactor, presented at the *6th International Conference on Environment Science and Technology*, (2012) June 25-29, Houston, USA.
9. Praveen P, Loh K-C., Two-phase biodegradation of phenol in a hollow fiber supported liquid membrane bioreactor, presented at the *104th Annual AIChE Meeting*, (2012) Oct 28-Nov 02, Pittsburgh, USA.